Replication of damaged DNA

Amy Louise Upton, B.Sc. (Hons.)

A thesis submitted
to the University of Nottingham
for the degree of Doctor of Philosophy,
June 2009

The University of
Nottingham

Abstract

DNA is under constant attack from numerous damaging agents and our cells deal with thousands of lesions every day. With such constant damage it is inevitable that the template will not be completely cleared of lesions before the replication complex arrives. The consequences of the replisome meeting an obstacle will depend upon the nature of the obstacle. I have focussed upon replication in *Escherichia coli* and the effect of UV-induced lesions, which would block synthesis by the replicative polymerases. It is accepted that a UV lesion in the lagging strand template can be bypassed by the replisome complex, but the consequences of meeting a lesion in the leading strand template remain unclear. A lesion in the leading strand template could block replisome progression and the fork might require extensive processing in order to restart replication. However, it has also been proposed that the replisome could progress past these lesions by re-priming replication downstream and leaving a gap opposite the lesion.

The results of my studies revealed that all modes of synthesis are delayed after UV. I have demonstrated that when synthesis resumed, the majority reflected the combined effects of *oriC* firing and the initiation of inducible stable DNA replication. These modes of synthesis mask the true extent of the delay in synthesis at existing replication forks. The results also revealed that all synthesis after UV is dependent upon DnaC, suggesting that the replicative helicase and possibly the entire replisome, needs to be reloaded. A functional RecFOR system is required for efficient replication restart, without these proteins replication is capable of resuming but only after a long delay. My data support models proposing that replication forks require extensive processing after meeting a lesion in the leading strand template. Whilst I cannot exclude the possibility that replication forks can progress past some such lesions, my data indicate that they cannot progress past many before stalling.

Overall, my results demonstrate the importance of measuring all modes of DNA synthesis when assessing the contribution of any particular protein to recovery after UV

irradiation. Thus, although net synthesis in cells lacking RecG appears similar to wild type after UV, the mode of replication is in fact quite different. A dramatic increase in the level of stable DNA replication appears to account for much of the overall synthesis detected and coincides with a major chromosome segregation defect. The importance of stable DNA replication in irradiated *recG* cells has not previously been considered because the different modes of synthesis were ignored. The significance of this pathology and of the other findings reported in this thesis is discussed in relation to current models of DNA repair and replication restart.

Acknowledgements

First of all, I would like to thank Bob Lloyd for enabling me to study for a PhD. I will miss talking to you about science on such a regular basis. I am indebted to Bob and Christian Rudolph, who together have supervised my projects and taught me how to think scientifically and to ask appropriate questions. Your enthusiasm has inspired me and I hope that I will have the same outlook in my future endeavours. I also thank Geoff Briggs for introducing me to biochemistry. Thanks to Carol, Lynda, Akeel, Jane, Tim, Stuart, Jing and Jing and to everyone else in C5. I have valued your knowledge and of course, your friendship. A big thank you to my family for supporting me throughout my education and having faith in me even when I did not. And finally to Christian, thanks for lots of hugs and support, and for living with me and my thesis!

Statement

The work presented here was carried out solely by the author (unless cited) during three years from September 2005 in the Institute of Genetics, University of Nottingham, whilst registered as a full-time PhD student. This thesis is comprised of original work, which has not been presented for examination in any other form. This research was supported by the MRC.

Whilst carrying out the work described in this thesis, I was fully aware of the hazards associated with the materials and techniques I was using, as advised in the Control of Substances Hazardous to Health regulations. The guidelines laid down in these regulations, and departmental rules, were adhered to at all times. I was also aware of, and followed, the regulations concerning the use and disposal of radioisotopes.

Table of Contents

Introduction

The human soma possesses stem cells, which give it the capacity to maintain tissues over time and thus, prolong life. However, the proliferation of stem cells has to be controlled since the capacity for renewal comes with the immense danger of malignant transformation. Cells are permanently accumulating genetic damage, and corruption of the mechanisms regulating and restricting proliferation can lead to cancer. Cells that have accumulated DNA damage beyond a certain threshold are normally eliminated (apoptosis) or placed in a state where division is prevented (senescence). Therefore, cells that are at risk of transforming into cancer cells are removed. However, the removal of stem cells will lead to a reduction of tissue maintenance and a change of the cellular environment, which are characteristics of ageing. Hence, damage prevention and repair are processes that increase longevity by reducing the potential of cells developing into cancer but also by keeping damage below the threshold that leads to cell removal and ageing (van Heemst *et al.* 2007).

My research has focussed on studies of how cells control the cell cycle and manage to achieve accurate genome duplication in the face of DNA damage. For my studies I have exploited the bacterium *Escherichia coli* as a model, where the machinery for DNA replication and repair has been extensively studied. Whilst prokaryotes such as *E. coli* have a single circular chromosome, eukaryotes have to organise replication of their multiple, linear chromosomes. However, despite their differences many similarities still exist such as the necessity to control the cell cycle, in particular the process of DNA replication. For example, although the details are different, parallels can be drawn between the general mechanisms that control replication initiation in *E. coli* and eukaryotes (Nielsen and Lobner-Olesen 2008). Multiple initiations at the same origin are restricted such that the genome is replicated only once in a cell cycle. The ability to make comparisons allows us to study a simpler, although still complex, organism and to consider larger questions such as the relationship between DNA damage and genomic instability. Genomic instability is a characteristic of cancer as well as ageing (Finkel *et al.* 2007).

Replication initiation in Escherichia coli

Replication of the *E. coli* chromosome is initiated at a single origin, named *oriC*, where two replication forks are set up and proceed to replicate the chromosome bi-directionally. Replication is initiated by the initiator protein DnaA, binding to sequences in *oriC* that are referred to as DnaA boxes. DnaA can form a complex with either ADP (adenosine diphosphate) or ATP (adenosine triphosphate). While both forms can bind to *oriC*, only the ATP-DnaA complex is active in initiation. When active DnaA binds to its boxes in *oriC*, it enables more ATP-DnaA to bind lower affinity boxes in the region. This cooperative binding to the origin promotes the unwinding of an AT-rich region which is stabilised in this open form by further binding of ATP-DnaA to boxes in the single-stranded region (reviewed by Messer 2002; Kaguni 2006). DnaA is the only protein specific to initiation in *E. coli* and the levels of DnaA available in the cell are critical in regulating the frequency of replication initiation (Lobner-Olesen *et al.* 1989).

Once the AT-rich region at *oriC* has been unwound, DnaA recruits two protein complexes each consisting of the hexameric DnaB helicase and the helicase loader DnaC ($DnaB_6$-$DnaC_6$). DnaB is the replicative helicase, it moves along the lagging strand template unwinding the parental DNA strands and allowing movement of the replication fork (Fang *et al.* 1999; Messer 2002). One DnaB hexamer is needed for each replication fork. Thus, at *oriC* two DnaB hexamers are loaded onto opposite strands with the assistance of DnaA and DnaC (Fang *et al.* 1999; Carr and Kaguni 2001). Once the helicases have been loaded, DnaC dissociates from the complex and the two helicases move past one another and begin to unwind the DNA (Fang *et al.* 1999). Further unwinding of the region allows DnaG (primase) to bind the DNA and create the RNA primers necessary to prime replication. Priming of replication allows the β-subunit (sliding clamp) of the replication complex and the replicative polymerase (polymerase III) to bind (Fang *et al.* 1999).

Once the replicative complexes, often referred to as replisomes, have fully assembled at *oriC*, they proceed to replicate the chromosome bi-directionally. The stages of replication initiation are illustrated in Figure 1.

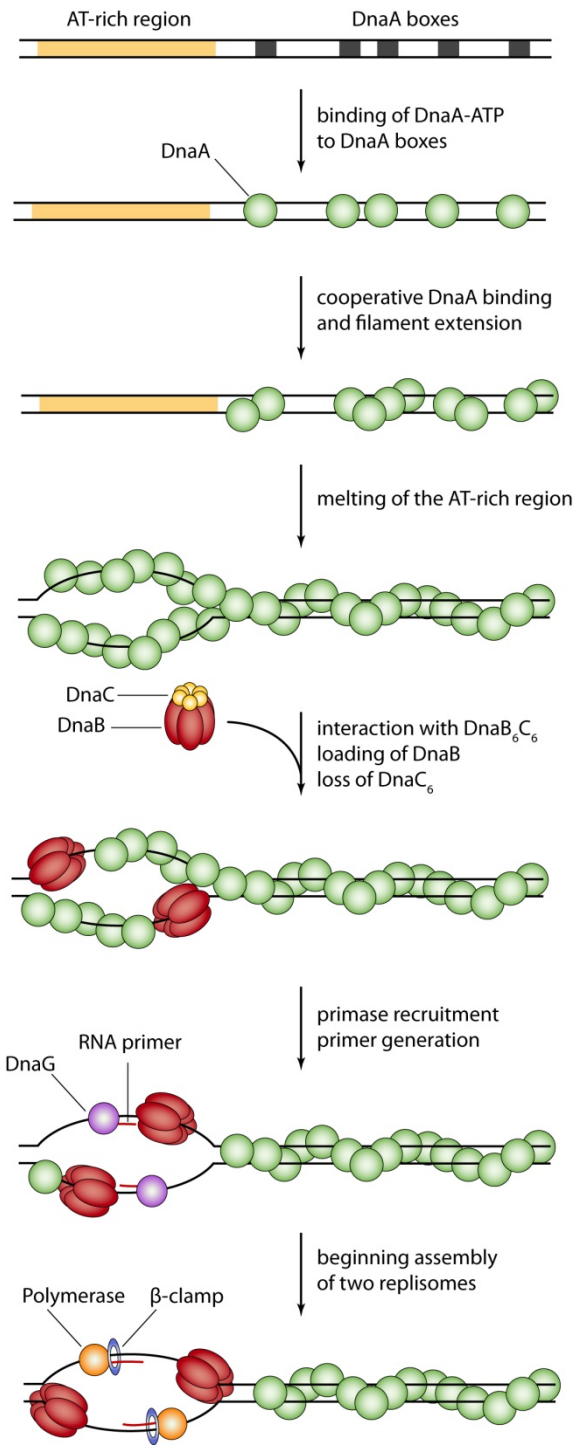

Figure 1. Initiation of replication at *oriC*.

Control of replication initiation in Escherichia coli

In all organisms it is critical that the entire genome is fully replicated before cell division occurs but also that it is replicated once and only once per cell cycle. If replication is allowed to initiate more than once per cell cycle, this re-replication can lead to genomic instability (reviewed by Arias & Walter (2007) and Blow & Gillespie (2008)). How is replication initiation limited to once per cell cycle?

Slow-growing *E. coli* have a simple cell cycle, consisting of three periods, B, C & D. After cell division when a new cell is born, there is a period of time leading up until initiation of replication, the B-period. The C-period consists of DNA replication, from initiation through to termination, lasting approximately forty minutes. Afterwards, the D-period is the time between replication termination and cell division. However, *E. coli* is capable of dividing at a rate faster than would be expected from the time taken for replication forks to move from the origin to the terminus. It does this by creating overlapping cell cycles, meaning that when the cells are growing fast the next cell cycle is initiated (by replication initiation, since there is no B-period) before the current cell cycle has ended (see review Haeusser and Levin 2008). This leads to the presence of multiple chromosomes within a cell and replication of these is normally initiated synchronously. Re-initiation at an origin is inhibited first of all by inactivating *oriC* for a period after initiation and secondly by reducing the availability of active DnaA. Thus, 'old' origins are initiated synchronously and after initiation they become distinctly recognisable to the cell as 'new' origins (newly replicated), which need to be inactivated for a period of time. During this period the levels of active DnaA available for initiation are reduced by titration to other regions of the chromosome, as well as by inactivating DnaA and reducing its transcription (see reviews (Boye *et al.* 2000; Messer 2002; Kaguni 2006; Nielsen and Lobner-Olesen 2008) and see below).

These control mechanisms combined prevent re-initiation of replication within a cell cycle, giving the cells time in which to replicate their chromosomes and allowing them to promote initiation of a new cell cycle only when they are ready to do so. When the cells do initiate replication, the multiple copies of *oriC* initiate synchronously in what has been suggested to be an initiation cascade, explained by the release of active DnaA from a newly replicated origin and its immediate binding to an old origin (Lobner-Olesen *et al.* 1994).

Origin sequestration

Dam methyltransferase targets GATC sites in the *E. coli* chromosome and methylates the adenine base at these sites. Newly replicated origins are recognisable because they contain multiple GATC sites which, after replication, are only methylated on the parental strand (hemi-methylated) (Boye *et al.* 2000; Messer 2002; Kaguni 2006; Nielsen and Lobner-Olesen 2008).

Generally Dam methyltransferase begins to methylate GATC sites immediately after a replication fork has passed. However, *oriC* and the promoter region of the *dnaA* gene remain hemi-methylated for a longer period of time, around one third of the cell cycle (Campbell and Kleckner 1990). Studies of initiation *in vivo* have shown that initiation does not occur at hemi-methylated origins (Russell and Zinder 1987). Interestingly this is not supported by *in vitro* studies (Landoulsi *et al.* 1989; Boye 1991), suggesting that there is something acting *in vivo* to specifically inactivate hemi-methylated origins. This inactivation is referred to as sequestration and is dependent upon a factor called SeqA (Lu *et al.* 1994). SeqA binds preferentially to hemi-methylated DNA (Slater *et al.* 1995) and delays re-methylation by Dam methyltransferase *in vitro* (Kang *et al.* 1999). SeqA might inhibit initiation by interfering with DnaA binding to low affinity sites at *oriC* (Nievera *et al.* 2006).

The level of Dam methyltransferase in cells influences the duration of the sequestration period (von Freiesleben *et al.* 2000). During this period, the potential of cells to initiate replication is reduced by additional mechanisms that act specifically upon DnaA and these are discussed below. Cells that are mutant for one of the various mechanisms often display phenotypes related to defects in replication initiation timing (Boye *et al.* 2000; Messer 2002; Kaguni 2006). For example, origin re-firing occurs in cells lacking SeqA (Lu *et al.* 1994; von Freiesleben *et al.* 1994; Boye *et al.* 1996) and the mutants form small colonies on rich media, have an increased doubling time and the cells are filamentous (Lu *et al.* 1994). These *seqA* mutant phenotypes are alleviated somewhat by growing the cultures in minimal media presumably because the reduction of growth rate also reduces the rate of initiation in these cells (Lu *et al.* 1994).

Reducing the availability of active DnaA

Controlling DnaA expression

Expression of *dnaA* is auto-regulated. The level of DnaA in the cell influences the level of expression of *dnaA* and other genes. DnaA is transcribed from two promoters and binding of DnaA to its own promoter region (both inactive and active DnaA) represses transcription. Active (ATP-bound) DnaA is a stronger repressor than the inactive form (Messer and Weigel 1997; Messer 2002).

Along with the ability of *dnaA* expression to be controlled by the level of DnaA itself, the promoter of *dnaA* is also bound by SeqA and sequestered in the same manner as *oriC*. This sequestration blocks transcription from the *dnaA* gene (Campbell and Kleckner 1990; Boye *et al.* 2000). Thus, whilst *oriC* is sequestered and unable to re-initiate, the promoter of *dnaA* is also sequestered meaning that no new DnaA can be synthesized during this period.

Inactivation of DnaA

During the sequestration period the levels of active ATP-DnaA within the cell are reduced by promoting the conversion to inactive ADP-DnaA by ATP hydrolysis. This mechanism is sometimes referred to as 'regulatory inactivation of DnaA' (RIDA) (Boye *et al.* 2000; Messer 2002; Kaguni 2006). Binding of the β-subunit (sliding clamp) to DNA during initiation stimulates ATP hydrolysis by DnaA, inactivating the initiator and rendering it unable to promote re-initiation of replication as the replication complex leaves *oriC* (Katayama *et al.* 1998).

There is evidence to suggest that replication stimulates inactivation of DnaA (Kurokawa *et al.* 1999). Since lagging strand synthesis requires loading of a β-subunit for every Okazaki fragment (see page 17, Pomerantz and O'Donnell 2007), the presence of multiple β-subunits during replication might continue to stimulate inactivation of DnaA. Inactivation of DnaA after initiation would appear to conflict with the idea of an initiation cascade where active DnaA is thought to be released from a newly replicated origin and can bind immediately to an old origin leading to synchronous initiation of all origins within a cell (Lobner-Olesen *et al.* 1994). However, as replication also stimulates inactivation of DnaA, it is possible that it is not inactivated immediately but over a period of time after initiation. This means that there could still be active DnaA available to

initiate any origins that have not yet initiated and the levels would be relatively high since the sequestration of origins would remove some of the potential DnaA binding sites.

Titration of DnaA to other locations

There are multiple DnaA binding sites around the chromosome of *E. coli*. One site in particular, named *datA*, seems to have the highest affinity for DnaA. It can bind about eight fold more DnaA than the region of *oriC* and its neighbouring gene *mioC* combined (Kitagawa *et al.* 1996). The *datA* region would be replicated whilst *oriC* is still sequestered and it has been suggested that its replication would create a sink for DnaA. It would be able to bind twice as much DnaA after its replication and therefore significantly reduce the levels of free DnaA within the cell (Kitagawa *et al.* 1998).

Replication initiation in eukaryotes

Since *E. coli* growing under optimal conditions have multiple albeit identical origins, that initiate synchronously, coordination of initiation in these cells can be compared to that of eukaryotes. Eukaryotes contain multiple chromosomes and replication is initiated at multiple origins spread along the length of these chromosomes. Although eukaryotes have a different genome organisation, they are still faced with the challenge of ensuring that their entire genome is replicated once, but only once per cell cycle. This means replication initiation has to be regulated at the numerous origins such that all of the chromosomes are replicated during S-phase (DNA synthesis phase of the cell cycle). I will briefly describe some of the mechanisms of regulation employed in eukaryotes in relation to those in *E. coli*. Eukaryotic replication and initiation are described in detail in many review articles (Weinreich *et al.* 2004; Arias and Walter 2007; Sclafani and Holzen 2007; Nielsen and Lobner-Olesen 2008).

Replication initiation in eukaryotes occurs in a series of steps, similar to those in prokaryotes. The first stage of initiation is the recognition of the replication origins by the binding of an initiation factor. In *E. coli* this factor is DnaA, and in eukaryotes the origins are bound by the origin recognition complex (ORC). DnaA binds to specific sequences of DNA (DnaA boxes) with varying degrees of affinity, whereas with the exception of budding yeast (*Saccharomyces cerevisiae*) there is no consensus DNA sequence for origin

recognition complexes in eukaryotes. It is possible that the chromatin structure around origin sites defines these sites as origins (Sclafani and Holzen 2007). In *E. coli*, origins fire synchronously whereas eukaryotic origins are different from one another, with some origins firing early in S-phase and some firing late and with varying degrees of efficiency in replicating the chromosome (some fire in almost every cell, others do not) (Weinreich *et al.* 2004).

Just as DnaA recruits the DnaB-DnaC complex to *oriC*, in eukaryotes ORC provides a site that allows loading of the MCM complex. The MCM complex is believed to be the replicative helicase in eukaryotes (Sclafani and Holzen 2007; Costa and Onesti 2008). This stage, at which the replicative helicase has been loaded (known as the pre-replicative complex) is often referred to as 'licensing'. Origin licensing occurs before S-phase of the cell cycle, during late mitosis and G1 phase (Arias and Walter 2007; Sclafani and Holzen 2007; Nielsen and Lobner-Olesen 2008).

In order to enter S-phase the helicase needs to be activated and the replisome complex must be loaded. This seems to be able to happen immediately in the case of *E. coli*. In eukaryotes this requires the activity of multiple proteins, in particular protein kinases which modify proteins by phosphorylation. Once this stage has occurred, replication forks proceed bi-directionally until they meet other forks or telomeric chromosome ends in the case of eukaryotes (Arias and Walter 2007; Sclafani and Holzen 2007; Nielsen and Lobner-Olesen 2008).

As discussed in the sections above there are several mechanisms acting in *E. coli* to prevent immediate re-initiation at newly replicated origins. Since eukaryotes contain multiple origins, it is necessary to turn off the origin licensing system before initiation to ensure that origins cannot reacquire the potential to fire during S-phase as this could lead to genomic instability (Arias and Walter 2007; Blow and Gillespie 2008).

Prevention of loading of the replicative helicase at an origin after initiation is the critical mechanism that prevents re-initiation and therefore re-replication in both prokaryotes and eukaryotes. Just as mechanisms act in *E. coli* to sequester *oriC* and reduce the availability of active DnaA, mechanisms in eukaryotes also regulate the activity of proteins involved in helicase loading at origins. The precise mechanisms vary from species to species but they act to achieve the same end, prevention of MCM re-loading during S- and G2-phases (Arias and Walter 2007; Sclafani and Holzen 2007; Blow and

Gillespie 2008; Nielsen and Lobner-Olesen 2008). There appears to be a link between some of these regulatory mechanisms and active DNA replication (Blow and Gillespie 2008; Nielsen and Lobner-Olesen 2008), providing a parallel with *E. coli* since DnaA inactivation is also linked with the loading of the replisome (the β subunit in particular). Although the general mechanisms of replication initiation have been conserved throughout evolution, the proteins that function in these processes have not. Therefore, bacterial studies do not provide information about the specific proteins involved, but about the general mechanisms of control that may be required. Replication initiation is tightly controlled in order to prevent chromosome under- or over-replication and therefore reduce the risk of genomic instability which in the case of humans can lead to cancer.

Replication elongation

Replication initiation ends with the assembly of two replisome complexes at an origin of replication which then proceed to replicate the chromosome bi-directionally. Many of the components of the replisome have already been mentioned above, but will be described briefly in order to explain how the replication forks proceed (Figure 2).

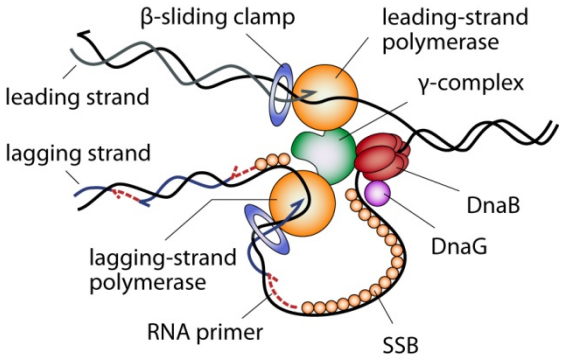

Figure 2. The *E. coli* replisome complex.

The replicative helicase DnaB encircles the lagging strand template and unwinds the parental duplex DNA as it moves along, allowing the polymerases to copy the template DNA. Progression of DnaB along the chromosome creates a fork-shaped DNA structure which is referred to as a replication fork. Each DNA polymerase is tethered to the template DNA by a β-subunit (sliding clamp) which encircles the template and slides

along it, increasing the processivity of the polymerase. Each β-subunit is loaded at a primer by the γ-complex (Pomerantz and O'Donnell 2007). DNA is antiparallel, meaning that the two strands within the duplex run in opposite directions to one another. DNA synthesis begins at the 3′-hydroxyl end of a primer. Replication of the leading strand is thought to be continuous from *oriC* until termination as its template is oriented such that it is replicated in the same direction as fork progression, suggesting there would be no need to re-prime synthesis. Although this has been confirmed by *in vitro* data, there is *in vivo* data suggesting that leading strand synthesis is discontinuous. Despite this, the idea of continuous leading strand synthesis is generally accepted (Wang 2005).

Since lagging strand synthesis occurs in the opposite direction to fork movement it is synthesised in a discontinuous manner. As shown in Figure 2, the lagging strand is synthesised in segments, each newly primed by DnaG and running in the opposite direction to leading strand synthesis. These segments are called Okazaki fragments and DnaG synthesizes a new RNA primer at the beginning of each fragment. The lagging strand template is thought to loop out from the replisome complex allowing the synthesis of the two strands to be coupled. This template loop is coated with single-stranded DNA binding protein (SSB). When the lagging strand polymerase meets the 5′ end of the previous Okazaki fragment, it dissociates from the template and is recruited to the newly synthesised Okazaki fragment primer and a new β-subunit. The Okazaki primers are degraded and the gaps filled in by DNA polymerase I. The Okazaki fragments are finally ligated to create a continuous, newly synthesised, lagging strand (Pomerantz and O'Donnell 2007).

Replication termination

In order to complete replication in *E. coli*, the two replication forks set up at *oriC* must travel around the chromosome until they meet each other. The process of forks meeting is termed replication termination (reviewed by Neylon *et al.* 2005). Studies of chromosomal replication had determined that replication terminates in the chromosomal region opposite *oriC*. By inserting a new origin into the chromosome and inactivating *oriC* using a *dnaA* mutant it was demonstrated that if the origin was situated nearer to the terminus region this did not change the location at which replication forks meet. However, when

bi-directional replication is set up from an origin nearer to the terminus region, one of the forks will enter this region much sooner than the fork moving in the opposite direction. This led to the suggestion that termination occurred in a particular area because fork movement in this region is inhibited (Kuempel *et al.* 1977; Louarn *et al.* 1977). Further experiments of this type narrowed down the locations of termination to specific termination sites, that are now called *Ter* sequences, and which act as polar inhibitors of replication (de Massy *et al.* 1987; Hill *et al.* 1987). The *Ter* sites are spread throughout the terminus region and let forks pass through in one direction but not the other. The positioning of *Ter* sites means that forks can enter the terminus region but not leave again. They create a replication fork trap (Neylon *et al.* 2005).

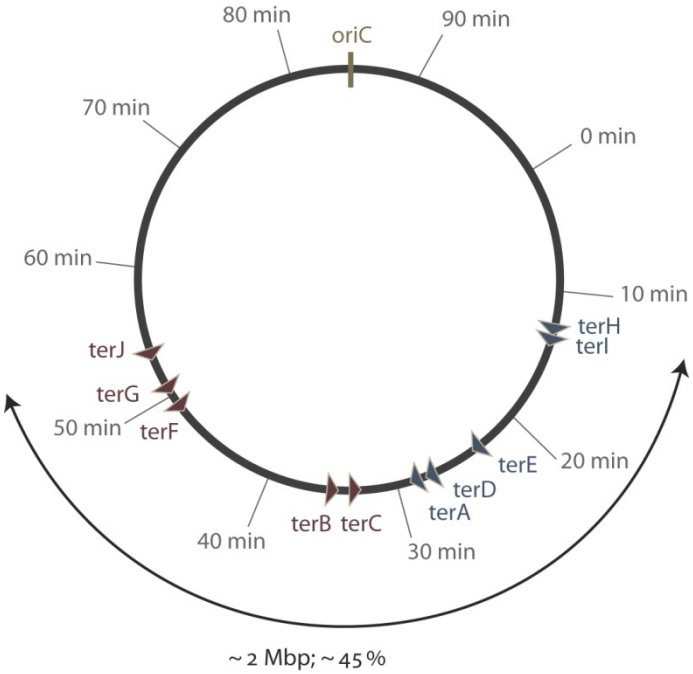

Figure 3. Map of *E. coli* chromosome.

Figure 3 shows a map of the *E. coli* chromosome and the locations of the 10 *Ter* sites that have now been identified (Neylon *et al.* 2005). These sites span approximately 45% of the chromosome, creating a broad zone in which termination can occur. Replication forks travelling clockwise around the chromosome pass through *TerH*, *TerI*, *TerE*, *TerD* and *TerA* but are blocked by *TerC*. Forks moving anti-clockwise pass through *TerJ*, *TerG*, *TerF*, *TerB*, and *TerC* but are blocked by *TerA*. Thus, the chromosome is divided in two, with each half replicated by only one of the forks initiated at *oriC*. If one fork is delayed on its

journey around the chromosome the other fork will pause in the termination zone and wait for it to arrive (Neylon *et al.* 2005). This would explain the existence of mechanisms that promote repair and restart of damaged or stalled replication forks (reviewed in McGlynn and Lloyd 2002; Michel *et al.* 2004; Heller and Marians 2006b; Rudolph *et al.* 2006; Michel *et al.* 2007). If one of the forks does not reach the terminus zone then replication of the chromosome will be incomplete and could lead to cell death (Sharma and Hill 1995). So how do *Ter* sites inhibit replication forks?

The *tus* gene is necessary for replication termination at the *Ter* sites (Hill *et al.* 1989). The gene encodes a protein, Tus, which binds to *Ter* sequences (Sista *et al.* 1989). The Tus-*Ter* interaction was shown to inhibit the action of the replicative helicase DnaB *in vitro*. This inhibition occurs only when the *Ter* sequence is in a particular orientation (Khatri *et al.* 1989; Lee *et al.* 1989). It was also shown that this interaction blocked replication forks *in vitro* (Lee *et al.* 1989; Hiasa and Marians 1994). This polar inhibition by Tus explains why forks moving in one direction can pass through *Ter* sites but not when moving in the opposite direction. The precise mechanism by which Tus is able to create a polar block was difficult to explain (Neylon *et al.* 2005), but recently the work of Mulcair *et al.* (2006) has demonstrated a difference in the ability of Tus to bind *Ter* when the DNA is unwound at one side or the other. DNA unwinding at the permissive side of Tus (the side that lets forks pass) led to rapid dissociation of Tus, whereas unwinding at the non-permissive face caused Tus to lock onto the DNA in a stable complex (Mulcair *et al.* 2006). However, another study has shown that unwinding is not necessary for polarity of the helicase block and suggests that protein-protein interactions between the helicase and Tus are also important (Bastia *et al.* 2008). In essence, the interaction of Tus-*Ter* and Tus with the helicase, forces forks to terminate replication within a specific region of the chromosome.

When a replication fork meets Tus-*Ter*, leading strand replication ends very close to the *Ter* site and it has been suggested that the replisome complex dissociates upon termination (Hill and Marians 1990). If the replisome dissociates when a fork terminates then the opposing replication fork should be able to converge with it. The Tus-*Ter* system does not prevent forks from meeting in the middle of the terminus zone, in between the *Ter* sites, before either fork has been blocked. It is not clear what happens when two forks meet away from Tus-*Ter*. As two replication forks converge, an excess of positive

supercoils would accumulate in front of the forks. It is assumed that this could slow these forks down and perhaps prevent them from meeting. A recent paper has suggested a mechanism dependent upon the combined efforts of RecQ helicase and topoisomerase III that may resolve converging forks, enabling termination of replication (Suski and Marians 2008).

What is the purpose of the replication fork trap?

Studies using ectopic *Ter* sites placed such that both replication forks would be blocked approximately halfway between *oriC* and the terminus zone led Bidnenko *et al.* (2002) to conclude that forks pause at Tus-*Ter* and are stable until the next round of replication. They suggested that the first forks remain paused at the ectopic *Ter* sites but the next round of replication forks copy until the end of the original forks creating linear DNA. Such a situation might occur naturally if one of the forks replicating the chromosome is substantially delayed on its route from *oriC* to the terminus zone, perhaps by DNA damage, an event which may be quite frequent and which is discussed later (page 23). Why would cells have a replication fork trap, if it can prevent the completion of chromosomal replication in the event of one of the forks stalling?

Studies of *E. coli* Δ*tus* mutants demonstrated that they were indistinguishable from wild type cells in respect of growth rate as well as sensitivity to DNA damage (Duggin *et al.* 2008). The biological importance of Tus-*Ter* termination is still not clear, but the presence of multiple *Ter* sites in *E. coli* and similar systems in other bacteria (for example, *Bacillus subtilis,* Neylon *et al.* 2005; Duggin *et al.* 2008) suggests that the system has a significant function.

As discussed in a review by Rudolph *et al.* (2007a), many bacterial genomes are organised such that most of the highly expressed genes are transcribed in the same direction as replication (Brewer 1988). Studies suggest that head-on collisions between replication forks and transcription complexes are particularly inhibitive of replication (French 1992; Mirkin and Mirkin 2005). The replication fork trap may have evolved to limit these events by ensuring that replication forks do not enter regions where transcription would be mostly head-on (Rudolph *et al.* 2007a). This general organisation of replication and transcription in the same direction is not seen in eukaryotes. However, in *S. cerevisiae* replication forks mostly move in a co-directional manner through a region

that contains ~200 copies of the highly transcribed ribosomal RNA genes. Forks moving in the opposite direction are stopped by a replication fork barrier at the end of the gene (Brewer and Fangman 1988; Rudolph *et al.* 2007a). Is the purpose of Tus-*Ter* simply to prevent forks progressing towards *oriC*?

As discussed earlier (page 12), there are several mechanisms acting to limit replication initiation to once per cell cycle as re-replication may lead to genomic instability. There are several studies suggesting that the role of Tus-*Ter* may be to prevent over-replication of the chromosome (reviewed in Mirkin and Mirkin 2007; Duggin *et al.* 2008). A study of *in vitro* replication using minichromosomes containing *oriC* and *TerB* sites found that Tus is required to prevent over-replication from occurring when two forks meet (Hiasa and Marians 1994). When Tus was present, replication was terminated at one or the other *Ter* site. One fork was blocked by Tus-*Ter* and this interaction stopped the other fork when it reached the same site. Over-replication occurred when two forks met in the absence of Tus. This over-replication was dependent upon DNA ligase (joins Okazaki fragments together). It was concluded that over-replication occurred when forks met because a replisome was capable of unwinding the 3'-end of the nascent leading strand of the opposing fork and that the polymerase switched from its original template to use the nascent leading strand instead. It was suggested that the purpose of Tus-*Ter* was to prevent over-replication rather than to ensure accurate termination (Hiasa and Marians 1994; Mirkin and Mirkin 2007; Duggin *et al.* 2008).

This suggestion was supported further by *in vivo* replication studies of the plasmid R1 which contains its own *Ter* sites. Krabbe *et al.* (1997) demonstrated that in the absence of Tus, replication of the plasmid does not terminate but leads to plasmid multimers, further replication via rolling-circle replication and a loss of stability of the plasmid. Recently, a study using flow cytometry has revealed that a fraction of cells in a Δ*tus* strain over-produce chromosomal DNA (Markovitz 2005). Thus, it appears that the function of Tus-*Ter* may be to prevent over-replication of the chromosome.

Replication forks travel some distance from *oriC* to the termination zone and there is a high likelihood that at least one of the forks will be delayed on its route to the terminus by one of the numerous impediments to replication that will be discussed in the following sections. Therefore, it is likely that one fork will be stalled at Tus-*Ter* before the

other fork has arrived in the region. However, if two forks should meet between the *Ter* sites, Tus-*Ter* might act to prevent any over-replication from proceeding out of this zone.

Replication termination in eukaryotes

Since eukaryotes have multiple replication origins (Weinreich *et al.* 2004; Sclafani and Holzen 2007), multiple replication forks traverse the chromosome and consequently there must be multiple sites at which forks meet. In contrast to *E. coli*, there do not appear to be specific sites at which forks meet in eukaryotes and little is known about termination of replication.

An imperfect DNA template

As has been mentioned above, in *E. coli* a replication fork might be delayed on its route to the terminus zone. The Tus-*Ter* system does not allow forks to easily pass through the terminus region, so if a fork is damaged and cannot reach the terminus region, part of the chromosome will remain un-replicated and this may result in cell death. The path between *oriC* and the terminus region is often corrupted, with estimates ranging from forks arresting in 15-50 % of cells in the absence of exogenous damaging agents (Cox *et al.* 2000; Maisnier-Patin *et al.* 2001). This means that a large proportion of the population has failed to maintain a perfect DNA template ahead of the replication fork.

How is the DNA template corrupted? The genome is under a constant threat from numerous agents that can damage DNA. Damaging agents can originate from within the cell (endogenous damage), such as oxygen species and from the environment (exogenous damage), such as UV light (Lindahl and Wood 1999). Prokaryotic and eukaryotic cells encode multiple repair systems that can deal with the damage (Friedberg *et al.* 2006). Although cells are equipped with repair mechanisms, they are not always able to clear the DNA template of all damage ahead of a replication fork. The different types of DNA damage and obstacles on the template will lead to different consequences if met by a replication fork. Along with chemical damage to the DNA, single-stranded gaps or nicks in the DNA and protein-DNA complexes also pose a threat to replication. If a replication fork were to meet a single-stranded gap in the template DNA and replicate to the edge of this gap, the fork would collapse creating a double-stranded DNA end (Kuzminov 1995),

which can be a toxic lesion (Helleday *et al.* 2007) and is a target for recombination enzymes. Increasing evidence suggests that recombinase activity (recombinases initiate recombination) is limited to when it is necessary in both prokaryotes (Flores *et al.* 2005; Mahdi *et al.* 2006) and eukaryotes (Krejci *et al.* 2003; Veaute *et al.* 2003). Recombination carries the risk of genetic rearrangements and recombination intermediates can delay chromosome segregation and cell division.

Protein-DNA complexes can be obstacles for replication and as in the examples mentioned previously, Tus-*Ter* complexes (page 18) and transcription complexes (page 21) can even block replication fork progression. DNA damage can cause RNA polymerases to stall. As discussed in a review by Rudolph *et al.* (2007a), the high number of transcription complexes moving on DNA means that the replisome is likely to meet a transcription complex stalled at a lesion. In highly transcribed regions this obstacle may actually be an array of stalled transcription complexes where the first complex is actually stalled at a lesion and blocks the rest. Several factors are proposed to prevent replication from encountering such blocks by either aiding the resumption of transcription or dislodging stalled complexes from the template (Trautinger *et al.* 2005).

My studies have focused largely on replication of a UV-irradiated DNA template. UV irradiation can lead to the formation of pyrimidine dimers and 6-4 photoproducts (in both cases, pyrimidine bases situated next to one another become covalently linked), which can block the replicative polymerase. Pyrimidine dimers, in particular T-T dimers, are thought to be the major DNA lesion induced by UV-irradiation (Friedberg *et al.* 2006). Hence, it is not surprising that multiple systems can repair or deal with these lesions. The process of photoreactivation in *E. coli* can reverse the joining of adjacent pyrimidines when certain wavelengths of light are shone onto the cell (Sancar 1996b; Sancar 2000; Beukers *et al.* 2008). The major repair pathway for pyrimidine dimers is nucleotide excision repair (NER), which can also repair a variety of different lesions (Sancar 1996a; Truglio *et al.* 2006). It is dependent upon several proteins that act together to recognise DNA lesions and cleave phosphodiester bonds of the damaged DNA strand, releasing an oligonucleotide and leaving a gap that can be filled in. In *E. coli*, UvrA dimers bind to UvrB forming a damage recognition complex that can recognise anomalies in DNA structure. UvrA facilitates tight binding of UvrB to the damaged DNA strand and then dissociates. The UvrB-DNA complex is recognised by UvrC. Binding of UvrC leads to

incision of the damaged strand either side of the damage. After incision UvrC dissociates from the DNA. The UvrD DNA helicase binds to the nicks created and unwinds the DNA, releasing the excised oligonucleotide. UvrB remains bound to the gapped DNA and is displaced as DNA polymerase I fills the gap. DNA ligase seals the end of the newly synthesised DNA, leaving an intact DNA template. During NER 12-13 nucleotides are excised and replaced (Sancar 1996a; Truglio *et al.* 2006).

Excision repair can be coupled to the process of transcription, which means that transcription can act as a scanning mechanism for DNA damage. If an RNA polymerase stalls at a lesion the complex is recognised by a transcription factor (Mfd) that can release the polymerase and recruit the UvrA-UvrB complex (Sancar 1996a; Hanawalt and Spivak 2008).

The importance of NER is illustrated by various human diseases associated with defective excision repair (Sancar 1995; Sancar 1996a; van Heemst *et al.* 2007). Xeroderma pigmentosum is caused by reduced levels of excision repair and individuals with the disease are sensitive to UV-irradiation and prone to skin cancers. Cockayne's syndrome is thought to be the result of defects related to transcription coupled repair, suggesting that the scanning of DNA by transcription is an important mechanism for recognition of damage. Individuals with this disease suffer from numerous symptoms including mental retardation as well as some overlapping symptoms with Xeroderma pigmentosum (Sancar 1995; Sancar 1996a; van Heemst *et al.* 2007). They also show features of premature ageing, which has been explained by the idea that transcription coupled repair removes cytotoxic lesions that would otherwise lead to apoptosis and cell death, contributing to ageing (van Heemst *et al.* 2007).

The entire genome must be duplicated in order for cells to survive. Since eukaryotes have multiple forks traversing the chromosome and no known termination zones, if one fork stalls it might not pose much of a risk to the cell because a fork coming from an adjacent origin can still converge with it. Any stalled or damaged replication forks in *E. coli* must be repaired and restarted in order for replication forks to reach the terminus zone (McGlynn and Lloyd 2002; Michel *et al.* 2004; Heller and Marians 2006b; Rudolph *et al.* 2006). Several models for the ability of replication forks to bypass lesions and for the repair of stalled or damaged replication forks are prominent in the literature and these are summarised in the following sections. Whereas a protein-DNA complex might block

the replicative helicase and therefore fork progression, single-stranded DNA lesions only block the replicative polymerase and thus, may not inhibit fork progression.

Lagging strand blocks can be bypassed

Although DNA lesions like pyrimidine dimers will block the replicative polymerases, it is generally accepted that this is not a problem for fork progression if the lesion is on the lagging strand template (see Meneghini and Hanawalt 1976 and reviews McGlynn and Lloyd 2002; Rudolph *et al.* 2006). As discussed above (page 17), the lagging strand is synthesised in Okazaki fragments. Each individual Okazaki fragment is newly primed by DnaG, the primase. Higuchi *et al.* (2003) used an *in vitro* replication system with purified replisome components and an *oriC* plasmid to study the effect of a lagging strand template lesion upon replication fork progression. They demonstrated that when the lagging strand polymerase stalls at a lesion only synthesis of that particular Okazaki fragment is blocked. Lagging strand synthesis continues at the next Okazaki fragment once it has been primed. Therefore, replication fork progression is not inhibited by lesions on the lagging strand template. A gap will be left in the nascent lagging strand opposite the lesion (Higuchi *et al.* 2003). Further *in vitro* experiments suggested that as the fork progresses accumulation of single-stranded DNA on the lagging strand template can lead to dissociation of the stalled lagging strand polymerase and recycling to a new primer (McInerney and O'Donnell 2004). If unrepaired, single-stranded DNA gaps can cause a replication fork to collapse and so must be filled in before the next round of replication (Kuzminov 1995).

It is possible that some gaps may be filled in by translesion polymerases (see page 30, Tippin *et al.* 2004). Most gaps are probably filled using a recombination mediated mechanism (Figure 4, for a review see Kreuzer 2005; Michel *et al.* 2007). In order for RecA, the *E. coli* recombinase, to catalyse recombination it needs to bind to the gapped DNA. Single-stranded DNA gaps will be coated by single-stranded DNA binding protein (SSB), which inhibits RecA binding. RecFOR mediates loading of RecA onto SSB-coated single-stranded DNA (Morimatsu and Kowalczykowski 2003). RecA proteins form a filament on the DNA which can invade a double-stranded DNA homologue. This strand invasion leads to pairing of the single-stranded DNA with its complementary strand in the duplex DNA. DNA synthesis using the double-stranded homologue as a template leads to repair

of the gap and results in the linkage of the two molecules by Holliday junctions (Kreuzer 2005; Michel *et al.* 2007). A Holliday junction is a four-stranded DNA junction that can be resolved by the action of RuvABC, the Holliday junction endonuclease, via cleavage of two strands at the branch point of the junction (Zerbib *et al.* 1998). After Holliday junction resolution the gap has been filled via strand exchange (Figure 4) and the lesion can now be repaired so that the template DNA is once again intact, ready for the next round of replication.

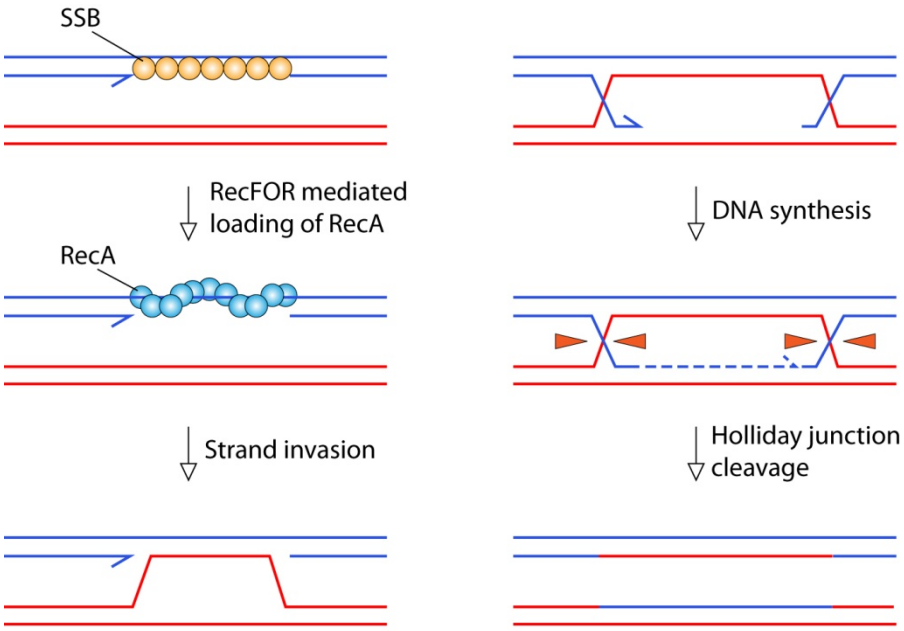

Figure 4. Recombination mediated gap repair. The sites of RuvABC cleavage are illustrated by orange arrowheads.

Thus, lesions blocking synthesis of the lagging strand can be bypassed and the gaps filled in later. However, the ability of the replisome to bypass leading strand template lesions remains a matter of contention.

Do lesions in the leading strand template block replication fork progression?

Rupp and Howard-Flanders (1968) proposed that the replication fork can also progress past leading strand template lesions. They studied the effects of UV irradiation on DNA replication in an excision repair defective (*uvrA*) mutant of *E. coli*. By using an excision defective strain and preventing photoreactivation, they ensured that the damage would

not be repaired. They observed that the rate of replication is reduced after UV irradiation and that the extent of this reduction was dependent upon the UV dose, i.e. the number of pyrimidine dimers induced in the template DNA. Analysis of the newly synthesised DNA showed that short fragments are synthesised after UV irradiation, and that they are subsequently converted into larger fragments over time. They interpreted the results as showing that the DNA contains gaps, which they assumed would be opposite lesions. A model was proposed, that pyrimidine dimers blocked DNA synthesis and that synthesis resumed downstream leaving gaps opposite the lesions with an estimated delay of only ten seconds per lesion (Figure 5). They suggested that these gaps could be filled in later by a RecA-mediated recombination reaction (Rupp and Howard-Flanders 1968), and in a later study they provided evidence that recombination does occur after UV irradiation of excision defective strains (Rupp *et al.* 1971). It was demonstrated that photoreversal of lesions promoted conversion of small DNA fragments to large fragments, leading to the suggestion that the gaps were situated opposite lesions (Bridges and Sedgwick 1974) and that lesions led to the appearance of gaps after UV irradiation.

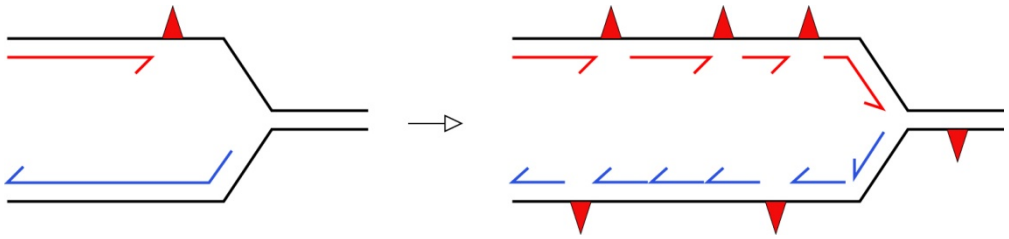

Figure 5. Model for replication restart: replication forks proceed past lesions. The lesions (red triangles) block synthesis by the polymerase. Synthesis is able to resume downstream leaving gaps in the nascent strands. 3' ends of the leading and lagging strands are shown by arrowheads.

Lesion bypass during leading strand synthesis is contrary to the widely accepted view of continuous leading strand synthesis. It was thought that leading strand synthesis can only be primed at *oriC*, probably as another level of control preventing initiation more than once per cell cycle. Lesion bypass and resumption of replication downstream of the block would require a new 3' end to prime further synthesis. Recently, Heller and Marians (Heller and Marians 2006a), have demonstrated that leading strand synthesis could be initiated *de novo* at fork structures, at least *in vitro*. Using fork substrates that represented blocked leading strands, they demonstrated that two different replication restart systems (dependent upon either PriC or PriA proteins) were able to load the

replicative helicase onto these substrates and that this was sufficient to induce priming of both the leading and lagging strands by DnaG primase (Heller and Marians 2006a). If such a system operates *in vivo*, it would enable replication forks to bypass lesions that block leading strand synthesis. Although this is an appealing idea (Heller and Marians 2006b; Langston and O'Donnell 2006; Lehmann and Fuchs 2006), such a system would require many recombination events to fill the gaps remaining in the DNA after replication.

Many studies have provided evidence that replication forks can, and do, stall in cells that are growing normally and in cells that have been exposed to damaging agents. Using an *in vitro* plasmid replication system with purified replisome components, Higuchi *et al* (2003) demonstrated that a lesion on the leading strand template causes a replication fork to stall. The lesion halted leading strand synthesis, however approximately two-thirds of the replication forks encountering this lesion were able to maintain lagging strand synthesis for approximately 1 kb beyond the lesion. This suggests that a replication fork may be able to progress past a lesion for some distance before stalling, resulting in a fork structure where the lagging strand has extended past the leading strand.

Indeed, Pages and Fuchs (2003) demonstrated that replication of the leading and lagging strands can become uncoupled when the fork meets a leading strand template lesion. Using an *in vivo* plasmid replication system they observed that when the leading strand is blocked, lagging strand synthesis can continue past the lesion. Replication of the leading strand was delayed for a substantial period, conflicting with the Rupp and Howard-Flanders model. This observation fits with data showing that the rate of DNA synthesis drops dramatically immediately after UV irradiation (Khidhir *et al.* 1985; Courcelle *et al.* 2005).

It is still unclear as to what exactly happens when the replisome meets lesions. Lagging strand blocks do not seem to stop fork progression but the consequences of leading strand blocks are controversial. In some instances the replisome may be able to prime synthesis downstream of the lesion leaving gaps that need to be repaired. However, as discussed above, there are numerous *in vitro* and *in vivo* studies that provide evidence that leading strand template lesions can disrupt the coupled synthesis of leading and lagging strands, and that they can cause significant delays to replication fork progression.

Replication restart pathways

Stalled replication forks may have various structures depending on the nature of the blocking lesion. For example a protein that is stably bound to the DNA, such as a stalled RNA polymerase, could block unwinding of the template DNA, whereas a damaged DNA base could block DNA synthesis by a polymerase (McGlynn and Lloyd 2002). Whatever the nature of the replicative block, the block needs to be removed or bypassed in order for replication to continue. In the case of a polymerase blocking lesion, unwinding of the template DNA prior to polymerase stalling and fork blockage will leave the lesion in single-stranded DNA, which repair enzymes cannot deal with. How can replication resume in such a situation? Several pathways for fork reactivation have been suggested, these involve either replicative bypass of the lesion or movement of the lesion into double-stranded DNA so that it can be repaired.

Lesion bypass by translesion synthesis

Translesion polymerases are capable of replicating past sites of DNA damage that would block the replicative polymerase. However, these translesion polymerases are error prone. They insert incorrect nucleotides (mismatches) into the DNA at a higher rate than the replicative polymerase and can also cause DNA deletions. In *E. coli* translesion polymerases are induced to higher levels of expression after DNA damage (see page 37), which may be a mechanism of limiting mutagenic repair to occasions when replication forks have stalled or when the genome is heavily damaged (Tippin *et al.* 2004). Courcelle and co-workers have demonstrated that translesion polymerase mutants have little effect on the rate of recovery of DNA synthesis after UV irradiation in *E. coli* (Courcelle *et al.* 2005). This suggests that error-prone lesion bypass by translesion polymerases is not the primary pathway for dealing with stalled forks.

Replication fork reversal

An alternative to translesion synthesis is to repair the blocking lesion, so that replication can resume avoiding the risk of error-prone synthesis. Several models have been proposed that describe pathways in which various recombination enzymes can act to aid the removal of replicative blocks and re-establish active replication forks. Higgins *et al.* (1976) suggested that branch migration of a stalled replication fork would allow the nascent strands to anneal to each other and the parental strands to re-anneal and form a

"chicken foot" structure (Figure 6). This structure is known as a Holliday junction and they observed such structures by electron microscopy after mammalian cells were treated with DNA damaging agents (Higgins *et al.* 1976). The formation of a Holliday junction would move the blocking lesion back into double-stranded DNA and would give repair enzymes an opportunity to repair the damage.

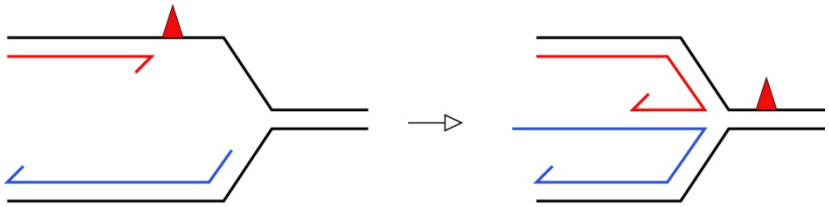

Figure 6. Replication fork reversal. Branch migration of the replication fork allows the nascent strands to anneal to each other and the parental strands to re-anneal. The lesion (red triangle) is moved back into double-stranded DNA. In this case the lagging strand has extended past the leading strand. 3' ends of the leading and lagging strands are shown by arrowheads.

In *E. coli*, arrest of replication due to inactivation of the replicative helicase has been shown to induce the formation of double-stranded DNA breaks in certain genetic backgrounds (Michel *et al.* 1997). Seigneur *et al.* (1998) proposed that these double-stranded DNA breaks result from the reversal of an arrested replication fork into a Holliday junction and its subsequent cleavage. They demonstrated that replication arrest no longer leads to double-stranded breaks in cells lacking the Holliday junction endonuclease. The idea of fork reversal leading to the formation of a Holliday junction has proven to be popular because it would allow re-modelling and potentially error-free repair of the stalled replication fork (McGlynn and Lloyd 2002; Kreuzer 2005; Rudolph *et al.* 2006).

Several enzymes in *E. coli* have been proposed to facilitate fork reversal into a Holliday junction structure because of both genetic and biochemical data. These enzymes are RecA (Seigneur *et al.* 2000; Robu *et al.* 2001), RuvAB (Seigneur *et al.* 1998; McGlynn and Lloyd 2001a) and RecG (McGlynn and Lloyd 2000). Lambert *et al.* (2005) demonstrated that recombination proteins associate with sites of fork stalling in yeast and that this can lead to genomic rearrangements. Several enzymes have recently also been proposed to perform fork reversal reactions in eukaryotes (Kanagaraj *et al.* 2006; Blastyak *et al.* 2007; Gari *et al.* 2008; Sun *et al.* 2008). It is unclear how often Holliday

junction structures arise from fork reversal in wild type cells, as the only way in which they have been visualised was in mutants in which replication was compromised (Seigneur *et al.* 1998) and in checkpoint mutants in yeast (Sogo *et al.* 2002). It is possible that fork reversal may simply be a transient event in wild type cells that is difficult to observe unless the ability to deal with such structures is compromised (Klein 2007).

Replication fork reversal and the formation of a Holliday junction would move the polymerase blocking lesion back into double-stranded DNA, enabling its repair. However, the replication fork structure needs to be re-formed so that replication can be restarted. Several mechanisms have been proposed that could lead to reconstitution of the fork structure. If replication fork progression continued whilst the leading strand polymerase was stalled and polymerase uncoupling led to an extended lagging strand (Higuchi *et al.* 2003; Pages and Fuchs 2003), the Holliday junction formed by fork reversal would have a tail consisting of double-stranded DNA with a single-stranded overhang. Any single-stranded DNA overhang could be digested by a single-stranded exonuclease, resulting in a Holliday junction with a double-stranded DNA tail (Figure 7, see (Viswanathan *et al.* 2001) and references therein for details of single-stranded exonucleases).

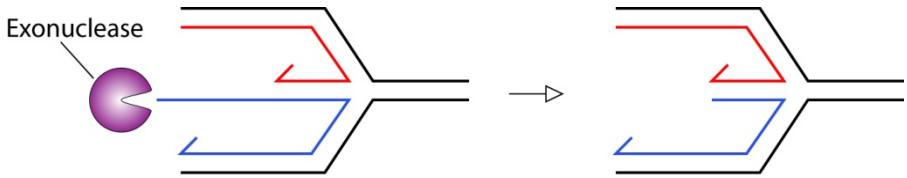

Figure 7. Exonuclease digestion of the extended lagging strand. 3' ends of the leading and lagging strands are shown by arrowheads.

RecBCD is a double-stranded DNA exonuclease (Dillingham and Kowalczykowski 2008) and it could target the double-stranded tail of a Holliday junction produced by fork reversal (Seigneur *et al.* 1998). If RecBCD digests the DNA right up to the junction the fork structure would be directly reformed (Figure 8a). Alternatively, branch migration of the reversed fork in the opposite direction would also re-form the fork structure. RecG is a double-stranded DNA translocase. It has been shown *in vitro* to unwind fork structures (McGlynn and Lloyd 2000) and Holliday junction substrates (Lloyd and Sharples 1993)

and it has been postulated that it could convert a Holliday junction back into a fork structure (Figure 8b, McGlynn and Lloyd 2000).

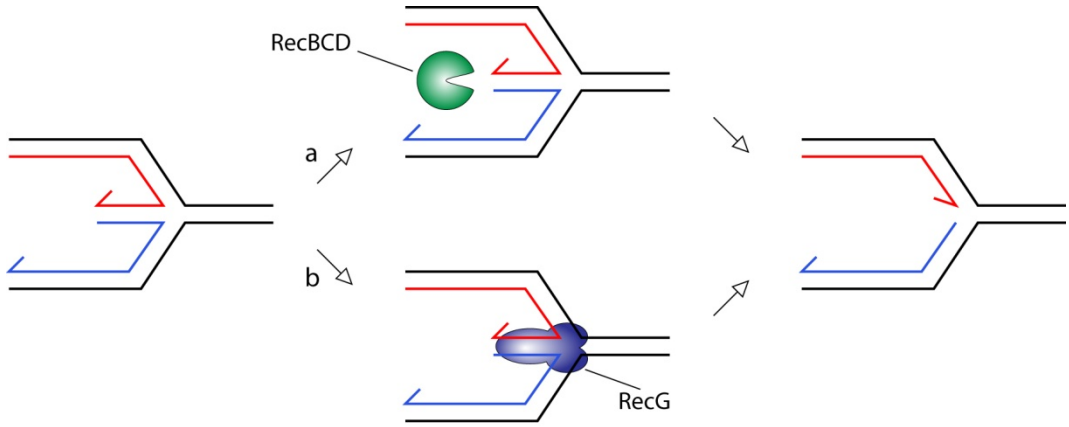

Figure 8. Direct resetting of the fork structure. (a) The double-stranded tail of the Holliday junction could be digested by RecBCD right up to the junction, re-forming the fork structure. (b) Alternatively branch migration of the junction, catalysed by a protein such as RecG, could convert the Holliday junction back into a fork structure. In both cases, the resulting structure is suitable for re-loading of the replisome. 3' ends of the leading and lagging strands are shown by arrowheads.

Instead of directly resetting the fork structure by degradation or branch migration, recombination could also lead to the formation a structure recognisable as a replication fork (reviewed in McGlynn and Lloyd 2002). RecBCD enzyme will not re-set the fork structure if it recognises a χ (Chi) sequence in the double-stranded tail of the reversed fork (Seigneur *et al.* 1998). Upon encountering a χ site RecBCD initiates recombination by preferentially digesting only one of the DNA strands and leaving a 3' single-stranded DNA overhang onto which RecA is loaded (Dillingham and Kowalczykowski 2008). RecA can catalyse invasion of the single-stranded 3' end into the homologous re-annealed parental strands, forming a D-loop (DNA-loop) (Cox 2007) and a second Holliday junction (Figure 9a). A D-loop is a target for the PriA-dependent restart system, which can re-load the replisome complex at certain fork structures (see page 36). Resolution of the Holliday junctions by RuvABC would separate the sister duplexes (Figure 9b,c), which is necessary for the chromosomes to segregate later at cell division.

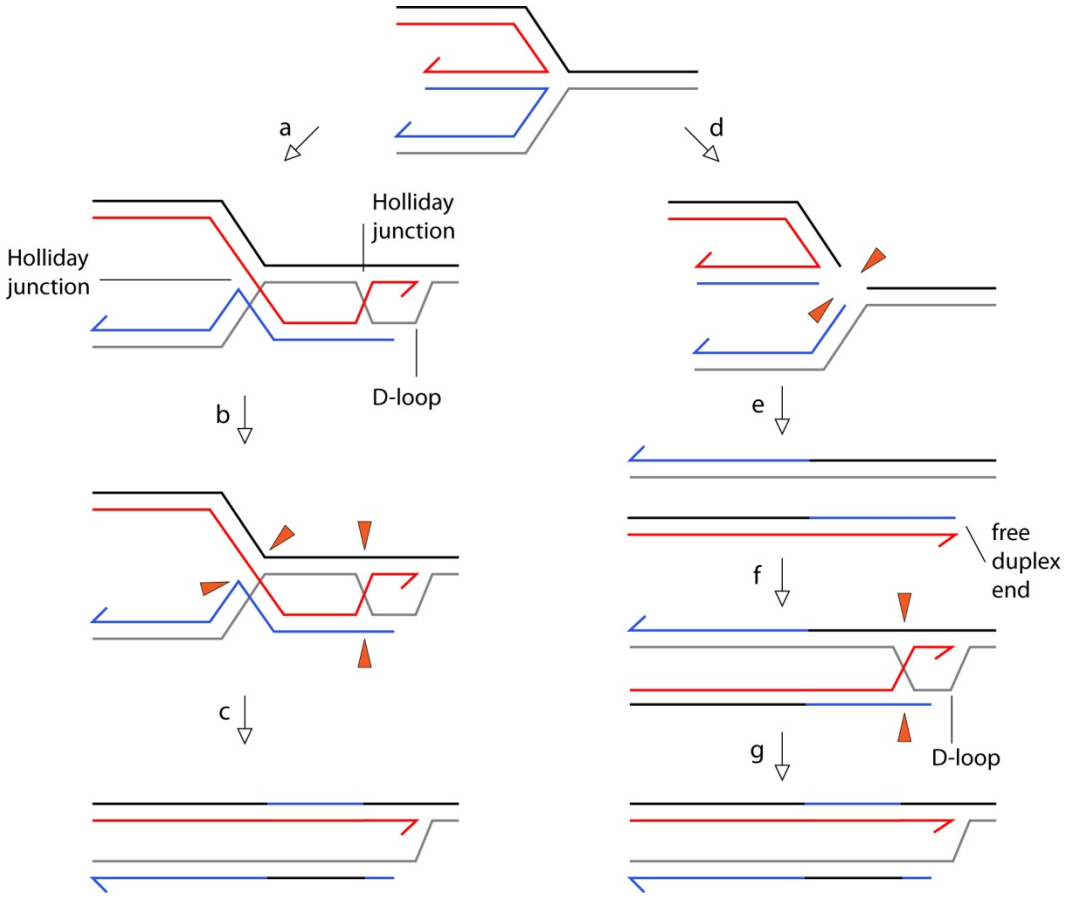

Figure 9. Re-forming a replication fork via recombination. (a) The double-stranded tail of the Holliday junction can invade the homologous re-annealed parental strands, forming a D-loop and a second Holliday junction. (b) Both Holliday junctions can be targeted by RuvABC and junction cleavage will result in a fork structure (c). (d) Alternatively, the Holliday junction formed by fork reversal could be cleaved immediately, releasing a double-stranded DNA end (e). (f) The double-stranded end could invade the duplex, forming a D-loop and a Holliday junction. Cleavage of the Holliday junction would result in a fork structure (g). The sites of RuvABC cleavage are illustrated by orange arrowheads. 3' ends of the leading and lagging strands are shown by arrowheads.

However, the RuvABC complex could cleave the junction created by fork reversal before any other processing occurs (Figure 9d, Seigneur *et al.* 1998; McGlynn and Lloyd 2000). Cleavage of the junction results in a free double-stranded DNA end (Figure 9e), which is one of the most toxic forms of DNA damage (Helleday *et al.* 2007). The double-stranded end would be targeted by RecBCD, which could initiate recombination. Recombination of this end with the chromosome would create a D-loop suitable for restarting replication (Figure 9f, Seigneur *et al.* 1998; McGlynn and Lloyd 2000). Again a Holliday junction would be formed that links the two sister duplexes together and requires resolution (Figure 9g). This second recombination pathway might increase the risk of illegitimate

recombination. By cleaving the Holliday junction initially and releasing a free double-stranded end, the ability of that end to move around the cell and recombine with another chromosomal region would be increased (McGlynn and Lloyd 2002). Seigneur *et al.* (1998) have proposed that RecBCD limits cleavage of the Holliday junction in *E. coli*, reducing the risk of illegitimate recombination.

Whilst replication fork reversal would enable the polymerase blocking lesion to be repaired, it was initially proposed that it would allow lesion bypass via a template switching reaction. Higgins *et al.* (1976) proposed that a fork, in which the lagging strand is extended past the blocked leading strand, could be reversed and that the lagging strand could then provide an alternative template for extension of the leading strand. If the Holliday junction is migrated back in the opposite direction a fork structure could be re-formed. Extension of the leading strand using an alternative template would enable it to bypass the lesion in an error-free manner and the fork can progress before the lesion has been repaired (Figure 10). Template strand switching is an appealing model but has not yet been demonstrated directly.

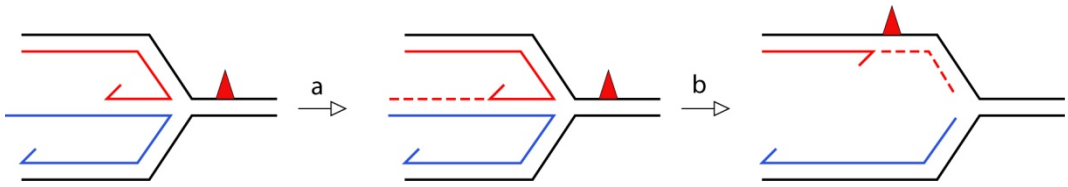

Figure 10. Replication restart by template strand switching. (a) The extended lagging strand could be used as an alternative template for leading strand synthesis. (b) Branch migration of the Holliday junction back into a fork structure, would result in a fork in which the leading strand has been extended past the lesion. 3' ends of the leading and lagging strands are shown by arrowheads.

RecA-mediated excision repair

Recently Bichara *et al.* (2007) proposed a mechanism that would enable the repair of a leading strand template lesion after fork stalling, without the need to reverse the replication fork. They suggested that the actions of RecFOR and RecA could facilitate nucleotide excision repair of such a lesion by promoting pairing of the damaged template DNA with an undamaged homologous sequence. This intermediate would move the lesion into double-stranded DNA and facilitate excision repair of the lesion. Disruption of the pairing after repair would leave a clear leading strand template enabling replication to restart (Bichara *et al.* 2007).

Replication restart depends on reloading of the replisome

If the replisome has been dismantled after fork stalling it must be reloaded in order for replication to restart. Since replication initiation is strictly controlled so that replisome loading occurs via a DnaA-dependent mechanism at *oriC*, the loading of the replisome complex at damaged forks must circumvent these control mechanisms. Consequently, replication restart is dependent upon the formation of specific fork structures that are recognised by the restart proteins. Upon recognising their substrates, the restart proteins PriA or PriC are able to reload the replicative helicase via a series of protein-protein interactions. Loading of the replicative helicase initiates the binding of the rest of the replisome complex. Whilst *priC* mutants have an almost wild type phenotype (Sandler *et al.* 1999), *priA* mutants suffer from slow growth and reduced viability and are sensitive to UV (Lee and Kornberg 1991; Kogoma *et al.* 1996), indicating that PriA-dependent loading of the replicative helicase is the primary restart pathway at least after UV irradiation. For a review of the various replication restart mechanisms refer to Heller and Marians (2006b).

Heller and Marians (2005) have demonstrated using *in vitro* substrates that PriA and PriC recognise and load the replisome at different structures. PriA requires the 3′ end of the leading strand to be present at the branch point of the fork. The ability to load DnaB via PriA is reduced by increasing the distance between the 3′ end and the branch point. However, restart via PriC does not require a leading strand to be present at the branch point of the fork. In fact, the ability of PriC to load DnaB is increased by increasing the size of the leading strand gap (Heller and Marians 2005). Thus, PriC can reload the replicative helicase and restart replication at forks with a leading strand gap (Figure 11b). Whereas PriA prefers fork substrates that have a leading strand 3′ end near to the branch point (Heller and Marians 2005) such as a D-loop (McGlynn *et al.* 1997; Liu *et al.* 1999), an R-loop (RNA-loop) (Masai *et al.* 1994) or a stalled fork that contains a nascent leading strand (Figure 11a, Gregg *et al.* 2002; Heller and Marians 2005).

The synthetic lethality of *priA* and *priC* mutations demonstrates the importance of replication restart systems, even in undamaged cells (Sandler 2000). The combined actions of recombination and DNA repair enzymes, specialised polymerases and restart proteins allow replication forks to be restarted after stalling and thus enable the completion of replication in the face of DNA damage.

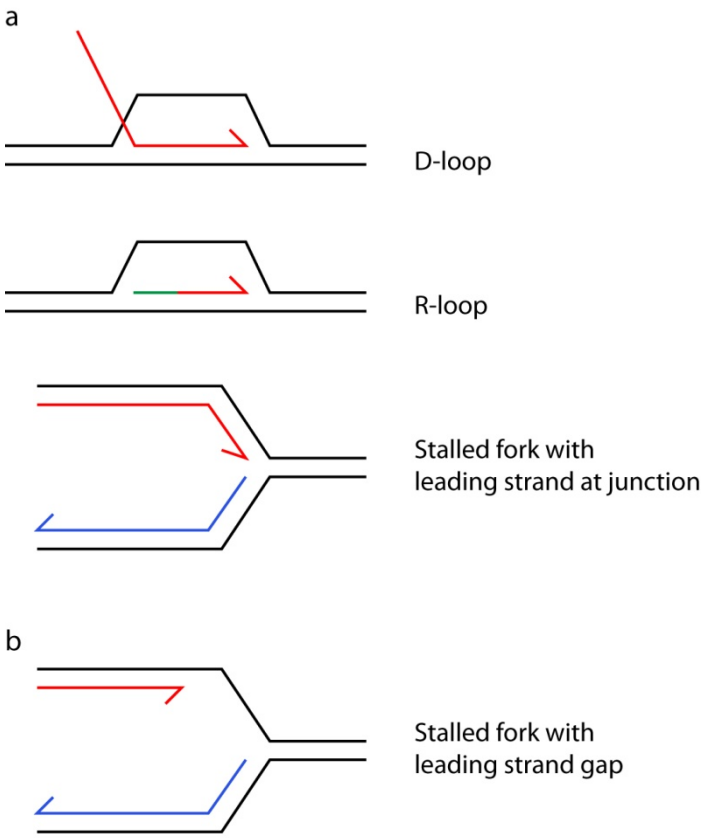

Figure 11. Replication restart structures. (a) The PriA-dependent restart pathway targets D-loops, R-loops (green strand represents RNA) and stalled fork structures with a leading strand at the junction. (b) The PriC-dependent restart pathway targets stalled fork structures with a leading strand gap at the junction. 3' ends of the leading and lagging strands are shown by arrowheads.

The SOS response

The activities of many proteins ensure that replication is completed each cell cycle. How does the cell ensure that all of the proteins necessary to facilitate replication are present when needed? Studies over the last 50 years (reviewed by Sutton *et al.* 2000; Janion 2001; Michel 2005; Schlacher and Goodman 2007) have led to the understanding of the DNA damage-inducible response, originally proposed by Miroslav Radman in 1970 (as reproduced in Bridges 2005), that leads to the up-regulation of more than forty genes (Courcelle *et al.* 2001). Many of the up-regulated genes are involved in DNA replication, recombination and repair. This response, referred to as the SOS response, allows bacteria to survive increased levels of DNA damage.

The SOS response is induced by a wide range of DNA-damaging agents. It has also been found that mutations of certain genes involved in DNA repair or replication can

lead to chronic SOS induction (Janion 2001). The SOS response has been studied extensively in *E. coli* and the following review articles have described aspects of the response previously (Sutton *et al.* 2000; Janion 2001; Michel 2005; Schlacher and Goodman 2007). The SOS response is controlled by the combined actions of LexA and RecA, which negatively and positively regulate the response, respectively. LexA is a repressor, which under normal cellular conditions binds to SOS boxes in the promoter regions of SOS-regulated genes. Binding of LexA reduces expression of genes to varying degrees depending on the affinity of LexA for a specific SOS box and the strength of the gene promoter. The inducing signal for the SOS response is single-stranded DNA bound by RecA. When the cells suffer DNA damage this leads to the accumulation of single-stranded DNA, either due to the formation of double-stranded DNA breaks and RecBCD degradation or as a result of polymerase uncoupling leading to regions of single-stranded DNA at or behind replication forks (Sutton *et al.* 2000; Janion 2001; Michel 2005; Schlacher and Goodman 2007). RecA is loaded onto single-stranded DNA by the actions of RecFOR at gapped DNA (Morimatsu and Kowalczykowski 2003), and RecBCD at double-stranded DNA ends (Dillingham and Kowalczykowski 2008). Thus, depending on the nature of the damage, an efficient SOS response requires the actions of RecFOR and/or RecBCD (Michel 2005). RecA forms a nucleoprotein filament when it is loaded onto single-stranded DNA which activates the co-protease activity of RecA, promoting self-cleavage of the LexA repressor. This leads to de-repression of the SOS-regulated genes (Sutton *et al.* 2000; Janion 2001; Michel 2005; Schlacher and Goodman 2007).

The SOS-regulated genes are not all induced at the same time. It is thought that the SOS response is divided into the early expression of genes involved in accurate repair processes and the late expression of error-prone repair genes (Tippin *et al.* 2004). The early expressed genes include *uvrA*, *uvrB* and *uvrD* that are involved in nucleotide excision repair, as well as LexA itself. The late expressed genes include those that encode the error-prone translesion polymerase V. It is thought that the temporal separation of expression of these genes allows nucleotide excision repair the chance to remove the damage that has blocked replication before the error-prone repair genes are expressed. This means that the SOS signals could be removed and the SOS-regulated genes repressed again by LexA before polymerase V is expressed and activated (Michel 2005;

Rudolph *et al.* 2006). Thus, error-prone repair is limited to situations where either the damage cannot be repaired or the level of damage is too high to be removed in time.

The induction of the SOS response after DNA damage enables *E. coli* cells to control the expression of proteins involved in repairing damage and restarting replication such that they are expressed at times of stress when they are most needed. The SOS response plays an important role in ensuring that replication forks can reach the terminus region and complete replication. It has also been shown to lead to the induction of DNA replication. Little is known about the nature or the purpose of this replication.

Stable DNA replication

In spite of the control mechanisms that act to limit replication initiation to once and only once per cell cycle, DNA damage can induce replication initiation in *E. coli* independently of DnaA and at sites away from *oriC*. This DNA damage inducible replication has been termed inducible stable DNA replication (iSDR). The name stable DNA replication refers to the fact that this replication, unlike *oriC*-initiated replication, is resistant to inhibition of protein synthesis. Inducible SDR is, in fact, independent of transcription. Induction of the SOS response is necessary to induce this replication and thus, any form of damage that elicits the SOS response leads to SDR. Tokio Kogoma was the major investigator of SDR and has written an extensive review of the subject (Kogoma 1997).

As discussed above, the restart proteins PriA and PriC enable the replicative helicase to be loaded at forked structures away from *oriC* (page 36). These restart pathways are necessary during the repair of stalled replication forks, however they could also allow the inappropriate priming of new replication forks at substrates that have not been formed by the processing of stalled forks. PriA protein is necessary for the induction of iSDR (Masai *et al.* 1994) and it is thought that iSDR might be initiated from recombination intermediates such as D-loops (Asai *et al.* 1993). It has been suggested that iSDR is initiated at a site within *oriC* and also at a site in the terminus region, however the mechanism that might lead to a recombination intermediate that can prime replication at a specific site is not yet understood (Kogoma 1997).

Strains of *E. coli* lacking RNase HI exhibit SDR, and this is referred to as constitutive stable DNA replication (cSDR) (Kogoma 1997). RNase HI specifically degrades the RNA from RNA:DNA hybrids (Stein and Hausen 1969; Hausen and Stein 1970), such as RNA-

loops (R-loops) where an RNA molecule has invaded duplex DNA and bound to its complementary DNA sequence. The level of replication induced in a strain lacking RNase HI is sufficient to maintain cell viability in *dnaA* mutants and in *oriC* deletion mutants (Kogoma and von Meyenburg 1983). Constitutive SDR is thought to be initiated at R-loops (von Meyenburg *et al.* 1987). This idea is supported by the fact that cSDR is observed in mutants lacking RNase HI, in which R-loops would be stabilised. RecA protein, which has been shown to promote the formation of R-loops *in vitro* (Kasahara *et al.* 2000), is necessary for cSDR (Torrey and Kogoma 1982), as is transcription (von Meyenburg *et al.* 1987) which would be required in order to create the invading RNA.

Strains lacking RecG exhibit cSDR and iSDR (without DNA-damaging treatment) (Hong *et al.* 1995). RecG can also unwind R-loops, at least *in vitro* (Vincent *et al.* 1996). The appearance of iSDR in cells lacking RecG is explained by the observation that these cells suffer from chronic SOS induction (Asai and Kogoma 1994). The absence of both RNase HI and RecG is lethal (Hong *et al.* 1995), suggesting that accumulation of R-loops has toxic consequences, possibly by leading to too much cSDR. Although SDR has been studied extensively, the nature of this replication i.e. whether it has a beneficial effect after SOS induction or is an evolutionary relic from a time when replication was less strictly controlled is still unclear (Kogoma 1997). These questions will be addressed further in this thesis.

Summary

In order for organisms to survive and reproduce they must faithfully duplicate their genomes. DNA replication is strictly controlled so that it occurs once and only once per cell cycle. It is assumed that re-replication resulting from uncontrolled initiation leads to genomic instability. However, the DNA template is often corrupted by DNA damage or other lesions and this can cause replication forks to stall. A stalled fork is a dangerous intermediate if unprotected, as enzymes within the cell may cleave this intermediate creating double-stranded DNA breaks. All studied organisms possess mechanisms that enable replication forks to be reconstituted and for the replication machinery including the replicative helicase to be re-loaded at these forks. Studies suggest that replication forks may undergo extensive processing before replication continues after DNA damage.

However, the issue is still under debate due to evidence that forks can bypass lesions leaving behind recombinogenic gaps and data that suggests that recombination proteins such as those that may be involved in fork reversal (RecG and RuvAB) are not required for restart of replication after DNA damage (Donaldson *et al.* 2004). The following questions are not fully answered: Do replication forks skip lesions on both the leading and lagging strand templates *in vivo*, and if so how often does this occur? How are stalled replication forks processed? Does stable DNA replication play an important role in genome synthesis after DNA damage?

In this thesis several approaches were taken in order to study the effect of DNA damage upon replication in *E. coli*. Various replication and repair mutants were used to analyse the effects of UV irradiation upon DNA synthesis and cell cycle progression. These studies have given further insight into the effect of DNA damage upon replication and have enabled me to address the questions posed above.

Materials and Methods

Materials

Chemicals & enzymes

Any specific chemicals used are detailed in the appropriate method. All restriction enzymes were purchased from New England Biolabs (NEB). DyNAzyme EXT DNA polymerase (from FINNZYMES) was purchased from NEB, as was *Taq* DNA polymerase. All buffers and solutions used are detailed in the appropriate methods.

Growth media & agar

Luria & Burrows (LB) medium

Broth: 1% bacto tryptone, 0.5% yeast extract, 0.05% sodium chloride, 0.002 M sodium hydroxide, pH~7.0. For agar, broth was dispensed in 300 ml portions and 1.5% agar added (4.5 g).

Mu medium

Broth: 1% bacto tryptone, 0.5% yeast extract, 1% sodium chloride, 0.002 M sodium hydroxide, pH~7.0. For agar, broth was dispensed in 300 ml portions and 1% agar added (3 g).

YT medium

Broth: 0.8% bacto tryptone, 0.5% yeast extract, 0.5% sodium chloride, 0.002 M sodium hydroxide, pH 7.2-7.4

2YT medium (for fermenter)

Broth: 1.6% bacto tryptone, 1% yeast extract, 0.5% sodium chloride

SOB broth

2% bacto tryptone, 0.5% yeast extract, 0.06% sodium chloride and 0.02% potassium chloride.

SOC broth

2 % bacto tryptone, 0.5 % yeast extract, 10 mM sodium chloride, 2.5 mM potassium chloride, 10 mM magnesium chloride, 10 mM magnesium sulphate and 20 mM glucose.

56/2 salts medium

56 salts: 155 mM potassium dihydrogen phosphate (KH_2PO_4), 245 mM disodium hydrogen orthophosphate (Na_2HPO_4), 3.2 mM magnesium sulphate ($MgSO_4 \cdot 7\ H_2O$), 60 mM ammonium sulphate ($(NH_4)_2SO_4$), 0.17 mM calcium nitrate ($Ca(NO_3)_2 \cdot 4\ H_2O$), 0.01 mM iron sulphate ($FeSO_4 \cdot 7\ H_2O$). For 56/2 salts dilute 56 salts 2-fold and add appropriate supplements. For 56/2 salts agar mix 250 ml of 56 salts (with required supplements) with 250 ml of molten 3 % minimal agar.

Davis medium

0.7 % dipotassium hydrogen phosphate (K_2HPO_4), 0.3 % potassium dihydrogen phosphate (KH_2PO_4), 0.1 % ammonium sulphate ($(NH_4)_2SO_4$), 0.05 % tri-sodium citrate ($Na_3C_6H_5O_7 \cdot 2\ H_2O$). After autoclaving add 0.01 % magnesium sulphate ($MgSO_4 \cdot 7\ H_2O$) and 0.4 % glucose.

Strains, Plasmids and Oligonucleotides

The strains, plasmids and oligonucleotides used during my studies are detailed in Table 1, Table 2, and Table 3 respectively. For strains and plasmids derived during this work, the construction of these is also described in the tables.

The RecG C-terminal deletion strains were constructed as follows. The relevant gene constructs for these deletions were cloned into a pT7-7 derivative (Table 2). The kanamycin resistance gene was cloned downstream of these *recG* mutant genes in order create pAU115 (*recGΔC5-kan*), pAU116 (*recGΔC10-kan*), pAU117 (*recGΔC15-kan*), pAU118 (*recGΔC20-kan*), pAU119 (*recGΔC25-kan*) and pAU120 (*recGΔC30-kan*) (Table 2). In the case of *recGΔC5-kan*, the C-terminal region of the mutant and the kanamycin resistance gene were amplified as one fragment using the primers GSB55 and ALU2. The PCR product was used to engineer the *recGΔC5-kan* allele onto the chromosome replacing the wild type *recG* allele, following the protocol of Datsenko & Wanner (2000) (see page 61). Primer ALU2 formed unspecific PCR products. In order to avoid this problem the other deletion mutants were engineered onto the chromosome using primers GSB55 and ALU3.

The wild type control for the C-terminal deletions, *recG-kan* was also cloned into a pT7-7 derivative by cloning the kanamycin resistance gene downstream of the full length *recG* gene in pAU121, creating pAU122. Unfortunately one of the primers used to create the full length *recG* sequence in pAU121 caused an erroneous nucleotide to be incorporated within the C-terminal region. However, the *recG-kan* allele was successfully engineered into the chromosome because the recombination event took place downstream of the nucleotide change. Thus, the *recG-kan* allele is a full length wild type *recG* gene with a kanamycin resistance gene inserted downstream. The position of the *kan* marker gene was checked via diagnostic PCR using primer pairs ALU4 & ALU5 and ALU6 & ALU7. The *recG* mutations were then confirmed by DNA sequencing.

Table 1. *Escherichia coli* K-12 strains

Strain	**Relevant Genotype**[a]	**Source**[a]
BW6164	*thr-43::*Tn*10*	CGSC
JC12337	*tnaA::*Tn*10*	A. J. Clark
NY171	*deo-41 dnaC7*	CGSC
RUC663	*tnaA::*Tn*10 dnaA46*	Tove Atlung
SS1791	*tnaA300::*Tn*10 dnaA167*	Steve Sandler
SS2241	*tnaA300::*Tn*10 dnaA204*	Steve Sandler
W3110 derivatives		
N3072	*recA269::*Tn*10*	(Mahdi *et al.* 2006)
AB1157 derivatives		
IL01	*att*Tn*7::lacO240::kan*	David J. Sherratt
IL04	*zdd/e::tetO240::gen att*Tn*7::lacO240::kan*	David J. Sherratt
N3793	*ΔrecG263::kan*	(Al-Deib *et al.* 1996)
N4452	*ΔrecG265::cat*	(Jaktaji and Lloyd 2003)
N4454	*ΔruvABC::cat*	(Jaktaji and Lloyd 2003)
BL21 derivatives		
STL5827	*F⁻ ompT hsdS* (r_B^- m_B^-) *dcm gal λDE3*	Susan Lovett
AU1115	*ΔrecG::apra*	P1.N6052 × STL5827 to Apra^r
AU1118	pLysS *ΔrecG::apra*	pLysS × AU1115 to Cm^r

N1141 derivatives

N1141	F⁻ *lacI3 lacZ118 metE70 leuB6 proC32 thyA54 deo(BC) malA38 ara-14 mtl-1 xyl-5 str-109 spc-15*	Low thymine requiring derivative of KB Low strain KL266
AU1068	*tnaA::*Tn*10 dnaA46*	P1.RUC663 × N1141 to Tc^r
AU1072	*tnaA::*Tn*10 dnaA46 ΔuvrA::apra*	P1.N6024 × AU1068 to $Apra^r$
AU1073	*thr-43::*Tn*10 dnaC7*	P1.N6594 × N1141 to Tc^r
AU1074	*tnaA::*Tn*10*	P1.JC12337 × N1141 to Tc^r
AU1075	*ΔuvrA::apra*	P1.N6024 × N1141 to $Apra^r$
AU1080	*dnaC7 deo(BC)*	P1.N1141 × AU1073 to Thr^+
AU1090	*tnaA::*Tn*10 dnaA46 ΔrecG263::kan*	P1.N3793 × AU1068 to Km^r
AU1093	*tnaA::*Tn*10 dnaA167*	P1.SS1791 × N1141 to Tc^r
AU1094	*tnaA::*Tn*10 dnaA204*	P1.SS2241 × N1141 to Tc^r
AU1106	*ΔrecG263::kan*	P1.N3793 × N1141 to Km^r
AU1110	*ΔrecO::kan*	P1.AM1746 × N1141 to Km^r
AU1112	*ΔrecO::kan tnaA::*Tn*10 dnaA46*	P1.RUC663 × AU1110 to Tc^r

MG1655 derivatives

MG1655	*F⁻ dnaC⁺ dnaA⁺ thr⁺ tnaA⁺ uvrA⁺ rec⁺ ruv⁺ rnhA⁺ pri⁺ lac⁺*	(Bachmann 1996)
AM1662	*ΔrecO::dhfr*	A. Mahdi and RGL, unpublished
AM1746	*ΔrecO::kan*	A. Mahdi and RGL, unpublished
AM1955	*ΔruvABC::apra*	A. Mahdi and RGL, unpublished
APS301	*att*Tn*7::lacO240::kan*	P1.IL01 × MG1655 to Km^r
APS345	*att*Tn*7::lacO240::kan zdd/e::tetO240::gen*	P1.IL04 × APS301 to Gen^r
AU1006	pJJ100 (*lac⁺ recG⁺*) *ΔlacIZYA ΔrecG::apra ΔrnhA::cat*	P1.N4704 × JJ1119 to Cm^r Ap^r
AU1012	pJJ100 (*lac⁺ recG⁺*) *ΔlacIZYA ΔrecG::apra ΔrnhA::cat recA269::*Tn*10*	P1.N3072 × AU1006 to Tc^r Ap^r
AU1017	pJJ100 (*lac⁺ recG⁺*) *ΔlacIZYA priA300 ΔrecG::apra ΔrnhA::cat*	P1.N4704 × JJ1078 to Cm^r Ap^r
AU1018	pAM383 (*recA⁺ lac⁺*) *ΔlacIZYA recA269::*Tn*10 ΔrnhA::cat*	P1.N4704 × N6121 to Cm^r Ap^r
AU1019	pAM383 (*recA⁺ lac⁺*) *ΔlacIZYA ΔrnhA::cat*	P1.N4704 × N6335 to Cm^r Ap^r
AU1020	pJJ100 (*lac⁺ recG⁺*) *ΔlacIZYA ΔrnhA::cat*	P1.N4704 × N6283 to Cm^r Ap^r

AU1032	pJJ100 (*lac*$^+$ *recG*$^+$) *ΔlacIZYA ΔrecG::apra recA269::*Tn*10*	P1.N3072 × JJ1119 to Tc^r Ap^r
AU1033	pJJ100 (*lac*$^+$ *recG*$^+$) *ΔlacIZYA priA300 ΔrnhA::cat*	P1.N4704 × JJ1076 to Cm^r Ap^r
AU1034	pJJ100 (*lac*$^+$ *recG*$^+$) *ΔlacIZYA recA269::*Tn*10*	P1.N3072 × N6283 to Tc^r Ap^r
AU1101	*att*Tn*7::lacO240::kan zdd/e::tetO240::gen ΔrecO::dhfr*	P1.AM1662 × APS345 to Tm^r
AU1120	pDIM113 (eYFP-RecG eCFP-SeqA) *ΔrecG263::kan*	pDIM113 × N4256 to Ap^r
AU1122	pDIM133 (eYFP-RecGΔwedge) *ΔrecG263::kan*	pDIM133 × N4256 to Ap^r
AU1150	pAU108 (eYFP-RecGΔC30) *ΔrecG263::kan*	pAU108 × N4256 to Ap^r
AU1157	pAU109 (eYFP-RecGCterm) *ΔrecG263::kan*	pAU109 × N4256 to Ap^r
AU1158	pAU110 (eYFP-RecGΔC5) *ΔrecG263::kan*	pAU110 × N4256 to Ap^r
AU1159	pAU111 (eYFP-RecGΔC10) *ΔrecG263::kan*	pAU111 × N4256 to Ap^r
AU1160	pAU112 (eYFP-RecGΔC15) *ΔrecG263::kan*	pAU112 × N4256 to Ap^r
AU1161	pAU113 (eYFP-RecGΔC20) *ΔrecG263::kan*	pAU113 × N4256 to Ap^r
AU1162	pAU114 (eYFP-RecGΔC25) *ΔrecG263::kan*	pAU114 × N4256 to Ap^r
AU1178	pAM390 (*lac*$^+$ *ruvABC*$^+$) *ΔlacIZYA ΔrnhA::cat*	P1.N4704 × N6254 to Cm^r Ap^r
AU1179	pAM390 (*lac*$^+$ *ruvABC*$^+$) *ΔlacIZYA ΔruvABC::apra*	P1.AM1955 × N6254 to Apra^r Ap^r
AU1181	pAM390 (*lac*$^+$ *ruvABC*$^+$) *ΔlacIZYA ΔruvABC::apra Δrnh::cat*	P1.N4704 × AU1179 to Cm^r Ap^r
AU1190	*ΔlacIZYA ΔrnhA::cat*	Plasmid free derivative of AU1178[b]
AU1191	*ΔlacIZYA ΔruvABC::apra*	Plasmid free derivative of AU1179[b]
AU1192	*ΔlacIZYA ΔruvABC::apra Δrnh::cat*	Plasmid free derivative of AU1181[b]
AU1194	*recGΔC5-kan*	This work[c]
AU1195	*recGΔC10-kan*	This work[c]
AU1196	*recGΔC15-kan*	This work[c]
AU1197	*recGΔC20-kan*	This work[c]
AU1198	*recGΔC25-kan*	This work[c]
AU1199	*recGΔC30-kan*	This work[c]
AU1200	*recGΔC5-kan*	P1.AU1194 × MG1655 to Km^r
AU1201	*recGΔC10-kan*	P1.AU1195 × MG1655 to Km^r
AU1202	*recGΔC15-kan*	P1.AU1196 × MG1655 to Km^r
AU1203	*recGΔC20-kan*	P1.AU1197 × MG1655 to Km^r
AU1204	*recGΔC25-kan*	P1.AU1198 × MG1655 to Km^r

AU1205	*recGΔC30-kan*	P1.AU1199 × MG1655 to Km^r
AU1210	pJJ100 (*lac$^+$ recG$^+$*) *ΔlacIZYA ΔrnhA::cat recGΔC5-kan*	P1.AU1194 × AU1020 to Km^r
AU1211	pJJ100 (*lac$^+$ recG$^+$*) *ΔlacIZYA ΔrnhA::cat recGΔC10-kan*	P1.AU1195 × AU1020 to Km^r
AU1212	pJJ100 (*lac$^+$ recG$^+$*) *ΔlacIZYA ΔrnhA::cat recGΔC15-kan*	P1.AU1196 × AU1020 to Km^r
AU1213	pJJ100 (*lac$^+$ recG$^+$*) *ΔlacIZYA ΔrnhA::cat recGΔC20-kan*	P1.AU1197 × AU1020 to Km^r
AU1214	pJJ100 (*lac$^+$ recG$^+$*) *ΔlacIZYA ΔrnhA::cat recGΔC25-kan*	P1.AU1198 × AU1020 to Km^r
AU1215	pJJ100 (*lac$^+$ recG$^+$*) *ΔlacIZYA ΔrnhA::cat recGΔC30-kan*	P1.AU1199 × AU1020 to Km^r
AU1216	*recG-kan*	This work[c]
AU1217	pJJ100 (*lac$^+$ recG$^+$*) *ΔlacIZYA ΔrnhA::cat recG-kan*	P1.AU1216 × AU1020 to Km^r
AU1218	*recG-kan*	P1.AU1216 × MG1655 to Km^r
AU1219	*recGΔC5-kan ΔruvABC::apra*	P1.AM1955 × AU1200 to Apra^r
AU1220	*recGΔC10-kan ΔruvABC::apra*	P1.AM1955 × AU1201 to Apra^r
AU1221	*recGΔC15-kan ΔruvABC::apra*	P1.AM1955 × AU1202 to Apra^r
AU1222	*recGΔC20-kan ΔruvABC::apra*	P1.AM1955 × AU1203 to Apra^r
AU1223	*recGΔC25-kan ΔruvABC::apra*	P1.AM1955 × AU1204 to Apra^r
AU1224	*recGΔC30-kan ΔruvABC::apra*	P1.AM1955 × AU1205 to Apra^r
AU1225	pJJ100 (*lac$^+$ recG$^+$*) *ΔlacIZYA recG-kan*	P1.AU1216 × N6283 to Km^r
AU1226	pJJ100 (*lac$^+$ recG$^+$*) *ΔlacIZYA recGΔC5-kan*	P1.AU1194 × N6283 to Km^r
AU1227	pJJ100 (*lac$^+$ recG$^+$*) *ΔlacIZYA recGΔC10-kan*	P1.AU1195 × N6283 to Km^r
AU1228	pJJ100 (*lac$^+$ recG$^+$*) *ΔlacIZYA recGΔC15-kan*	P1.AU1196 × N6283 to Km^r
AU1229	pJJ100 (*lac$^+$ recG$^+$*) *ΔlacIZYA recGΔC20-kan*	P1.AU1197 × N6283 to Km^r
AU1230	pJJ100 (*lac$^+$ recG$^+$*) *ΔlacIZYA recGΔC25-kan*	P1.AU1198 × N6283 to Km^r
AU1231	pJJ100 (*lac$^+$ recG$^+$*) *ΔlacIZYA recGΔC30-kan*	P1.AU1199 × N6283 to Km^r
AU1232	*recG-kan ΔruvABC::apra*	P1.AM1955 × AU1218 to Apra^r
JJ1017	pJJ100 (*lac$^+$ recG$^+$*) *ΔlacIZYA ΔrecG265::cat*	pJJ100 × N5742 to Ap^r
JJ1060	*ΔlacIZYA priA300*	Plasmid free derivative of N5933[b]
JJ1075	*ΔlacIZYA priA300 ΔrecG::apra*	P1.N6052 × JJ1060 to Apra^r
JJ1076	pJJ100 (*lac$^+$ recG$^+$*) *ΔlacIZYA priA300*	pJJ100 × JJ1060 to Ap^r
JJ1078	pJJ100 (*lac$^+$ recG$^+$*) *ΔlacIZYA priA300 ΔrecG::apra*	pJJ100 × JJ1075 to Ap^r

JJ1119	pJJ100 (*lac*$^+$ *recG*$^+$) *ΔlacIZYA ΔrecG::apra*	P1.N6052 × JJ1017 to Apra^r Ap^r
N4256	*ΔrecG263::kan*	(Mahdi *et al.* 2006)
N4280	*uvrA277::*Tn*10*	RGL, unpublished
N4560	*ΔrecG265::cat*	(Mahdi *et al.* 2006)
N4583	*ΔruvABC::cat*	(Jaktaji and Lloyd 2003)
N4704	*ΔrnhA::cat*	RGL, unpublished
N4971	*ΔrecG263::kan ΔruvABC::cat*	P1.N4454 × N4256 to Cm^r
N5742	*ΔlacIZYA ΔrecG265::cat*	P1.N4452× TB28 to Cm^r
N5933	pAM374 (*priA*$^+$ *lac*$^+$) *ΔlacIZYA priA300*	(Mahdi *et al.* 2006)
N6024	*ΔuvrA::apra*	RGL, unpublished
N6052	*ΔrecG::apra*	RGL, unpublished
N6121	pAM383 (*recA*$^+$ *lac*$^+$) *ΔlacIZYA recA269::*Tn*10*	(Mahdi *et al.* 2006)
N6254	pAM390 (*lac*$^+$ *ruvABC*$^+$) *ΔlacIZYA*	pAM390 × TB28 to Ap^r
N6283	pJJ100 (*lac*$^+$ *recG*$^+$) *ΔlacIZYA*	pJJ100 × TB28 to Ap^r
N6310	*ΔlacIZYA ΔruvABC::cat rus-2*	(Mahdi *et al.* 2006)
N6329	pAM390 (*lac*$^+$ *ruvABC*$^+$) *ΔlacIZYA ΔruvABC::cat rus-2*	pAM390 × N6310 to Ap^r
N6335	pAM383 (*recA*$^+$ *lac*$^+$) *ΔlacIZYA*	pAM383 × TB28 to Ap^r
N6594	*dnaC7 thr-43::*Tn*10*	P1.BW6164 × RCe79 to Tc^r
N7253	pAM390 (*lac*$^+$ *ruvABC*$^+$) *ΔlacIZYA rus-2 ΔruvABC::apra*	P1.AM1955 × N6329 to Apra^r Ap^r
N7256	pAM390 (*lac*$^+$ *ruvABC*$^+$) *ΔlacIZYA rus-2 ΔruvABC::apra ΔrnhA::cat*	P1.N4704 × N7253 to Cm^r Ap^r
RCe79	*dnaC7*	P1.NY171 × RCe98 to Thr$^+$
RCe98	*thr-43::*Tn*10*	P1.BW6164 × MG1655 to Tc^r
RCe120	*dnaC7 uvrA277::*Tn*10*	P1.N4280 × RCe79 to Tc^r
RCe190	*dnaC7 ΔrecO::kan*	P1.AM1746 × RCe79 to Km^r
TB28	*ΔlacIZYA<>frt* (Km^s)	(Bernhardt and de Boer 2004)[d]

[a]The abbreviations, *kan, cat, apra, dhfr* and *gen* refer to insertions conferring resistance to kanamycin (Km^r), chloramphenicol (Cm^r), apramycin (Apra^r), trimethoprim (Tm^r) and gentamycin (Gen^r), respectively. Tn*10* confers resistance to tetracycline (Tc^r). Ap^r refers to ampicillin resistance. Strains carrying *dnaA46, dnaA167, dnaA204* or *dnaC7* are temperature-sensitive for growth. CGSC: Coli Genetic Stock Center, Yale University.

[b]Plasmid free derivatives were identified as white colonies on LB agar supplemented with X-Gal and IPTG.

[c]For detailed information of the *recG* deletion constructs see page 43. The original recombinant strains were used as P1 donors only.

[d]Abbreviated to *ΔlacIZYA* in derivatives.

Table 2. Plasmids used

Plasmid	Description[a]	Source[a]
pBAD24 derivatives		
pAU108	eYFP-RecGΔC30	The *Kpn*I-*Hin*dIII fragment from pAU107 was cloned between the *Kpn*I and *Hin*dIII sites of pDIM071.
pAU109	eYFP-RecGCterm	The last 47 codons of *recG* were amplified using primers that added *Bsr*GI site at 5′ end (ALU1) and *Hin*dIII site at 3′ end (GSB64). The PCR product was cloned between the *Bsr*GI and *Hin*dIII sites of pDIM071.
pAU110	eYFP-RecGΔC5	The *Kpn*I-*Hin*dIII fragment from pAU102 was cloned between the *Kpn*I and *Hin*dIII sites of pDIM071.
pAU111	eYFP-RecGΔC10	The *Kpn*I-*Hin*dIII fragment from pAU103 was cloned between the *Kpn*I and *Hin*dIII sites of pDIM071.
pAU112	eYFP-RecGΔC15	The *Kpn*I-*Hin*dIII fragment from pAU104 was cloned between the *Kpn*I and *Hin*dIII sites of pDIM071.
pAU113	eYFP-RecGΔC20	The *Kpn*I-*Hin*dIII fragment from pAU105 was cloned between the *Kpn*I and *Hin*dIII sites of pDIM071.
pAU114	eYFP-RecGΔC25	The *Kpn*I-*Hin*dIII fragment from pAU106 was cloned between the *Kpn*I and *Hin*dIII sites of pDIM071.
pDIM071	eYFP-RecG	Tim Moore. *recG* was amplified from pIM02 encoding RecG with an N-terminal linker[b], using primers that introduced *Bsr*GI site at 5′ end and *Xba*I site at 3′ end. The PCR product was cloned between the *Bsr*GI and *Xba*I sites of pLau18.
pDIM083	eCFP-SeqA	Tim Moore. *seqA* was amplified using primers that introduced *Bsr*GI site at the 5′ end and *Xba*I site at 3′ end. The PCR product was cloned between the *Bsr*GI and *Xba*I sites of pLau17.
pDIM113	eYFP-RecG eCFP-SeqA	Tim Moore. The *Nhe*I-*Hin*dIII fragment from pDIM083 was cloned between the *Xba*I and *Hin*dIII sites of pDIM071.

pDIM133	eYFP-RecGΔwedge	Tim Moore. *recGΔwedge* was amplified from pGB010 with primers that added an N-terminal linker region[b] and *Bsr*GI site at 5′ end and *Xba*I site at 3′ end. The PCR product was cloned between the *Bsr*GI and *Xba*I sites of pLau18.
pDIM141	*kan*^{r}	Tim Moore, unpublished plasmid. The kanamycin resistance cassette is encoded within the *Hin*dIII fragment of this vector. The *kan*^{r} gene is flanked by FRT sites.
pLau17	eCFP	(Lau *et al.* 2003)
pLau18	eYFP	(Lau *et al.* 2003)
pLau53	LacI-eCFP TetR-eYFP	(Lau *et al.* 2003)
pRC7 derivatives		
pAM374	*priA*$^+$	(Mahdi *et al.* 2006)
pAM383	*recA*$^+$	(Mahdi *et al.* 2006)
pAM390	*ruvABC*$^+$	(Mahdi *et al.* 2006)
pJJ100	*recG*$^+$	(Mahdi *et al.* 2006)
pT7-7 derivatives		
pAU102	RecGΔC5	The C-terminal region of *recG* was amplified from pQW120. The 5′ primer bound to the *Pst*I site within *recG* (GSB55). The 3′ primer specified the size of the C-terminal deletion and added a *Hin*dIII site (GSB56).
pAU103	RecGΔC10	The C-terminal region of *recG* was amplified from pQW120. The 5′ primer bound to the *Pst*I site within *recG* (GSB55). The 3′ primer specified the size of the C-terminal deletion and added a *Hin*dIII site (GSB57).
pAU104	RecGΔC15	The C-terminal region of *recG* was amplified from pQW120. The 5′ primer bound to the *Pst*I site within *recG* (GSB55). The 3′ primer specified the size of the C-terminal deletion and added a *Hin*dIII site (GSB58).
pAU105	RecGΔC20	The C-terminal region of *recG* was amplified from pQW120. The 5′ primer bound to the *Pst*I site within *recG* (GSB55). The 3′ primer specified the size of the C-terminal deletion and added a *Hin*dIII site (GSB59).

pAU106	RecGΔC25	The C-terminal region of *recG* was amplified from pQW120. The 5′ primer bound to the *Pst*I site within *recG* (GSB55). The 3′ primer specified the size of the C-terminal deletion and added a *Hin*dIII site (GSB60).
pAU107	RecGΔC30	The C-terminal region of *recG* was amplified from pQW120. The 5′ primer bound to the *Pst*I site within *recG* (GSB55). The 3′ primer specified the size of the C-terminal deletion and added a *Hin*dIII site (GSB61).
pAU115	*recGΔC5-kan*	The *Hin*dIII fragment (*kan*^{r} cassette) from pDIM141 was cloned into the *Hin*dIII site of pAU102.
pAU116	*recGΔC10-kan*	The *Hin*dIII fragment (*kan*^{r} cassette) from pDIM141 was cloned into the *Hin*dIII site of pAU103.
pAU117	*recGΔC15-kan*	The *Hin*dIII fragment (*kan*^{r} cassette) from pDIM141 was cloned into the *Hin*dIII site of pAU104.
pAU118	*recGΔC20-kan*	The *Hin*dIII fragment (*kan*^{r} cassette) from pDIM141 was cloned into the *Hin*dIII site of pAU105.
pAU119	*recGΔC25-kan*	The *Hin*dIII fragment (*kan*^{r} cassette) from pDIM141 was cloned into the *Hin*dIII site of pAU106.
pAU120	*recGΔC30-kan*	The *Hin*dIII fragment (*kan*^{r} cassette) from pDIM141 was cloned into the *Hin*dIII site of pAU107.
pAU121	RecGW683G	Full length C-terminus sequence of *recG* was amplified from pAU115 using primers GSB55 and ALU8. ALU8 should add back the last 5 amino acids of the *recG* sequence. PCR using ALU8 incorporates an erroneous nucleotide resulting in the amino acid change W683G. The PCR product was cloned between the *Pst*I and *Hin*dIII sites of pAU102.
pAU122	*recG*$_{W683G}$*-kan*	The *Hin*dIII fragment (*kan*^{r} cassette) from pDIM141 was cloned into the *Hin*dIII site of pAU121.
pGB010	RecGΔwedge	(Briggs *et al.* 2005)
pQW120	RecGF96A,97A	(Briggs *et al.* 2005)
pQW145	RecGQ640R	(Briggs *et al.* 2004)

[a]The relevant description of plasmids and either the source (including construction) or reference for the plasmid is given. PCR primers can be found listed in the oligonucleotide table (Table 3).

[b]The N-terminal linker was based on the sequence of the region that links the DNA binding domain of *Thermotoga maritima* RecG to an extra N-terminal domain. The amino acid sequence of the linker is: MELYLIDYLEC.

Table 3. Oligonucleotides used

Oligonucleotide	Sequence 5′-3′
ALU1	gct tgt aca aag tgg cgg att tac tgc g
ALU2	cgg cag gaa ggt agg gta acc tga aat ggc ggt ctt ctc act gcc gcc tta agc ttg aag ttc cta tac ttt cta g
ALU3	cgg cag gaa ggt agg gta acc tga aat ggc ggt ctt ctc act gcc gcc ttc tca tgt ttg aca gct tat cat cg
ALU4	gga agc tac ctg gga aga gt
ALU5	cgc tac ctt tgc cat gtt tca ga
ALU6	gcc gat ttt tgc cgg tta acc ga
ALU7	gct cag gcg caa tca cga atg aa
ALU8	cat aaa gct tac gca ttc cag taa cgt tcc gtc tcc ggc atc ca
GSB55	gga tga aac ctg cag aga aac agg
GSB56	cat aaa gct tat tcc gtc tcc ggc atc cag c
GSB57	cat aaa gct tac cag cgt tct atc agg gc
GSB58	cat aaa gct tag gct ttt gcc tgt tgt ggg
GSB59	cat aaa gct tat ggg taa cgt tcg tga ata tgg c
GSB60	cat aaa gct taa ata tgg cgt gcc agg cg
GSB61	cat aaa gct tag cgc tga act tcc ggg atc
GSB64	cca tac caa acg acg agc gtg aca cc
5′ mioC	aca ggt aat cac cgt gct caa ca
3′ mioC	tca cca tat cgt tca gag agg ca
MW12	gtc gga tcc tct aga cag ctc cat gat cac tgg cac tgg tag aat tcg gc
MW14	caa cgt cat aga cga tta cat tgc tac atg gag ctg tct aga gga tcc ga
PM17	tag caa tgt aat cgt cta tga cgt t
RGL13	gac gct gcc gaa ttc tgg ctt gct agg aca tct ttg ccc acg ttg acc c
RGL14	tgg gtc aac gtg ggc aaa gat gtc cta gca atg taa tcg tct atg acg tt
RGL15	caa cgt cat aga cga tta cat tgc tag gac atg ctg tct aga gac tat cga
RGL16	Atc gat agt ctc tag aca gca tgt cct agc aag cca gaa ttc ggc agc gt
5′ ribA	tca tgc agc tta aac gtg tgg ca
3′ ribA	tca ttg acg cca agg agt ttg aa

Methods

Maintenance and propagation of bacterial strains

All bacterial strains were stored at −20°C in 30 % glycerol. Routinely, 20 µl (sometimes ~ 100 µl for old or sick strains) of a frozen stock were streaked to single colonies on a LB agar plate (containing antibiotics if required) and incubated overnight at 37°C. For DNA synthesis experiments, strain N1141 and its derivatives were streaked on agar plates containing high levels of thymine (0.005 %). All strains that carried temperature-sensitive alleles such as *dnaA46* were cultured at 30°C. For all experiments, fresh 5 ml liquid medium was inoculated with a single colony and the cultures grown overnight at the required temperature in a tube rotator. To begin an experiment, overnight cultures were routinely diluted in fresh medium to an optical density (A_{650}) of 0.05. The optical density of cultures was measured using either a Thermo Spectronic or a Beckman Coulter spectrophotometer.

Antibiotics

When required, antibiotics were used at the following final concentrations: ampicillin (50 µg/ml); carbenicillin, kanamycin and apramycin (40 µg/ml); chloramphenicol, tetracycline and trimethoprim (10 µg/ml); streptomycin (100 µg/ml). Kanamycin and gentamicin were used at final concentrations of 15 µg/ml and 6 µg/ml, respectively for testing strains carrying chromosomal DNA arrays tagged with genes encoding resistance to these antibiotics. For reasons that are unclear, the levels of resistance encoded by these tags are unusually low.

Testing bacterial strains

All new strains were tested by performing a streak test. Also strains not created by myself were tested in this manner before use. Single colonies were used to inoculate fresh overnight cultures and once grown these were streaked out (~10 µl) onto various diagnostic test plates, to give a qualitative overview of the phenotype of the strain in comparison to the necessary control strains. Many of the strains used carried ampicillin, chloramphenicol, kanamycin, tetracycline or apramycin resistance genes so strains were routinely tested on these antibiotics as part of a streak test. Strains were also tested to

various degrees with DNA damaging agents depending upon the nature of the strain. Routinely strains were tested on LB plates irradiated with 30 and 60 J/m² UV, as well as on plates containing 0.2 and 0.5 μg/ml Mitomycin C (with and without irradiation with 30 J/m² UV). These tests would confirm the presence of mutations conferring sensitivity to DNA damage.

Testing strains via replica plating

When a strain was created by transduction using linkage to a specific marker located near to the mutant allele of interest, not all colonies that received the marker would necessarily have received the mutant allele. For example, in the case of *dnaA46* strains, the mutant *dnaA46* allele is linked to *tnaA*::Tn*10* and tetracycline resistant transductants may or may not have received the mutant allele. In such cases, 100 colonies would be picked and re-grown in a regular array on a single agar plate, creating a master grid of potential strains. The plate would be incubated until the grid had grown and then replica plated using sterile velvets onto various test plates ending with a control plate on which all genotypes should grow. The replica plates were incubated overnight and screened the next day for strains with the correct phenotype. Several of them would be purified to single colonies and then tested using the standard streak test described above.

Preparation of bacteriophage P1 lysates

Buffers & solutions:
MC buffer: 0.1 M magnesium sulphate ($MgSO_4$), 5 mM calcium chloride ($CaCl_2$)

Liquid culture lysates

A fresh overnight culture of the host strain was diluted to an optical density A_{650} of 0.05 in 8 ml of fresh Mu broth and grown at 37°C with vigorous shaking to an A_{650} of 0.4. At this stage 0.1 ml of calcium chloride (0.5 M) was added to the culture and incubation continued for a further 10 minutes because the phage requires calcium ions for infection of the cells. A stock of P1 bacteriophage that has been grown on the wild type strain W3110 is maintained in the lab. An amount of phage P1 grown on *E. coli* strain W3110 (designated P1.W3110) that contained ~10^7-10^8 plaque forming units of phage (30 μl) was added and the culture was incubated with vigorous shaking until cell lysis had occurred (3-4 hours). Once lysis had occurred, 0.5 ml of chloroform was added and the mixture

was vortexed and incubated at room temperature for 5 minutes. The chloroform completes lysis and kills any phage resistant cells. The lysate was spun (10000 rpm, 4°C, 20 minutes, Sorvall SS-34 rotor) to pellet the cellular debris. The supernatant, which contains the new stock of phage, was transferred to a clean tube and 0.5 ml of chloroform added (mixed by inverting). P1 lysates can be stored for long periods at 4°C.

Plate lysates

For most strains, growing a liquid culture lysate is the most suitable method because it is quick and efficient. Occasionally a plate lysate may be required if liquid culture lysis of the strain occurs at a low efficiency. A fresh overnight culture of the host strain was diluted to an optical density A_{650} of 0.05 in 8 ml of fresh Mu broth containing 0.1 ml calcium chloride (0.5 M) and grown at 37°C with vigorous shaking to an A_{650} of 0.8. The phage stock P1.W3110 was diluted 10-fold and 100-fold in MC buffer, so that there was approximately 10^9 and 10^8 plaque forming units per ml. Once the cells were grown, 0.1 ml of the culture was overlaid onto P1 agar plates (Mu agar containing 0.1 % glucose, 5 mM calcium chloride) in 3 ml of Mu soft agar (0.4 %, kept molten at 42°C) containing either 300, 200, 100 or 0 µl of the diluted phage. The plates were not dried before use and were incubated in moist conditions overnight (the plates are not turned in this case because the overlay agar is very soft). If the lysis has not worked a lawn of cells will grow on the plates. If lysis has occurred the plates will have phage plaques on the lawn of cells and if lysis was very efficient there will be a lawn of phage and only isolated colonies growing. The new stock of phage was harvested by scraping off the overlay into a clean tube, mixing with 1 ml of MC buffer and 0.5 ml of chloroform. The mix was spun down (10000 rpm, 4°C, 20 minutes, Sorvall SS-34 rotor). The supernatant was transferred to a clean tube and 0.5 ml chloroform added for storage at 4°C.

Transduction with bacteriophage P1

Buffers & solutions:
MC buffer: 0.1 M magnesium sulphate ($MgSO_4$), 5 mM calcium chloride ($CaCl_2$)
Sodium citrate: 1 M tri-sodium citrate ($C_6H_5Na_3O_7$)

Transduction of antibiotic resistance markers

A fresh overnight culture of the recipient strain was diluted to an optical density A_{650} of 0.05 in 8 ml of fresh Mu broth and grown at 37°C with vigorous shaking to an A_{650} of ≥

0.8. The culture was pelleted (6000 rpm, 4°C, 5 minutes, Sorvall SS-34 rotor). The cell pellet was resuspended in 1 ml of MC buffer and incubated at room temperature for 15 minutes. MC buffer provides the calcium ions required by the phage for infection of cells. The cells (200 µl) were mixed with 0, 50 and 200 µl of P1 phage which had been grown on the appropriate donor strain and which was normally at a concentration of ~10^{10} pfu/ml (plaque forming units per ml). As a control, cells with no phage added were included to demonstrate that the recipient strain would not grow on the selective plates without transduction of the antibiotic resistance marker. The cells and phage were incubated together for 20-25 minutes at 37°C in a static water bath to allow infection of the cells with phage. Incubation should not be allowed to continue for longer as this will result in lysis of the recipient strain. After incubation 200 µl of sodium citrate was added immediately to chelate the calcium ions and stop the infection. The cells were mixed with 3 ml of Mu soft agar (0.6%, kept molten at 42°C), overlaid onto the appropriate selective plates and incubated until transductant colonies were visible (12-72 hours). Transductant colonies were purified on fresh plates and then tested for the presence of antibiotic markers and for any phenotype (see page 53).

Transduction of nutritional markers

These transductions were carried out in similar manner to those described above. However, cells were overlaid using molten 0.7% water agar onto the appropriate selective plates. In this case the selective plates were minimal media lacking the particular nutrient the recipient strain cannot grow on without transduction of the necessary gene.

Cloning DNA fragments

Preparation of plasmid DNA

Plasmid DNA was extracted from cells using a Qiagen miniprep kit. Fresh overnight cultures of strain DH5α carrying the desired plasmid were grown and ~ 4 ml of culture was pelleted (13000 rpm, room temperature, 1 minute, Eppendorf 5415 D). The cell pellet was processed and applied to a QIAprep spin column following the protocol provided. In principle, the cells were lysed in alkaline conditions in a buffer containing SDS. The alkaline conditions of the buffer denature both chromosomal and plasmid DNA, as well

as proteins. RNase A was also added to remove cellular RNAs. The mixture was rapidly neutralised, allowing renaturation of plasmid DNA, but causing chromosomal DNA and cellular debris to precipitate. The mixture was spun to pellet the precipitate and the supernatant was applied to a QIAprep column and washed with a buffer containing ethanol. Plasmid DNA was eluted from the spin column in 30 μl of elution buffer.

For larger preparations of plasmid DNA the Qiagen Plasmid Midi kit was used, with a Qiagen-tip 100 and a different set of buffers. The preparations followed the same principle as set out above.

Agarose gel electrophoresis

Buffers & solutions:
TAE buffer (50 ×): 2 M Tris, 1 M acetic acid, 0.05 M EDTA. To make 1 L, 242 g Tris, 57.1 ml glacial acetic acid, 100 ml EDTA 0.5 M (pH 8.0), add water to 1000 ml
TBE buffer (10 ×): 0.89 M Tris, 0.89 M boric acid, 0.02 M EDTA. To make 1 L, 108 g Tris, 55 g boric acid, 40 ml EDTA 0.5 M (pH 8.0), add water to 1000 ml
5 × Saccharose loading dye (10 ml): 6 g saccharose (sucrose), 10 mg bromophenol blue, 10 mg xylene cyanol, made up to 10 ml with 1 × TBE buffer

DNA fragments were routinely separated using 1% agarose (Geneflow) gels. Gels made with TBE can be run at a higher voltage than TAE gels and so run quicker; however, the borate in TBE can interfere with enzymes, so if the fragments were subsequently purified from the gel for the purpose of cloning a TAE gel was used. Gels also contained ethidium bromide (0.5 μg/ml) to enable visualisation of the DNA. DNA samples were loaded with saccharose loading dye (diluted to 1 × in the DNA sample). Alongside the samples, 0.5 μg of either a 1 kb DNA ladder (NEB) or a 100 bp DNA ladder (NEB) was loaded on the gels, depending on the size of the fragments to be separated. Minigels were run at a constant voltage of 90 V (TBE) or 45 V (TAE). DNA was visualised by exposing the gels to UV light using either a Bio-Rad Gel Doc or a transilluminator. If the DNA fragments were required for further applications they were excised from gels using a clean scalpel blade.

Extraction of DNA from agarose gels

DNA fragments were excised from gels and then extracted from the agarose using a Qiagen gel extraction kit. The provided buffers solubilise the agarose and allow the DNA to bind the QIAquick spin column whilst the agarose and other impurities flow through. The DNA is washed by an ethanol containing buffer and then eluted in 30 μl of elution buffer.

Polymerase chain reaction

Buffers & solutions:
10 × Taq buffer: 500 mM potassium chloride, 100 mM Tris (pH9.0),
15 mM magnesium chloride, 1% triton X-100

The polymerase chain reaction (PCR) was used for amplification of DNA fragments for the purpose of cloning and for amplifying fragments to send for DNA sequencing. PCR was also used as a diagnostic tool for checking the locations of insertions of antibiotic resistance genes into the chromosome. Plasmid DNA was preferentially used as template DNA at a final concentration of ~10000 copies per reaction. In a 50 μl PCR, 1 μl of a 10-fold diluted standard Qiagen miniprep was suitable as the template. When a colony was used to provide the template, a hot start PCR was employed (see below).

Taq DNA polymerase was used for diagnostic PCRs. When the PCR product was required for cloning, a higher fidelity polymerase DyNAzyme EXT was used. The Taq buffer described was used with *Taq* polymerase and the buffer provided by the manufacturer was used with DyNAzyme. PCRs were typically set up with primers at a final concentration of 1 μM, dNTPs at a final concentration of 0.2 mM (per dNTP), 1 unit of polymerase, in 1 × reaction buffer made up to a final volume of 50 μl with water.

A typical PCR program:
95°C for 5 minutes (initial denaturation of DNA)
Then 30 cycles of:
95°C for 45 seconds (denaturation)
53°C for 45 seconds (primer annealing)
72°C for 1 minute (primer extension – this time varies according to the enzyme efficiency and length of the desired product).
A final period of 5 minutes at 72°C was used to complete unfinished products and then the reaction was cooled to 4°C.

PCR products were analysed by agarose gel electrophoresis (see page 57). If necessary the DNA was extracted from the gel (see page 57).

Hot start PCR

Hot start PCRs were used when a colony was used to provide the template DNA. The reaction was set up with a 30 μl lysis mix consisting of water and buffer (1 ×) in which a small amount of the colony to be tested was resuspended (touch the colony with a tip and pipette it up and down in the mix). The rest of the PCR mix was set up in 20 μl with the components as normal (for a final reaction volume of 50 μl). The PCR program used was

a modified version of a standard PCR. First of all the lysis mix is heated to 98°C for 5 minutes and then the reaction is cooled to 85°C to allow addition of the rest of PCR mix. This avoids stressing the polymerase at 98°C. The program then runs into the PCR cycles and finishes as normal.

Cloning restriction fragments

For cloning, DNA fragments were amplified using primers that contained restriction enzyme sites. The PCR products were purified on agarose gels, the DNA extracted and cleaved with the appropriate restriction enzymes. The vector into which the fragment would be cloned was also cleaved. For cloning a 20 µl digest was set up containing ~0.1-1 µg DNA (visible on a gel), the appropriate buffer, 1 µl BSA (1 mg/ml) and 0.5 µl restriction enzyme(s). The digests were incubated according to the manufacturer's suggestions.

The digested DNA was purified on an agarose gel and extracted as described (page 57). A ligation reaction (10-15 µl) was set up using T4 DNA ligase (NEB), the buffer provided, vector and insert DNA and made up to the correct volume with water. Ligation reactions should contain ~200 ng of vector DNA. In order to work out how much insert DNA to use, the number of moles of vector DNA used should be calculated and 5 × the amount of insert DNA (in moles) should be used. Ligations were incubated overnight at 15°C and the next day the ligation mix was used to transform DH5α (see page 60).

DNA sequencing

All DNA sequencing, including the sequencing reactions were performed by the Biopolymer Synthesis and Analysis Unit, The University of Nottingham. Either purified plasmid DNA or a clean PCR product was sent up as a template for the reactions along with sequencing primers.

Bacterial transformation

Electroporation

Electroporation is an efficient method for bacterial transformation and was used routinely for transformation of strains with plasmid DNA, as well as with linear DNA. The following protocol was used for transforming cells with plasmid DNA. A method for transformation with linear DNA is detailed in the section "Chromosomal genetic

engineering" (page 61). A fresh overnight culture of the strain to be transformed was diluted to an optical density A_{650} of 0.05 in 8 ml of fresh LB broth and grown at 37°C with vigorous shaking to an A_{650} of 0.6. A 2 ml sample of the culture was pelleted (6000 rpm, 4°C, 5 minutes, Eppendorf 5810 R). From this point the cells were kept ice-cold. The cells were pelleted and resuspended in decreasing volumes of ice-cold sterile distilled water, with a 10 minute wait between resuspension and spinning. The volumes used for resuspension were 10 ml, 5 ml, 1 ml and 0.5 ml. The washes are necessary to remove any traces of salt left from the medium, which would cause arcing during the electroporation and prevent transformation.

After the last spin, the supernatant was poured away and the cells were resuspended in the remaining drop of liquid (~50-100 μl). At this point plasmid DNA was added to the cells, typically 0.5-2 μl of a standard Qiagen mini-prep. The cells were incubated with plasmid DNA for 10 minutes and then transferred into a cold electroporation cuvette. Cells were electroporated with 1.75 kV (Bio-Rad *E. coli* pulser). Immediately after electroporation 2 × 800 μl of SOC broth was added to the cells and they were transferred to a fresh tube and left to recover at 37°C in a tube rotator. It is important that SOC broth is added to the cells immediately after electroporation as this can affect efficiency. Cells were left to recover for 45 minutes and then 50 μl was streaked to single colonies on the appropriate selective plate. The remaining cells can be pelleted and streaked on another plate in case of low efficiency.

Chemical competence

Buffers & solutions:

TFB-I: 100 mM potassium chloride, 50 mM manganese chloride, 30 mM potassium acetate, 10 mM calcium chloride, 15% glycerol, adjust to pH 5.6-6.2 with acetic acid. Sterile filtered.

TFB-II: 10mM Mops, 10 mM potassium chloride, 75 mM calcium chloride, 15% glycerol, adjust to pH 7.0. Sterile filtered.

Chemically competent cells can be stored for long periods. A fresh overnight culture of the strain to be transformed was used (1 ml) to inoculate 100 ml of fresh SOC broth and grown with vigorous shaking at 37°C to an optical density A_{650} of 0.6. The cells were centrifuged (4000 rpm, 4°C, 5 minutes, Eppendorf 5810 R) and the cell pellet resuspended in 30 ml of cold TFB-I. Cells were kept ice-cold from this point. The cells were incubated on ice for an hour and then centrifuged again (4000 rpm, 4°C, 5 minutes, Eppendorf 5810

R). The cell pellet was resuspended in 4 ml of cold TFB-II and the competent cells were stored in 200 µl aliquots at −80°C.

For transformation of chemically competent cells, one aliquot was used per transformation. The aliquot was thawed on ice and the plasmid DNA (typically 0.5-2 µl of a standard Qiagen mini-prep or a whole ligation reaction) was mixed with the cells and incubated on ice for 5 minutes. Cells were heat shocked at 42°C for 1 minute and placed immediately onto ice again. The cells were incubated on ice for 5 minutes, 800 µl of SOC broth was added and the cells were left to recover at 37°C for 45 minutes in a tube rotator. Cells were streaked (100 µl) on the appropriate selective plates and incubated overnight. The remaining cells can be pelleted and streaked on another plate in case of low efficiency.

Chromosomal Genetic Engineering

Chromosomal mutations were engineered following the method of Datsenko and Wanner (2000). The mutant allele was cloned onto a plasmid and linked with an antibiotic resistance marker. The antibiotic resistance and the sequence changes were amplified by PCR with primers that contained ~50 base pairs of homology to the chromosome, defining the site at which the PCR product would be recombined into the chromosome. PCR products were run on an agarose gel and extracted as above (page 57).

The temperature-sensitive (grow at 30°C) plasmid pKD46 encoding the arabinose-inducible λ Red recombinase was used for this procedure. The Red system inhibits *E. coli* RecBCD enzyme so that it does not degrade the PCR product, enabling the recombinase to promote recombination between the PCR product and the chromosome (Datsenko and Wanner 2000). A fresh overnight culture of strain MG1655 carrying the plasmid pKD46 was used to inoculate 8 ml of fresh SOB broth (supplemented with 50 µg/ml Ampicillin and 0.2% arabinose) to an optical density A_{650} of 0.05. Cultures were grown at 30°C to an A_{650} of 0.6 and then made electrocompetent as follows. A 5 ml sample of culture was spun down (6000 rpm, 4°C, 5 minutes, Eppendorf 5810 R) and from this point the cells were kept ice-cold. The cells were pelleted and resuspended in decreasing volumes of ice-cold 10% glycerol with no delay between resuspension and spinning. The volumes used for resuspension were 10 ml, 5 ml, 1 ml and 0.5 ml. After the last spin, the supernatant was poured away and the cells were resuspended in the remaining drop of liquid (~50-

100 µl). The cells had been concentrated 100-fold. At this point ~60 ng of PCR product was mixed with the cells and then transferred into a cold electroporation cuvette. Cells were electroporated with 1.75 kV (Bio-Rad *E. coli* pulser). Immediately after electroporation 1 ml of SOC broth was added to the cells and they were transferred to a fresh tube and left to recover at 37°C in a tube rotator. Cells were left to recover for 1 hour and then 500 µl were spread on the appropriate selective plate and incubated at 37°C. The remaining cells were left at room temperature overnight and spread on selective plates if there were no recombinants on the first set of plates. The plasmid should be lost during growth at 37°C.

Recombinant colonies were purified on LB plates and tested by a streak test, diagnostic PCR and sequencing. To ensure that the mutations were characterised in a clean strain background, they were always transferred to a clean MG1655 strain by transduction (see page 55).

Synthetic lethality assays

This method was described previously (Mahdi *et al.* 2006). Strain TB28 and its derivatives, carrying plasmids derived from the plasmid pRC7 were used in these experiments. The plasmids are easily lost from cells when they are not grown with ampicillin selection. Fresh overnight cultures (LB supplemented with ampicillin) were diluted to an optical density A_{650} of 0.05 in fresh LB broth without ampicillin and grown at 37°C to an A_{650} of 0.48. Cells were diluted in a series of 10-fold steps to 10^{-5} in 56/2 salts and then spread on LB agar plates containing X-gal (66.67 µg/ml) and IPTG (0.15 mM). Typically, the following dilutions were spread on plates: 10^{-4} (200, 100 and 50 µl) and 10^{-5} (200 and 100 µl). Plates were incubated at 37°C for 48 hours, photographed and the numbers of blue and white colonies scored.

Measuring survival after DNA damage

Semi-quantitative UV survival

Fresh overnight cultures of the strains to be tested were diluted to an optical density A_{650} of 0.05 in 8 ml of fresh LB broth and grown at 37°C with vigorous shaking to an A_{650} of 0.48. Once grown, the cultures were chilled on ice and then diluted in a series of 10-fold

steps to 10^{-5} in chilled 56/2 salts. The dilutions were spotted onto LB plates (10 μl spots) and left to dry. Once the spots had dried the plates were irradiated with UV. The standard UV doses used were 0, 5, 10, 20, 30, 45 and 60 J/m². When strains were more sensitive to UV irradiation, for example Δ*recG* Δ*ruv* double mutants, lower doses of 1 and 3 J/m² were included in the assay. The plates were incubated overnight at 37°C until colonies were visible enough to be counted. The numbers of colonies were scored for each strain at each UV dose, by counting the number of colonies for a dilution at which individual colonies were visible. The fraction of cells surviving was calculated by comparison to the 0 J/m² plate, taking into account the dilution at which the colonies were scored. For example, if there are 12 colonies at a 10^{-5} dilution on the unirradiated plate and 6 colonies at a 10^{-4} dilution after 30 J/m², then the fraction surviving is calculated as: $6/(12 \times 10) = 0.05$, where 10 is the dilution factor (i.e. the difference between 10^{-5} and 10^{-4}).

Qualitative mitomycin C survival

These assays were carried out using the same method as for quantitative UV survival, except that the dilutions were spotted on plates that contained mitomycin C. The standard plates used for these assays contained 0.2 and 0.5 μg/ml mitomycin C, with and without 30 J/m² UV, along with LB plates that received UV doses of 0, 30 and 60 J/m². These plates were incubated overnight at 37°C until colonies were visible. Strains that are sensitive to mitomycin C do not produce colonies that are countable (Figure 44), so the plates from these assays were photographed for a qualitative comparison only.

Measurement of DNA synthesis

This method is as previously described (Rudolph *et al.* 2007b). Strain N1141 and its derivatives were used for measuring DNA synthesis. N1141 encodes a *thyA54* and a *deo* mutation, meaning that the strain only grows in media supplemented with low levels of thymine. The dependence of this strain on thymine for growth means that it incorporates [^{3}H]thymidine into newly synthesised DNA at a level suitable for measuring DNA synthesis. All cultures for these experiments were grown in Davis medium (see page 43) supplemented with 0.0001% thiamine, 0.4% glucose, 0.01% magnesium sulphate, 1% casamino acids and 5 μg/ml thymidine. Fresh overnight cultures of the required strains

were diluted to an optical density A_{650} of 0.05 in 10 ml fresh Davis medium supplemented as above. Cultures were grown with vigorous shaking at 30°C to an A_{650} of 0.2 and then split into 2 × 4 ml and filtered onto 0.22 μm cellulose acetate (Corning). The cells were UV-irradiated directly on the filter or mock-irradiated and then resuspended in 3 ml filtrate. [^{3}H]thymidine (specific activity 80.0 Ci/mmol, Amersham) was added to 600 μl of resuspended cells to a final concentration of 2 μCi/ml and cultures were incubated at 42°C using an Eppendorf Thermomixer comfort, shaking at 1200 rpm. Twenty-microliter samples were taken at intervals, applied to 2.5 cm² filters (Whatman 3MM) and immediately immersed in ice-cold 5% trichloroacetic acid for a minimum of 30 minutes. Filters were washed in three changes of fresh trichloroacetic acid and two of ethanol (100%) and then dried. Filters were placed in scintillation tubes with 4 ml of scintillation fluid (Emulsifier scintillator plus, PerkinElmer) and the bound radioactivity was counted using a scintillation counter (Tri-carb 2100TR, Packard).

Fluorescence microscopy

Using chromosomal arrays

This method is as previously described (Rudolph *et al.* 2007b). These experiments used derivatives of the strain MG1655 carrying *lacO240* and *tetO240* arrays transformed with a plasmid, pLAU53, encoding arabinose-inducible LacI-eCFP (enhanced cyan fluorescent protein) and TetR-eYFP (enhanced yellow fluorescent protein) repressors. When expressed, the fluorescent repressor proteins bind to the arrays, labelling their position within the cell (Lau *et al.* 2003). Fresh overnight cultures of the required strains were diluted to an optical density A_{650} of 0.05 and grown with vigorous shaking at 37°C to an A_{650} of 0.2 in 10 ml of LB broth supplemented with 0.5 mM IPTG and 40 ng/ml anhydrotetracycline to reduce repressor binding, without compromising focus formation. A 1 ml sample was removed and expression of the repressors induced at high levels by adding arabinose to a final concentration of 0.2%. The rest of the culture was pelleted (5000 rpm, 4°C, 5 minutes, Eppendorf 5810 R). The supernatant was filter-sterilized using a 0.45 μm syringe-end filter (Satorius Stedim Biotech Minisart). The cells were resuspended in 250 μl of LB broth and spread on the surface of a dried LB agar plate for irradiation with the desired UV dose. By creating a thin and dry layer of cells on the surface of a plate any absorption or shielding effects were reduced. Our standard

medium contained traces of glucose, which interfered with expression of fusion proteins so to avoid this problem the irradiated cells were resuspended in the original filter-sterilised supernatant and incubation was continued at 37°C. Further 1 ml samples were taken at the intervals indicated and induced with arabinose. Cells were induced with arabinose for 30 minutes and then a 3 μl sample was transferred to a thin 1% LB agarose layer on a microscopic slide. The cells were visualized using a BX-52 Olympus microscope equipped with a coolSNAP™HQ camera (Photometrics). eCFP and eYFP foci were visualized using the JP4-CFP-YFP filterset 86002v2 (Chroma). Images were taken and analyzed by MetaMorph 6.2 (Universal Imaging) and processed using MetaMorph and Adobe Photoshop.

Using fluorescently tagged proteins

Strain MG1655 and its derivatives were used for these experiments. Strains were transformed with plasmids which encoded arabinose-inducible fusions of the protein of interest to either eYFP or eCFP. Fresh overnight cultures of the strains were diluted to an optical density A_{650} of 0.05 in 8 ml of LB broth and grown with vigorous shaking to an A_{650} of 0.2. Expression of the fusion proteins was induced by adding arabinose to a final concentration of 0.2%. Cells were induced for an hour and then a 3 μl sample was transferred to a thin 1% 56/2 agarose layer on a microscopic slide. The cells were visualized as described above.

Southern analysis of the origin to terminus ratio

Treatment of samples

This method is as previously described (Rudolph *et al.* 2007b). Strains used for these experiments were derivatives of a MG1655 *dnaC7* strain. Fresh overnight cultures of the required strains were diluted to an optical density A_{650} of 0.05 in 24 ml of LB broth and incubated with vigorous shaking at 30°C to an A_{650} of 0.15. The cells were then synchronized by shifting the cultures to 42°C for 45 minutes. The cells were pelleted (6000 rpm, 4°C, 5 minutes, Eppendorf 5810 R). The supernatant was filtered using a 0.45 μm syringe-end filter (Satorius Stedim Biotech Minisart). The cells were resuspended in 250 μl of LB broth and spread on the surface of a dried LB agar plate for irradiation with the desired UV dose. The cells were resuspended in the original filter-sterilized

supernatant and then incubated with shaking at 30°C. A 4 ml sample was taken immediately after irradiation and this was the time zero sample. The optical density A_{650} of the sample was measured and was usually ~0.4. Samples were taken every 30 minutes up to 180 minutes and were diluted so that the equivalent of 4 ml of culture at an optical density A_{650} of 0.4 was spun down. Spinning down samples with equivalent cell densities meant that the samples would have similar DNA concentrations. The cell pellets were stored at −20°C. At this stage the samples can be stored overnight.

Preparation of chromosomal DNA

Buffers & solutions:
NET buffer: 10 mM Tris (pH 8.0), 10 mM NaCl, 10 mM EDTA, filtered.
TE buffer: 10 mM Tris-HCl (pH 8.0), 1 mM EDTA

Cell pellets were resuspended in 500 µl of NET resuspension buffer and transferred to 2 ml tubes before adding 1 µl RNase A (30 mg/ml), 50 µl Triton X-100 (10 %) and 50 µl lysozyme (5 mg/ml) and incubating for 30 minutes (37°C, 600 rpm, Eppendorf Thermomixer). After incubation, 60 µl Proteinase K (5 mg/ml) was added and the samples were incubated for 2 hours (65°C, 600 rpm, Eppendorf Thermomixer comfort).

After Proteinase K treatment the DNA was extracted using phenol-chloroform. One volume of phenol/chloroform/isoamylalcohol (Sigma) was added to each sample, vortexed and centrifuged (14000 rpm, 4°C, 10 minutes, Eppendorf 5417 R). The supernatant was transferred into a fresh tube and again 1 volume of phenol/chloroform/isoamylalcohol was added. Samples were centrifuged as before. The supernatant was transferred into a fresh tube and washed with 1 volume of chloroform, vortexing until mixed. Samples were centrifuged as before. Phenol denatures proteins within the sample and because water and phenol do not mix, the proteins are separated into the phenol phase during centrifugation. The final wash with chloroform removes any remaining phenol from the sample.

The supernatant was transferred to a fresh tube. Two volumes of ethanol (100 %) and 1/10 volume of potassium acetate (3 M) were added to each sample to precipitate the DNA. Samples were left to precipitate overnight at 4°C.

The next day the samples were centrifuged, (14000 rpm, 4°C, 30 minutes, Eppendorf 5417 R). There should be a visible DNA pellet at this stage. The supernatant was poured out and 900 µl of ethanol (70 %) was carefully added and the samples were left at room

temperature for 10-15 minutes. The samples were spun for 30 minutes as before. The ethanol was removed with a pipette taking care not to dislodge the pellet and the tube was spun briefly and the rest of the ethanol removed. The pellets were dried at 37°C for 15 minutes and then 50 µl of TE was added. The samples were vortexed and then incubated for 10 minutes (65°C, 600 rpm, Eppendorf Thermomixer comfort), vortexed and heated again. The samples were vortexed once more and spun down briefly.

The concentrations of the DNA samples were determined using a spectrophotometer (Beckman coulter, DU 530). Chromosomal DNA was stored at 4°C.

Digest of DNA and fragment separation by gel electrophoresis

Buffers & solutions:
TAE buffer (50 ×): 2 M Tris, 1 M acetic acid, 0.05 M EDTA. To make 1 L, 242 g Tris, 57.1 ml glacial acetic acid, 100 ml EDTA 0.5 M (pH 8.0)
TBE buffer (10 ×): 0.89 M Tris, 0.89 M boric acid, 0.02 M EDTA. To make 1 L, 108 g Tris, 55 g boric acid, 40 ml EDTA 0.5 M (pH 8.0), add water to 1000 ml
5 × Saccharose loading dye (10 ml): 6 g saccharose (sucrose), 10 mg bromophenol blue, 10 mg xylene cyanol, made up to 10 ml with 1 × TBE buffer

Chromosomal DNA (3 µg) samples were digested overnight with *Xma*I and *Hpa*I. The digests were made up to a final volume of 25 µl with sterile distilled water and contained the required amount of DNA, 2.5 µl of NEBuffer 4 (NEB), 2.5 µl BSA (1 mg/ml) and 0.5 µl of each enzyme. The digests were incubated overnight at 37°C in a static water bath.

The digested DNA fragments were resolved on a 0.7 % agarose TAE gel (1.7 g agarose, 250 ml 1 × TAE). The large gel tank requires 1.5 L of TAE gel running buffer (1 ×). The digested chromosomal DNA was loaded with 5 µl of 5 × Saccharose loading dye. Gels were run for 16 hours at 45 V (normally overnight). After the gel had run, it was stained with 500 ml of ethidium bromide solution (0.5 µg/ml) to confirm that there was DNA on the gel and that it had run properly.

Preparation of the membrane

Buffers & solutions:
Southern transfer buffer: 0.5 M sodium hydroxide, 1.5 M sodium chloride
20 × SSPE: 3 M sodium chloride, 200 mM sodium dihydrogen phosphate ($NaH_2PO_4 \cdot H_2O$), 20 mM EDTA, pH 7.4

The gel was treated for 20 minutes in 500 ml of hydrochloric acid (0.25 M) which creates apurinic (AP) sites in the DNA. The gel was then washed twice with water for 10 minutes

and treated with Southern transfer buffer for 45 minutes to induce nicks in the DNA backbone at the AP sites (the shorter DNA fragments will transfer to the membrane during blotting).

The DNA was transferred to the membrane by vacuum transfer. The membrane (15 × 25 cm, Zeta-Probe GT membrane, Bio-Rad) was rinsed briefly in water, soaked in fresh transfer buffer for 5 minutes and placed on the wet foam support of the vacuum blotter. The wet gasket was placed over the membrane, the edges must be sealed. The lid was placed on top and the clamps put in place but not tightened. The gel was transferred on top of the membrane and 500 ml of Southern transfer buffer poured over it to seal the machine. The pump was turned on (pressure set to ~50 mBar) and the lid sealed by tightening the clamps. The gel was blotted for 45-60 minutes.

After blotting it is important that no buffer drips onto the membrane during removal of the gel, the lid and the gasket. The membrane was rinsed in 500 ml of SSPE (2 ×). Excess liquid was removed using Whatman paper and the damp membrane was cross-linked to the membrane using 120 mJ/cm² UV (UV crosslinker). The membrane was wrapped in Saran wrap and stored at −20°C.

Prehybridisation

Buffers & solutions:

SSPE (20 ×): 3 M sodium chloride, 200 mM sodium dihydrogen phosphate ($NaH_2PO_4 \cdot H_2O$), 20 mM EDTA, pH 7.4

Denhardt's (100 ×): 10 g ficoll 400, 10 g polyvinylpyrrolidone K30, BSA 10 g, water to 500 ml, aliquot (2 ml) and freeze.

Prehybridisation buffer: 22 ml water, 12 ml SSPE (20 ×) mixed and heated to 65°C. Once heated add 4 ml SDS solution (10%), 2 ml Denhardt's (100 ×) and 800 µl denatured fish sperm DNA (Roche, 10 mg/ml – for denaturation the fish DNA was heated for 5 minutes to 100°C and then quenched on ice).

The membrane was transferred into a hybridisation tube. The prehybridisation buffer was heated to 65°C and 40 ml added to the membrane. Prehybridisation should take ~4 hours.

Probe preparation

Buffers & solutions:

TE buffer: 10 mM Tris-HCl (pH 8.0), 1 mM EDTA

For generation of probes 100 ng of DNA was used, except for the DNA ladder probe where 1 ng of DNA was used. The origin probe was created by PCR using primers 5'mioC and 3'mioC (Table 3) which bind near to *oriC* and give a product size of 413 base pairs. The terminus probe was created by PCR using primers 5'ribA and 3'ribA (Table 3) which bind near to *terA* and give a product size of 388 base pairs. The DNA probes were mixed together and water was added to give a final volume of 14 µl. The DNA was heated to 100°C for 5 minutes and quenched on ice and then 4 µl of High prime (Roche) and 2 µl of α^{32}P dCTP (GE healthcare) were added to give a final volume of 20 µl. The mixture was incubated at 37°C for 15-30 minutes and then 30 µl of TE buffer was added and the hot probe purified using a Micro Bio-Spin 30 column (Bio-Rad).

Hybridisation

Buffers & solutions:
SSPE (20 ×): 3 M sodium chloride, 200 mM sodium dihydrogen phosphate ($NaH_2PO_4 \cdot H_2O$), 20 mM EDTA, pH 7.4
Hybridisation buffer: 16.5 ml water, 9 ml SSPE (20 ×), mixed and heated to 65°C. Once heated, add 1.5 g dextrane sulphate and 3 ml SDS solution (10 %)

The hybridisation buffer was heated to 65°C. The hot probe was added to 450 µl of fish sperm DNA (Roche, 10 mg/ml) and the mixture was heated to 100°C for 5 minutes. The prehybridisation buffer was removed and the warm hybridisation buffer was added immediately to the membrane and then the probe/fish DNA mixture was added. Hybridisation was carried out overnight.

Washing of the membrane

Buffers & solutions:
20 × SSPE: 3 M sodium chloride, 200 mM sodium dihydrogen phosphate ($NaH_2PO_4 \cdot H_2O$), 20 mM EDTA, pH 7.4
2 × washing buffer: 2 × SSPE, 0.5 % SDS
0.2 × washing buffer: 0.2 × SSPE, 0.5 % SDS

The hybridisation liquid was removed and the membrane washed at 65°C with pre-warmed washing buffers. First the membrane was washed for 5 minutes with 2 × washing buffer, then 20 minutes with 2 × washing buffer and then twice with 0.2 × washing buffer for 30 minutes. The membrane was removed from the hybridisation tube and excess liquid was dried with Whatman paper. The damp membrane was placed on Whatman paper, wrapped in Saran wrap and then placed in a cassette. The signal visualized using

a Kodak Storage Phosphor Screen, scanned with a STORM scanner system (Molecular Dynamics) and quantified using ImageQuant 5.2 (Molecular Dynamics). For calculation of the corrected relative origin to terminus ratio, the signal intensity of the origin signal was divided by the intensity of the terminus signal and all ratios were divided by the ratio of the very first sample (taken directly after synchronization).

Purification of *Escherichia coli* RecG

SDS-PAGE analysis of proteins

Buffers & solutions:
Resolving gel buffer: 1.5 M Tris pH 8.8, 0.4% SDS
Resolving gel (10% polyacrylamide gel, 7.5 ml): 3.1 ml distilled water, 2.5 ml 30% acrylamide/bis-acrylamide (Severn Biotech), 1.875 ml resolving gel buffer, 37.5 µl 10% ammonium persulphate and 3.75 µl TEMED (tetramethylethylenediamine).
Stacking gel buffer: 0.5 M Tris pH 6.8, 0.4% SDS
Stacking gel (3% polyacrylamide, 2 ml): 0.77 ml distilled water, 0.2 ml 30% acrylamide/bis-acrylamide (Severn Biotech), 1 ml stacking gel buffer, 25 µl 10% ammonium persulphate, 2.5 µl TEMED (tetramethylethylenediamine).
5 × SDS-PAGE loading dye: 50 mM Tris pH 6.8, 100 mM DTT, 2 % SDS, 0.1 % bromophenol blue, 10 % glycerol
SDS-PAGE running buffer: 0.25 M Tris, 1.92 M glycine, 1% SDS

Protein samples were separated and analysed on SDS-PAGE gels using the X-Cell SureLock Mini-Cell (Invitrogen) gel apparatus. Gels were made in cassettes (Invitrogen). Recipes for gels are written above. First a resolving gel was poured, with a layer of isopropanol on top to leave a flat surface. Once the resolving gel had set, the isopropanol was washed off and a stacking gel was poured and a comb inserted. Protein samples were mixed with 5 × SDS-PAGE loading dye (to a final concentration of 1 ×) and then heated to 100°C for 2 minutes. Samples were loaded onto the gel along with a sample (5 µl) of the PageRuler Unstained protein ladder (Fermentas). The gels were run for 75 minutes in 1 × SDS-PAGE running buffer (200 V, 35 mA per gel). Gels were stained with PageBlue protein staining solution (Fermentas) according to the manufacturer's protocol.

Small-scale overexpression of RecG proteins

Buffers & solutions:
TNE: 50 mM Tris, 100 mM sodium chloride, 1 mM EDTA, pH 7.5, filtered and degassed

Wild type and mutant *recG* genes were all cloned into the pT7-7 vector for protein expression under the control of the T7 promoter. The proteins were expressed using the following plasmids: wild type RecG (pAM210), RecGΔC5 (pAU102), RecGΔC15 (pAU104), RecGΔC25 (pAU106). Strain AU1115, a derivative of BL21 (DE3), was used for overexpression of RecG proteins. AU1115 is a *xonA endA* mutant reducing the risk of exonuclease contamination in protein preparations. It is also a *ΔrecG* mutant, which means that there will be no wild type protein contaminating mutant protein preparations. AU1115 was transformed with pLysS (chloramphenicol resistant, making strain AU1118) encoding T7 lysozyme, which is expressed at low levels and is a natural inhibitor of the T7 RNA polymerase and therefore prevents basal expression of the target gene until expression is induced.

AU1118 was transformed with the appropriate expression vector and expression was first tested on a small scale, to check that the protein is expressed and that it is in the soluble protein fraction. A fresh overnight culture of the transformed AU1118 was diluted 100-fold in 2 × 8 ml of fresh Mu broth (supplemented with Ampicillin and Chloramphenicol to maintain both pLysS and the expression plasmid) and grown at 37°C to an optical density A_{650} of 0.5. One culture was left as an uninduced control and the other culture was induced to express protein by addition of IPTG (0.5 mM final concentration) to the culture. The cultures were incubated at 37°C for 3-4 hours. The cells were spun down (5000 rpm, 4°C, 5 minutes, Eppendorf 5810 R) and the cell pellet resuspended in 1 ml TNE. TNE stabilises the proteins after cell lysis. The cells were lysed by sonication (MSE soniprep 150, Sanyo) and kept on ice to prevent overheating and denaturation of the protein. At this point a sample (5 μl) of the total proteins was taken to be run on a gel later. The lysed induced cells were centrifuged (13000 rpm, 4°C, 10 minutes, Eppendorf 5417 R). The soluble proteins were in the supernatant and the insoluble proteins were in the pellet. A sample (5 μl) of the supernatant was taken for a gel and the pellet was resuspended in TNE + 6 M Urea (1 ml). The urea denatures the proteins in the pellet and allows them to be re-solubilised. A sample of the re-solubilised protein pellet was also taken. The protein samples were run on a gel (see page 70). The uninduced total proteins were compared with the induced total proteins, which should indicate if the protein has been expressed. The soluble and insoluble fractions of proteins

from the induced sample were also compared to check that the protein was expressed in a soluble form which could then be purified.

Large-scale overexpression of RecG proteins

If the results of the small-scale overexpression were promising the proteins were expressed on a large scale for purification. Fresh overnight cultures of the AU1118 transformed with the expression plasmid were diluted 100-fold in 300 ml fresh YT broth (containing ampicillin and chloramphenicol) in 1 L baffled flasks and grown at 37°C (unless otherwise stated) to an optical density A_{650} of 0.5. Normally 6 flasks of culture were grown per protein and the cell pellets pooled. Cells were induced to express protein by addition of IPTG (0.5 mM final concentration) and incubation continued for 3 hours. The cultures were spun down (6000 rpm, 4°C, 6 minutes, Sorvall SLA 3000 rotor) and the cell pellets stored at −80°C.

When a larger volume of culture was required for protein expression, a fermenter (Electrolab Fermac 310) was used. The glass vessel containing 2YT media (6-10 L) was autoclaved (123°C for 90 minutes). The glass vessel was connected up to the fermenter system and left at 37°C overnight, to check that there was no bacterial contamination. An overnight culture (100 ml) was grown for inoculation of the fermenter. The fermenter was set up for protein expression the next day. The media was aerated with filtered air and the rotor set to 600 rpm to calibrate the oxygen probe (antifoam was injected if necessary) to 100 % dissolved oxygen. The rotor speed was turned back down to 200 rpm and the antibiotics, Ampicillin (300 mg in 10 ml sterile distilled water) and Chloramphenicol (60 mg in 1 ml ethanol) were injected. The fermenter was inoculated (1:100, overnight culture: fresh media) and the culture grown at 37°C to an optical density A_{650} of 0.5. The speed of the rotor was controlled by the dissolved oxygen levels such that the oxygen was kept above 80 % dissolved oxygen. The oxygen demand of the culture increases as it grows. The culture was induced to express protein by addition of IPTG (0.5 mM final concentration). Cells were incubated at 37°C (unless otherwise stated) for 3 hours and then spun down (6000 rpm, 4°C, 6 minutes, Sorvall SLA 3000 rotor) and the cell pellets stored at −80°C.

Purification of RecG using an ÄKTA FPLC

Buffers & solutions:

TNE: 50 mM Tris, 100 mM sodium chloride, 1 mM EDTA, pH 7.5, filtered and degassed
Buffer A: 50 mM Tris, 1 mM EDTA, 1 mM DTT, pH 7.5, filtered and degassed
Gel filtration buffer: 20 mM Tris, 150 mM sodium chloride, pH 7.5, filtered and degassed
Storage buffer: 50 mM Tris, 1 mM EDTA, 1 mM DTT, 100 mM sodium chloride, 50% glycerol, pH 7.5

RecG proteins were expressed as described above (page 72). The purification of RecG proteins was performed at 4°C and has been described previously (Mahdi *et al.* 2003). The induced cell pellet was resuspended in ~20 ml of TNE and the cells lysed by sonication (MSE soniprep 150, Sanyo). The lysed cells were centrifuged (16000 rpm, 4°C, 30 minutes, Sorvall SS-34 rotor) and the supernatant was filtered with a 0.45 μm syringe-end filter (Satorius Stedim Biotech Minisart). The supernatant was loaded onto a 10 ml (2 × 5 ml) HiTrap SP HP column and eluted with a gradient of sodium chloride (0-1 M) in buffer A. Fractions containing RecG were pooled and diluted with buffer A so that the conductivity was low enough that the proteins would bind to the next column. The diluted fractions were loaded onto a 5 ml HiTrap Heparin HP column and RecG was eluted with a gradient of sodium chloride (0-1 M) in buffer A. Fractions containing RecG were pooled and ammonium sulphate was added to a final concentration of 0.5 M. The fractions were loaded onto a 5 ml HiTrap Phenyl-Sepharose HP column and RecG was eluted with a stepped gradient of ammonium sulphate (0.5-0 M) in buffer A. RecG elutes in 0% ammonium sulphate in a broad peak of 800 ml and so it was concentrated by binding directly to a 5 ml HiTrap Heparin HP attached downstream of the Phenyl-Sepharose column. RecG was eluted from the Heparin column as above. The eluted RecG was then loaded onto a 16/60 Sephacryl S-200 HR column (gel filtration) and eluted in gel filtration buffer. The fractions containing RecG were pooled and concentrated by loading onto a 5/5 Mono-S HR (1 ml) column and RecG was eluted with gradient of sodium chloride (0-1 M) in buffer A. The pure RecG protein was dialysed overnight against two changes of storage buffer (2 × 500 ml) and stored at −80°C. RecG preparations can be contaminated with nucleases, however no nuclease activity was observed at the highest concentrations used in the DNA binding assays (Figure 48).

Measuring protein concentration

Protein concentrations were measured using a protein assay kit (Bio-Rad). Bovine serum albumin (BSA) was used as a protein standard. BSA was diluted in sterile distilled water to a volume of 800 μl and then 200 μl of reagent was added. The final concentrations of

BSA samples were 2.5, 5, 10 and 15 μg/ml. After 15 minutes the optical density A_{595} was measured and compared with the optical density of the protein samples (also diluted in water to a final volume of 800 μl plus 200 μl reagent).

Biochemical analysis of RecG protein

Purification of oligonucleotides

Buffers & solutions:
Elution buffer: 10 mM Tris-HCl (pH 8.5)
TBE buffer (10 ×): 0.89 M Tris, 0.89 M boric acid, 0.02 M EDTA. To make 1 L, 108 g Tris, 55 g boric acid, 40 ml EDTA 0.5 M (pH 8.0), add water to 1000 ml
Sequencing gel (12 %): 40 ml 30 % acrylamide/bis-acrylamide (Severn Biotech), 10 ml TBE (10 ×), 46 g urea, made up to 100 ml with sterile distilled water. Plus, 100 μl 25 % ammonium persulphate, 100 μl TEMED (tetramethylethylenediamine)
Formamide loading buffer (2 ×): 10 ml formamide, 400 μl EDTA (0.5 M, pH 8.0), 10 mg xylene cyanol, 10 mg bromophenol blue

Oligonucleotides were concentrated overnight at −20°C by ethanol precipitation with 2 volumes 100 % ethanol plus 0.1 volumes of 3 M sodium acetate. The precipitated DNA was spun (14000 rpm, 4°C, 30 minutes, Eppendorf 5417 R) and the liquid removed carefully so as not to disturb the pellet. The pellet was washed with 70 % ethanol and the samples were left at room temperature for 10-15 minutes. The samples were spun for 30 minutes as before. The ethanol was removed carefully with a pipette and the pellet air dried at 37°C for ~15 minutes. The DNA pellet was resuspended in elution buffer.

All oligonucleotides used for biochemical assays were purified using a sequencing gel to remove any degraded oligonucleotides. A 12 % sequencing gel (suitable for 20-60 nucleotide oligos) was poured the night before and left to set with both ends covered with a damp cloth to prevent the gel from drying. The concentrated oligonucleotides were mixed with formamide loading buffer (2 ×) and loaded onto the sequencing gel (1-5 nmol loaded) and it was run at 1000 V for 3 hours. The gel was wrapped in Saran wrap and the bands were visualised by UV shadowing, cut from the gel and eluted overnight in elution buffer. The oligonucleotides were concentrated by ethanol precipitation (as above) and their concentration measured using a spectrophotometer (Beckman coulter, DU 530).

Labelling oligonucleotides with radioisotope

One of the DNA strands in each substrate is labelled with a radioisotope so that the substrate can be visualised on a gel. The oligonucleotides were labelled at the 5′ end using [γ-^{32}P]ATP (PerkinElmer). Approximately 1000 ng of oligonucleotide was labelled in a 20 µl reaction containing 3 µl [γ-^{32}P]ATP, 3 µl T4 kinase (NEB, 10000 units/ml) and 2 µl 10 × buffer (provided with enzyme). The reaction was made up to 20 µl with sterile distilled water. The reaction was incubated at 37°C for 1 hour and then at 65°C for 15 minutes to denature the enzyme.

Labelled oligonucleotides were purified using a Micro Bio-Spin 30 column (Bio-Rad). The column was mixed, left to settle and then spun twice at (5000 rpm, 4°C, 2 minutes, Heraeus Biofuge Fresco) to remove any excess liquid. The labelling reaction (+ 20 µl sterile distilled water) was loaded onto the column and spun at 5000 rpm at 4°C for 4 minutes, collecting the labelled oligonucleotides in a fresh tube.

The volume of labelled oligonucleotide recovered was measured and the concentration calculated assuming 90 % recovery of the oligonucleotide.

Preparation of labelled substrate

Buffers & solutions:
SSC (10 ×): 1.5 M sodium chloride, 150 mM sodium citrate, pH 7.0
TBE buffer (10 ×): 0.89 M Tris, 0.89 M boric acid, 0.02 M EDTA. To make 1 L, 108 g Tris, 55 g boric acid, 40 ml EDTA 0.5 M (pH 8.0), add water to 1000 ml
10 % polyacrylamide TBE gel: 33.3 ml sterile distilled water, 6 ml 10 × TBE, 20 ml 30 % acrylamide/bis-acrylamide (Severn Biotech), 0.6 ml 10 % ammonium persulphate, 30 µl TEMED (tetramethylethylenediamine)
5 × Saccharose loading dye (10 ml): 6 g saccharose (sucrose), 10 mg bromophenol blue, 10 mg xylene cyanol, made up to 10 ml with 1 × TBE buffer
TE buffer: 10 mM Tris-HCl (pH 8.0), 1 mM EDTA

Substrates were made by annealing oligonucleotides together, including a labelled oligonucleotide. The Holliday junction substrate, J12, was made using the following oligonucleotides: RGL13, RGL14, RGL15 and RGL16 (labelled). The partial replication fork substrate was made using the following oligonucleotides: MW12, MW14 and PM17 (labelled). These oligonucleotides are detailed in Table 3. An annealing reaction was carried out in 1 × SSC buffer and oligonucleotides were mixed at a ratio of 2.5:1, unlabelled:labelled DNA. The annealing reaction was heated to 95°C and left to cool slowly to room temperature overnight.

The substrates were purified on a pre-chilled 10% polyacrylamide TBE gel using a Bio-Rad Protean II gel kit. The samples were loaded with Saccharose loading dye. The gel was run in 2.5 L of 1 × TBE running buffer at 190 V for 2 hours. The gel was wrapped in Saran wrap and the radio-labelled substrates were visualised by exposure to X-Omat UV Plus film (Kodak). The film was used as a template for cutting the gel fragment containing the substrate and the substrate was eluted overnight in TE buffer containing 50 mM sodium chloride.

The volume of substrate recovered was measured. The activities of the substrate and labelled oligonucleotide were measured by adding a 2 µl sample to 4 ml scintillation fluid (Emulsifier scintillator plus, PerkinElmer) and counting the radioactivity using a scintillation counter (Tri-carb 2100TR, Packard). The activities measured were compared and used to estimate the concentration of the labelled substrate.

Branched DNA unwinding assays

Buffers & solutions:
Helicase buffer (5 ×): 100 mM Tris pH 7.5, 0.5 mg/ml BSA, 10 mM DTT, stored in 300 µl aliquots at −20°C.
Stop buffer (5 ×): 100 mM Tris pH 7.5, 0.5% SDS, 200 mM EDTA, 10 mg/ml Proteinase K
TBE buffer (10 ×): 0.89 M Tris, 0.89 M boric acid, 0.02 M EDTA. To make 1 L, 108 g Tris, 55 g boric acid, 40 ml EDTA 0.5 M (pH 8.0), add water to 1000 ml
5 × Saccharose loading dye (10 ml): 6 g saccharose (sucrose), 10 mg bromophenol blue, 10 mg xylene cyanol, made up to 10 ml with 1 × TBE buffer
10% polyacrylamide TBE gel: 33.3 ml sterile distilled water, 6 ml 10 × TBE, 20 ml 30% acrylamide/bis-acrylamide (Severn Biotech), 0.6 ml 10% ammonium persulphate, 30 µl TEMED (tetramethylethylenediamine)

The procedure for these assays was modified from previously published methods (McGlynn and Lloyd 1999). For standard 20 µl reactions, RecG protein was mixed with 0.3 nM [γ-^{32}P]-labelled substrate in helicase buffer (1 ×) plus 5 mM ATP and 5 mM magnesium chloride and incubated at 37°C for 20 minutes. To stop the reaction, 5 µl of stop buffer (5 ×) was added and it was incubated for a further 10 minutes at 37°C.

The percentage of substrate dissociation was analysed using the Bio-Rad Protean II gel kit, by adding 5 µl Saccharose loading dye (5 ×) to the samples and loading a 12 µl sample on a pre-chilled 10% polyacrylamide TBE gel. The gels were run in 2.5 L of 1 × TBE running buffer at 190 V for 90 minutes. Gels were transferred onto filter paper (Whatman 3MM) and covered with a layer of Saran wrap and dried using a gel dryer

(Bio-Rad, model 583). The gel was placed in a cassette and the signal visualised using a Kodak Storage Phosphor Screen, scanned with a STORM scanner system (Molecular Dynamics) and quantified using ImageQuant 5.2 (Molecular Dynamics). The gel was also exposed to X-Omat UV Plus film (Kodak) to obtain a quality image of the gel.

The rates of junction dissociation were measured using bulk reactions. All components of the reaction were mixed together except for the protein and pre-incubated at 37°C for 5 minutes. RecG was added to the bulk mix at the concentration indicated, to start the reaction. Samples (20 µl) were removed at the times indicated and incubated with 5 µl of stop buffer at 37°C for 10 minutes. After the reaction had been stopped the samples were loaded onto a pre-chilled 10% polyacrylamide TBE gel and analysed as above.

DNA binding assays

Buffers & solutions:

Binding buffer (5 ×): 250 mM Tris pH 8.0, 0.5 mg/ml BSA, 5 mM DTT, 25 mM EDTA, 30% glycerol, stored in 300 µl aliquots at −20°C

LIS buffer (10 ×): 67 mM Tris pH 8.0, 33 mM sodium acetate, 20 mM EDTA

4% polyacrylamide LIS gel: 45.4 ml sterile distilled water, 6 ml 10 × LIS, 8 ml 30% acrylamide/bis-acrylamide (Severn Biotech), 0.6 ml 10% ammonium persulphate, 30 µl TEMED (tetramethylethylenediamine)

DNA binding assays were essentially as described previously (Mahdi *et al.* 2003). For standard 20 µl reactions, RecG protein was mixed with 0.3 nM [γ-^{32}P]-labelled substrate in binding buffer (1 ×) and incubated on ice for 20 minutes. The percentage of substrate bound was analysed using the Bio-Rad Protean II gel kit and loading 15 µl samples on a pre-chilled 4% polyacrylamide gel in low ionic strength (LIS) buffer. Samples were loaded very carefully without dye to prevent binding from being disrupted. The gels were run in 2.5 L of 1 × LIS running buffer at 160 V for 75 minutes.

Gels were transferred onto filter paper (Whatman 3MM) and covered with a layer of Saran wrap and dried using a gel dryer (Bio-Rad, model 583). The gel was placed in a cassette and the signal visualised using a Kodak Storage Phosphor Screen, scanned with a STORM scanner system (Molecular Dynamics) and quantified using ImageQuant 5.2 (Molecular Dynamics). The gel was also exposed to X-Omat UV Plus film (Kodak) to obtain a quality image of the gel.

DNA replication in UV-irradiated *Escherichia coli* cells

The cell cycle in *E. coli* is completed when newly replicated chromosomes segregate and cell division occurs (Haeusser and Levin 2008; Reyes-Lamothe *et al.* 2008). In order to investigate the effect of DNA damage on replication and segregation of chromosomes, Christian Rudolph employed fluorescent microscopy to follow replication of the origin and terminus regions of the chromosome (Rudolph *et al.* 2007b). The origin and terminus regions were tagged with 240 copies of the *lac* and *tet* operators, respectively. The strain carried a plasmid encoding LacI-eCFP (enhanced cyan fluorescent protein) and TetR-eYFP (enhanced yellow fluorescent protein) repressors, which would bind to and decorate these arrays (Lau *et al.* 2003). To avoid a general effect of repressor-DNA binding, expression of the fluorescent repressors was only induced in samples taken for analysis. Expression of the repressors was induced by addition of arabinose to a sample of the culture 30 minutes prior to visualisation under the microscope (see page 64). During exponential growth, cells create overlapping cell cycles and therefore would be expected to contain several copies of the origin region (see page 12). Indeed, unirradiated cells had an overall origin to terminus ratio of 3:1, with the majority of cells having 3 or 4 origin foci and 1 or 2 terminus foci (Figure 12A, 0 min = no UV). Analysing multiplication of origin and terminus foci after UV irradiation should give an indication of the delay of replication after DNA damage.

An otherwise wild type strain carrying the *lac* and *tet* operator arrays and the plasmid encoding the fluorescent repressors was irradiated with 30 J/m² UV. This UV dose should induce ~1200 pyrimidine dimers per chromosome, which means there is approximately one dimer every 4 kb of double-stranded DNA, or one dimer every 8 kb per single strand (Sedgwick 1975; Courcelle *et al.* 2006; Rudolph *et al.* 2007b). After such a UV dose, the leading strand polymerase would encounter a lesion every 8 kb and thus, at a fork speed of 1000 nucleotides per second (Baker and Bell 1998), the fork could encounter a potentially blocking lesion within 8 seconds of irradiation.

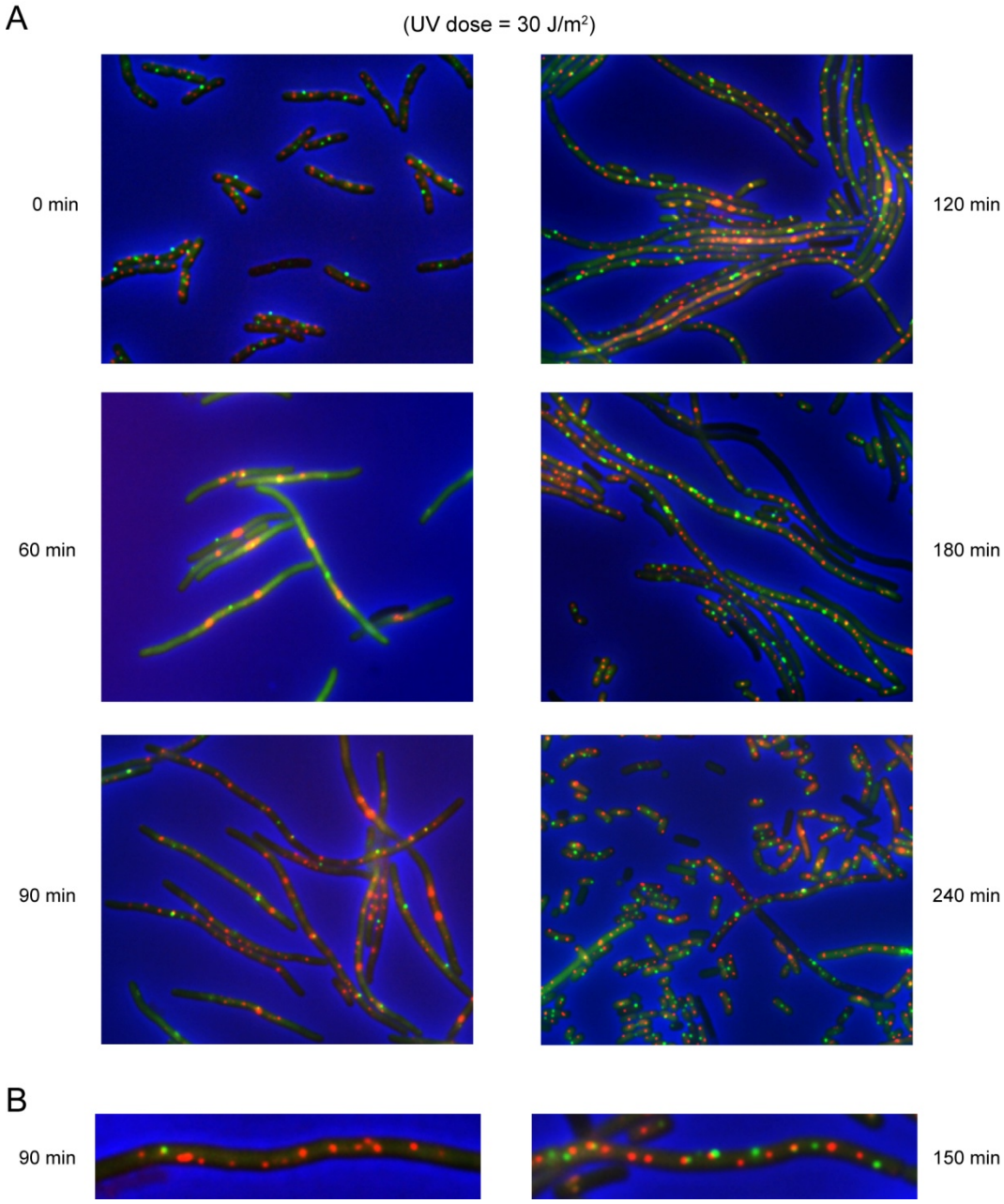

Figure 12. Effect of UV on cell cycle progression. (A) Fluorescence microscopy showing multiplication of origin (red foci) and terminus (green foci) regions of the chromosome. Pictures are combined phase contrast and fluorescence images. The strain used was APS345. The incubation time after UV irradiation is indicated. (B) Enlargements of filaments from a repeat of the experiment in A. Experiment performed and figure produced by Christian Rudolph.

Irradiation caused the cells to filament and by 60 minutes after irradiation, whilst the origin to terminus ratio remained largely unchanged, the origin foci gave a very intense signal (Figure 12A). The high signal intensity of the origin foci had mostly disappeared

by 90 minutes after irradiation. However, the number of origin foci had increased to an average of 12.5 per cell and these foci were spread along the filaments. At this stage the number of terminus foci per filament was still low (Figure 12A,B). This suggests that the origin of replication continues to fire after UV irradiation, supporting previous studies (Billen 1969). The number of foci indicated that origin firing occurred roughly every 30 minutes. Since the unirradiated cells grow with a measured doubling time of 30.4 minutes this suggests that not only does the origin fire after UV, but in most cells it continues to fire at the normal rate.

The pattern of foci changed dramatically around 120-150 minutes after irradiation. Not only did the number of terminus foci increase to an average of 4.6 per filament, these foci were also spread along the filaments and interspersed with the origin foci (Figure 12A,B), suggesting that the replicated chromosomes were segregating along the filaments ready for cell division. Indeed, after 180 minutes normal sized cells began to appear with a more normal origin to terminus ratio, and by 240 minutes these cells dominated the population and few filaments remained.

The data suggest that at early time points after irradiation, replication forks are blocked and thus, replication of the terminus region is delayed. This supports models proposing that replication forks stall and require time-consuming processing (McGlynn and Lloyd 2002; Michel *et al.* 2004; Rudolph *et al.* 2006). The origin of replication continues to fire at the normal rate, but after a relatively high UV dose the inter-lesion distance is small and so the newly set up forks cannot travel far before stalling. Therefore, stalled forks would accumulate somewhere near to the origin of replication preventing this region from segregating and leading to an intense origin focus. After a period of time the replication forks are able to resume replication. Fork progression away from the origin would allow the region to segregate and explains the apparently sudden increase in the number of origin foci. Eventually the terminus region is replicated and the chromosomes can fully segregate and the cells divide.

There are several types of DNA synthesis after UV irradiation

Many of the studies of replication after UV have been dependent upon measures of net DNA synthesis (Rupp and Howard-Flanders 1968; Donaldson *et al.* 2004; Courcelle *et al.* 2005). However, the data described above, have implications for models proposing that replication forks continue to progress towards the terminus with little delay, by reinitiating downstream of lesions (Rupp and Howard-Flanders 1968). These models were based on studies of net DNA synthesis, but the increased number of origin foci after irradiation clearly shows that the origin of replication continues to fire and therefore contributes to net synthesis. This means the delay in net synthesis might not represent the delay at existing replication forks. I wanted to assess the relative contributions of existing replication forks and origin firing to net synthesis.

DnaA functions specifically to initiate replication and is therefore an essential protein. A strain carrying the *dnaA46* mutant allele is temperature-sensitive; the strain will grow at 30°C, but not at 42°C (see Figure 50 for the wild type *dnaA* DNA and protein sequence and Figure 51 for the sequence changes in the *dnaA46* allele). The temperature-sensitive protein does not function at higher temperatures, meaning that replication cannot be initiated. This mutant should reveal the level of net synthesis attributable to origin firing after UV irradiation and therefore the contribution of replication forks existing at the time of irradiation.

Newly synthesised DNA can be labelled by growing cells in a medium that contains a labelled DNA base such as [^{3}H]thymidine, which is incorporated into the DNA during replication. The level of radioactive label incorporated can be quantified by taking samples from a culture and precipitating the chromosomal DNA using trichloroacetic acid (see page 63). This method measures net incorporation, which is the sum of the incorporated label minus any label removed by DNA degradation. The experiments depend upon using *thyA* mutant strains, which require thymine in the medium in order to grow and so incorporate levels of [^{3}H]thymidine that allow robust measurements of DNA synthesis. Therefore all cultures contained an amount of cold (unlabelled) thymidine to ensure growth. To ensure that the data were directly comparable, after UV

all cultures, including all controls, were shifted to 42°C, at which temperature-sensitive mutants do not initiate replication.

The total level of [^{3}H]thymidine incorporated into the DNA of an unirradiated wild type culture increases with time because the growing cells are replicating their DNA. The rate of incorporation in a wild type strain after UV irradiation was reduced, suggesting that DNA synthesis was delayed for at least 10 minutes, consistent with previous studies (Figure 13, Khidhir *et al.* 1985; Courcelle *et al.* 1997). After this delay, DNA synthesis continued at a similar rate to that in unirradiated cells.

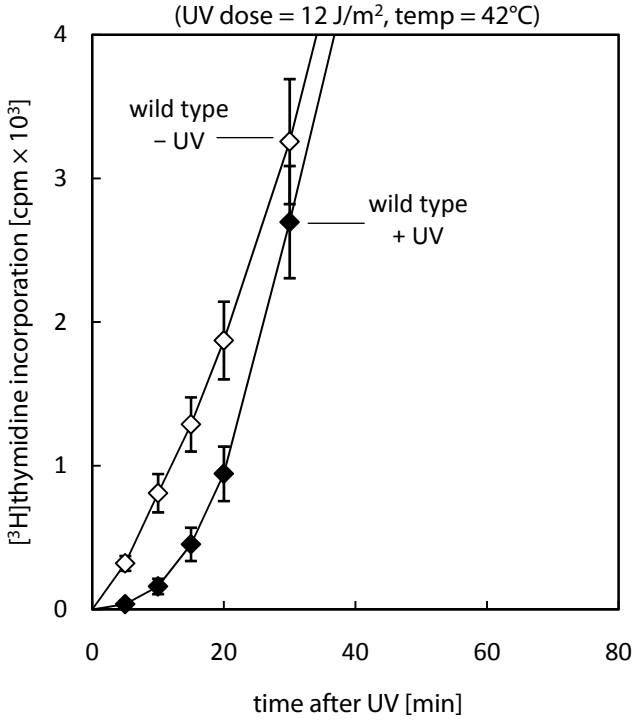

Figure 13. Effect of UV on DNA synthesis. [^{3}H]thymidine incorporation in a wild type strain (N1141). Data are the mean (±SE) of three experiments.

The *dnaA46* allele was moved into strains via transduction by selection for a linked allele, *tnaA*::Tn*10*. [^{3}H]thymidine incorporation was measured in a *tnaA* single mutant with and without UV, as a control. The *tnaA* mutant looks like a wild type strain; it has no effect on incorporation either before or after UV irradiation (Figure 14). Unirradiated *dnaA46* cells shifted to 42°C continue incorporating [^{3}H]thymidine for some time, before levelling off (Figure 15). At 42°C no new rounds of replication are initiated in *dnaA46* cells, but the existing rounds of replication lead to incorporation until they are completed.

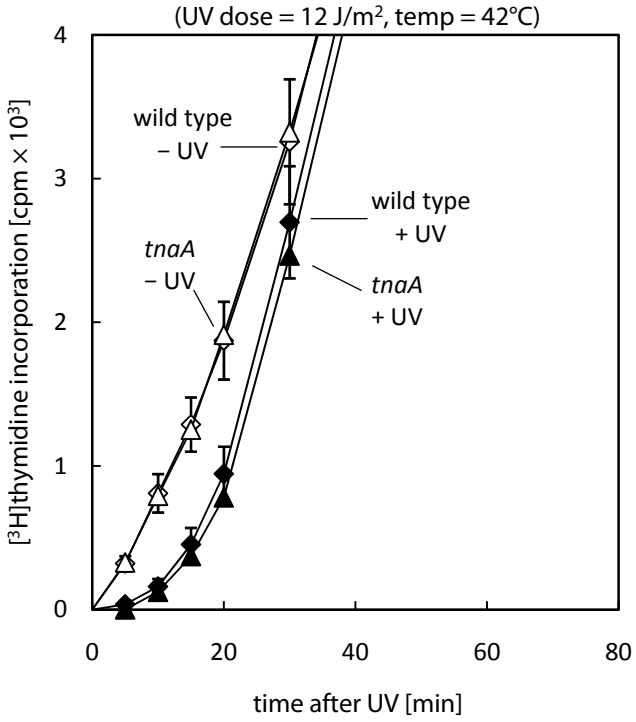

Figure 14. DNA synthesis is not affected by *tnaA*. [³H]thymidine incorporation in wild type (N1141) and *tnaA* (AU1074) cells. Data for *tnaA* are the mean of two experiments that gave very similar values. The data for the wild type are reproduced from Figure 13 for comparison.

After UV irradiation, the level of incorporation in *dnaA46* cells is much lower than in wild type cells, showing that *oriC* firing contributes significantly to the level of net synthesis measured in the wild type (Figure 15). This is consistent with the fluorescent microscopy data of Christian Rudolph showing that the origin continues to fire even when the terminus cannot be replicated (Figure 12). However, the incorporation in irradiated *dnaA46* cells is significantly higher than in unirradiated cells, as also reported by Jonczyk & Ciesla (1979). It is most likely due to initiation of DnaA-independent stable DNA replication (iSDR), which is induced after DNA damage (see page 39, Kogoma 1997). Indeed, by 70 minutes after irradiation, the *dnaA46* cells have incorporated more than twice the amount of [³H]thymidine than the unirradiated cells, suggesting that new forks have been set up. Since UV induces DnaA-independent synthesis, the analysis of *dnaA* mutants does not reveal the level of incorporation due to forks present at the time of irradiation. The *dnaA* experiment was repeated with two other temperature-sensitive alleles, *dnaA167* and *dnaA204* (see Figure 50 for the wild type *dnaA* DNA and protein

sequence and Figure 51 for the sequence changes in the mutant alleles), and almost identical results were obtained (Figure 16).

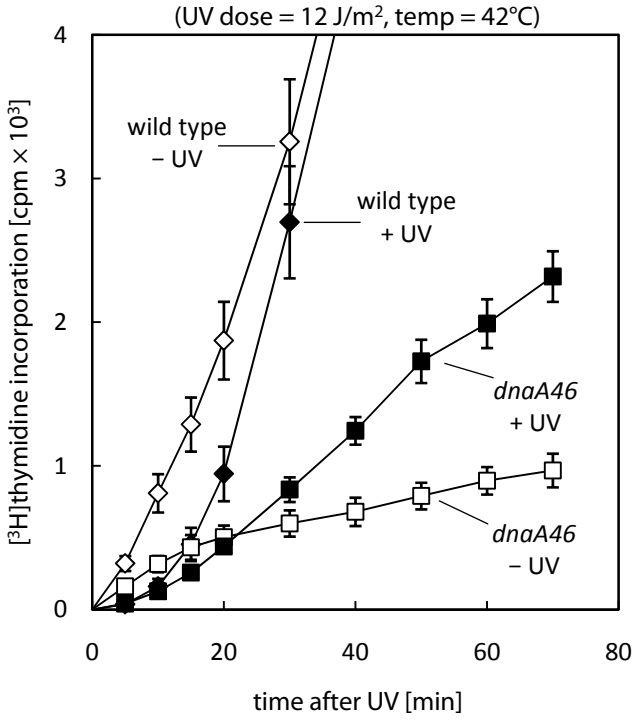

Figure 15. Effect of UV on DNA synthesis in *dnaA46* strains. [³H]thymidine incorporation in wild type (N1141) and *dnaA46* (AU1068) cells. Data for unirradiated *dnaA46* cells are the mean (±SE) of five experiments. Data for irradiated *dnaA46* cells are the mean (±SE) of four experiments. The data for the wild type are reproduced from Figure 13 for comparison.

The data presented so far indicate that a large fraction of the synthesis measured in wild type cells after UV irradiation is comprised of DnaA-dependent *oriC* firing and UV-induced DnaA-independent synthesis. Together these two types of synthesis mask the incorporation attributable to replication forks present at the time of irradiation and thus, the true extent of the delay at these forks. Therefore, measures of total net synthesis are not suitable for studying the effect of UV irradiation on existing replication forks.

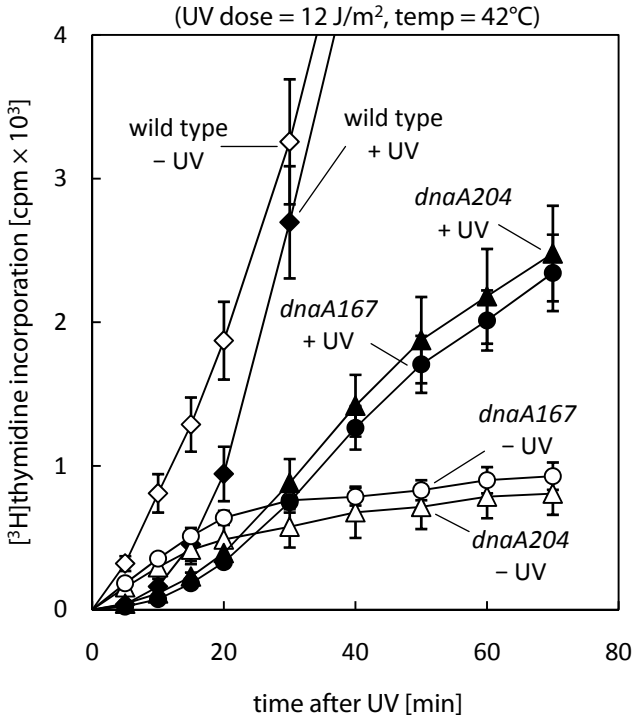

Figure 16. Effect of UV on DNA synthesis in *dnaA* strains. [³H]thymidine incorporation in wild type (N1141), *dnaA167* (AU1093), and *dnaA204* (AU1094) cells. Data are the mean (±SE) of three to four experiments. The data for the wild type are reproduced from Figure 13 for comparison.

Origin firing and excision repair contribute significantly to the amount of net DNA synthesis measured after UV irradiation

Rupp and Howard-Flanders (1968) studied net synthesis after UV irradiation in nucleotide excision-defective *uvrA* cells, which could not repair the lesions. Since the lesions could not be repaired, they assumed that the total delay measured was equivalent to the sum of the delays caused by individual lesions. Therefore, based on the number of lesions induced, they calculated that replication forks are delayed by ~10 seconds per lesion (Rupp and Howard-Flanders 1968). The recent demonstration by Heller & Marians (Heller and Marians 2006a), that replication *in vitro* can be primed *de novo* downstream of a lesion on the leading strand, has brought attention back to the model of Rupp & Howard-Flanders.

However, as demonstrated above, origin firing and UV-induced synthesis will mask the delay in progression of existing forks and are likely to lead to an underestimate of this

delay. Therefore, the total level of [³H]thymidine incorporation was compared in *uvrA* and *dnaA46 uvrA* strains at 42°C after UV.

Incorporation in unirradiated *uvrA* cells is similar to that measured in wild type cells (compare Figure 13 and Figure 17), just as incorporation in unirradiated *dnaA46 uvrA* cells, is similar to *dnaA46* cells (compare Figure 15 and Figure 17).

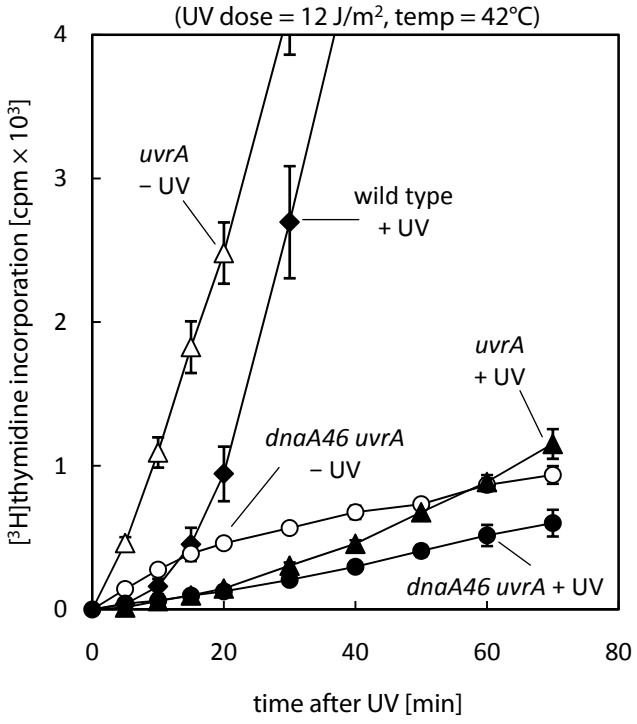

Figure 17. Effect of UV on DNA synthesis in *uvrA* cells. [³H]thymidine incorporation in wild type (N1141), *uvrA* (AU1075) and *dnaA46 uvrA* (AU1072) cells. Data are the mean (±SE) of three to six experiments. Data for the wild type are reproduced from Figure 13 for comparison.

After UV irradiation the incorporation measured in *uvrA* cells is much lower than that in wild type cells, in fact it is lower than in a *dnaA* culture (compare Figure 15 and Figure 17). Incorporation in the *dnaA uvrA* double mutant was even lower than in *uvrA* cells, demonstrating that origin firing still has a significant effect on the level of incorporation in an *uvrA* background (Figure 17). UV-induced synthesis is also detectable, but after this dose it is substantially delayed (12 J/m², data not shown). This synthesis is readily detectable after a lower UV dose (5 J/m², Figure 18). Since there is no excision repair in *uvrA* cells, this rules out the possibility that UV-induced synthesis is due to the filling in of gaps created during excision repair. These data demonstrate that the total delay of

incorporation measured by Rupp & Howard-Flanders in *uvrA* cells was an underestimate of the delay in progression of existing forks. Any estimates made from the *dnaA uvrA* double mutant will also be inaccurate because they will not take into account the level of UV-induced replication.

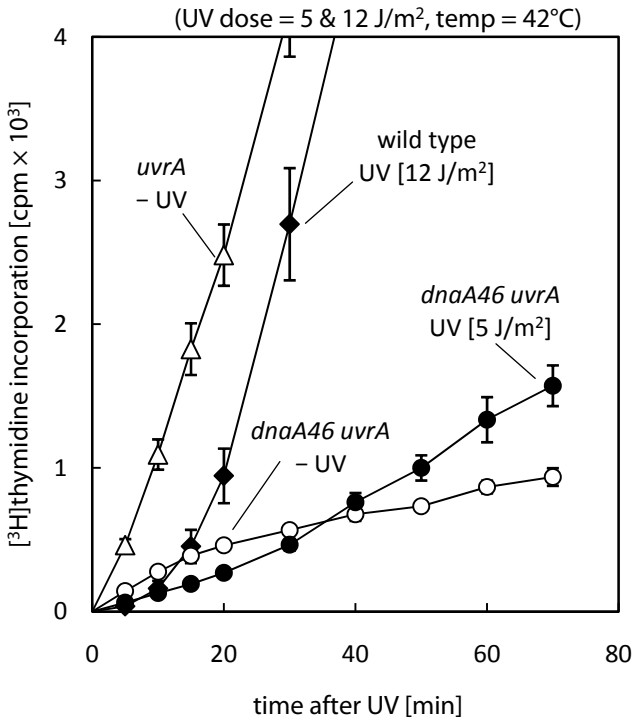

Figure 18. UV-induced synthesis is detectable in *uvrA* strains. [³H]thymidine incorporation in wild type (N1141), *uvrA* (AU1075) and *dnaA46 uvrA* (AU1072). Data for *dnaA46 uvrA* (5 J/m²) are the mean (±SE) of three experiments. All other data are reproduced from Figure 17 for comparison.

After a lower UV dose, the level of incorporation in *uvrA* cells is much improved (Figure 19). The amount of incorporation resulting from *oriC* firing after 5 J/m² in *uvrA* cells is substantially higher than that after 12 J/m², indicating that origin firing results in less DNA synthesis after a higher UV dose. Presumably this is due to an increased level of damage at or near to *oriC*, which in *uvrA* cells cannot be removed. Forks coming from the origin may not progress very far before stalling and might also limit the ability of the origin to fire again. A high UV dose might therefore influence the ability of origins to fire if the lesions cannot be removed, which could explain the complete lack of DNA synthesis measured in *uvrA* mutants after much higher UV doses (Courcelle *et al.* 1999; Courcelle *et al.* 2005; Courcelle *et al.* 2006).

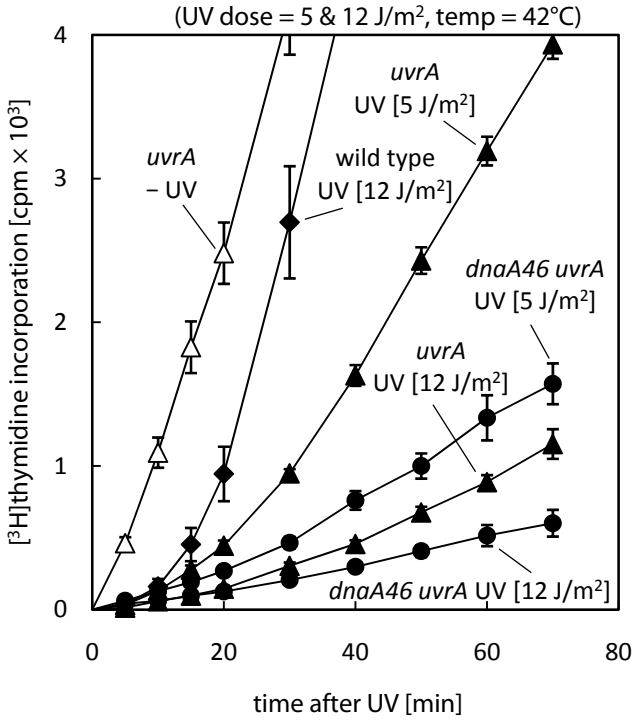

Figure 19. Changing the UV dose affects *uvrA* strains. [³H]thymidine incorporation in wild type (N1141), *uvrA* (AU1075) and *dnaA46 uvrA* (AU1072). Data for *uvrA* (5 J/m²) are the mean (±SE) of three experiments. All other data are reproduced from Figure 17 and Figure 18 for comparison.

Total net synthesis is not suitable for studying existing replication forks

The contribution of replication restart to DNA synthesis after UV irradiation and therefore the extent of the delay in progression of existing replication forks is masked by origin firing and UV-induced synthesis. This means that the average delay per lesion at existing forks cannot be calculated based on measurements of total net [³H]thymidine incorporation. Estimations of the average delay per lesion have been calculated for several of the strains used in these studies in order to demonstrate the effect of origin firing and therefore the dangers of ignoring the fact that several types of synthesis occur after irradiation. The following calculations are based upon these assumptions:

(1) Cells growing in minimal salts medium have two forks per cell on average.

(2) Each fork takes ~40 minutes to replicate from *oriC* to the terminus.

(3) With a genome of ~4600 kb, replication proceeds in unirradiated cells at a rate of ~2 kb per second (4600 kb is replicated in 2400 seconds).

(4) A UV dose of 1 J/m² induces ~40 pyrimidine dimers per chromosome (Sedgwick 1975; Courcelle *et al.* 2006), which means there is approximately one dimer every 115 kb. Therefore a UV dose of 12 J/m² introduces a lesion every 10 kb or so, and a dose of 5 J/m² introduces a lesion every 23 kb.

The total delay in incorporation was estimated using the data in Figure 13 and Figure 19, which measured [³H]thymidine incorporation after a UV dose of 12 J/m² or 5 J/m². The delay was estimated as the extra time taken for irradiated cells to incorporate the same amount of [³H]thymidine as in unirradiated wild type cells. The estimations were based upon the amount of incorporation in *dnaA uvrA* cells at 70 minutes after irradiation. The unirradiated wild type cells took 8 minutes to incorporate this level of [³H]thymidine. The times taken to reach this level of incorporation and therefore the estimated delays for each strain are as follows:

(1) Unirradiated wild type = 8 min, no delay.
(2) Irradiated wild type = 16 min, a delay of 8 min.
(3) Irradiated *uvrA* = 43 min, a delay of 35 min.
(4) Irradiated *dnaA uvrA* = 70 min, a delay of 62 min.
(5) Irradiated *uvrA* (5 J/m²) = 23 min, a delay of 15 min.
(6) Irradiated *dnaA uvrA* (5 J/m²) = 33 min, a delay of 25 min.

The unirradiated wild type should replicate ~960 kb of DNA in 8 minutes. Assuming that irradiated cells have replicated the same length of DNA, the replication forks would have encountered ~96 pyrimidine dimers after a UV dose of 12 J/m², or 42 pyrimidine dimers after a UV dose of 5 J/m². Using the estimated delays for each strain, the average delay per dimer can be calculated to the nearest second:

(1) Wild type = 5 sec.
(2) *uvrA* = 22 sec.
(3) *dnaA uvrA* = 39 sec.
(4) *uvrA* (5 J/m²) = 21 sec.
(5) *dnaA uvrA* (5 J/m²) = 36 sec.

These calculations reinforce the conclusions drawn from the experiments. UV lesions delay fork progression, and by removing lesions the nucleotide excision repair system promotes replication. This can be seen by the increased delay in *uvrA* mutants in

comparison to the wild type. A significant amount of the synthesis measured after UV irradiation is due to *oriC* firing (compare delay in *uvrA* with *dnaA uvrA*).

The calculations above demonstrate that averaging the total delay in incorporation over the number of lesions induced, whilst ignoring the fact that new synthesis is initiated, is a dangerous analysis to make. Given that net thymidine incorporation in a *dnaA uvrA* strain includes UV-induced synthesis, it is still not clear what the measured delay in incorporation actually reflects. For example, the assumption is that if unirradiated cells have replicated ~960 kb then the irradiated cells must have replicated the same distance, however the incorporation equivalent to this amount of synthesis is not just coming from existing replication forks. Indeed it could all result from multiple initiations of synthesis at *oriC* or elsewhere. Any estimates made, as to the delay per lesion, are dangerous unless it is certain as to where the incorporation measured is coming from, i.e. in a strain in which both origin firing and UV-induced synthesis are eliminated.

Replication after UV irradiation is dependent upon DnaC

DnaC binds to the replicative helicase DnaB and is necessary for DnaB loading during replication initiation at *oriC* (see page 10, Messer 2002; Kaguni 2006) and also during restart of stalled forks at sites away from *oriC* (Marians 2004). Initiation of iSDR is also dependent upon DnaC (Kogoma 1997). A strain carrying the *dnaC7* mutant allele is temperature-sensitive. At 42°C the protein does not function, meaning that DnaB cannot be loaded to initiate any new synthesis or reloaded during replication restart. Therefore, by monitoring incorporation in this mutant at 42°C, only synthesis from replisomes existing at the time of the temperature shift will be measured. Shifting the cells to 42°C immediately after UV irradiation, should give an indication of the contribution of existing replisomes to total incorporation after UV.

In unirradiated *dnaC7* cells incorporation continued for a time at 42°C before levelling off, consistent with existing rounds of replication coming to an end and no new rounds initiating (Figure 20).

Almost no incorporation was detected in *dnaC7* cells after UV irradiation (Figure 20). This suggests that after UV, replication is dependent upon reloading of DnaB, even

though pyrimidine dimers are not expected to block progression of the replicative helicase. It appears that replisomes present at the time of irradiation cannot progress past many pyrimidine dimers; they stall and disassemble, at least partially. Therefore, restart of replication after UV irradiation requires reloading of the replicative helicase.

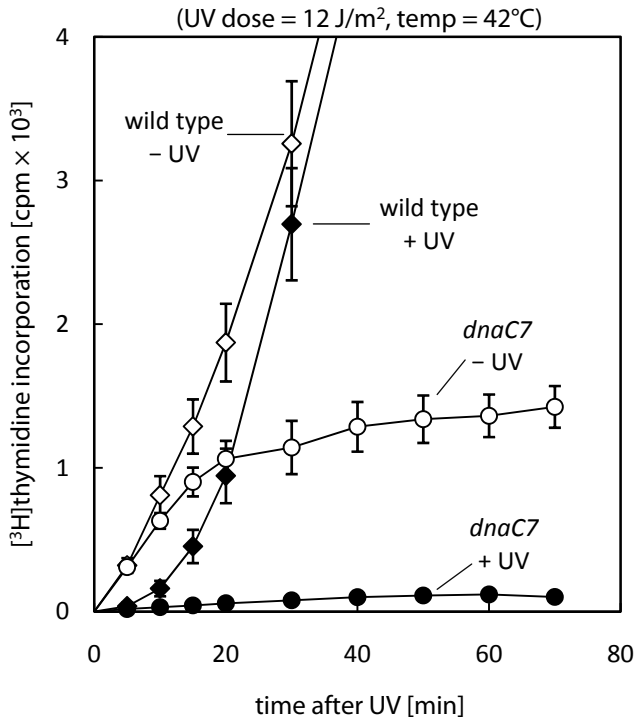

Figure 20. Effect of UV on DNA synthesis in *dnaC7* strains. [³H]thymidine incorporation in wild type (N1141) and *dnaC7* (AU1080) cells. Data are the mean (±SE) of three experiments. The data for the wild type are reproduced from Figure 13 for comparison.

The inter-lesion distance after a UV dose of 12 J/m² is one pyrimidine dimer every 9 kb of double-stranded DNA or one dimer every 18 kb per single strand. This means there would be approximately 18 seconds after UV irradiation before the replisome meets a leading strand template lesion. However, since there is a slight delay between irradiation and the addition of [³H]thymidine, any DNA synthesis leading up to replication fork stalling probably occurs before the label is added. Although this result does not exclude the idea that new replisomes may assemble downstream of a lesion and allow forks to resume replication with only a minor delay (Heller and Marians 2006a), it does suggest that whilst lagging strand template lesions may be skipped, existing replisomes are

unable to proceed past many leading strand template lesions, if any, before stalling and disassembling.

Discussion

The majority of the data presented in this chapter have been published (Rudolph *et al.* 2007b). In eukaryotes, UV irradiation can induce checkpoint responses that prevent cell cycle progression during DNA repair. In particular, the G_1-S transition checkpoint inhibits replication initiation whilst there are lesions present. This delay allows the cells time to repair the lesions so that when replication does initiate it can proceed unhindered (Sancar *et al.* 2004; Callegari and Kelly 2007). Whilst studying the effects of UV irradiation upon replication and cell cycle progression in *E. coli* using fluorescent microscopy, Christian Rudolph observed that the origin of replication appears to fire at times when the terminus region cannot be replicated. Analysis of the multiplication of origin foci after UV shows that *oriC* continues to fire at the normal rate in the majority of cells, indicating that *E. coli* is lacking a control mechanism that inhibits replication initiation when the template is damaged.

The data presented in this chapter demonstrate that undamaged origins of replication continue to fire after UV irradiation and that UV induces synthesis that is independent of the initiator protein, DnaA. These data are supported by experiments using 5-Bromo-2'-deoxyuridine (BrdU) to label newly synthesised DNA (Rudolph *et al.* 2007b). The BrdU labelled DNA was digested with a rare-cutting restriction enzyme and the DNA fragments separated using pulsed-field gel electrophoresis. These experiments allow visualisation of the chromosomal locations, as well as the timing, of DNA synthesis after irradiation. BrdU incorporation in wild type cells demonstrated that synthesis is greatly reduced in all chromosomal fragments during the first 15-20 minutes after UV, indicating that progression of all replication forks is delayed. However, those fragments situated at or near to *oriC* appeared to give an even stronger signal than expected at early times after irradiation (Rudolph *et al.* 2007b). BrdU incorporation experiments in *dnaA* cells at 42°C after UV showed that all fragments had a similar initial delay to that observed in wild type cells, but the disproportionate labelling of the *oriC*-proximal fragments was no longer evident (Rudolph *et al.* 2007b). Therefore, the BrdU incorporation, fluorescent

microscopy and [^{3}H]thymidine incorporation data together, demonstrate that pre-existing replication forks are delayed for at least 15-20 minutes after UV irradiation, and that *oriC* continues to fire during this delay. The true extent of this delay is masked by *oriC* firing and DnaA-independent UV-induced synthesis in assays measuring net DNA synthesis.

Interestingly, the BrdU experiments demonstrate that replication is delayed for approximately 15-20 minutes but that after this period incorporation appears to occur synchronously in all fragments. After a relatively high UV dose (30 J/m^2), ~80 % of the pyrimidine dimers are removed within 20 minutes (Courcelle *et al.* 1999; Rudolph *et al.* 2007b), which coincides with the time at which replication restarts.

Finally, I have also demonstrated that synthesis after UV irradiation depends upon DnaC activity (Figure 20), indicating that at least the replicative helicase needs to be reloaded and possibly the entire replisome. This observation fits with *in vitro* studies showing that when the leading strand polymerase stalls, the replicative helicase continues to unwind the template leaving behind the polymerase stably bound at the arrest site (McInerney and O'Donnell 2007). The actions of RecFOR and RecA have been shown to displace the stalled polymerase *in vitro* (McInerney and O'Donnell 2007), supporting the idea that the entire replisome needs to be reloaded. This implies that whilst replication forks do recover and continue replication, the replisomes completing replication are not those that were set up at *oriC*.

The data support models proposing that UV lesions cause replication forks to stall and that these stalled forks require processing in order for replication to be restarted (see page 30). It is thought that lagging strand template lesions do not block progression of replication forks and synthesis of the lagging strand continues at the next Okazaki fragment, leaving a gap opposite the lesion. Leading strand template lesions, however, have been proposed to block the leading strand polymerase, leading to uncoupling of the leading and lagging strand polymerases (Higuchi *et al.* 2003; Pages and Fuchs 2003). Progression of the replication fork whilst the leading strand is blocked would expose a single-stranded region of the leading strand template onto which RecA could be loaded, inducing the SOS response. The action of RecA or other fork binding proteins, could lead to replication fork reversal, moving the lesion back into double-stranded DNA, creating an opportunity for repair of the lesion and of the stalled fork. After the fork has been

processed, reloading of the replicative helicase via DnaC and either the PriA- or PriC-dependent restart pathway would enable replisome assembly and restart of replication.

Why should replication be delayed for at least 15 minutes? DnaC dependent reloading of the replicative helicase and perhaps replisome assembly may be a slow process. But also, since *oriC* continues to fire and UV induces extra synthesis, there is increased demand within the cell for replisome components, which are limited in supply (~10 copies of the polymerase III holoenzyme per cell, Kelman and O'Donnell 1995). It has been suggested that RecA might be involved in stabilisation of a stalled fork (Courcelle *et al.* 1999) and also in replication fork reversal (Seigneur *et al.* 1998; Robu *et al.* 2001). Processing of stalled forks may also require time. It has been suggested that cells deliberately delay replication restart after DNA damage in order to allow repair proteins additional time to repair the lesions (Opperman *et al.* 1999).

During the period that replication is delayed after UV irradiation, SOS induction will have led to an increase in the expression of proteins involved in nucleotide excision repair (Michel 2005; Rudolph *et al.* 2006). This enables the rapid repair of the majority of lesions (Courcelle *et al.* 1999; Rudolph *et al.* 2007b), such that when replication does resume, the path to the terminus region should be relatively clear. The data in Figure 13 and the BrdU data of Christian Rudolph demonstrate that the rate of replication after the delay is similar to that in unirradiated cells (Rudolph *et al.* 2007b), consistent with the idea that after the delay replication restarts and proceeds unhindered. Cells lacking the ability to repair lesions, such as *uvrA* mutants, are very UV sensitive and suffer from extensive delays in synthesis after UV (Figure 17, Rupp and Howard-Flanders 1968; Courcelle *et al.* 1999; Rudolph *et al.* 2007b), consistent with the idea that replication forks stall at lesion after lesion and require replisome reassembly each time.

The idea of replication forks stalling at a leading strand lesion and requiring a period of time equivalent to the total replication delay in order to restart is in contrast to the idea of forks proceeding past lesions, resuming synthesis downstream and leaving gaps opposite the lesions. Based on measured delays in incorporation, Rupp & Howard-Flanders (1968) suggested that replication forks would be delayed on average by approximately 10 seconds per lesion. However, the net [^{3}H]thymidine incorporation data presented in this chapter provide evidence that origin firing and UV-induced synthesis contribute significantly to the synthesis measured after UV and that averaging the total

delay in synthesis over the number of lesions induced is very misleading. The overall delays in synthesis measured in *uvrA* cells (35 min) and *dnaA uvrA* cells (62 min) are in line with data showing that in repair-deficient cells a leading strand lesion can be bypassed by translesion synthesis after a delay of ~50 minutes (Pages and Fuchs 2003).

Rupp & Howard-Flanders observed that after UV irradiation, newly synthesised DNA appeared to be in short fragments, which were converted to larger fragments over time. By considering the lesion density and the size of the small fragments, they assumed that the newly synthesised DNA contained gaps opposite lesions, which were filled in over time (Rupp and Howard-Flanders 1968). Further experiments demonstrated that photoreversal of lesions promoted this conversion of small DNA fragments into larger fragments, supporting the idea that the gaps were opposite lesions (Bridges and Sedgwick 1974). However, newly synthesised DNA, initiated at *oriC* or induced by UV (DnaA-independent), would appear initially as small fragments that would increase in size over time. This newly initiated synthesis would also be affected by the lesion density and would progress further if lesions were repaired by photoreversal, creating larger DNA fragments. The data in Figure 15 suggests that such synthesis represents a large majority of the newly synthesised DNA after UV, providing a new explanation for these early observations.

Why is origin firing allowed to continue as normal when replication restart is delayed after DNA damage? If the origin continues to fire, the newly set up forks will also stall at lesions. However, when replication resumes, a cluster of replication forks can proceed from the origin region to replicate the chromosome, creating multiple chromosomal copies at once. Cell filaments can therefore divide down into multiple viable cells which may, at least in part, compensate for the delay caused by the initial blocking lesions. This idea is supported by the observation that after a low UV dose, cellular division in a wild type culture is delayed for a period, but then resumes at a rate higher than that in unirradiated cells. The viable cell count of the irradiated culture appears to catch up with that of the unirradiated culture and then continues to increase at the same rate as unirradiated cells (Rudolph *et al.* 2008).

The data presented cannot eliminate the idea that a replication fork can proceed past some lesions on the leading strand template, leaving gaps to be filled in by recombination. However, the much delayed replication of the terminus region that has

been observed in *uvrA* mutants (Rudolph *et al.* 2007b), can be explained if replication stops or slows down dramatically soon after encountering a leading strand template lesion. DNA synthesised in a UV-irradiated *uvrA* strain does contain gaps, but it is not clear whether these are in both nascent strands (Iyer and Rupp 1971). Gaps are likely to occur if the first lesion encountered by a fork is on the lagging strand template. However, wild type cells are unlikely to have to deal with many gaps, given the rapid stalling of replication forks after UV and the apparent coupling of restart with lesion removal. It is possible that replication forks may be able to proceed past a few leading strand template lesions (Heller and Marians 2006a), but a more sensitive assay would be required to distinguish between progression past a leading or lagging strand lesion.

Given that the majority of wild type cells can survive UV doses that induce more than a thousand pyrimidine dimers, the idea of replication forks stalling for a period of time is very appealing. The delay in restart would mean that only a small fraction of the lesions induced would actually be encountered by a replication fork. If replication forks were to proceed, as suggested by Rupp & Howard-Flanders, even when nucleotide excision repair was active, many gaps could be left behind the forks each requiring a recombination event to repair them. Recombination can lead to genetic rearrangements and the intermediates can also delay chromosome segregation and cell division. An elevated level of recombination is one of the cellular phenotypes observed in some of the human disorders characterised by cancer predisposition (Hickson 2003). There is increasing evidence suggesting that recombination is limited in both eukaryotes (Krejci *et al.* 2003; Veaute *et al.* 2003) and prokaryotes (Flores *et al.* 2005; Mahdi *et al.* 2006). Delaying replication restart after DNA damage may be another means of avoiding the dangers of excessive recombination.

RecFOR promotes efficient restart after UV irradiation

Several studies have demonstrated that restart is delayed in UV-irradiated cells lacking RecA and also in cells lacking any of the RecFOR proteins (Courcelle *et al.* 1997; Courcelle *et al.* 2003). Induction of the SOS response is delayed in *recFOR* cells (Hegde *et al.* 1995; Whitby and Lloyd 1995), but lesions are removed at a rate comparable to wild type cells, ruling out a simple explanation for the observed delay (Courcelle *et al.* 1999). It was also observed that extensive nascent DNA degradation occurs in cells lacking RecF after UV irradiation (Courcelle *et al.* 1997). This excessive degradation is due to the combined action of RecQ helicase and RecJ exonuclease, which also degrade nascent DNA to a lesser extent in wild type cells before replication recovers after UV (Courcelle and Hanawalt 1999). Courcelle *et al.* (2006) suggested that nascent DNA degradation is necessary in order for efficient replication restart after UV irradiation. The RecFOR proteins have been shown to enable loading of RecA protein onto single-stranded DNA coated with SSB (single-stranded DNA binding protein) (Morimatsu and Kowalczykowski 2003). It was suggested that the function of the RecFOR proteins and RecA is to prevent excessive degradation and thus, stabilise and protect stalled replication forks (Courcelle *et al.* 2003). This is a similar concept to what has been proposed in eukaryotes. In yeast cells, the replicative polymerase and the putative helicase subunits are thought to be stabilised at stalled forks. When this replication checkpoint is disabled, the cells suffer from an increase in chromosomal rearrangements (Branzei and Foiani 2007; Tourriere and Pasero 2007).

[^{3}H]thymidine incorporation was used to study the effect of UV irradiation on DNA synthesis in cells lacking any of the RecFOR proteins or RecA. Interestingly, no synthesis was observed for at least 90 minutes after UV and it was concluded that DNA synthesis does not recover without these proteins (Courcelle *et al.* 2003). However, I have demonstrated that there are several modes of DNA synthesis after UV, resulting from (a) DnaA-dependent origin firing, (b) DnaA-independent UV-induced synthesis (iSDR) and (c) restart of replication at pre-existing forks (see page 81, Rudolph *et al.* 2007b). Therefore, this observed lack of synthesis in UV-irradiated *recF* cells reported by

Courcelle *et al.* (2003), does not only have implications for replication restart, it suggests that all modes of replication are inhibited. Whilst studies have shown that iSDR is slightly reduced in cells lacking RecF (Asai *et al.* 1993), there is no evidence that RecFOR or RecA are required for *oriC* firing. I investigated the effect of UV irradiation on replication and cell cycle progression in *E. coli* cells lacking RecF or RecO, in order to assess whether or not origin firing and UV-induced synthesis are delayed in these cells.

Multiplication of the origin is delayed in recO mutants

Fluorescent microscopy was employed to follow replication and segregation of the origin and terminus regions of the chromosome in cells lacking RecF or RecO. The procedure was identical to that employed by Christian Rudolph to study wild type cells (see pages 64 and 78, Rudolph *et al.* 2007b). The pattern of multiplication of the origin and terminus foci in *recF* and *recO* mutants after UV irradiation was compared with that observed in a wild type strain (see page 78, Rudolph *et al.* 2007b). The initial results for *recF* and *recO* mutants were virtually identical and therefore I will present data for the *recO* derivative only.

Unirradiated *recO* cells appeared similar to wild type cells; with regard to cell size they were not filamentous and they had similar numbers of origin and terminus foci (Figure 21, also refer to quantification of foci in Figure 23). Multiplication of origin and terminus foci was analysed in a *recO* derivative after a UV dose of 30 J/m², the most informative time points are presented in Figure 21 and images for all of the time points can be found in the appendix (Figure 52). By 60 minutes after irradiation, similar to the wild type, *recO* cells showed very little change in the number of origin and terminus foci. However, whilst the intensity of the origin foci increased dramatically in wild type cells, this was not evident in *recO* cells. This indicates that origin firing is delayed in *recO* cells after UV. Although the cells did filament after UV, the filament lengths were more variable, which might be explained by delayed induction of the SOS response (Hegde *et al.* 1995; Whitby and Lloyd 1995).

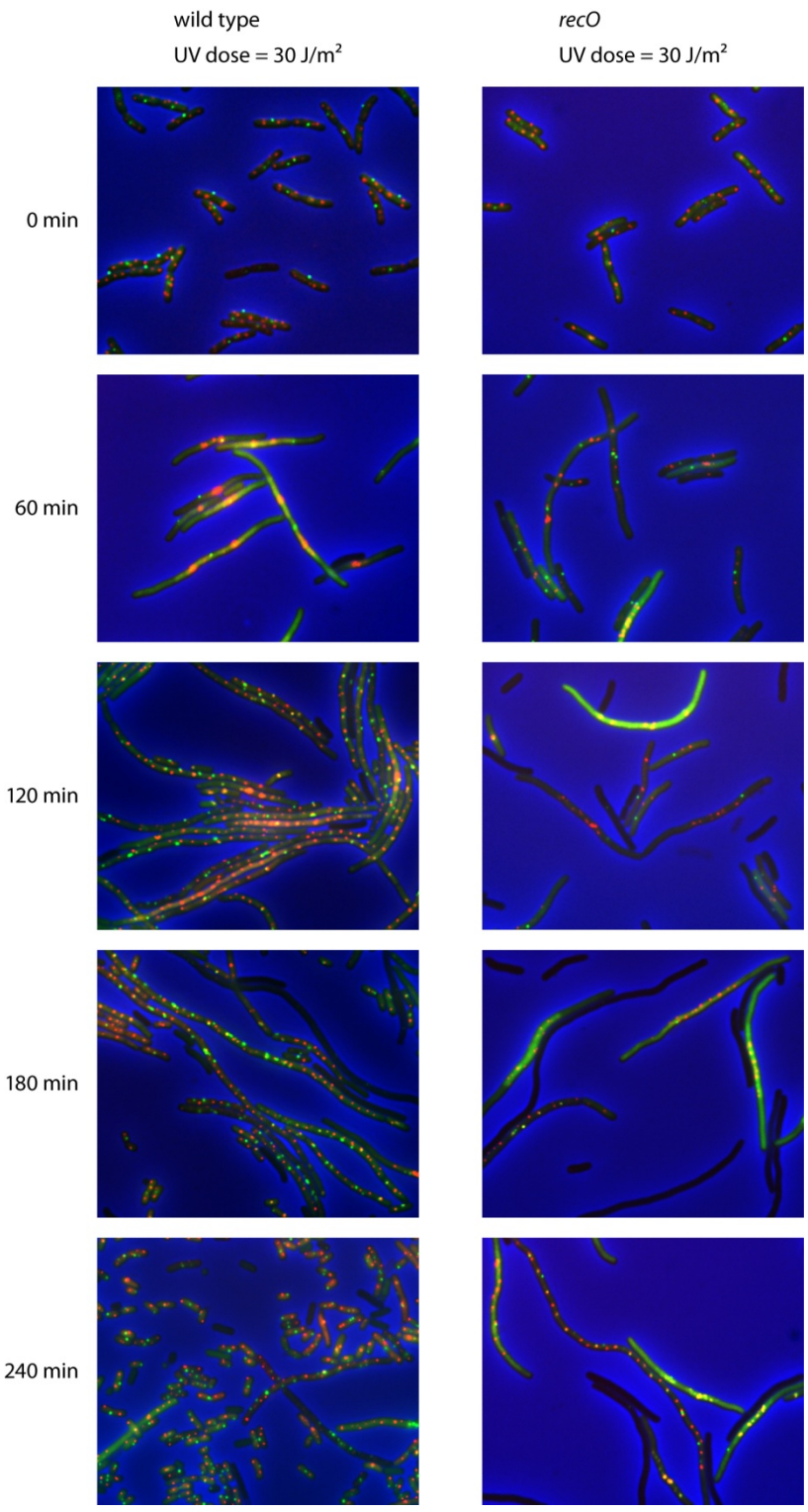

Figure 21. Effect of UV on cell cycle progression in *recO* cells. Fluorescence microscopy showing multiplication of the origin (red foci) and terminus (green foci) regions of the chromosome. Pictures are combined phase contrast and fluorescence images. The strain used was AU1101 (*recO*). The UV dose as well as incubation times after irradiation are indicated. Data for the wild type (APS345) were reproduced for comparison from Figure 12.

The origin foci in *recO* cells showed some increase in both number and signal intensity by 90 minutes after irradiation, whilst the number of terminus foci remained low. Over the course of the experiment the origin foci spread along the filaments showing that at least the origin region of the chromosome was beginning to segregate. In contrast to the wild type, by 240 minutes after irradiation only some cells showed an increase in the number of terminus foci and normal sized cells were few and far from dominating the culture. In fact, the majority of cells showed either no foci (>75%) or aggregation of both fluorescent repressor proteins (10%), probably signalling cell death.

Whilst more than 60% of wild type cells survive a UV dose of 30 J/m², only 2-3% of *recO* cells survive ((Trautinger *et al.* 2005) and data not shown). The experiment was repeated using a lower UV dose of 5 J/m², which increases the survival of *recO* cells to about 50% (Trautinger *et al.* 2005; Rudolph *et al.* 2008). A dose of 5 J/m² should induce ~200 pyrimidine dimers per chromosome, which means there is approximately one dimer every 23 kb of double-stranded DNA, or one dimer every 46 kb per single strand (Sedgwick 1975; Courcelle *et al.* 2006; Rudolph *et al.* 2007b). The leading strand polymerase would encounter a lesion every 46 kb and given that replication forks move at a speed of 1000 nucleotides per second (Baker and Bell 1998) this means the fork could encounter a potentially blocking lesion within 46 seconds.

Multiplication of the origin and terminus foci in *recO* cells after the lower UV dose (5 J/m²) occurs in a similar pattern to that observed in wild type cells after the higher UV dose (30 J/m²). The most informative time points are presented in Figure 22 and images for all of the time points can be found in the appendix (Figure 52). Although the intense origin foci were not observed in *recO* cells, the number of foci had already increased by 60 minutes after irradiation. It is assumed that an inability to segregate newly replicated origins results in the intense foci observed in wild type cells (see page 78). The inter-lesion distance might be large enough after this lower UV dose, such that forks resulting from origin firing do not stall close enough to the origin to prevent segregation of this region. Whilst origin firing appeared to be delayed after a UV dose of 30 J/m², this lower UV dose does not appear to affect origin firing.

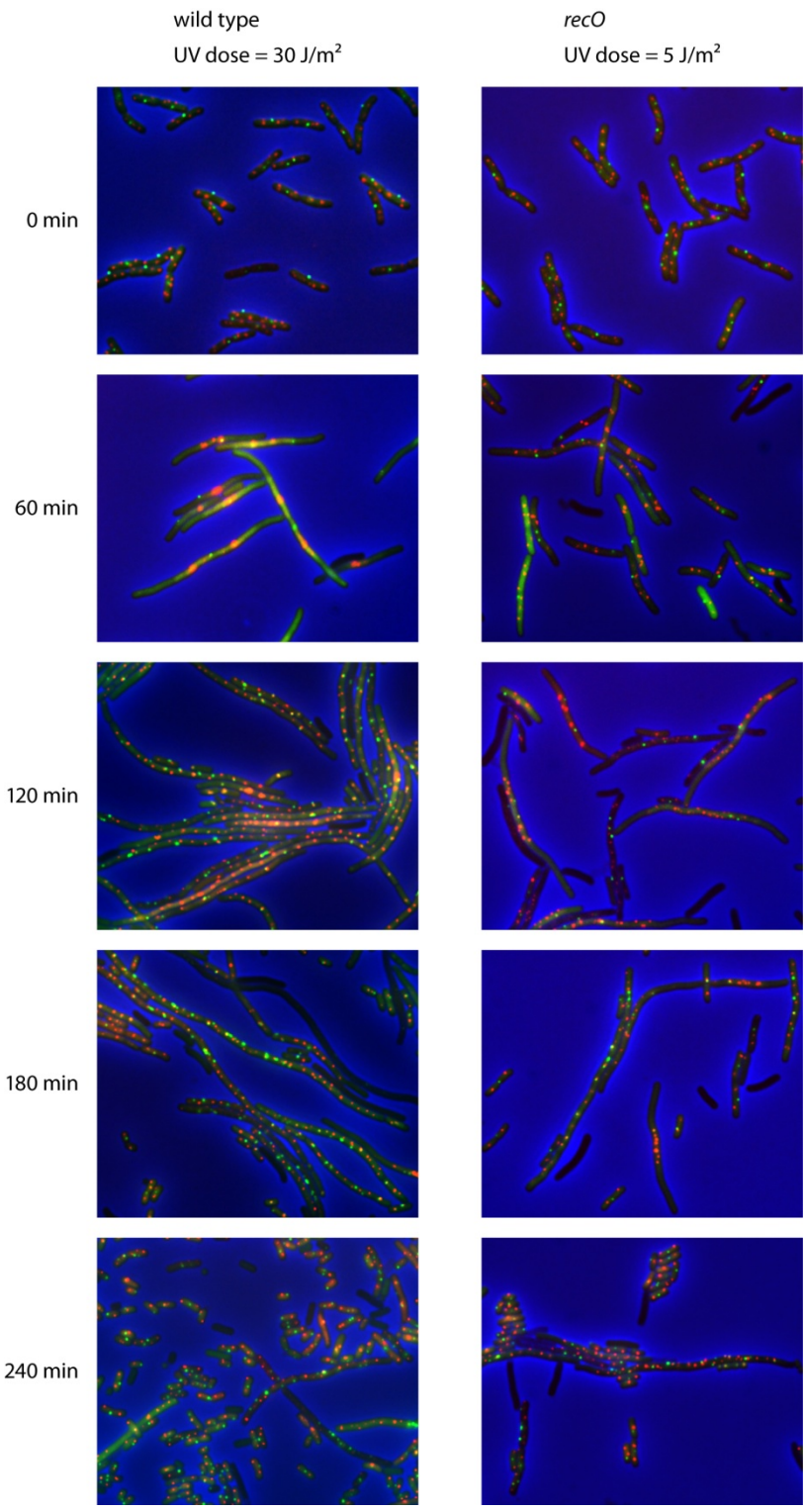

Figure 22. Effect of a low UV dose on cell cycle progression in *recO* cells. Fluorescence microscopy showing multiplication of the origin (red foci) and terminus (green foci) regions of the chromosome. Pictures are combined phase contrast and fluorescence images. The strain used was AU1101 (*recO*). The UV dose as well as incubation times after irradiation are indicated. Data for the wild type (APS345) were reproduced for comparison from Figure 12.

After 90 minutes, the origin foci had spread along the length of the filaments, confirming that the region was able to segregate. The terminus foci multiplied between 120 and 180 minutes after UV irradiation, but the multiplication was delayed in comparison to the wild type (compare images taken after 120 minutes, Figure 22). As with the wild type, normal sized cells began to appear around 180 minutes after irradiation and these dominated the culture by the end of the experiment. I would like to re-iterate that whilst the wild type was irradiated with 30 J/m², the pattern observed in *recO* cells was only comparable after a much lower UV dose (5 J/m²).

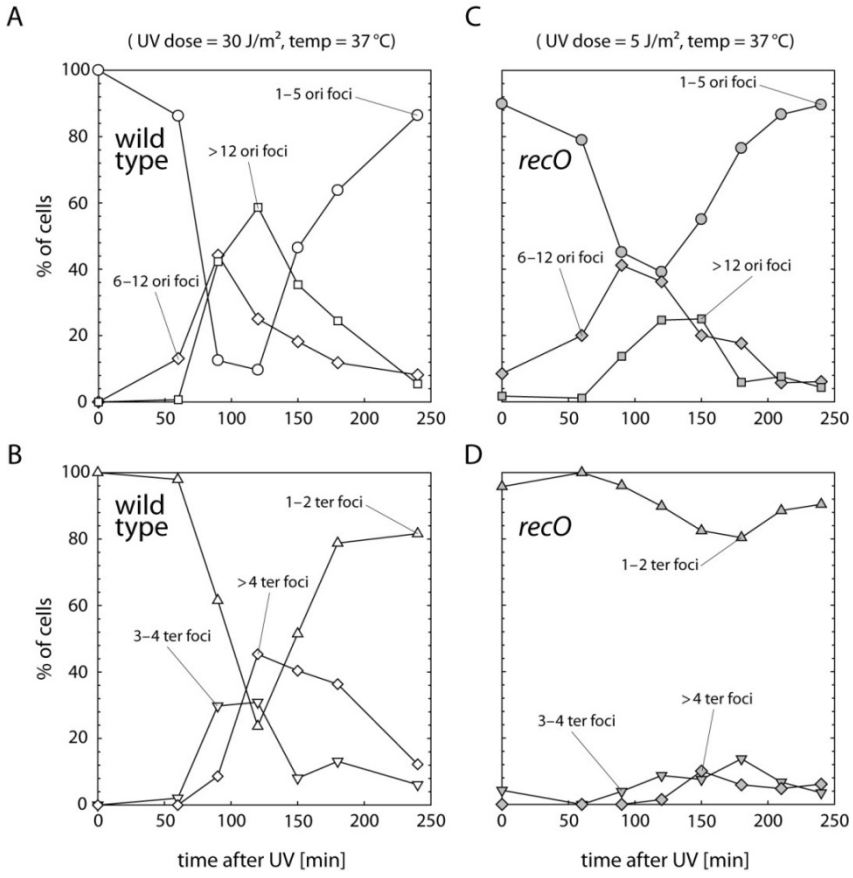

Figure 23. Effect of UV on multiplication of origin and terminus foci in *recO* cells. For quantification of the number of origin and terminus foci, several microscopical fields were analysed from at least two independent experiments. The foci were counted in every cell and then the cells were divided into classes. For origin foci, 90% of unirradiated cells contained no more than 5 origin foci, leading to the definition of the first class of cells, with 1-5 foci. Cells with 6-12 origin foci were classed as cells with an elevated number of foci. A third class, with more than 12 origin foci represented cells with a highly elevated number of foci. Similar classes were defined for the terminus foci (1-2 [95% in unirradiated cells], 3-4 and more than 4 foci per cell). (A-B) Changes in the number of origin (A) and terminus (B) foci per cell in wild type cells irradiated with 30 J/m² UV. The strain used was APS345. (C-D) Changes in the number of origin (C) and terminus (D) foci per cell in *recO* cells irradiated with 5 J/m² UV. The strain used was AU1101.

The numbers of origin and terminus foci were quantified by counting the number of foci per cell at each time point. The changes in foci number are illustrated in Figure 23. The quantification supports the observations discussed above. Whilst multiplication of the origin foci in *recO* cells after the lower UV dose showed a similar pattern to wild type, multiplication of the terminus foci was delayed. Cells which lacked either the origin or terminus signal or both were not included in the quantification. However, it was noted that the number of *recO* cells lacking both signals increased rapidly after irradiation, reaching a maximum of 50 %. This value supports the data showing that 50 % of *recO* cells survive a UV dose of 5 J/m² (Trautinger *et al.* 2005; Rudolph *et al.* 2008).

The delay in multiplication of the terminus region in *recO* cells after UV was supported by quantification of the origin to terminus ratio in synchronised *recO* cells. The experiments were carried out using temperature-sensitive *dnaC7* derivatives and cells were synchronised by shifting the cultures to 42°C for 45 minutes prior to irradiation. After irradiation, cultures were incubated at 30°C so that replication was able to initiate and samples were taken and processed. The ratio of the origin and terminus regions was investigated by Southern analysis using probes specific for these regions (see page 65). The results for the *recO* derivative have been compared to the data of Christian Rudolph for wild type and *uvrA* derivatives (Rudolph *et al.* 2007b). In unirradiated wild type cells the origin to terminus ratio (set to 1 for zero samples, assuming that cells are fully synchronised) increased to a ratio of 1.5, showing that the cells initiate replication once the cultures are shifted back to 30°C (Figure 24A). If all cells initiate replication, the origin signal should double giving a ratio of 2 however, microscopic analysis showed that the cells were not perfectly synchronised (data not shown). After the initial increase the ratio remained relatively constant over ~90 minutes, consistent with a population of growing cells, which are expected to have an increased number of origins. By 90 minutes the ratio began to decrease, because the cells were entering stationary phase and no longer initiating replication (Rudolph *et al.* 2007b). The origin to terminus ratio in unirradiated *recO* cells changes over time in a similar way to wild type cells, except that the ratio in *recO* is slightly increased (Figure 24B). This probably reflects a slight overall delay in replication of the terminus due to spontaneous fork stalling, resulting in over-representation of the origin region.

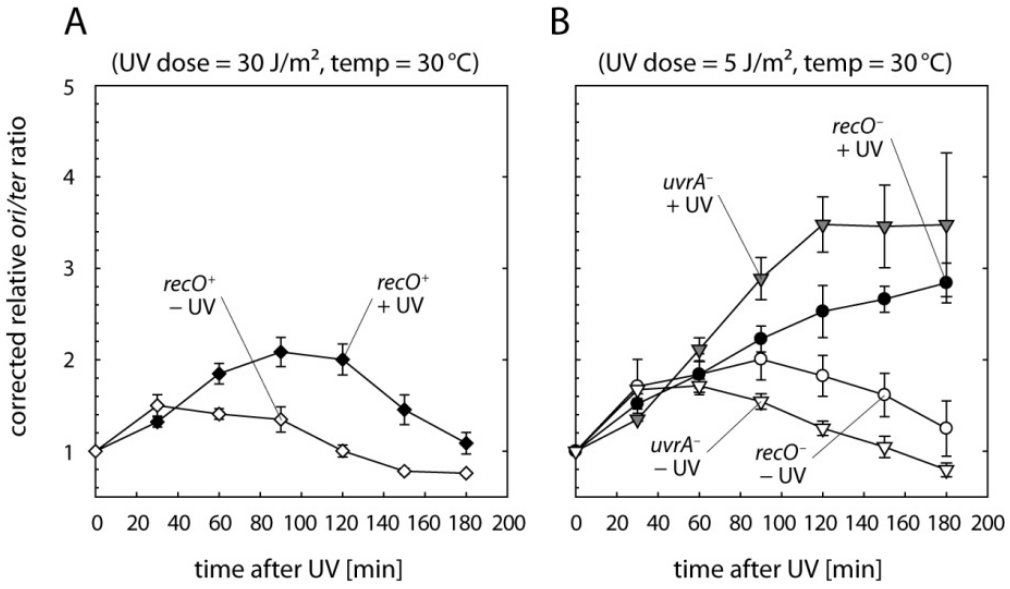

Figure 24. Effect of UV on multiplication of origin and terminus regions in *recO* cells. (A and B) Changes in the origin to terminus ratio during incubation of irradiated and unirradiated cells. The strains used were RCe79 (*dnaC7*), RCe120 (*dnaC7 uvrA*) and RCe190 (*dnaC7 recO*). The UV doses are indicated. Data are means (±SE) of three experiments. The data for RCe79 and RCe120 were reproduced for comparison from (Rudolph *et al.* 2007b).

In wild type cells irradiated with 30 J/m² UV, the origin to terminus ratio increased after a slight delay and it increased to a much greater extent than in unirradiated cells confirming that the origin is replicating at times when the terminus cannot. After 120 minutes the ratio decreased as the terminus region was finally replicated and the cells began to enter stationary phase (Figure 24A, Rudolph *et al.* 2007b). In *recO* cells, UV also slightly delayed the increase in the origin to terminus ratio, but in contrast to the wild type the ratio continued to increase for the duration of the experiment (Figure 24B). This confirms that replication of the terminus region is delayed in comparison to the wild type, in spite of the lower UV dose with which *recO* cells were irradiated (5 J/m²). This continuous increase in the origin to terminus ratio is similar to that observed in *uvrA* mutants (Figure 24B), but the increase is less rapid, suggesting that origin firing is affected in *recO* mutants even after the lower dose of 5 J/m².

These studies suggest that origin firing does occur in irradiated *recO* cells and given that 50 % of cells survive a UV dose of 5 J/m² the cells must complete chromosome replication, as indicated by multiplication of the terminus foci. However, the delay in the increase of the origin to terminus ratio in comparison to *uvrA* mutants indicates that

origin firing is delayed slightly in *recO* mutants. The fluorescent microscopy indicates that after a higher UV dose (30 J/m²) replication of the origin and terminus regions is dramatically delayed in comparison to the wild type, which may explain the complete lack of synthesis for 90 minutes observed in *recF* mutants in previous studies (Courcelle *et al.* 2003).

All modes of DNA synthesis are delayed in recO mutants

The fluorescent microscopy experiments using the *lac* and *tet* operator arrays, as well as the origin to terminus ratio experiments allow the analysis of replication of only two regions of the chromosome. DNA synthesis was measured using [³H]thymidine incorporation to give an overall picture of the level of synthesis in cells lacking RecFOR. As with the fluorescent microscopy, initial experiments demonstrated that the results were virtually identical in *recO* and *recF* cells, so only the data for *recO* cells are presented. Unirradiated *recO* cells incorporate [³H]thymidine at a similar rate to wild type cells (Figure 25) demonstrating that under normal growth conditions origin firing is not affected in cells lacking RecFOR.

The cells were irradiated with a UV dose of 12 J/m², so that the results would be directly comparable with those in the previous chapter. After this UV dose, all modes of DNA synthesis, although delayed, can still be observed in *uvrA* cells, which are much more UV sensitive than *recFOR* mutants (Figure 17 and data not shown). After UV irradiation, incorporation in *recO* cells is delayed for a substantially longer period than wild type cells but, after this delay, incorporation recovers and continues at a similar rate to that observed in unirradiated cells (Figure 25), consistent with previous studies (Courcelle *et al.* 1997). This shows clearly that although replication is severely delayed after UV, in contrast to the conclusion made by Courcelle *et al.* (2003), it does recover in cells lacking RecFOR and to a rate similar to unirradiated cells. The contrasting observations most likely reflect a difference in the UV doses used. Whilst Courcelle *et al.* generally use relatively high UV doses (25 J/m²) which kill the majority of *recFOR* mutant cells, the lower dose used here results in an approximately ten-fold higher survival rate ((Trautinger *et al.* 2005) and data not shown).

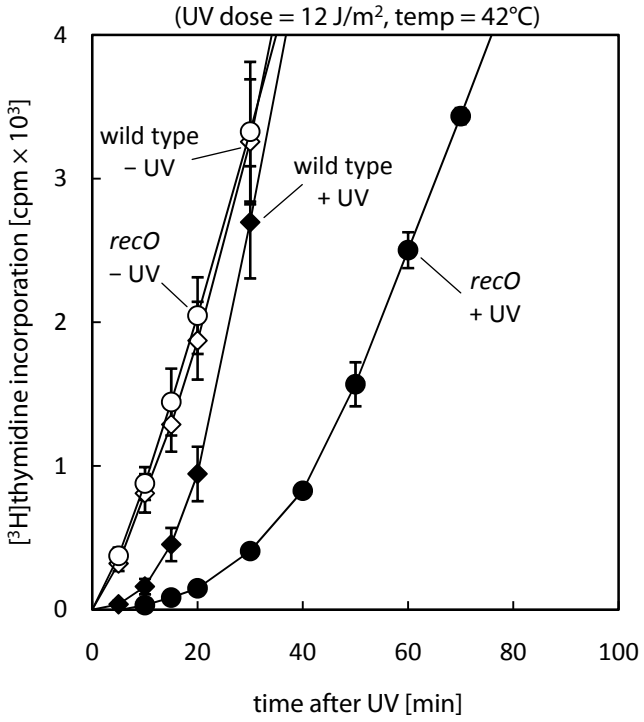

Figure 25. Effect of UV on DNA synthesis in *recO* cells. [³H]thymidine incorporation in wild type (N1141) and *recO* (AU1110) cells. Data for *recO* cells are the mean (±SE) of three experiments. The data for the wild type are reproduced from Figure 13 for comparison.

The majority of synthesis in wild type cells early after UV irradiation results from *oriC* firing and UV-induced synthesis (see page 81). Such a long delay of synthesis in *recO* cells after UV suggests that these modes of replication are delayed. The fluorescent microscopy and origin to terminus ratio experiments have already indicated that origin firing is delayed in *recO* mutants. DNA synthesis was monitored by [³H]thymidine incorporation in *dnaA46 recO* cells, in order to investigate if UV-induced synthesis is also delayed in *recO* mutants. Incorporation in unirradiated *dnaA46 recO* cells at 42°C is similar to that measured in *dnaA46* cells (Figure 26). Incorporation continues for some time and then levels off, consistent with existing rounds of replication coming to an end and no new rounds of replication initiating without functional DnaA. However, the level of incorporation in these two strains is quite different after UV. After an initial delay, *dnaA46* cells incorporate [³H]thymidine to a level significantly higher than that in unirradiated cells, consistent with the initiation of UV-induced synthesis (Figure 15). Incorporation in *dnaA46 recO* cells is considerably delayed in comparison to *dnaA46*, but after this delay incorporation continues and eventually exceeds the level measured in

unirradiated cells (Figure 26). This increase in incorporation can also be explained by the initiation of UV-induced synthesis (iSDR), but there is initially less of this synthesis than in *dnaA46* cells indicating that UV-induced synthesis is also delayed in cells lacking RecO. This is consistent with previous studies showing that iSDR is reduced in cells lacking RecF (Asai *et al.* 1993). The delayed SOS response observed in *recFOR* cells (Hegde *et al.* 1995; Whitby and Lloyd 1995) may be partially responsible for the delayed appearance of this mode of synthesis, since iSDR is dependent upon SOS induction (Kogoma 1997).

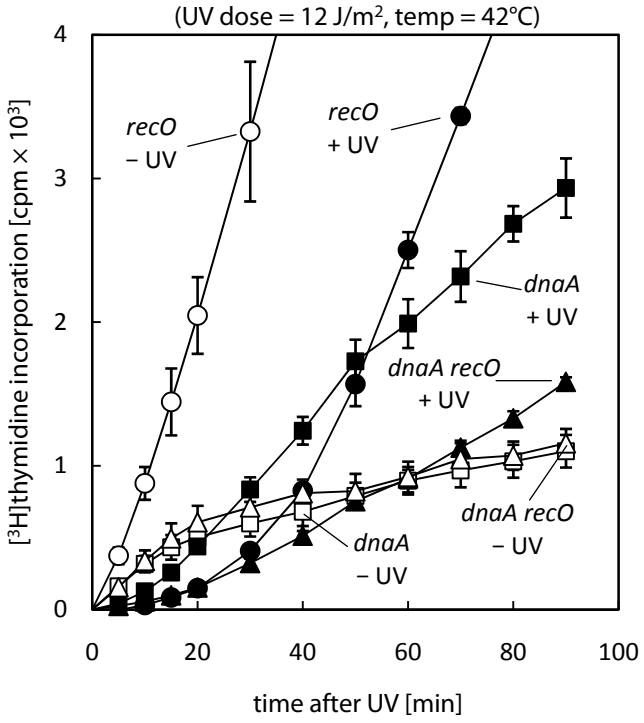

Figure 26. UV-induced synthesis is delayed in *recO* cells. [³H]thymidine incorporation in *recO* (AU1110), *dnaA46* (AU1068) and *dnaA46 recO* (AU1112) cells. Data for *dnaA46 recO* cells are the mean (±SE) of three experiments. The data for the *recO* (Figure 25) and *dnaA46* (Figure 15) are reproduced for comparison.

Taken together, these data suggest that RecFOR does promote efficient restart. After irradiation, all modes of synthesis are delayed in cells lacking RecFOR, but eventually synthesis recovers to a rate similar to that observed in unirradiated cells. The extent of the delay in cells lacking RecFOR appears to be dependent upon the UV dose used. The majority of the data presented in this chapter have been published (Rudolph *et al.* 2008).

Discussion

My previous experiments have shown that there are three modes of DNA synthesis after UV irradiation that contribute to [^{3}H]thymidine incorporation: DnaA-dependent initiation of replication at *oriC*, DnaA-independent UV-induced synthesis (iSDR) at other chromosomal locations and replication associated with restart of replication forks present at the time of irradiation (see page 78, Rudolph *et al.* 2007b). However, measurements of DNA synthesis in cells lacking RecFOR had indicated a complete lack of DNA synthesis for at least 90 minutes after UV, leading to the suggestion that replication does not recover in these cells (Courcelle *et al.* 2003). This lack of synthesis implied that, in addition to existing replication forks, UV-induced synthesis as well as initiation of replication at *oriC* were affected in irradiated *recF* cells. Although previous studies had shown that UV-induced synthesis was slightly reduced in *recF* mutants, this synthesis was still detectable (Asai *et al.* 1993) and no link has previously been made between RecFOR and *oriC* firing. The studies in this chapter have demonstrated that indeed all modes of DNA synthesis are delayed in cells lacking RecO, but that after a delay synthesis does recover and to a rate similar to that observed in unirradiated cells. This suggests that whilst RecFOR aids efficient restart, replication is capable of restarting in cells lacking RecFOR. DnaA-dependent origin firing and UV-induced synthesis still occur in irradiated *recO* mutants, but these new replication forks are also delayed. The data presented are consistent with experiments using BrdU labelling to study DNA synthesis at specific chromosomal locations within the cell. The BrdU experiments demonstrated that after a delay synthesis recovers at all chromosomal locations, confirming that replication is indeed able to restart in the absence of RecFOR (Rudolph *et al.* 2008).

The fluorescent microscopy data suggested that origin firing was increasingly delayed after a higher UV dose (compare 60 minutes image in Figure 21 & Figure 22). The origin to terminus ratio after the lower UV dose does not show a substantial delay in the increase of the ratio, indicating that the origin can fire soon after irradiation. However, the increase in the ratio is significantly less than that observed in *uvrA* cells, indicating that although the origin can fire, it is not capable of firing at the frequency observed in *uvrA* cells.

Why should origin firing be delayed after UV irradiation in cells lacking RecFOR? In the previous chapter it was observed that increased UV doses could affect origin firing in

uvrA cells, which were unable to remove the lesions. It was assumed that this was due to the persistence of lesions at or near to *oriC* preventing replication forks from progressing very far and limiting the ability of the origin to fire again (see page 85). However, previous studies have demonstrated that lesions in *recF* cells are removed with kinetics comparable to the wild type (Courcelle *et al.* 1999), so it is unlikely that persisting lesions are preventing origin firing in this case. Efficient excision repair does not mean that the template DNA is free of damage, previous replication forks may have stalled near to the origin and in *recO* cells these forks would suffer from a delay in restart. Whilst a leading strand template lesion could stall a replication fork, a lagging strand template lesion might simply be skipped leaving a gap (Meneghini and Hanawalt 1976; Higuchi *et al.* 2003; McInerney and O'Donnell 2004). Nascent strand gaps are filled in by recombination or by translesion synthesis, both of which are dependent upon the efficient loading of RecA via RecFOR (Kreuzer 2005; Fujii *et al.* 2006; Michel *et al.* 2007). Therefore, stalled replication forks or nascent strand gaps left near to *oriC* may prevent newly initiated replication forks from progressing very far and might also hamper the ability of *oriC* to fire at the normal rate in UV-irradiated cells lacking RecFOR.

If new replication forks initiated at *oriC* run into nascent strand gaps or stalled forks, they could run off the end of the nascent strands creating double-stranded DNA ends (Kuzminov 1995; Bidnenko *et al.* 2002). Such DNA ends would be targeted by exonucleases. In order to investigate the effect of origin firing on nascent DNA degradation, Christian Rudolph studied *dnaA46 recO* cells, in which origin firing could be prevented by shifting the culture to 42°C after UV. He demonstrated that origin firing results in a small amount of the extensive nascent DNA degradation observed in *recO* mutants (Rudolph *et al.* 2008). This supports the idea that replication initiated at *oriC* after UV might be limited by the damaged template in cells lacking RecFOR.

The [^{3}H]thymidine incorporation assays in *recO* mutants shed more light on the issue of replication fork progression past lesions. Can replication forks resume synthesis downstream of lesions on the leading strand template, leaving gaps behind? Re-priming of leading strand synthesis and replication fork progression past lesions should result in a detectable amount of synthesis if this is not a rare event. However, the complete lack of synthesis in *recO* cells for a substantial period after UV suggests that the majority of replication forks stall rather than progress.

The idea that the function of the RecFOR proteins and RecA is to prevent excessive degradation and thus, stabilise and protect stalled replication forks (Courcelle *et al.* 2003), was tested by simulating a delay in replication restart in the presence of RecFOR and RecA (Rudolph *et al.* 2008). I have demonstrated that all replication is blocked in UV-irradiated *dnaC7* temperature-sensitive cells and that no restart occurs, at least in the 2-hour period monitored after UV (Figure 20 and data not shown). Christian Rudolph found that if replication restart was prevented by shifting *dnaC7* cells to 42°C immediately after UV, these cells suffered from extensive DNA degradation even though RecFOR and RecA were present. The degradation pattern was similar to that observed in irradiated *recFOR* cells, suggesting that degradation occurs in these cells because replication restart is delayed rather than because the forks are not protected. Therefore, degradation is limited in wild type cells by efficient, RecFOR-mediated replication restart (Rudolph *et al.* 2008).

In conclusion, the data presented so far, combined with those of Christian Rudolph, indicate that after UV irradiation the majority of replication forks stall almost immediately at leading strand template lesions. The replisome dissociates from the fork structure, at least partially, and processing involving RecFOR-mediated loading of RecA enables replication to restart. By the time replication restarts, the majority of the lesions have been removed and replication can proceed at a rate similar to unirradiated cells. Some nascent strand degradation occurs whilst replication forks are stalled, but this is limited by the ability of the cells to restart replication efficiently. In the absence of RecFOR, greatly delayed replication restart exposes the nascent DNA strands to extensive exonuclease attack (Rudolph *et al.* 2007b; Rudolph *et al.* 2008).

Pathological replication in UV-irradiated *Escherichia coli* cells lacking RecG

Extensive genetic studies in the Lloyd laboratory suggested that the RuvABC and RecG proteins have partially overlapping activities with respect to DNA repair and recombination (Lloyd 1991; Lloyd and Buckman 1991). It became clear that the RuvAB proteins catalyse branch migration of Holliday junctions, enabling RuvC to resolve these to duplex products via a sequence specific endonuclease activity ((Zerbib *et al.* 1998) and references therein). It was thought that RecG might also act in the late stages of recombination, providing an alternative pathway for Holliday junction resolution (Lloyd 1991).

The idea of RecG playing a role in resolving recombination intermediates was supported by *in vitro* studies showing that RecG can catalyse branch migration of Holliday junctions (Lloyd and Sharples 1993). However, with the exception of the RusA resolvase, which is normally very poorly expressed (Mandal *et al.* 1993; Sharples *et al.* 1994; Mahdi *et al.* 1996), an alternative Holliday junction specific nuclease that could act alongside RecG has not been found. But investigation of the RusA resolvase provided evidence that RecG can act on Holliday junctions *in vivo*. Activation of RusA can suppress a *ruv* mutant, but only if RecG is present (Mandal *et al.* 1993; Mahdi *et al.* 1996). Since RusA can only resolve Holliday junctions, it is thought that RecG must provide the branch migration activity necessary to suppress a *ruv* mutation (Mandal *et al.* 1993; Sharples *et al.* 1994; Mahdi *et al.* 1996).

RecG has also been implicated in replication restart. PriA-dependent loading of the replicative helicase is thought to be the major replication restart pathway (see page 36, Heller and Marians 2006b) and helicase deficient mutants of PriA, such as PriAK230R encoded by *priA300*, which are still capable of assembling a replisome (Heller and Marians 2006b), have been shown to suppress the defects of *recG* single mutants (Al-Deib *et al.* 1996; Jaktaji and Lloyd 2003). RecG can also catalyse branch migration of forked structures *in vitro*; in fact it is able to interconvert fork and Holliday junction structures (McGlynn and Lloyd 2000). It was proposed that RecG may act at stalled replication forks

and catalyse replication fork reversal, enabling repair of the lesion and thus aiding replication restart (see page 30, McGlynn and Lloyd 2000). Whilst there is evidence for a role in recombination and in restart of stalled replication forks, there is also evidence to suggest that RecG performs another role within the cell.

Strict controls act to limit replication initiation to a DnaA-dependent event at *oriC* once per cell cycle (see page 12), but alternative, DnaA-independent, modes of DNA synthesis can be initiated at other sites under special circumstances. These modes of synthesis are referred to as stable DNA replication (see page 39). Cells lacking RecG or RNase HI exhibit DnaA-independent replication, referred to as constitutive stable DNA replication (cSDR) (Hong *et al.* 1995). RNase HI can degrade the RNA from R-loops (Stein and Hausen 1969; Hausen and Stein 1970) and RecG has been shown to unwind R-loops *in vitro* (Vincent *et al.* 1996). It is thought that the persistence of R-loops in strains lacking either RNase HI or RecG, leads to the initiation of cSDR (Kogoma 1997). DNA damage can also induce a form of DnaA-independent replication, referred to as inducible stable DNA replication (iSDR) (reviewed by (Kogoma 1997). Inducible SDR has also been observed in undamaged cells lacking RecG (Hong *et al.* 1995). These observations suggest another potential *in vivo* role for RecG; to limit the initiation of replication such that it occurs only in a DnaA-dependent manner at *oriC*.

In order to further investigate the *in vivo* function of RecG, Christian Rudolph compared cell cycle progression of *recG* and wild type cells after UV irradiation. Cultures were irradiated with a UV dose of 10 J/m², which the majority of wild type cells and ~50 % of *recG* cells survive (Jaktaji and Lloyd 2003). A sample of culture was irradiated on a microscope slide and incubated at ~35°C on a heated microscope stage and pictures were taken at 5 minute intervals. Time-lapse photography of irradiated wild type and *recG* cells was compared. Wild type cells filament after UV and begin to bud off small cells from the ends of the filaments between 60 and 70 minutes after irradiation. As the experiment progresses, the filaments divide down into normal-sized growing cells (Figure 27, Rudolph *et al.* unpublished).

After UV irradiation, cells lacking RecG filament extensively (Figure 27, Rudolph *et al.* unpublished), confirming previous studies (Ishioka *et al.* 1997). Whilst the *recG* filaments also bud off small cells between 60 and 70 minutes after irradiation, unlike wild type cells, these are rarely viable. At later times, most filaments bud off small cells, which

either filament or divide like unirradiated cells (Rudolph *et al.* unpublished). These late budded cells indicate recovery of the population, but complete division of the *recG* filaments into normal-sized cells is rarely seen (Figure 27). These data indicate that the majority of the biomass produced by *recG* cells immediately after irradiation is wasted and that only rare cells budded off from the filaments are capable of growing and dividing normally.

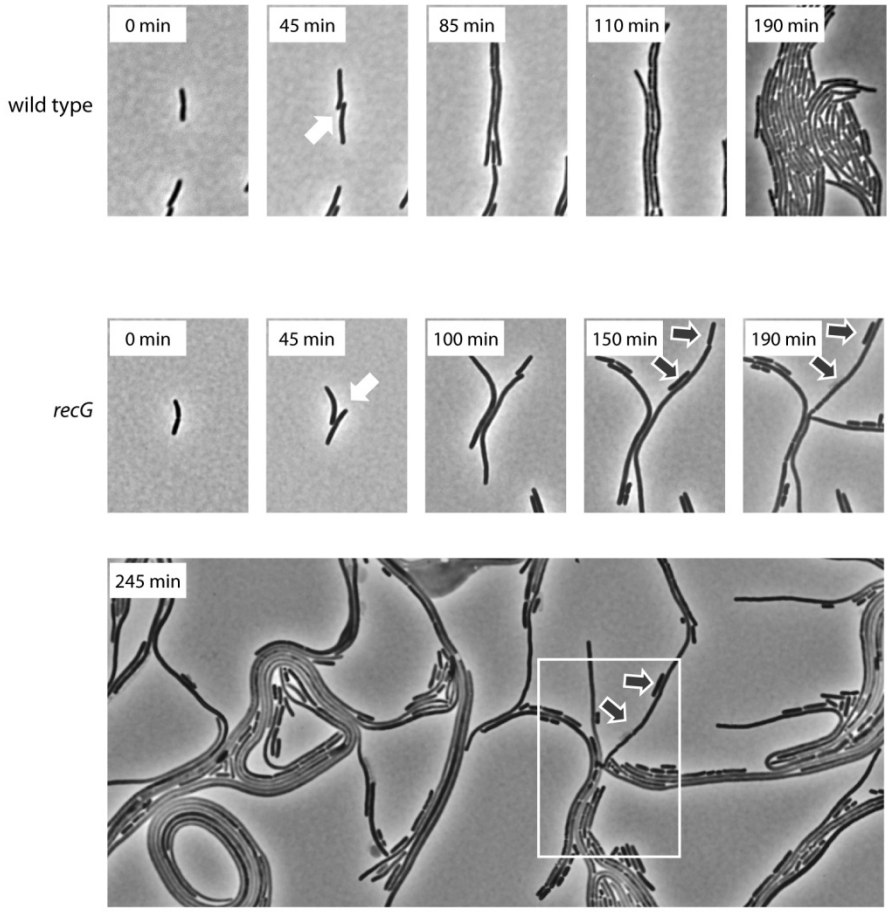

Figure 27. Effect of RecG on cell cycle progression after UV irradiation. Time-lapse photography following the growth of single cells after UV irradiation. The strains used were MG1655 (wild type) and N4560 (*recG*). White arrows indicate last divisions before the cells start to filament. Photographs for the most informative time points are presented. The dark arrows indicate two dead cells budded off a *recG* filament; one that bursts leaving a "ghost" visible at 245 minutes; and one that no longer grows. Experiment performed and figure produced by Christian Rudolph.

This is a rather extreme phenotype in comparison to the mild UV sensitivity of *recG* cells indicated by assays of survival. Since a filament only needs to produce one viable cell in order to form a colony, the wasted biomass would not be visible in standard UV survival

experiments where the colonies are counted after overnight incubation. This explanation is supported by photographs of UV survival plates at earlier times after irradiation (10 hours); *recG* colonies are much smaller than wild type colonies even after a low UV dose (Figure 28, Rudolph *et al.* unpublished). These data suggest that irradiated *recG* cells have a problem segregating their chromosomes before cell division, as was suggested previously (Ishioka *et al.* 1997).

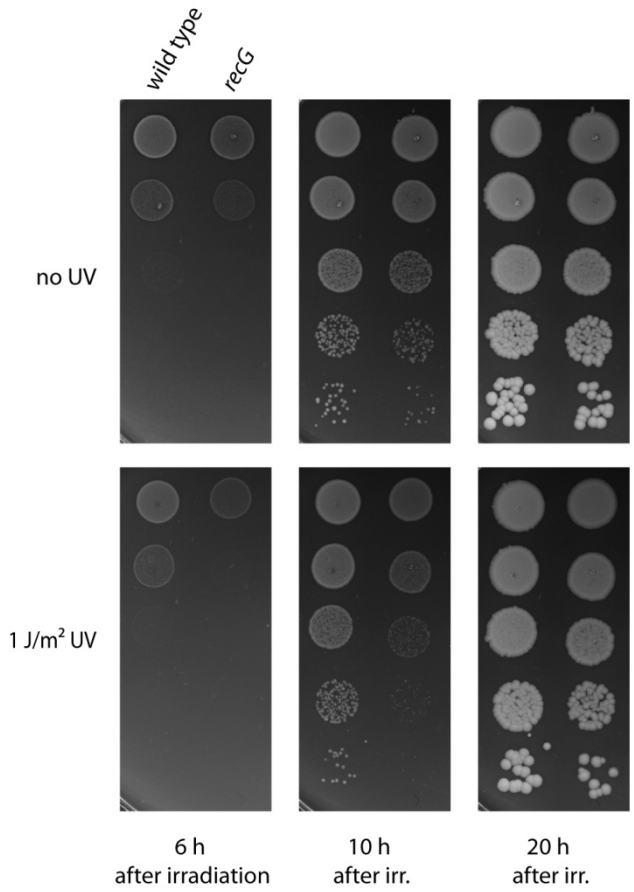

Figure 28. Effect of RecG on viability and cell cycle progression after UV irradiation. Procedure was the same as a semi-quantitative UV survival experiment (see page 62). The plates were photographed at the times indicated to illustrate the delay in cell division as well the difference in viability. The strains used were MG1655 (wild type) and N4560 (*recG*). Experiment performed and figure produced by Christian Rudolph.

Since RecG has been implicated in replication restart, these data could also be explained if irradiated *recG* cells have a problem in completing replication of the chromosome. However, it has been observed that *recG* mutations have no obvious effect on net DNA synthesis after UV irradiation (Donaldson *et al.* 2004). I have already demonstrated that

measures of net DNA synthesis are not suitable for studying replication after DNA damage because the different modes of synthesis cannot be distinguished from one another (see page 78). Given that undamaged *recG* cells already exhibit DnaA-independent replication (Hong *et al.* 1995), it is possible that SDR could mask an extended delay at existing replication forks after UV. I decided to further investigate the nature of the replication in irradiated *recG* cells.

The pattern of replication is different in irradiated recG cells

DnaA-independent synthesis can be observed by using *dnaA46* temperature-sensitive mutants (see page 81). Measures of DNA synthesis in both *recG* and *dnaA46 recG* cells, should give an indication of the relative contributions of the different modes of synthesis in cells lacking RecG.

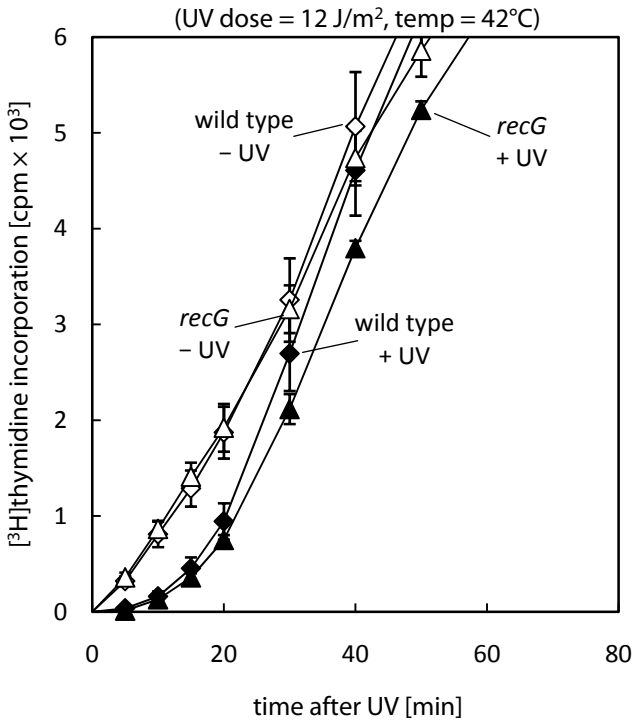

Figure 29. Effect of UV on DNA synthesis in *recG* cells. [³H]thymidine incorporation in wild type (N1141) and *recG* (AU1106) cells. Data for *recG* are the mean (±SE) of three experiments. The data for the wild type are reproduced from Figure 13 for comparison.

A *recG* mutation has hardly any effect on [^{3}H]thymidine incorporation either before or after UV irradiation, as reported (Figure 29, Donaldson *et al.* 2004). However, a *recG* mutation proved to have a dramatic effect upon the replication profile observed in a *dnaA46* background.

Unirradiated *dnaA46 recG* cells already incorporate significantly more [^{3}H]thymidine than unirradiated *dnaA46* cells (Figure 30). This is consistent with the studies reporting that undamaged *recG* cells exhibit cSDR (Hong *et al.* 1995). Incorporation in UV-irradiated *dnaA46 recG* cells is greatly increased, consistent with studies showing that initiation of iSDR is stimulated in *recG* cells (Figure 30, Asai and Kogoma 1994). However, incorporation in irradiated *dnaA46 recG* cells was increased almost to the level observed in a *recG* single mutant after UV (Figure 30). This result was quite unexpected; it suggests that the majority of the net synthesis measured in *recG* cells after UV irradiation could result from the initiation of SDR. In contrast to what has been observed in wild type cells, it appears as though very little of the synthesis in irradiated *recG* cells can be attributed to *oriC*-firing. However, analysis of the origin to terminus ratio in irradiated *recG* cells shows no difference to the wild type (Rudolph *et al.* unpublished), suggesting that *oriC* does still fire in these cells. By considering the fact that SDR requires the set-up of extra replication forks, these observations can be explained. Firstly, whilst the origin of replication might fire as normal in irradiated *recG* cells, the replication forks set up may not progress very far before meeting replication forks resulting from the initiation of SDR. This would mean that the level of net synthesis in irradiated *recG* cells would only be marginally reduced by inactivation of DnaA. Alternatively, given that the holoenzyme components are in limited supply (Kelman and O'Donnell 1995), inactivation of DnaA might enable more replication forks to be set up by stable DNA replication than is possible in a *recG* single mutant and thus, create the appearance of greatly increased levels of SDR in these cells. Both situations could account for the high levels of net synthesis measured in *dnaA46 recG* cells, even if *oriC*-firing continues as normal in irradiated *recG* cells, as suggested by the origin to terminus ratio.

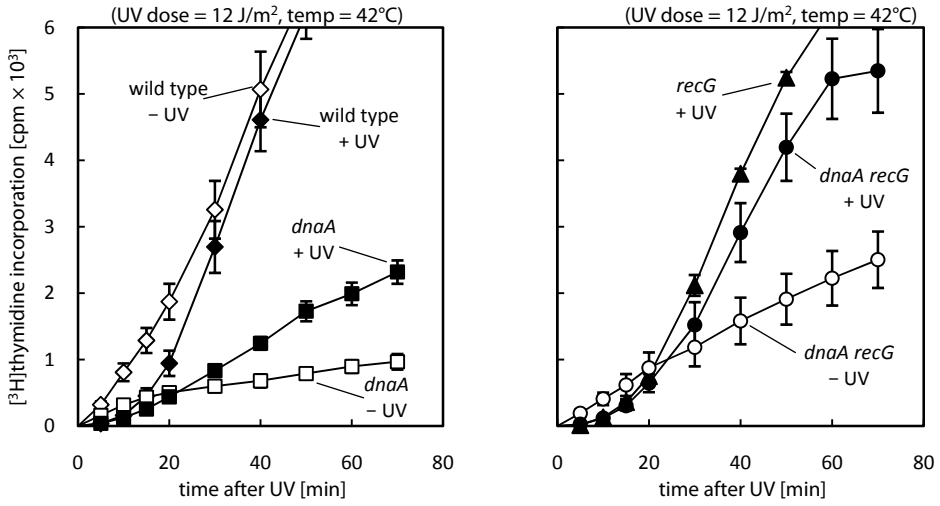

Figure 30. The pattern of replication is different in irradiated *recG* cells. [³H]thymidine incorporation in wild type (N1141), *dnaA46* (AU1068), *recG* (AU1106) and *dnaA46 recG* (AU1090) cells. Data for *dnaA46 recG* are the mean (±SE) of three experiments. The data for the wild type (Figure 13), *dnaA46* (Figure 15) and *recG* (Figure 29) are reproduced for comparison.

In contrast to previous reports (Donaldson *et al.* 2004), the pattern of replication in irradiated *recG* cells appears to be quite different to that observed in the wild type. These data suggest that a substantial level of the net synthesis measured in *recG* cells after UV results from the initiation of SDR rather from DnaA-dependent firing of *oriC*, which continues at a similar rate in wild type and *recG* cells. This synthesis appears to be a mixture of both cSDR induced by the lack of RecG and iSDR induced by UV. These results demonstrate very clearly that measuring net DNA synthesis is meaningless without considering which types of synthesis are being measured. A prolonged delay at existing replication forks might be completely masked by DnaA-independent synthesis in *dnaA46 recG* cells, so it is not possible to conclude whether or not RecG has a role in restart after DNA damage. However, these data also open up the possibility that the phenotypes observed in *recG* mutants may be due to complications arising from the initiation of DnaA-independent synthesis.

Can excessive stable DNA replication be lethal?

It is possible the high levels of SDR induced in irradiated *recG* cells could contribute to their phenotype. Is there any evidence that SDR can cause a problem? As mentioned above, cSDR is also observed in cells lacking RNase HI (*rnhA* mutants). It has been demonstrated previously that *rnhA recG* double mutants are inviable (Hong *et al.* 1995). This inviability could be caused by excessive levels of SDR, induced by the lack of both RNase HI and RecG. A synthetic lethality assay was used to investigate this inviability further. The assay was based on derivatives of pRC7, a *lac*$^+$ mini-F plasmid that is rapidly lost from the cells (de Boer *et al.* 1989; Bernhardt and de Boer 2004; Mahdi *et al.* 2006). Without ampicillin selection, loss of the plasmid is revealed in a Δ*lac* strain by the appearance of Lac$^-$ clones (white colonies or white sectors within blue colonies) on plates containing the β-galactosidase indicator (X-gal). White colonies are formed by a cell that had already lost the plasmid, and sectoring colonies show that the plasmid was lost during colony growth. By using derivatives of the plasmid that carry a copy of the gene of interest to cover a chromosomal deletion, the viability of that deletion in combination with other, uncovered mutations can be tested (Bernhardt and de Boer 2004; Mahdi *et al.* 2006).

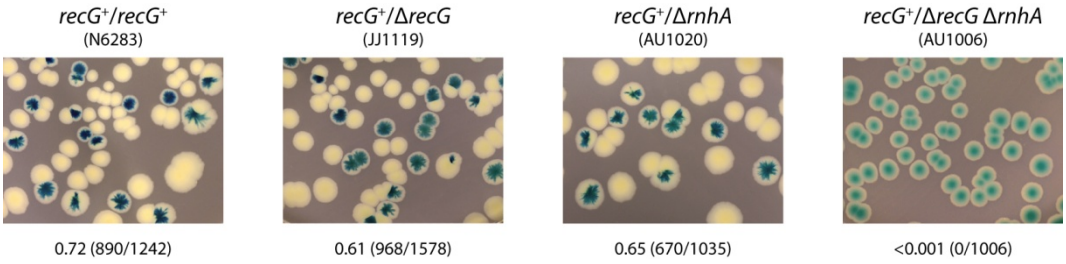

Figure 31. Cells lacking RecG and RNase HI are inviable. Synthetic lethality assays demonstrating the inviability of Δ*recG* Δ*rnhA* cells. The first three images are of the control strains. The relevant genotype is shown above each image, along with the strain number. The fraction of white colonies is shown below each image, with the number of white colonies/total colonies analysed in parentheses.

A *recG*$^+$ derivative of pRC7 was used to cover a chromosomal deletion of *recG*. The Δ*recG* strain is viable, as revealed by the presence of plasmid free, Lac$^-$ colonies on the X-gal plates (Figure 31). However, a Δ*recG* Δ*rnhA* double mutant only forms blue, Lac$^+$ colonies. The strain is unable to form colonies without the *recG*$^+$ plasmid, confirming that the combination of mutations is indeed synthetically lethal (Figure 31, Hong *et al.* 1995).

Since both RecG and RNase HI can remove R-loops, the inviability of Δ*recG* Δ*rnhA* suggests that cells might not be able cope with too many persisting R-loops, possibly because they lead to increased levels of SDR. Alternatively, since RecG was implicated to act during the late stages of recombination (Lloyd 1991; Lloyd and Buckman 1991), and Δ*rnhA* can provoke recombination, as measured by expansion of chromosomal duplications (Poteete 2009), this inviability could also indicate that Δ*rnhA* either provokes a level of recombination that is lethal for a *recG* mutant or requires recombination for survival. Since RuvABC acts during the late stages of recombination, a Δ*ruvABC* Δ*rnhA* strain can be used to test the possibility that the inviability of Δ*recG* Δ*rnhA* is due to a deficiency in the late stages of recombination.

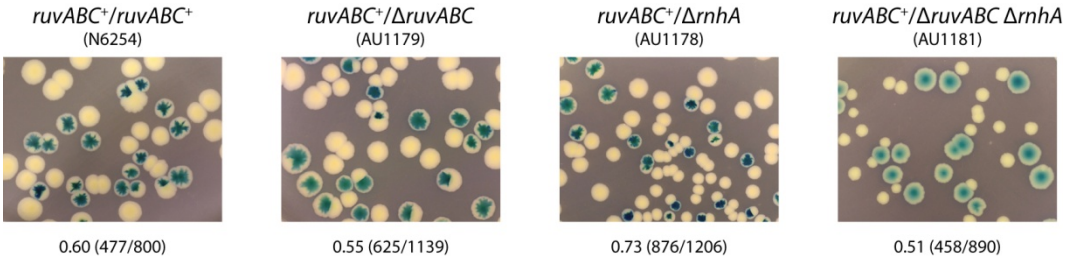

Figure 32. Cells lacking RuvABC and RNase HI are viable. Synthetic lethality assays demonstrating the viability of Δ*ruvABC* Δ*rnhA* cells. The first three images are of the control strains. The relevant genotype is shown above each image, along with the strain number. The fraction of white colonies is shown below each image, with the number of white colonies/total colonies analysed in parentheses.

A *ruvABC*⁺ derivative of pRC7 was used to cover a chromosomal deletion of the *ruvABC* genes. The Δ*ruvABC* Δ*rnhA* strain is viable (Figure 32), demonstrating that Δ*rnhA* does not provoke recombination to an extent that is incompatible with viability in cells lacking the Holliday junction resolvase. However, by comparing colony sizes it is obvious that in the case of the double mutant the Lac⁻ colonies are smaller than the Lac⁺ colonies, indicating that the viability is reduced. Since recombination is reduced by a similar amount in cells lacking either RecG or Ruv activity (see (Lloyd 1991) for a comparison of these mutants), the viability of Δ*ruvABC* Δ*rnhA* suggests that Δ*rnhA* does not provoke lethal levels of recombination. However, the reduction in viability does indicate that Δ*rnhA* cells are at least partially dependent upon recombination for viability. This is supported by the observation that the Lac⁻ colonies are no longer smaller than the Lac⁺ colonies when the RusA Holliday junction resolvase is expressed in Δ*ruvABC* Δ*rnhA* cells

(Figure 33). These observations suggest that the inviability of Δ*recG* Δ*rnhA* is not due to the possible role of RecG in promoting the late stages of recombination.

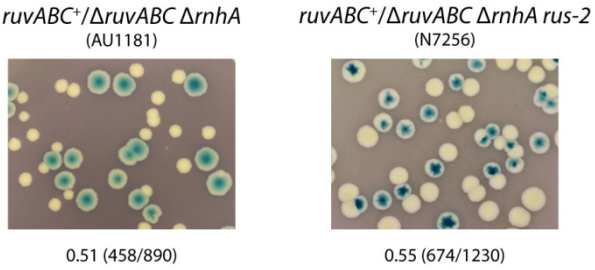

Figure 33. Expression of RusA improves the viability of Δ*ruvABC* Δ*rnhA* cells. A *rus-2* mutation increases expression of RusA and improves the viability of Δ*ruvABC* Δ*rnhA*. The relevant genotype is shown above each image, along with the strain number. The fraction of white colonies is shown below each image, with the number of white colonies/total colonies analysed in parentheses. The image for strain AU1181 is reproduced from Figure 32 for comparison.

RecG was initially implicated in the late stages of recombination because of the synergistic phenotype of Δ*recG* Δ*ruv* double mutants (Lloyd 1991). However, since RecG has several activities *in vitro*, it is possible that Δ*recG* exacerbates the recombination deficient phenotype of Δ*ruv* strains, by reducing the viability of transconjugant cells rather than creating further defects in recombination. The effect of Δ*rnhA* on the UV sensitivity of cells lacking RuvABC was investigated. Cells lacking RNase HI are only mildly sensitive to UV irradiation (Figure 34). Interestingly, the Δ*ruvABC* Δ*rnhA* double mutant is extremely sensitive. The phenotype suggests a synergistic interaction, but not to the extent seen in a Δ*ruvABC* Δ*recG* strain (Figure 34). Since the only common function between RNase HI and RecG is the ability to remove R-loops *in vitro* and to limit SDR *in vivo*, these results indicate that the synergism between Δ*ruvABC* Δ*recG* is at least partially due to the persistence of R-loops rather than a lack of recombination. Another link with SDR is provided by the fact that initiation of iSDR is stimulated in *ruv* mutant cells after SOS induction (Asai and Kogoma 1994).

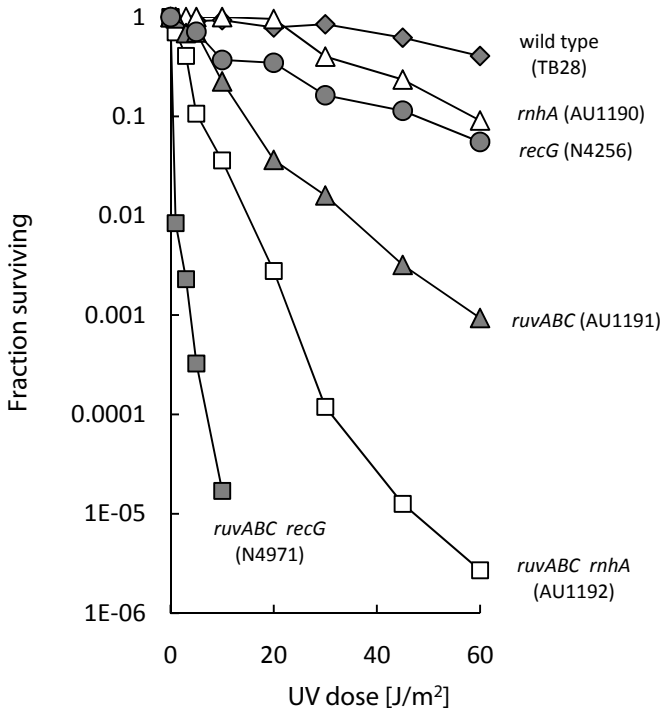

Figure 34. Effect of Δ*rnhA* and Δ*recG* on the UV sensitivity of strains lacking RuvABC. The strains used are identified in parentheses. The data are the mean of two to seven experiments.

A possible explanation for the inviability of Δ*recG* Δ*rnhA* strains is that too much stable DNA replication is toxic for the cell. I investigated the nature of this inviability further, by attempting to make a viable derivative of the double mutant. Since cSDR is dependent upon RecA (Torrey and Kogoma 1982), removing RecA activity in Δ*recG* Δ*rnhA* strains should prevent SDR. If SDR is the cause of the inviability, the Δ*recA* derivative should be viable. However, this was not the case. When Δ*recA* was introduced into Δ*recG* Δ*rnhA* strains, the strain was still unable to produce Lac$^-$ colonies (Figure 35). This result suggests that SDR alone is not the cause of the inviability. However, the Δ*recA* Δ*rnhA* double mutant already has reduced viability (Figure 35), supporting the idea that Δ*rnhA* cells are dependent on recombination for full viability. It has been proposed that RNase HI may have a role in Okazaki fragment maturation, the process of removing the RNA primers and replacing them with DNA to complete replication (Ogawa and Okazaki 1984). DNA Polymerase I (encoded by *polA*) has an important role in this process and strains lacking Pol I have been shown to be dependent on recombination (reviewed

in Kogoma 1997). A role of RNase HI in Okazaki fragment processing is supported by the synthetic lethality of Δ*polA* Δ*rnhA* strains. However, Δ*polA* Δ*recG* strains are also inviable (Hong *et al.* 1995), and these observations combined with the inability of Δ*recA* to suppress the inviability of Δ*recG* Δ*rnhA* illustrate the complexity of this phenotype.

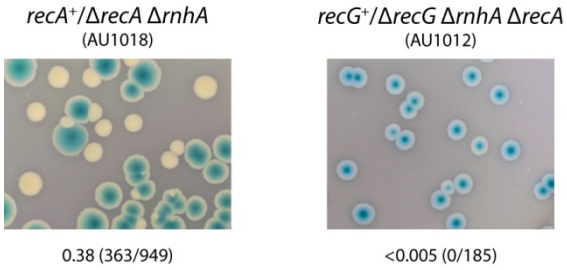

Figure 35. A *recA* mutation does not suppress the inviability of Δ*recG* Δ*rnhA* cells. The relevant genotype is shown above each image, along with the strain number. The fraction of white colonies is shown below each image, with the number of white colonies/total colonies analysed in parentheses. The full set of images of the control strains can be found in the appendix (Figure 53).

The DNA repair defects of cells lacking RecG can be suppressed by a *priA300* mutation (encoding PriAK230R), which inactivates the helicase activity of PriA (Al-Deib *et al.* 1996; Jaktaji and Lloyd 2003). It is interesting to note that a similar *priA* helicase mutation (encoding PriAK230D) can reduce both iSDR and cSDR (Tanaka *et al.* 2003). Since preventing SDR did not suppress the inviability of Δ*recG* Δ*rnhA*, a *priA300* allele was investigated. However, it was also incapable of suppressing the inviability (Figure 36). It seems the phenotype of Δ*recG* Δ*rnhA* strains is far more complex than was originally suspected. Identification of a suppressor of the lethality would have given an indication of the cause of this lethality.

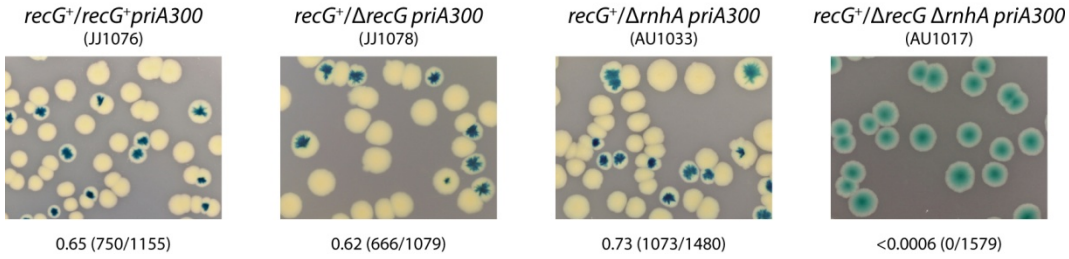

Figure 36. A *priA300* mutation does not suppress the inviability of Δ*recG* Δ*rnhA* cells. The relevant genotype is shown above each image, along with the strain number. The fraction of white colonies is shown below each image, with the number of white colonies/total colonies analysed in parentheses.

Discussion

RecG has multiple *in vitro* activities, making it difficult to determine its role within the cell. A combination of *in vitro* and *in vivo* studies has implicated RecG in several roles. It has been proposed that RecG acts during the late stages of recombination (Lloyd 1991; Lloyd and Sharples 1993), as well as in replication restart by catalysing branch migration of stalled fork structures (McGlynn and Lloyd 2000). It was also suggested that it limits replication initiation to *oriC*, by removing R-loops that can be used to initiate replication (Kogoma 1997).

Whilst investigating the effect of UV irradiation on cells lacking RecG, Christian Rudolph found that although these cells appear to be far less sensitive than other recombination mutants, they do in fact have a rather extreme phenotype, confirming previous observations (Ishioka *et al.* 1997). Cellular division of *recG* cells is delayed dramatically after UV irradiation and microscopy analysis of these cells demonstrated that the majority of the biomass created early after UV appears to be wasted (Figure 27 and Figure 28, Rudolph *et al.* unpublished). These observations suggested that after DNA damage, cells lacking RecG have a problem in chromosomal replication or segregation. Thus, the relatively high survival of UV-irradiated *recG* cells calculated from colony assays masks a defect in cell cycle progression. Further experiments have indicated that these cells do suffer from a segregation defect. The origin to terminus ratio and fluorescent microscopy have demonstrated that the origin and terminus regions of the chromosome are replicated in irradiated *recG* cells, but that they can cluster together rather than segregating ready for cell division (Rudolph *et al.* unpublished). These data support previous observations by Ishioka *et al.* (1997), who suggested that Holliday junctions are holding the newly replicated chromosomes together. These defects are suppressed by a *priA300* allele eliminating PriA helicase activity (PriAK230R mutant, Rudolph *et al.* unpublished). Since *priA300* does not suppress *ruv* mutations, and given that the Holliday junction resolvase RuvABC is present in *recG* cells, it seems unlikely that Holliday junctions are preventing segregation. Since *recG* cells can survive UV irradiation, some viable cells are created whilst the initial filaments persist, confirming that at least one entire chromosome can be replicated and segregate eventually.

Cells lacking RecG proved to be a very good example for why measurements of net DNA synthesis are not suitable for studying the effect of DNA damage on replication.

Since undamaged cells lacking RecG exhibit both iSDR and cSDR, it was surprising that studies of net DNA synthesis revealed no difference between irradiated wild type and *recG* cells (Donaldson *et al.* 2004). Since there are three modes of DNA synthesis after UV irradiation, it is important to consider which modes of synthesis are being measured in these assays. In contrast to wild type cells, the pattern of DNA synthesis in irradiated *recG* cells appeared to be quite different. A substantial level of the synthesis measured in irradiated *dnaA46 recG* cells results from the initiation of SDR (Figure 30). It is possible that the inactivation of DnaA allows a higher level of initiation of SDR than is possible in a *recG* single mutant, but the level induced in wild type and *recG* derivatives is clearly different. Even if the level of SDR observed in *dnaA46 recG* cells is artificial, this increased level means that a substrate capable of priming SDR is produced at a higher level in these cells than in a *dnaA46* single mutant.

The increased level of SDR in irradiated *recG* cells means that there are multiple replication forks traversing the chromosome. It is possible that the increased number of replication forks result in intermediates that prevent the newly replicated chromosomes from segregating properly. This possibility is supported by the fact that a *priA* helicase mutant suppresses the cell cycle defects of irradiated *recG* cells (Rudolph *et al.* unpublished) and that a similar *priA* helicase mutation (encoding PriAK230D instead of PriAK230R) can reduce both iSDR and cSDR (Tanaka *et al.* 2003). Thus, although the net synthesis measured in *recG* cells is not reduced in comparison to the wild type, a substantial level of this synthesis results from SDR and may be pathological. It is not clear whether or not SDR in irradiated *recG* cells is productive in generating fully replicated, transmissible chromosomes. Indeed, the cSDR in undamaged *recG* cells is not capable of supporting cell growth in the absence of *oriC* or *dnaA* (Hong *et al.* 1995). An obvious reason for the inviability of Δ*recG* Δ*rnhA* strains could be that too much SDR is toxic. However, my investigation of these strains proved that the inviability could not be suppressed by Δ*recA*, which should prevent SDR, suggesting that the inviability is more complicated than was suspected. A *priA300* allele, which can suppress *recG* DNA repair defects, was also unable to suppress Δ*recG* Δ*rnhA*. Little is known about the function of SDR or if it is purely a by-product of the ability of *E. coli* cells to reload the replisome at stalled fork structures, which can be mimicked by other intermediates such as R-loops and D-loops.

The level of SDR in irradiated *recG* cells is quite dramatic. In fact, the level is so dramatic that it seems impossible to determine the function of RecG without consideration of SDR. The synthetic lethality of Δ*recG* Δ*rnhA* cells suggests that RecG and RNase HI might have overlapping roles within the cell. This means the synergistic phenotypes of irradiated *ruvABC rnhA* and *ruvABC recG* cells could be related. The only known similarity between the activities of RecG and RNase HI is the ability to remove R-loops and to limit cSDR. Since RNase HI has never been implicated to act in recombination, it seems likely that an *rnhA* mutation exacerbates the phenotype of *ruv* cells by reducing the viability of these cells after UV, rather than by creating further defects in recombination. Indeed, it is already clear that Δ*rnhA* cells require recombination for full viability (Figure 33 and Figure 35). The fact that the synergism between *ruv* and *recG* mutations is more extreme than that between *ruv* and *rnhA* mutations may be explained by the fact that the SDR in these cells is clearly different. Undamaged *rnhA* cells are capable of maintaining sufficient chromosomal replication via cSDR such that *oriC* and *dnaA*, which are normally essential, can be deleted from these strains (Kogoma and von Meyenburg 1983), whereas this is not the case with *recG* cells (Hong *et al.* 1995). Also, RecG is required for the recovery of recombinants in conjugational crosses with *ruv* strains (assays in which viability is also considered) (Lloyd 1991). Thus, the more extreme synergism in irradiated *ruv recG* strains probably reflects the fact that cells lacking RecG do have some deficiency in recombination and that the survival after UV is also affected by the persistence of R-loops.

The *in vivo* function of RecG is still unclear. However, these data have led to the idea that the phenotypes of *recG* mutants could be explained by the possibility that the increased levels of SDR in these cells could be pathological and have consequences leading to a reduction in viability. Further investigations into the possibility that SDR might inhibit cellular replication after irradiation should shed more light onto the importance of SDR in the phenotypes of cells lacking RecG.

The C-terminus of RecG is necessary for cellular localisation and protein function

Whilst studying fluorescent fusion proteins, Tim Moore found that fluorescently tagged RecG (eYFP-RecG) localises within *E. coli* cells forming discrete foci. He also found that the fluorescent RecG co-localises with fluorescently tagged SeqA when these fusion proteins are expressed simultaneously. SeqA binds to newly replicated, hemi-methylated DNA immediately behind replication forks and therefore SeqA foci label the location of replication forks within the cell (Brendler *et al.* 2000; Molina and Skarstad 2004; Waldminghaus and Skarstad 2009). RecG is able to bind to several DNA structures *in vitro* (see page 111), so the localisation within the cell could have been due to DNA binding. However, when a RecG mutant in which the DNA binding domain had been deleted still localised within the cell, it was thought that localisation of RecG might be uninformative or even an artefact. Alternatively, instead of being localised by binding to a DNA substrate, I speculated that the localisation of RecG could be due to an interaction with a component of the replisome. Since RecG has been implicated to act at stalled replication forks (McGlynn and Lloyd 2000), I decided to investigate this localisation further.

Firstly, the experiments by Tim Moore were repeated to confirm that RecG foci co-localise with SeqA foci. The proteins are tagged fluorescently using a plasmid expression system that allows expression of the fusion proteins to be induced by the addition of arabinose to the culture (Lau *et al.* 2003). The N-terminus of RecG was tagged with eYFP, with a special linker region between the proteins. The linker region was designed by Geoff Briggs and was based on the sequence of the region that links the DNA binding domain of *Thermotoga maritima* RecG to an extra N-terminal domain that does not exist in the *E. coli* RecG (Singleton *et al.* 2001). The linker region in *T. maritima* RecG holds the extra N-terminal domain in position, away from the DNA binding domain. The position of the linker region is highlighted on the crystal structure of *T. maritima* RecG (Figure 37) and the sequence of this linker is shown in an alignment of the amino acid sequence of

T. maritima RecG against that of *E. coli* (Figure 54). The DNA binding and helicase domains are also indicated on these figures.

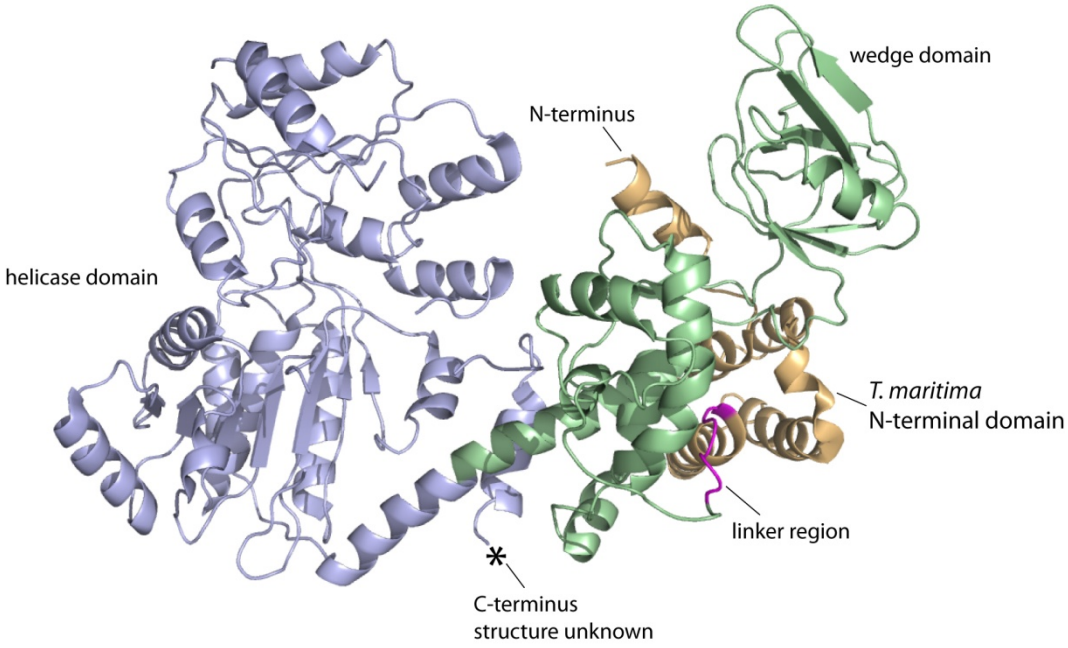

Figure 37. The crystal structure of *Thermotoga maritima* RecG. The linker region (LIDYLEC) utilised for fluorescently tagging *E. coli* RecG proteins is highlighted in magenta. The N-terminal domain of *T. maritima* that is not present in *E. coli* is shown in yellow. The DNA binding domain is shown in green and the wedge domain, which is important for binding to forked DNA, is highlighted. The helicase domain is shown in blue. The asterisk marks the most C-terminal residue (W755) resolved in the crystal structure. The structure is as determined by Singleton *et al.* (2001).

The linker region was included because previous attempts to create fusions to the N-terminus of *E. coli* RecG have failed and it was suggested that the fusion proteins were lethal (McGlynn *et al.* 2000). It is thought that the linker region will also position the fluorescent protein away from the DNA binding domains of *E. coli* RecG. Complementation analysis demonstrated that induction of the fluorescently tagged RecG protein complements the sensitivity of a Δ*recG* strain to UV irradiation and mitomycin C, confirming that the eYFP-RecG fusion protein is functional *in vivo* (data not shown). The N-terminus of SeqA was tagged with eCFP and the DNA fragment encoding this fusion was cloned downstream of the eYFP-RecG so that the fusion proteins could be expressed simultaneously. Fluorescently tagged SeqA has been used previously to label the location of replication forks within cells and it was confirmed that N-terminal tagged SeqA proteins are active *in vivo* (Brendler *et al.* 2000; Lau *et al.* 2003; Molina and Skarstad 2004).

All RecG fusion constructs were studied in a Δ*recG* strain to ensure that foci formation resulted from interactions of the fluorescently tagged RecG and was not due to an interaction of the tagged RecG with the untagged wild type protein. Expression of the fusion proteins was induced for 60 minutes prior to visualisation under the microscope, allowing sufficient time for expression and maturation of the proteins (see page 65).

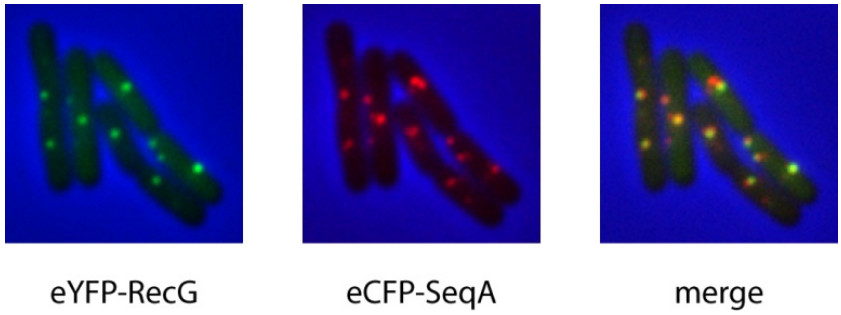

Figure 38. Co-localisation of RecG and SeqA foci. Fluorescence microscopy pictures showing eYFP-RecG foci (green) and eCFP-SeqA foci (red). Pictures are combined phase contrast and fluorescence images. The first two panels show the RecG and SeqA foci and the right panel is a merge of these images. The strain used was AU1120 (Δ*recG* + pDIM113).

As shown in Figure 38, both eYFP-RecG and eCFP-SeqA form discrete foci. A merged image shows that RecG and SeqA foci co-localise within the cell, confirming the observations of Tim Moore. I found that approximately 90 % of RecG foci are co-localised with SeqA (296 foci co-localised out of a total of 323 RecG foci analysed, in 164 cells from 3 independent experiments). As can be seen in Figure 38, when the eYFP and eCFP photos are merged there are some yellow foci, indicating close localisation and also examples where the foci are next to each other. Additional information about how closely these proteins localise may be provided by FRET (fluorescence resonance energy transfer) analysis, which relies on the phenomenon that when eYFP and eCFP are closely localised excitation of eCFP can transfer energy to eYFP such that an eYFP emission is observed (reviewed by Truong and Ikura 2001). Since a distance of 5.2 nm is required for 50 % energy transfer, FRET analysis might not be informative since I do not expect direct protein interactions between RecG and SeqA. In this instance SeqA has been used as a marker for the location of replication forks. FRET analysis could be used to investigate other potential interaction partners at the replication fork, with which RecG might interact directly.

The co-localisation with SeqA suggests that RecG interacts with one of the replisome components, which is in line with the fact that the DNA binding domain (referred to as the wedge) is not necessary for foci formation (Figure 39). These data are consistent with a study showing that localisation of RecG in *Bacillus subtilis* cells is dependent upon the C-terminus of the single-stranded DNA binding protein (SSB) (Lecointe *et al.* 2007). The *in vivo* microscopy data were supported by *in vitro* evidence for an interaction between *Bacillus* RecG and SSB (Lecointe *et al.* 2007). SSB is an essential protein, which binds to and protects single-stranded DNA as well as playing an organisational role in DNA replication, recombination and repair by interacting with many different proteins (reviewed by Shereda *et al.* 2008). SSB can be found coating the lagging strand template at replication forks (Pomerantz and O'Donnell 2007). This interaction of RecG with SSB might also offer an explanation for the apparent lethal effect of a fusion of maltose binding protein to the N-terminus of RecG (McGlynn *et al.* 2000). If *E. coli* RecG interacts with SSB, then a fusion protein in which the tag is not held in a specific position might disturb the protein components at a replication fork, which could cause inviability. Since the eYFP-RecG used in these studies was expressed without causing inviability, the extra linker region must hold the tag in a position where it does not interfere with the replisome.

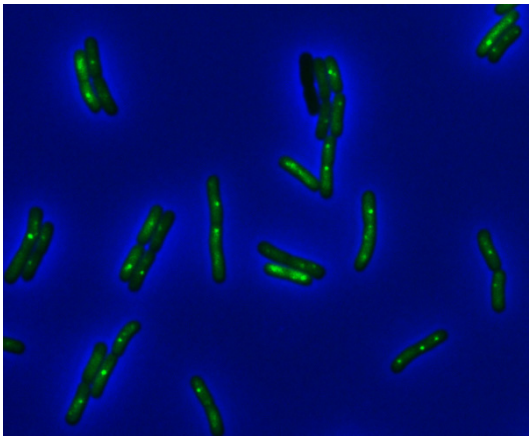

Figure 39. The DNA binding domain of RecG is not necessary for localisation. Fluorescence microscopy picture of eYFP-RecGΔwedge foci. The picture is a combined phase contrast and fluorescence image. The strain used was AU1122 (Δ*recG* + pDIM133).

The inability to create direct fusions to the N-terminus of RecG without the aid of a linker was overcome by deleting the last 32 amino acid residues from the C-terminus of RecG.

The mutant protein MBP-RecGΔC32 (RecG was fused to maltose binding protein), bound to junction DNA with an affinity similar to the wild type protein, but had very little helicase activity (McGlynn *et al.* 2000). Since the mutant protein still seems able to bind to its potential *in vivo* substrates, the lethality of the wild type fusion protein does not result from the protein binding to its substrate. The ability of the C-terminal deletion to enable fusions to the N-terminus suggests that the C-terminus might be involved in localisation of RecG within the cell. If the wild type fusion protein is lethal due to the tag interfering with the replisome, an inability of RecG to locate to the replisome would prevent the fusion protein from causing a problem. If the C-terminus of RecG is involved in localisation within the cell, deletions of the C-terminus might prevent foci formation when RecG is fused to eYFP.

The C-terminus of RecG is necessary for cellular localisation

A series of C-terminal deletions of RecG were created and the relevant gene constructs cloned into the fluorescent fusion vector. The largest deletion was 30 amino acid residues and the series of deletions decreased in size in steps of 5 residues down to a deletion of the last 5 residues from the C-terminus. Full details of the construction of these deletions, including details of primers and plasmids can be found in the Materials and methods chapter (page 43). Both eYFP-RecGΔC5 and eYFP-RecGΔC10 still form discrete foci when expression is induced (Figure 40). However, the larger deletions are no longer capable of forming foci. Instead, the majority of cells have a low level of fluorescence spread throughout the cell, consistent with an inability of the proteins to localise and confirming that the fluorescent fusions are still expressed. Figure 55 shows there is very little fluorescent signal detectable within the cells if expression of the fluorescent fusions is inhibited by growth in glucose instead of arabinose. Expression levels of the fluorescent RecG fusions could also be checked by western blot analysis using antibodies to either eYFP or RecG. A small percentage of the cells expressing the larger deletions contain aberrant foci (less than 10 % in all cases, Figure 40).

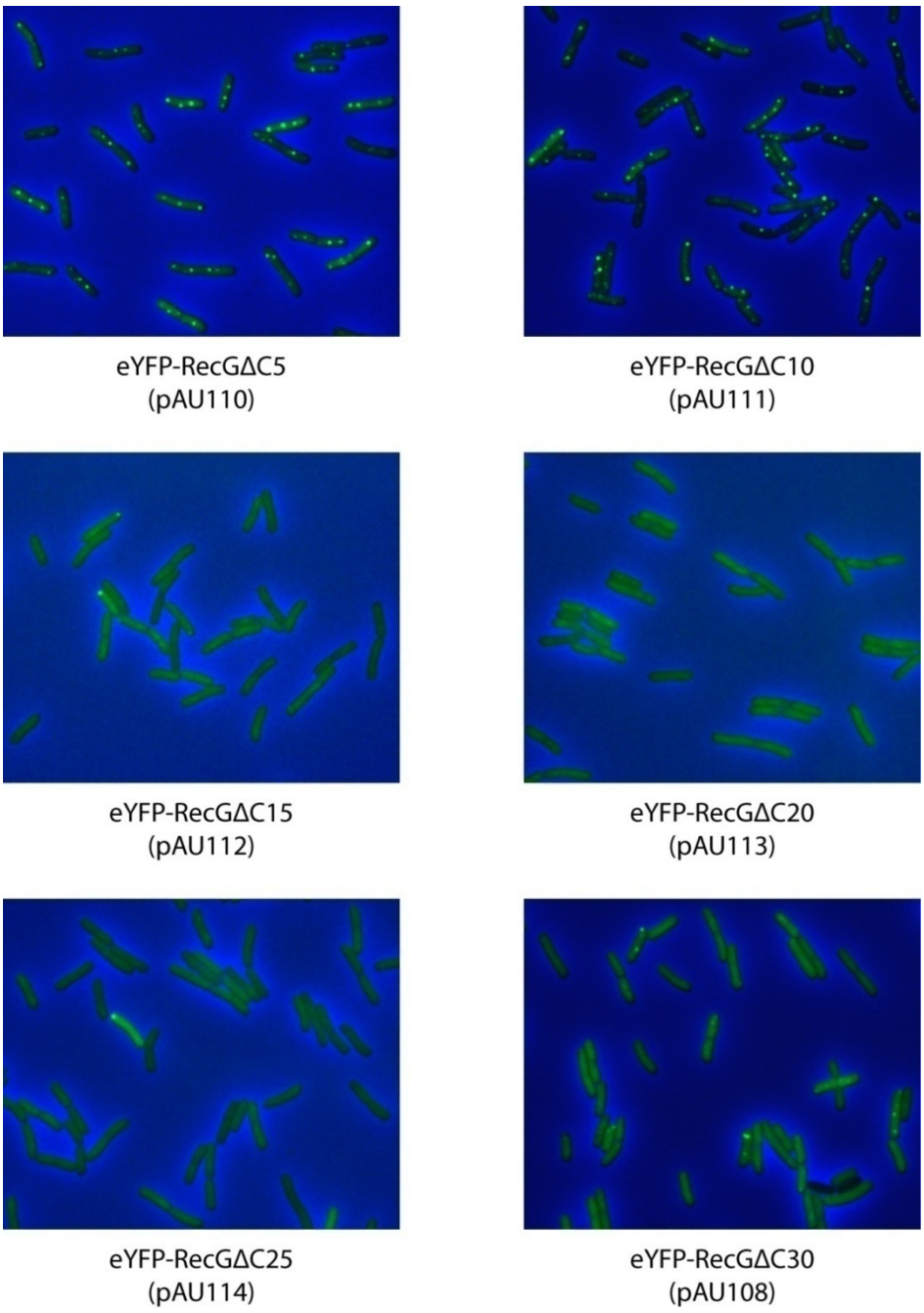

Figure 40. The C-terminus of RecG is necessary for localisation. Fluorescence microscopy pictures of eYFP fusions to C-terminus deletions of RecG. The pictures are combined phase contrast and fluorescence images. The strains used were AU1158 (Δ*recG* + pAU110), AU1159 (Δ*recG* + pAU111), AU1160 (Δ*recG* + pAU112), AU1161 (Δ*recG* + pAU113), AU1162 (Δ*recG* + pAU114) and AU1150 (Δ*recG* + pAU108).

Expression of eYFP-RecGΔC15 complements the UV irradiation and mitomycin C sensitivity of a Δ*recG* allele, at least when expressed from the plasmid, suggesting that the lack of foci formation is not due to an inability of the protein to fold correctly (data not

shown). These data indicate that the last 10 amino acid residues of RecG are not necessary for localisation within the cell. However, residues between 10 and 15 residues from the end of the C-terminus are needed for localisation. An alignment of the C-terminus assembled by Geoff Briggs shows that there is a conserved arginine and tryptophan (RW) residue 11 and 12 residues from the C-terminus that would be lost in RecGΔC15 (Figure 41). It is possible that these residues are conserved because they are required for localisation of RecG.

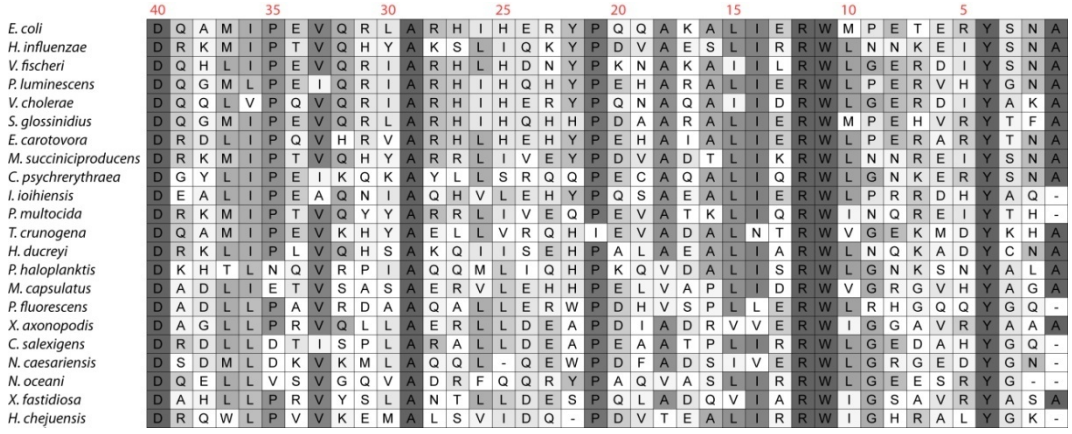

Figure 41. Amino acid sequence alignment of the extreme C-terminus region of RecG. The sequences aligned are from RecG proteins within the same RecG sequence family, which have a C-terminus region of similar length. Less closely related RecG proteins, such as that from *Thermotoga maritima*, have a different C-terminus region and are not informative in this instance. The level of shading indicates percent identity (darker shaded residues have a higher percent identity). The residues are numbered from the end of the C-terminus so that the numbers identify with the RecG C-terminus deletions used in this chapter. Alignment produced by Geoff Briggs.

The ability of the C-terminus alone to enable localisation in the cell was tested by creating a fluorescent fusion of the last 47 amino acids of RecG to eYFP (details are in Table 2). The eYFP-RecGCterm fusion protein did not localise within the cell, as can be seen from the complete lack of foci after induction (Figure 42).

No foci were observed in 100 cells analysed in different fields of view from independent experiments. As with the larger C-terminus deletions the cells had a low level of fluorescence spread throughout, consistent with expression of the fluorescent fusion but an inability to localise. These data combined suggest that the C-terminus of RecG is necessary but not sufficient for localisation of RecG within the cell. However, it is possible that the C-terminus of RecG (last 47 residues) was not folded properly when it was expressed without the other RecG domains.

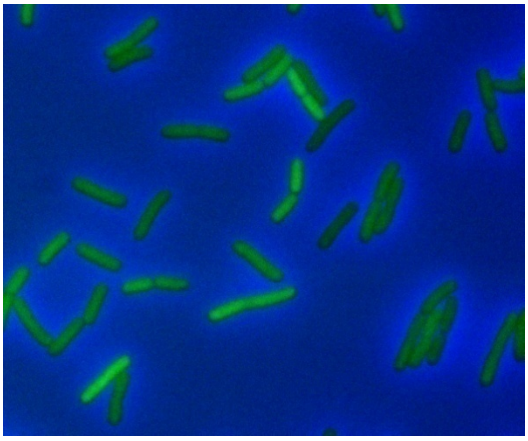

Figure 42. The C-terminus of RecG is not sufficient for localisation. Fluorescence microscopy picture of eYFP-RecGCterm foci. The picture is a combined phase contrast and fluorescence image. The strain used was AU1157 (Δ*recG* + pAU109).

RecG C-terminus deletions have an extreme phenotype in cells lacking RuvABC

The phenotypes of the RecG C-terminus deletions were analysed in order to assess whether or not cellular localisation of RecG is necessary for function. Since RecG is capable of unwinding R-loops, it can reduce the copy number of plasmids that rely on R-loops for initiation of replication. The copy number of plasmids carrying *recG*$^{+}$ is reduced severely (Vincent *et al.* 1996). This means that complementation studies using *recG* plasmids can be misleading. In order to avoid this, the *recG* alleles encoding C-terminus deletions were inserted into the chromosome, replacing wild type *recG*. The details of how these strains were made can be found in the Materials and methods chapter (page 43). All of the deletions were inserted with a kanamycin resistance gene downstream so that they could be transduced into other strains. Since *recG* is the last gene in an operon, the kanamycin marker should not have any downstream effects. As a control, the wild type *recG* allele was also inserted into the *recG* locus with a kanamycin marker (*recG-kan*, Figure 43).

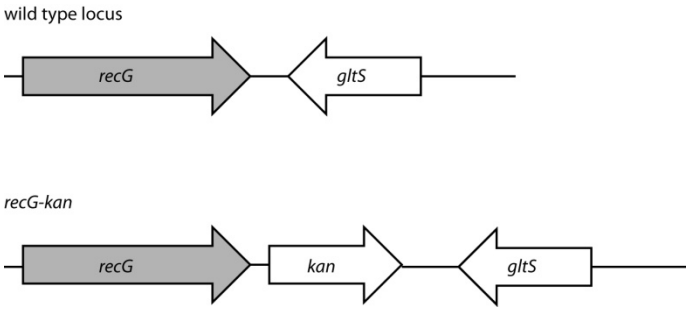

Figure 43. Representation of the *recG* locus. The kanamycin resistance gene (*kan*) was inserted into the region between *recG* and the downstream gene (*gltS*). Transcription of *gltS* is in the opposite direction to that of the *recG* and *kan* genes.

The strains were compared initially using mitomycin C survival assays (see page 63). Since *recG* mutants are sensitive to mitomycin C and do not form countable colonies on these plates, the assays are only qualitative, providing a picture of how the mutants compare to wild type strains. Photographs of the most informative DNA damaging treatments are presented in Figure 44 and the full set of photographs can be found in the appendix (Figure 56). The wild type control for the chromosomal insertions *recG-kan* looks like a wild type strain (compare *recG-kan* with *recG*$^+$ *ruv*$^+$). Also when the *recG-kan* allele is combined with Δ*ruvABC*, the strain does not look worse than a *ruv* strain, there are no signs that the *recG-kan* allele has any sort of defect. This was to be expected since the *recG-kan* allele is a full length wild type *recG* gene. Since the smaller C-terminus deletions still localise within the cell, I predicted that they would look like wild type *recG* strains. However, the C-terminus deletions had quite unexpected phenotypes.

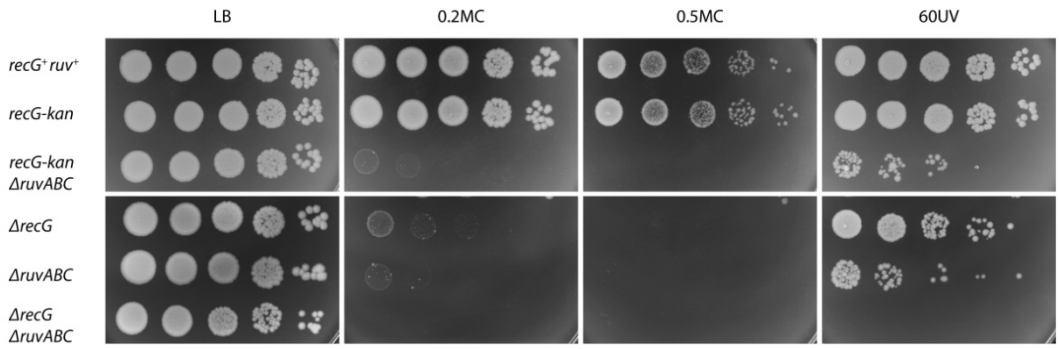

Figure 44. The *recG-kan* allele has a wild type phenotype. Mitomycin C survival assays demonstrating that the *recG-kan* allele is a wild type allele. The strains used were MG1655 (*recG*$^+$ *ruv*$^+$), AU1218 (*recG-kan*), AU1232 (*recG-kan* Δ*ruvABC*), N4256 (Δ*recG*), N7105 (Δ*ruvABC*) and N4971 (Δ*recG* Δ*ruvABC*). LB refers to an LB plate with no DNA-damaging treatment. 0.2MC and 0.5MC are LB plates containing 0.2 and 0.5 μg/ml of mitomycin C, respectively. 60UV refers to an LB plate irradiated with 60 J/m² UV.

The most informative photographs for the deletion mutants are presented in Figure 45, but the full set of photographs can be found in the appendix (Figure 56). The *recG*Δ*C5* strain grew as healthily as a wild type strain on plates containing 0.2 μg/ml mitomycin C or plates irradiated with 60 J/m² UV (Figure 45). However, the *recG*Δ*C5* strain was weaker than wild type on plates containing 0.5 μg/ml mitomycin C, though not to the extent of a Δ*recG* mutant (Figure 45). Although mild, this phenotype suggests that even the last 5 amino acid residues of RecG are important for full viability after DNA damage, which is interesting since there is currently no function assigned to the extreme C-terminus region of RecG. The *recG*Δ*C10*, *recG*Δ*C15* and *recG*Δ*C20* strains looked similar to the *recG*Δ*C5* strain (Figure 45). The *recG*Δ*C25* and *recG*Δ*C30* strains looked similar to a Δ*recG* strain. They were sensitive on plates containing 0.2 μg/ml mitomycin C and also looked weaker on plates irradiated with 60 J/m² UV (Figure 45).

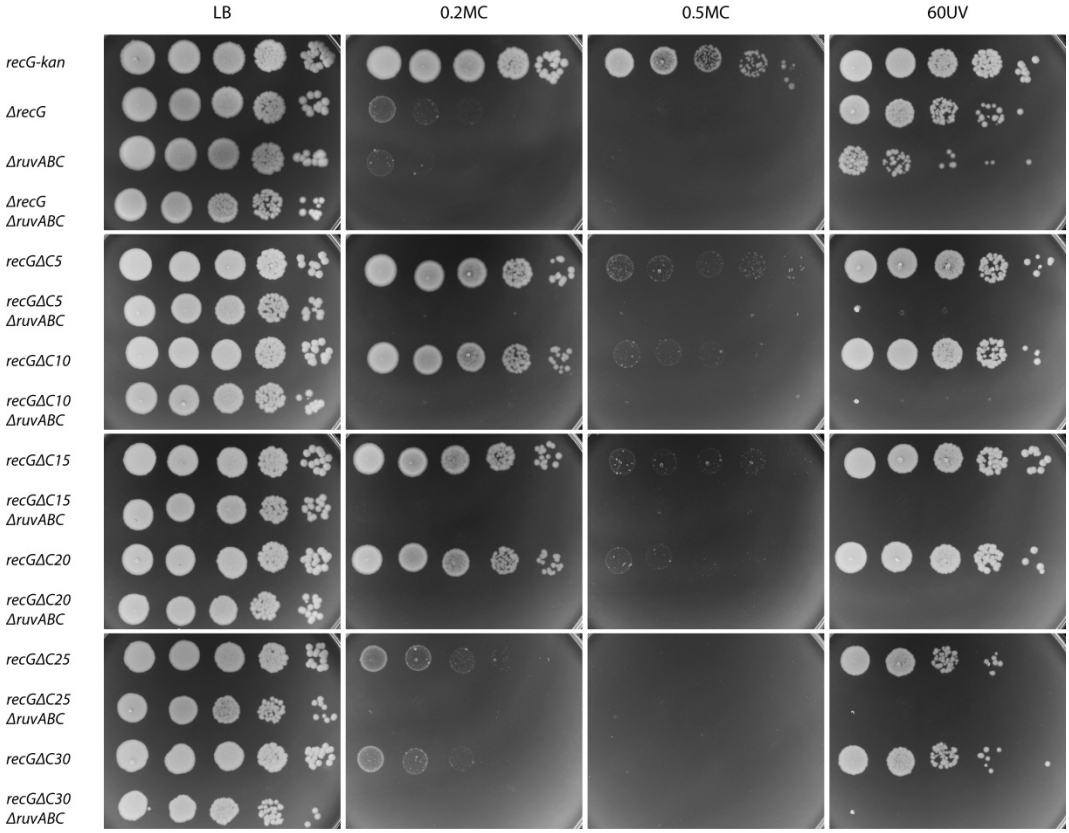

Figure 45. The *recG* C-terminus deletions are not like wild type. Mitomycin C survival assays illustrating the phenotypes of the *recG* C-terminus deletions. The strains used were AU1218 (*recG-kan*), N4256 (Δ*recG*), N7105 (Δ*ruvABC*), N4971 (Δ*recG* Δ*ruvABC*), AU1200 (*recG*Δ*C5*), AU1219 (*recG*Δ*C5* Δ*ruvABC*), AU1201 (*recG*Δ*C10*), AU1220 (*recG*Δ*C10* Δ*ruvABC*), AU1202 (*recG*Δ*C15*), AU1221 (*recG*Δ*C15* Δ*ruvABC*), AU1203 (*recG*Δ*C20*), AU1222 (*recG*Δ*C20* Δ*ruvABC*), AU1204 (*recG*Δ*C25*), AU1223 (*recG*Δ*C25* Δ*ruvABC*), AU1205 (*recG*Δ*C30*) and AU1224 (*recG*Δ*C30* Δ*ruvABC*).

Whilst the single mutants had only mild phenotypes (with the exception of *recG*Δ*C25* and *recG*Δ*C30*), when combined with Δ*ruvABC* the phenotype observed was that of a Δ*recG* Δ*ruvABC* strain in all cases. Indeed, even the *recG*Δ*C5* Δ*ruvABC* strain did not grow on plates containing 0.2 μg/ml mitomycin C or irradiated with a dose as low as 15 J/m² UV (Figure 45, appendix Figure 56).

The effect of the C-terminal deletions on survival after UV irradiation was investigated in order to examine whether or not they really were as sensitive as a Δ*recG* when in a Δ*ruvABC* background (see page 62). As expected, the *recG-kan* control looks like a *recG*⁺ strain after UV irradiation (compare *recG-kan* with *recG*⁺ *ruv*⁺, and *recG-kan* Δ*ruvABC* with *recG*⁺ Δ*ruvABC*; Figure 46). Both *recG*Δ*C5* and *recG*Δ*C10* single mutants are as resistant to UV irradiation as the wild type control (Figure 46).

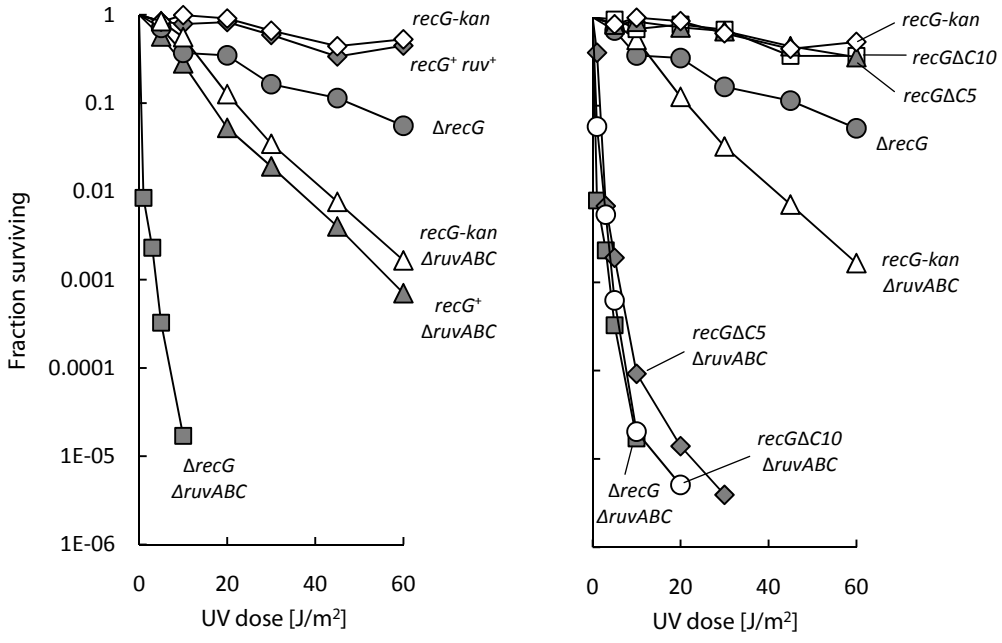

Figure 46. Effect of *recG*Δ*C5* and *recG*Δ*C10* on survival after UV irradiation. The strains used were MG1655 (*recG*⁺ *ruv*⁺), AU1218 (*recG-kan*), N4256 (Δ*recG*), N4583 (*recG*⁺ Δ*ruvABC*), AU1232 (*recG-kan* Δ*ruvABC*), N4971 (Δ*recG* Δ*ruvABC*), AU1200 (*recG*Δ*C5*), AU1219 (*recG*Δ*C5* Δ*ruvABC*), AU1201 (*recG*Δ*C10*), AU1220 (*recG*Δ*C10* Δ*ruvABC*). The data are the mean of three to six experiments. The data for N4583 are reproduced from Jaktaji *et al.* (2003) for comparison.

When these deletions are combined with Δ*ruvABC* they are extremely sensitive to UV irradiation (Figure 46), supporting the data from the mitomycin C survival assays. Therefore, after UV irradiation the smaller C-terminal deletions, as single mutants, show

no sign of being any different to wild type, but surprisingly when they are combined with Δ*ruvABC* the deletions appear almost as sensitive as a complete deletion of *recG*.

These data combined suggest that RecG C-terminal deletions of less than 20 residues can appear as wild type after DNA damage unless they are stressed by either constant DNA damage (high level of mitomycin C) or another DNA repair deficient mutation. Unfortunately, no conclusions can be drawn from these mutants about the importance of localisation of RecG within the cell because the *recG*Δ*C5* allele, which still forms fluorescent foci when tagged with eYFP, already has a phenotype. There is no obvious phenotypic difference between the two alleles that form foci when tagged and the *recG*Δ*C15* allele, which does not.

RecG C-terminus deletions are synthetically lethal with ΔrnhA

The C-terminus deletions were tested in a Δ*rnhA* background using the synthetic lethality assay (see pages 62 and 118). The strains were constructed using a *recG*$^{+}$ derivative of pRC7 to cover the chromosomal C-terminus deletions of *recG*. The *recG-kan* control allele is viable when combined with Δ*rnhA*, as revealed by the presence of plasmid free, Lac^{-} colonies on X-gal plates (Figure 47). In stark contrast to this viability, even a deletion of the last 5 amino acids of *recG* is inviable when combined with Δ*rnhA*; the double mutant only forms blue, Lac^{+} colonies (Figure 47). The other C-terminus deletions were also tested in the synthetic lethality assay and they too were inviable when combined with Δ*rnhA* (see appendix, Figure 57).

Another set of *recG* C-terminus mutants are now being investigated by Jane Grove. These new data indicate that a deletion of the last amino acid residue of *recG* is inviable when combined with Δ*rnhA*, although small Lac^{-} colonies have been observed on minimal media plates (Jane Grove, personal communication). The synthetic lethality assays demonstrate that the *in vivo* activity of the *recG* C-terminus mutants is not sufficient to maintain viability when combined with Δ*rnhA*.

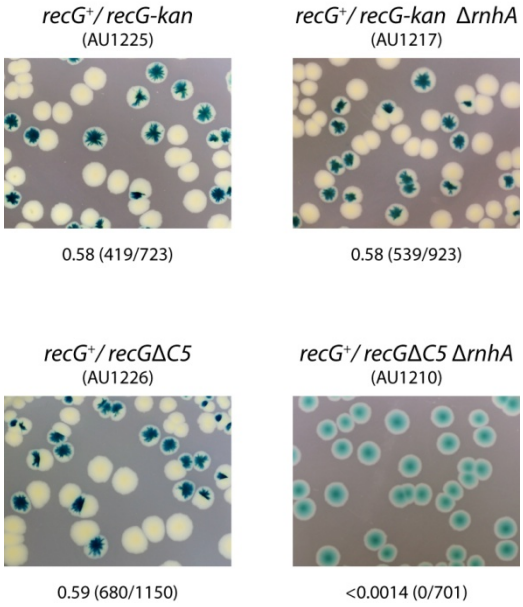

Figure 47. Deletions of the *recG* C-terminus are inviable when combined with Δ*rnhA*. Synthetic lethality assays demonstrating the inviability of *recGΔC5* Δ*rnhA*. The relevant genotype is shown above each image, along with the strain number. The fraction of white colonies is shown below each image, with the number of white colonies/total colonies analysed in parentheses.

RecGΔC5 significantly decreased in vitro RecG activity

There is currently no structure for the extreme C-terminus of RecG (Singleton *et al.* 2001). The N-terminal domain of RecG is involved in DNA binding and confers junction specificity. The helicase domains of RecG are near to the C-terminus (Lloyd and Sharples 1991; Mahdi *et al.* 1997). During the initial characterisation of the functional domains of RecG it was found that a deletion of the last 32 amino acids of the C-terminus of RecG had a moderate effect on DNA binding. However, this protein was tagged with a 20 amino acid N-terminal peptide containing six histidine residues to aid purification, which already reduced the binding ability of wild type RecG (Mahdi *et al.* 1997). As mentioned earlier, RecGΔC32, tagged at the N-terminus with maltose binding protein, bound to junction DNA with an affinity similar to the wild type protein (McGlynn *et al.* 2000). These conflicting results suggest that different N-terminal tags can affect the ability of RecG to bind to its substrate. The MBP-RecGΔC32 had very little helicase activity, indicating that such a large deletion was already removing residues necessary for helicase activity (McGlynn *et al.* 2000). The extreme C-terminus residues of RecG have not

been associated with RecG activity, but the phenotypes of the mutants described in this chapter suggest that the extreme C-terminus is necessary for full RecG function.

Based on their phenotypes, three of the C-terminus deletions were chosen for protein purification: the smallest deletion RecGΔC5, because it already has quite striking phenotypes; RecGΔC15 because it has lost the ability to localise within the cell when labelled with a fluorescent tag; and RecGΔC25, because its phenotype as a single mutant is similar to a full deletion of *recG*. Purification of these mutants was attempted without an N-terminal tag in order to avoid any problems of the tag interfering with the *in vitro* activity of the protein. The protocol for wild type RecG purification has been described previously (page 70, Mahdi *et al.* 2003). RecGΔC5 was expressed and purified according to the protocol for purification of wild type RecG. RecGΔC15 and RecGΔC25 have not been successfully purified. These two proteins are not expressed at such high levels as the wild type or RecGΔC5 proteins and during purification there were often multiple bands on the gels that proved to be RecG proteins, indicating that these mutants were susceptible to degradation. They also elute from the purification columns at slightly different salt concentrations, meaning that they are purified with a different set of contaminants.

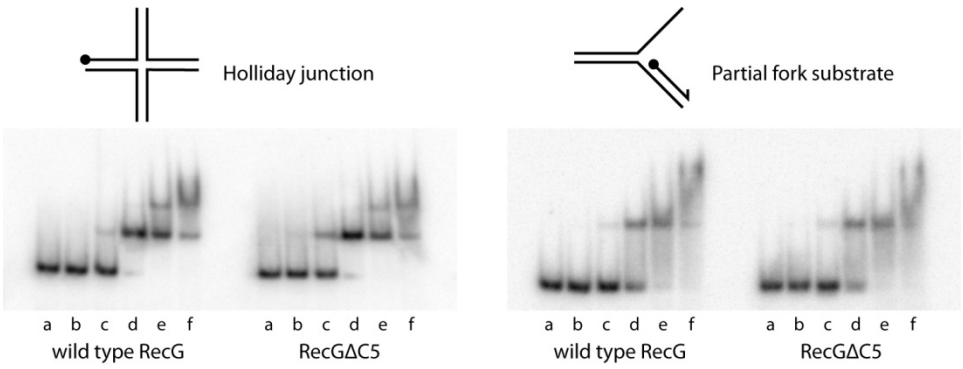

Figure 48. RecGΔC5 binds DNA substrates with a similar affinity to wild type RecG. DNA binding assays showing binding of wild type RecG and RecGΔC5 to a Holliday junction substrate and a partial fork substrate. Reactions used the proteins indicated at 0, 0.1, 1, 10, 50 or 100 nM (lanes a-f) and ^{32}P-labelled substrate DNA at 0.3 nM. The substrates were labelled at the 5' end of one strand as indicated.

Since such a small deletion from the extreme C-terminus has a large phenotypic effect *in vivo*, the *in vitro* activity of RecGΔC5 was examined. The ability of RecGΔC5 to bind to and unwind a Holliday junction substrate and a partial replication fork substrate was

compared to that of wild type RecG (see page 74). The Holliday junction substrate, J12, has been described before (Lloyd and Sharples 1993). It has a 12 base pair core of homology within which the branch point can migrate. The core is flanked by heterologous arms that prevent spontaneous dissociation of the junction. The partial replication fork structure lacked a leading strand; it is the preferred fork substrate of RecG and has been described before (McGlynn and Lloyd 2001b; Mahdi *et al.* 2003). The oligonucleotides used to make the DNA substrates are detailed in the Materials and methods chapter (Table 3 and page 75). Preliminary experiments indicate that RecGΔC5 binds to both substrates with a similar affinity to wild type RecG (Figure 48). This suggests that the last 5 amino acids at the RecG C-terminus are not involved in DNA binding. However, in comparison to wild type RecG, the deletion caused a significant reduction in ATP-dependent DNA unwinding of both substrates (Figure 49). A low level of unwinding of both substrates was visible at high concentrations of RecGΔC5. These preliminary data are now supported by the observation that RecGΔC3 has a similar deficiency (Jane Grove, personal communication). They indicate that the extreme C-terminus of RecG is necessary for full helicase activity and provide an explanation for the phenotypes of the C-terminus deletion mutants. It seems that such a reduced level of RecG activity is sufficient when the single mutants are exposed to UV irradiation or low levels of chronic DNA damage resulting from Mitomycin C. However, this level of activity is far from sufficient when the mutants are subjected to increased levels of chronic DNA damage or are combined with either a Δ*ruvABC* or Δ*rnhA* mutation.

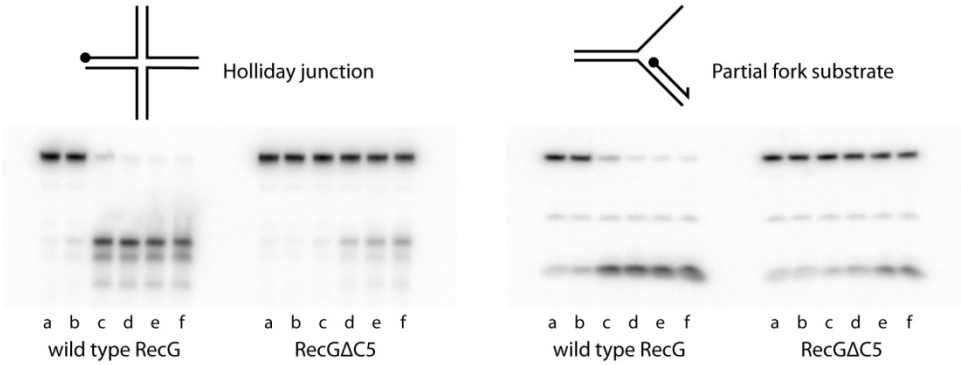

Figure 49. RecGΔC5 has significantly reduced ATP-dependent DNA unwinding activity. DNA unwinding assays comparing the ability of RecGΔC5 to unwind a Holliday junction substrate and a partial fork substrate with that of wild type RecG. Reactions used the proteins indicated at 0, 0.1, 1, 10, 50 or 100 nM (lanes a-f) and ^{32}P-labelled substrate DNA at 0.3 nM. The substrates were labelled at the 5' end of one strand as indicated.

Discussion

RecG can bind to and unwind several substrates *in vitro*. However, it is not clear whether or not RecG targets such structures within the cell (see page 111). Co-localisation of fluorescently tagged RecG and SeqA suggests that RecG localises to newly replicated DNA within *E. coli* cells and might interact with one of the replisome components. It was suggested previously that RecG might aid the restart of stalled replication forks by catalysing the inter-conversion of stalled fork structures and Holliday junctions (McGlynn and Lloyd 2000). The co-localisation of RecG with the replisome suggests that RecG would be localised in the vicinity of a stalled replication fork, supporting these models. In *B. subtilis*, RecG also localises with the replisome and this is dependent upon an interaction with the C-terminus of SSB (Lecointe *et al.* 2007). Recent *in vitro* studies have shown that *E. coli* RecG interacts with SSB and that this interaction is also via the C-terminus of SSB (Buss *et al.* 2008). Therefore, the localisation of RecG within *E. coli* cells might also be dependent upon an interaction with SSB. However, whilst SSB coats the lagging strand template during replication, it might also be found at recombination intermediates, such as D-loops, and also at R-loops. Although, RecG localises with the replisome this could be one of several structures to which SSB might target RecG. The length of the single-stranded DNA in these other structures might mean that only a small amount of SSB and RecG is capable of binding, so they might not be visible in assays such as these, at least with the fluorescent proteins I have used.

Since the high levels of SDR observed in *recG* cells are so dramatic, the role of RecG in limiting SDR needs to be considered when analysing *recG* phenotypes (see page 123). If RecG does localise to other intermediates, such as R-loops and D-loops, this means that it could be present at the initiation sites of stable DNA replication, as well as at the replication forks that have resulted from the initiation of SDR. Therefore, RecG may be uniquely qualified to limit the initiation of SDR and also be localised to these extra replication forks in case any problems should arise as a result of these forks. For example, multiple unregulated replication forks traversing the chromosome might be responsible for the segregation defects observed in *recG* cells after UV irradiation (see page 123).

Single-stranded DNA is exposed during most forms of DNA metabolism. SSB binds to and protects single-stranded DNA and therefore SSB-coated DNA is the substrate upon which many DNA metabolic enzymes must act. However, the role of SSB is more

complex. It can interact with at least 14 different proteins, which belong to systems involved in various aspects of DNA metabolism, including replication, recombination and repair. SSB is now thought to be involved in the organisation of these processes (reviewed by Shereda *et al.* 2008). Many of these interactions have been found to be mediated by the conserved C-terminus of SSB. A mutant (*ssb113*) encoding a substitution at one of these conserved C-terminal residues (P176S) is temperature-sensitive and hypersensitive to DNA damage at the permissive temperature. This mutant SSB does not interact properly with some of the SSB binding partners (refer to (Shereda *et al.* 2008) and references therein). Buss *et al.* (2008) demonstrated that the interaction between SSB and RecG is reduced when wild type SSB is replaced with SSB113 (P176S). Therefore, analysis of the ability of fluorescently tagged RecG to form foci and co-localise with SeqA in an *ssb113* derivative might confirm that the localisation of RecG is due an interaction with SSB.

Previous attempts to create fusions to the N-terminus of RecG suggested that such fusions were lethal to the cell. However, it was possible to create N-terminal fusions if the last 32 amino acid residues from the C-terminus of RecG were deleted (McGlynn *et al.* 2000). The fluorescent fusions used in this chapter depend upon a specially designed linker region that probably holds the fusion protein in a fixed position away from the DNA binding domains of RecG. I have demonstrated that localisation of fluorescently tagged RecG is dependent upon the C-terminus of RecG (Figure 40). If RecG co-localises with the replisome it is likely that a fusion protein, in which the extra N-terminal domains are not fixed in position, could interfere with the replisome components and cause lethality. This provides an explanation as to why the original fusions to wild type RecG were not possible unless the C-terminus was deleted.

Whilst a deletion of 10 residues from the C-terminus of RecG has no effect, a deletion of 15 residues or more prevents foci formation. A protein sequence alignment assembled by Geoff Briggs indicates that there is a conserved arginine and tryptophan between 10 and 15 residues from the end of the C-terminus (Figure 41). These residues might be important for localisation within the cell and targeted mutations within this region of the C-terminus should provide more information about the specific amino acid residues involved. As discussed above, the localisation of RecG might be due to the interaction with SSB. The inability of the larger RecG C-terminus deletions to localise within the cell

might therefore indicate that SSB interacts with the C-terminus of RecG. Since the fluorescently tagged RecG C-terminus alone did not form foci, it is possible that the interaction site includes residues from another domain of RecG, for instance the helicase domain. Purification and analysis of RecGΔC15, which does not form foci when tagged with eYFP, could indicate whether or not the C-terminus of RecG is necessary for the interaction with SSB.

The phenotypes of the C-terminus deletions were investigated with the aim of determining the importance of localisation of RecG. However, the smaller C-terminus deletions, which still localise within the cell, already had a phenotype. Therefore, it was impossible to determine whether or not the ability to localise is important. The DNA binding domain of RecG is situated at the N-terminus and the helicase motifs are towards the C-terminus (Lloyd and Sharples 1991; Mahdi *et al.* 1997). Given that no function has been assigned to the extreme C-terminal residues of RecG, it is surprising that a deletion of only 5 residues from the C-terminus could have such a dramatic effect on phenotype. When the C-terminus mutants were studied as single mutants they appeared to be far more resistant to DNA damage than a Δ*recG*, but unexpectedly when they were combined with Δ*ruvABC* the strains were almost as sensitive as a full deletion of *recG*. Indeed, the *recGΔC5* allele proved to be lethal when combined with Δ*rnhA* (Figure 47). Recent investigations of even smaller C-terminus deletions indicate that these can also have a dramatic phenotypic effect (Jane Grove, personal communication).

My studies of the *recG* deletions indicate that the C-terminus is necessary for protein function. The activity of purified RecGΔC5 was compared with wild type RecG. These preliminary experiments show that whilst RecGΔC5 binds Holliday junction and partial fork substrates with similar affinity to wild type, ATP-dependent unwinding of the substrates appears to be significantly reduced. At high protein concentrations a small amount of substrate unwinding is visible. It seems that the reduced ability to unwind substrates *in vitro* is sufficient for *in vivo* function provided the strains are not stressed by high levels of chronic DNA damage or by further mutations. These data combined with the *in vivo* phenotypes indicate that the extreme C-terminus of RecG is necessary for full function because it is involved in RecG helicase activity. There is currently no structure for the extreme C-terminus of RecG (Singleton *et al.* 2001). Since the C-terminus does not

appear to be involved in DNA binding, but affects the DNA unwinding activity it is possible that the extreme C-terminus interacts with the helicase motifs of the protein.

A deletion of the last 5 amino acid residues removes a conserved tyrosine residue situated 4 residues from the end of the C-terminus as well as a conserved alanine, which is the last residue (Figure 41). It is possible that these two residues have a role in DNA unwinding. A series of *recG* C-terminal mutants have been designed that should provide more information on the importance of these conserved residues. These mutants include *recGΔC3*, *recGΔC1*, *recGY690A* and *recGA693Q*, which Jane Grove is currently investigating. The importance of cellular localisation of RecG might also be determined if a functional protein that prevents localisation, can be designed. The first residues to be targeted will be the arginine and tryptophan between 10 and 15 residues from the end of the C-terminus. However, the extreme C-terminus obviously plays a role in helicase function so it might not be possible to create a mutant that prevents localisation, which does not affect *in vitro* activity.

General discussion

DNA is vulnerable to numerous endogenous and exogenous damaging agents. These damaging agents can induce a great number of DNA lesions. For example, every day human cells suffer from an estimated 18000 DNA depurination events alone (Friedberg *et al.* 2006). Depurination is only one of many forms of endogenous DNA damage that occur within these cells. With such constant damage, cells are heavily reliant upon DNA repair processes for survival. The situation is complicated by the fact that multicellular organisms such as humans are capable of renewing their tissues in order to prolong life. The ability of stem cells to keep dividing comes with the great risk of providing an opportunity for malignant transformation. It is inevitable that cells will accumulate genetic damage over time. However, if this damage enables the cells to proliferate in an unregulated manner it can lead to cancer. Whilst eliminating damaged cells or preventing them from further divisions protects against cancer early in life, it appears to be at a cost, namely ageing. Therefore the ability to repair DNA damage, promotes longevity not only by limiting genetic changes that might allow cells to proliferate uncontrollably but also by reducing the number of cells that have to be removed from the proliferating population (van Heemst *et al.* 2007).

I initially set out to study how cells are able to maintain the cell cycle and accurately replicate their genome in spite of the constant threat of DNA damage. I have focussed on the ability of *Escherichia coli* to complete replication and progress through the cell cycle when the cells have been exposed to UV irradiation, an environmental DNA damaging agent to which many organisms are exposed frequently. Replication is delayed by DNA damage, but what happens when a replication fork meets a lesion is still unclear. UV-induced lesions can block synthesis by the replicative DNA polymerases. Despite blocking the lagging strand polymerase, it is accepted that a lesion in the lagging strand template can be bypassed by priming a new Okazaki fragment and therefore does not affect replication fork progression. However, it is thought that a lesion in the leading strand template could block progression of the replication fork. In *E. coli*, a stalled replication fork must be reactivated so that replication can be continued. Numerous mechanisms for replication restart have been proposed. The replication fork might require extensive processing before replication can restart. Alternatively, it has been

proposed that replication could be re-primed downstream of a lesion in the leading strand template with little delay, but it is not clear if this actually happens *in vivo*, let alone how often.

Christian Rudolph observed that the origin of replication keeps firing at times when the terminus region cannot be replicated in UV-irradiated *E. coli* cells (see page 78, Rudolph *et al.* 2007b). This observation indicated that there is no control mechanism acting to inhibit replication initiation when the template DNA is damaged. This provides a contrast with eukaryotic cells, in which it is believed checkpoint mechanisms bring the cell cycle to a halt so that the damaged DNA might be repaired before continuing to the next step in the cycle. Whilst any existing replication forks could stall at DNA lesions, if the origin continues to fire in *E. coli*, these newly set up replication forks could also stall. However, if blocked replication forks can restart efficiently, albeit after a significant delay, continued firing of the origin could enable a cluster of active forks to rapidly complete replication and produce multiple copies of the chromosome once the blocking lesions have been removed. Our data suggested that when replication resumes, the majority of the lesions have already been repaired (Rudolph *et al.* 2007b). Therefore continued firing of the origin could compensate at least partially for the initial delay caused by the blocking lesions, which is consistent with the observation that after a low UV dose, cellular division in a wild type strain resumes, after a delay, at a higher rate than that in unirradiated cells (Rudolph *et al.* 2008).

In the case of eukaryotes, multiple checkpoint responses are thought to maintain genome stability by preventing progression through the cell cycle until all essential processes have been completed. The G_1-S transition checkpoint inhibits replication initiation when lesions are present on the template DNA (Sancar *et al.* 2004; Callegari and Kelly 2007). Since eukaryotic chromosomes have multiple replication origins and they do not initiate overlapping cell cycles, allowing these origins to fire when the template is damaged would simply increase the number of stalled forks that the cell has to deal with. Since loading of the replicative helicase is thought to be inhibited after replication initiation, at least in some eukaryotes, numerous stalled replication forks are dangerous intermediates. Indeed, my studies have demonstrated that in *E. coli* all synthesis after UV irradiation depends on DnaC activity, indicating that at least the replicative helicase and possibly the entire replisome needs to be reloaded. Eukaryotes have another checkpoint

system, which stabilises stalled replication forks and prevents replisome dissociation (Branzei and Foiani 2007; Tourriere and Pasero 2007), but numerous stalled forks might increase the risk of replisome dissociation. It has also been shown in yeast that stalled replication forks provoke recombination and genomic rearrangements (Lambert *et al.* 2005). Therefore, whilst it might be beneficial for the origin of replication to continue firing in *E. coli*, the consequences are different in eukaryotes, probably due to their different genomic structure.

Over forty years ago Rupp & Howard-Flanders made several observations that led to a theory of how replication proceeds after UV irradiation in *E. coli*. They found that if the delay in incorporation after UV was averaged over the number of lesions induced, it could correspond to a delay of approximately 10 seconds per lesion. They observed that newly synthesised DNA after UV irradiation is in short fragments and that over time these fragments increased in size (Rupp and Howard-Flanders 1968). Based on these observations it was concluded that replication forks are delayed at each lesion for approximately 10 seconds before proceeding and leaving a gap opposite the lesion (Figure 5). They suggested that the conversion of small DNA fragments into larger ones represented the filling in of these nascent strand gaps (Rupp and Howard-Flanders 1968).

The model of Rupp & Howard-Flanders requires that synthesis of the leading strand can be primed at sites away from *oriC*. But whilst it is accepted that lesions in the lagging strand template can be bypassed simply by priming replication downstream of the lesion, it has been argued that leading strand synthesis can be primed only at *oriC* and would therefore be blocked by a lesion in the leading strand template. Indeed, *in vitro* and *in vivo* studies have demonstrated that a lesion on the leading strand template prevents replication fork progression (Higuchi *et al.* 2003; Pages and Fuchs 2003). The Rupp & Howard-Flanders model has recently been revived by data demonstrating that leading strand synthesis can be initiated *de novo* at fork structures, at least *in vitro* (Heller and Marians 2006a).

However, these studies as well as those by several other groups (Khidhir *et al.* 1985; Courcelle *et al.* 2003; Donaldson *et al.* 2004; Courcelle *et al.* 2005), had ignored the fact that some of the net synthesis measured after UV could result from DnaA-dependent origin firing. I have demonstrated that the extent of the delay at existing forks is masked by continued origin firing and the initiation of inducible stable DNA replication (iSDR). This

means that a delay of only 10 seconds per lesion is an underestimate. Furthermore, these two modes of synthesis represent the majority of synthesis measured early after UV irradiation. Newly synthesised DNA, initiated at *oriC* or induced by UV, would initially appear as small fragments that would increase in size over time as these forks progress. Therefore, these two modes of synthesis could be responsible for the newly synthesised DNA fragments that Rupp & Howard-Flanders observed rather than the lesion skipping mechanism that they proposed. Finally, the complete lack of DNA synthesis in *recO* cells for a substantial period after UV suggests that the majority of replication forks are blocked by the lesions rather than proceeding past them.

What does happen to existing replication forks after UV irradiation? My data cannot exclude the possibility that replication forks progress past some lesions in the leading strand template, however it does indicate that forks cannot progress past many lesions before stalling. It is in line with models proposing that replication forks stall at lesions on the leading strand template and require extensive processing before replication can restart. The idea of forks stalling at lesions rather than proceeding past them leaving gaps behind is appealing. Any gaps created would require recombination to repair them, which is potentially harmful. Indeed, there is increasing evidence that recombination is limited in both prokaryotes (Flores *et al.* 2005; Mahdi *et al.* 2006) and eukaryotes (Krejci *et al.* 2003; Veaute *et al.* 2003).

When the leading strand polymerase is blocked, uncoupling of the leading and lagging strand polymerases (Higuchi *et al.* 2003; Pages and Fuchs 2003), would expose single-stranded DNA at the replication fork, which will rapidly be coated by single-stranded DNA binding protein (SSB). There is increasing evidence that SSB interacts with a variety of proteins (Shereda *et al.* 2008). Thus, binding of SSB to the lagging strand template during replication would explain the co-localisation of various proteins with the replication fork, including PriA, RecG and RecQ (see page 141, Lecointe *et al.* 2007). Since SSB has a variety of interaction partners, these might also be localised to active replication forks. Therefore, when replication forks stall several of the SSB interaction partners should be in the vicinity of the fork and able to act should their target substrates arise. SSB also interacts with RecO ((Shereda *et al.* 2008) and references therein), one of the RecA-mediators and this interaction might aid the loading of RecA onto the exposed single-stranded DNA at stalled forks, leading to induction of the SOS response.

A stalled replication fork must be processed such that replication can be restarted. The major priority is probably to either repair or bypass the blocking lesion. Whilst RecFOR activity is not required for lesion removal (Courcelle *et al.* 1999), it is necessary for efficient replication restart (see page 97). Since RecFOR mediates the loading of RecA, fork reactivation probably involves some sort of RecA-dependent reaction. This RecA activity could be replication fork reversal or RecA-mediated excision repair (see pages 30 and 35). My data indicates that at least the replicative helicase and possibly the entire replisome needs to be reloaded before replication can restart (see page 78). This idea is supported by *in vitro* studies showing that the replicative helicase leaves the stalled polymerase behind and that RecFOR and RecA can act to displace this polymerase (McInerney and O'Donnell 2007). Therefore, the RecA-dependent activity might be a fork clearing role allowing the damaged region to be accessed by repair proteins.

Replication restart does not occur for approximately 15-20 minutes, by which time the majority of the lesions have been repaired (Courcelle *et al.* 1999; Rudolph *et al.* 2007b). This means that when replication does resume, the path to the terminus should be relatively clear and forks should proceed unhindered. Indeed, after the delay DNA synthesis continues at a similar rate to that in unirradiated cells (see page 78).

My observation that the majority of synthesis early after UV irradiation results from origin firing and iSDR led me to re-investigate DNA synthesis in cells lacking RecFOR or RecG. In the case of cells lacking RecFOR, it had been observed that there is a complete lack of DNA synthesis for at least 90 minutes after UV irradiation and it was concluded that synthesis could not recover without these proteins (Courcelle *et al.* 2003). However, this lack of synthesis suggested that origin firing and iSDR were also affected in these cells. I demonstrated that all three modes of synthesis are delayed after UV irradiation in cells lacking RecO, but in contrast to the reports by Courcelle *et al.*, I found that, after a delay, synthesis can recover to a rate similar to that observed in unirradiated cells. My data suggest that these contrasting observations can be explained by the different UV doses used. In their original analysis of synthesis in *recF* cells, Courcelle *et al.* used a relatively high UV dose, which would result in the killing of the majority of *recFOR* cells. In contrast, by using a lower UV dose, I have been able to demonstrate that whilst RecFOR is required for efficient restart, replication is still capable of resuming in cells lacking these proteins.

RecG has been implicated in several pathways *in vivo*, including during the late stages of recombination (Lloyd 1991; Lloyd and Buckman 1991), during replication restart (McGlynn and Lloyd 2000), and in limiting stable DNA replication (Hong *et al.* 1995). Although it was known that SDR is elevated in *recG* mutants (Hong *et al.* 1995), this was not considered when DNA synthesis was measured in irradiated *recG* cells (Donaldson *et al.* 2004). My studies revealed dramatic levels of SDR after UV irradiation. This proved to be an excellent example as to why the different modes of DNA synthesis should be considered when measuring synthesis after UV irradiation. Although DNA synthesis does not appear to be affected in a *recG* single mutant, I have demonstrated that a substrate capable of initiating SDR is formed at a much higher rate in these cells and that SDR is greatly increased in comparison with *dnaA46* cells lacking the DnaA initiator protein. The much increased initiation of SDR in *recG* cells could prove important for understanding the phenotype of these mutants.

The role of iSDR is not clear. However, it has recently been proposed that in eukaryotes extra replication initiations can be triggered when replication is blocked. The multiple origins and lack of defined termination sites on eukaryotic chromosomes means that if one replication fork stalls, a fork from a neighbouring origin could replicate up to this fork, reducing the necessity to restart the stalled fork. In addition, recent experimental evidence has led to the hypothesis that even if two converging forks are stalled, replication of the region could be completed if a dormant origin was located in between (Ge *et al.* 2007). It was demonstrated that when replication is inhibited in human cells, these dormant origins help to maintain the rate of replication as well as cell viability (Ge *et al.* 2007). Since *E. coli* has only one origin of replication and a defined termination region, if one of the forks initiated at *oriC* is blocked and cannot restart, the other fork will be held up within the termination region and replication of the chromosome would be incomplete. Replication forks can eventually escape the termination region but this takes a long time (Possoz *et al.* 2006). Therefore, iSDR could provide a function similar to the dormant origins observed in eukaryotes and therefore be beneficial for the survival of bacterial cells after DNA damage.

Could stable DNA replication in *E. coli* cells fulfil this role? SDR is initiated after DNA damage independently of DnaA and *oriC*. Whilst specific chromosomal locations for the initiation of iSDR have been described (Kogoma 1997), the BrdU incorporation

experiments of Christian Rudolph have not shown any evidence of a specific initiation site (Rudolph *et al.* 2007b). Therefore, it is possible that iSDR can initiate at any chromosomal location, which means it could be a suitable mechanism for rescuing stalled replication forks. There is currently no evidence to support a possible beneficial role of iSDR after DNA damage. However, the increased levels of SDR in irradiated *recG* cells coincide with a severe segregation defect. This opens the possibility that SDR has a detrimental rather than a beneficial effect.

How could SDR cause segregation defects? Whilst the nature and significance of SDR are poorly understood, there is strong evidence that it results from the setting up of extra replication forks. This means that in irradiated *recG* cells there will be multiple replication forks traversing the chromosome, which would result in an increased number of replication fork encounters during each cell cycle. It is thought that both cSDR and iSDR occur in a bi-directional manner and therefore these forks could either follow and catch-up with *oriC*-initiated forks that have already replicated the region or converge with the *oriC*-initiated forks. Replication initiation in both prokaryotes and eukaryotes is strictly regulated to prevent initiation from occurring more than once per cell cycle. If cells do re-initiate replication early, this re-replication can lead to genomic instability (Simmons *et al.* 2004; Arias and Walter 2007; Blow and Gillespie 2008). The situation in which SDR initiates behind the *oriC*-initiated replication fork could have the same effect as re-initiation of an origin. In *E. coli* cells, the broad termination region limits convergence of forks to occur within this area. It is possible that converging forks could also result in de-stabilising DNA intermediates, especially perhaps if these meetings did not occur at Tus-*Ter*. Indeed, *in vitro* studies of replication suggested that without Tus, when two replisomes meet, one replisome might displace the 3′ end of the nascent leading strand of the opposing fork (Hiasa and Marians 1994). This could generate a structure that allows the replisome to use the nascent leading strand as a new template and re-replicate the already replicated DNA (Hiasa and Marians 1994). This was supported by *in vivo* studies showing that in the absence of Tus, replication of a plasmid does not terminate but leads to plasmid multimers, further replication via rolling-circle replication and loss of plasmid stability (Krabbe *et al.* 1997). Little is known about termination in eukaryotes but it appears that forks meet without the aid of any termination factors. It seems there is evidence that both fork catch-up events and fork convergence events (in prokaryotes) can

lead to re-replication of the chromosome. It is not clear what exactly might happen if re-replication occurs but it might explain the segregation defects observed in *recG* cells.

It is possible that the limited level of iSDR in wild type cells could have a beneficial role, but it is also possible that the presence of RecG in wild type cells prevents the SDR from causing pathology. Indeed, the localisation of RecG to replication forks could mean that RecG is in the immediate vicinity when two forks meet and could somehow limit the opportunity for re-replication to occur. RecG might perform a dual role, firstly by limiting the initiation of SDR by unwinding D-loops and R-loops, hence the lower levels observed in wild type cells and secondly by reducing the pathological effects resulting from SDR.

In conclusion, my studies have shed further light on the effect of UV irradiation on DNA synthesis. They support models proposing that replication forks stall at lesions on the leading strand template and require extensive processing in order to restart. I have demonstrated the importance of looking at the different modes of DNA synthesis, which were already known to occur. I also have highlighted the importance of stable DNA replication in *recG* cells and have suggested that the role of RecG in SDR must be considered when evaluating the phenotype of *recG* cells. The synergistic phenotype of *recG ruvABC* double mutants after UV irradiation has been explained by a possible role of RecG during the late stages of recombination, but an alternative Holliday junction resolvase that could act with RecG has yet to be found. However, it is possible that pathology resulting from the dramatic level of SDR in *recG* cells after UV irradiation could provide an alternative explanation for the synergistic phenotype of *recG ruvABC*, an idea that is supported by the possible synergism I have observed in *rnhA ruvABC* cells. Whilst RNase HI is not thought to be involved in recombination, it does have a role in limiting SDR. Therefore, the elevated levels of SDR in *recG* and *rnhA* cells might be responsible for the synergistic interactions of these mutants with *ruvABC* after UV irradiation. The ability of RecG to unwind a variety of branched DNA substrates *in vitro*, coupled with the pleiotropic phenotypes of *recG* mutant strains, has made it difficult to pin down exactly what RecG does *in vivo*. The results presented here indicate that limiting SDR might be a crucial role. They also suggest ways in which this idea might be probed in future studies.

References

Al-Deib, A.A., Mahdi, A.A., and Lloyd, R.G. 1996. Modulation of recombination and DNA repair by the RecG and PriA helicases of *Escherichia coli* K-12. *J Bacteriol* **178**: 6782-6789.

Arias, E.E. and Walter, J.C. 2007. Strength in numbers: preventing rereplication via multiple mechanisms in eukaryotic cells. *Genes Dev* **21**(5): 497-518.

Asai, T. and Kogoma, T. 1994. Roles of *ruvA, ruvC* and *recG* gene functions in normal and DNA damage-inducible replication of the *Escherichia coli* chromosome. *Genetics* **137**: 895-902.

Asai, T., Sommer, S., Bailone, A., and Kogoma, T. 1993. Homologous recombination-dependent initiation of DNA replication from DNA damage-inducible origins in *Escherichia coli*. *EMBO J* **12**: 3287-3295.

Bachmann, B.J. 1996. Derivations and genotypes of some mutant derivatives of *Escherichia coli* K-12. in *Escherichia coli and Salmonella Cellular and Molecular Biology, (Second Edition)* (ed. F.C. Neidhardt, R. Curtiss III, J.L. Ingraham, E.C.C. Lin, K.B. Low, B. Magasanik, W.S. Reznikoff, M. Riley, M. Schaechter, and H.E. Umbarger), pp. 2460-2488. ASM Press, Washington, D.C.

Baker, T.A. and Bell, S.P. 1998. Polymerases and the replisome: machines within machines. *Cell* **92**(3): 295-305.

Bastia, D., Zzaman, S., Krings, G., Saxena, M., Peng, X., and Greenberg, M.M. 2008. Replication termination mechanism as revealed by Tus-mediated polar arrest of a sliding helicase. *Proc Natl Acad Sci U S A* **105**(35): 12831-12836.

Bernhardt, T.G. and de Boer, P.A. 2004. Screening for synthetic lethal mutants in *Escherichia coli* and identification of EnvC (YibP) as a periplasmic septal ring factor with murein hydrolase activity. *Mol Microbiol* **52**(5): 1255-1269.

Beukers, R., Eker, A.P., and Lohman, P.H. 2008. 50 years thymine dimer. *DNA Repair (Amst)* **7**(3): 530-543.

Bichara, M., Pinet, I., Lambert, I.B., and Fuchs, R.P. 2007. RecA-mediated excision repair: a novel mechanism for repairing DNA lesions at sites of arrested DNA synthesis. *Mol Microbiol* **65**(1): 218-229.

Bidnenko, V., Ehrlich, S.D., and Michel, B. 2002. Replication fork collapse at replication terminator sequences. *EMBO J* **21**(14): 3898-3907.

Billen, D. 1969. Replication of the bacterial chromosome: location of new initiation sites after irradiation. *J Bacteriol* **97**(3): 1169-1175.

Blastyak, A., Pinter, L., Unk, I., Prakash, L., Prakash, S., and Haracska, L. 2007. Yeast Rad5 protein required for postreplication repair has a DNA helicase activity specific for replication fork regression. *Mol Cell* **28**(1): 167-175.

Blow, J.J. and Gillespie, P.J. 2008. Replication licensing and cancer – a fatal entanglement? *Nat Rev Cancer* **8**(10): 799-806.

Boye, E. 1991. The hemimethylated replication origin of *Escherichia coli* can be initiated *in vitro*. *J Bacteriol* **173**(14): 4537-4539.

Boye, E., Lobner-Olesen, A., and Skarstad, K. 2000. Limiting DNA replication to once and only once. *EMBO Rep* **1**(6): 479-483.

Boye, E., Stokke, T., Kleckner, N., and Skarstad, K. 1996. Coordinating DNA replication initiation with cell growth: differential roles for DnaA and SeqA proteins. *Proc Natl Acad Sci U S A* **93**(22): 12206-12211.

Branzei, D. and Foiani, M. 2007. Interplay of replication checkpoints and repair proteins at stalled replication forks. *DNA Repair (Amst)* **6**(7): 994-1003.

Brendler, T., Sawitzke, J., Sergueev, K., and Austin, S. 2000. A case for sliding SeqA tracts at anchored replication forks during *Escherichia coli* chromosome replication and segregation. *EMBO J* **19**(22): 6249-6258.

Brewer, B.J. 1988. When polymerases collide: replication and the transcriptional organization of the *E. coli* chromosome. *Cell* **53**: 679-686.

Brewer, B.J. and Fangman, W.L. 1988. A replication fork barrier at the 3' end of yeast ribosomal RNA genes. *Cell* **55**(4): 637-643.

Bridges, B.A. 2005. Error-prone DNA repair and translesion DNA synthesis. II: The inducible SOS hypothesis. *DNA Repair (Amst)* **4**(6): 725-726, 739.

Bridges, B.A. and Sedgwick, S.G. 1974. Effect of photoreactivation on the filling of gaps in deoxyribonucleic acid synthesized after exposure of *Escherichia coli* to ultraviolet light. *J Bacteriol* **117**(3): 1077-1081.

Briggs, G.S., Mahdi, A.A., Weller, G.R., Wen, Q., and Lloyd, R.G. 2004. Interplay between DNA replication, recombination and repair based on the structure of RecG helicase. *Philos Trans R Soc B* **359**(1441): 49-59.

Briggs, G.S., Mahdi, A.A., Wen, Q., and Lloyd, R.G. 2005. DNA binding by the substrate specificity (wedge) domain of RecG helicase suggests a role in processivity. *J Biol Chem* **280**(14): 13921-13927.

Buss, J.A., Kimura, Y., and Bianco, P.R. 2008. RecG interacts directly with SSB: implications for stalled replication fork regression. *Nucleic Acids Res* **36**(22): 7029-7042.

Callegari, A.J. and Kelly, T.J. 2007. Shedding light on the DNA damage checkpoint. *Cell Cycle* **6**(6): 660-666.

Campbell, J.L. and Kleckner, N. 1990. *E. coli oriC* and the *dnaA* gene promoter are sequestered from *dam* methyltransferase following the passage of the chromosomal replication fork. *Cell* **62**(5): 967-979.

Carr, K.M. and Kaguni, J.M. 2001. Stoichiometry of DnaA and DnaB protein in initiation at the *Escherichia coli* chromosomal origin. *J Biol Chem* **276**(48): 44919-44925.

Costa, A. and Onesti, S. 2008. The MCM complex: (just) a replicative helicase? *Biochem Soc Trans* **36**(Pt 1): 136-140.

Courcelle, C.T., Belle, J.J., and Courcelle, J. 2005. Nucleotide excision repair or polymerase V-mediated lesion bypass can act to restore UV-arrested replication forks in *Escherichia coli. J Bacteriol* **187**(20): 6953-6961.

Courcelle, C.T., Chow, K.H., Casey, A., and Courcelle, J. 2006. Nascent DNA processing by RecJ favors lesion repair over translesion synthesis at arrested replication forks in *Escherichia coli. Proc Natl Acad Sci U S A* **103**(24): 9154-9159.

Courcelle, J., Carswell-Crumpton, C., and Hanawalt, P.C. 1997. *recF* and *recR* are required for the resumption of replication at DNA replication forks in *Escherichia coli*. *Proc Natl Acad Sci USA* **94**(8): 3714-3719.

Courcelle, J., Crowley, D.J., and Hanawalt, P.C. 1999. Recovery of DNA replication in UV-irradiated *Escherichia coli* requires both excision repair and *recF* protein function. *J Bacteriol* **181**(3): 916-922.

Courcelle, J., Donaldson, J.R., Chow, K.H., and Courcelle, C.T. 2003. DNA damage-induced replication fork regression and processing in *Escherichia coli*. *Science* **299**(5609): 1064-1067.

Courcelle, J. and Hanawalt, P.C. 1999. RecQ and RecJ process blocked replication forks prior to the resumption of replication in UV-irradiated *Escherichia coli*. *Mol Gen Genet* **262**(3): 543-551.

Courcelle, J., Khodursky, A., Peter, B., Brown, P.O., and Hanawalt, P.C. 2001. Comparative gene expression profiles following UV exposure in wild-type and SOS-deficient *Escherichia coli*. *Genetics* **158**(1): 41-64.

Cox, M.M. 2007. Motoring along with the bacterial RecA protein. *Nat Rev Mol Cell Biol* **8**(2): 127-138.

Cox, M.M., Goodman, M.F., Kreuzer, K.N., Sherratt, D.J., Sandler, S.J., and Marians, K.J. 2000. The importance of repairing stalled replication forks. *Nature* **404**(6773): 37-41.

Datsenko, K.A. and Wanner, B.L. 2000. One-step inactivation of chromosomal genes in *Escherichia coli* K-12 using PCR products. *Proc Natl Acad Sci U S A* **97**(12): 6640-6645.

de Boer, P.A., Crossley, R.E., and Rothfield, L.I. 1989. A division inhibitor and a topological specificity factor coded for by the minicell locus determine proper placement of the division septum in *E. coli*. *Cell* **56**(4): 641-649.

de Massy, B., Bejar, S., Louarn, J., Louarn, J.M., and Bouche, J.P. 1987. Inhibition of replication forks exiting the terminus region of the *Escherichia coli* chromosome occurs at two loci separated by 5 min. *Proc Natl Acad Sci U S A* **84**(7): 1759-1763.

Dillingham, M.S. and Kowalczykowski, S.C. 2008. RecBCD enzyme and the repair of double-stranded DNA breaks. *Microbiol Mol Biol Rev* **72**(4): 642-671.

Donaldson, J.R., Courcelle, C.T., and Courcelle, J. 2004. RuvAB and RecG are not essential for the recovery of DNA synthesis following UV-induced DNA damage in *Escherichia coli*. *Genetics* **166**(4): 1631-1640.

Duggin, I.G., Wake, R.G., Bell, S.D., and Hill, T.M. 2008. The replication fork trap and termination of chromosome replication. *Mol Microbiol* **70**(6): 1323-1333.

Erzberger, J.P., Pirruccello, M.M., and Berger, J.M. 2002. The structure of bacterial DnaA: implications for general mechanism underlying DNA replication initiation. *EMBO J* **21**(18): 4763-4773.

Fang, L., Davey, M.J., and O'Donnell, M. 1999. Replisome assembly at *oriC*, the replication origin of *E. coli*, reveals an explanation for initiation sites outside an origin. *Mol Cell* **4**(4): 541-553.

Finkel, T., Serrano, M., and Blasco, M.A. 2007. The common biology of cancer and ageing. *Nature* **448**(7155): 767-774.

Flores, M.J., Sanchez, N., and Michel, B. 2005. A fork-clearing role for UvrD. *Mol Microbiol* **57**(6): 1664-1675.

French, S. 1992. Consequences of replication fork movement through transcription units *in vivo*. *Science* **258**(5086): 1362-1365.

Friedberg, E.C., Walker, G.C., Siede, W., Wood, R., Schultz, R., and Ellenberger, T. 2006. *DNA repair and mutagenesis*. ASM Press, Washington, DC.

Fujii, S., Isogawa, A., and Fuchs, R.P. 2006. RecFOR proteins are essential for Pol V-mediated translesion synthesis and mutagenesis. *Embo J* **25**(24): 5754-5763.

Gari, K., Decaillet, C., Delannoy, M., Wu, L., and Constantinou, A. 2008. Remodeling of DNA replication structures by the branch point translocase FANCM. *Proc Natl Acad Sci U S A* **105**(42): 16107-16112.

Ge, X.Q., Jackson, D.A., and Blow, J.J. 2007. Dormant origins licensed by excess Mcm2-7 are required for human cells to survive replicative stress. *Genes Dev* **21**(24): 3331-3341.

Gregg, A.V., McGlynn, P., Jaktaji, R.P., and Lloyd, R.G. 2002. Direct rescue of stalled DNA replication forks via the combined action of PriA and RecG helicase activities. *Mol Cell* **9**: 241-251.

Haeusser, D.P. and Levin, P.A. 2008. The great divide: coordinating cell cycle events during bacterial growth and division. *Curr Opin Microbiol* **11**(2): 94-99.

Hanawalt, P.C. and Spivak, G. 2008. Transcription-coupled DNA repair: two decades of progress and surprises. *Nat Rev Mol Cell Biol* **9**(12): 958-970.

Hansen, F. G., Koefoed, S., and Atlung, T. 1992. Cloning and nucleotide sequence determination of twelve mutant *dnaA* genes of *Escherichia coli. Mol Gen Genet* **234**(1): 14-21.

Hausen, P. and Stein, H. 1970. Ribonuclease H. An enzyme degrading the RNA moiety of DNA-RNA hybrids. *Eur J Biochem* **14**(2): 278-283.

Hegde, S., Sandler, S.J., Clark, A.J., and Madiraju, M.V. 1995. *recO* and *recR* mutations delay induction of the SOS response in *Escherichia coli. Mol Gen Genet* **246**(2): 254-258.

Helleday, T., Lo, J., van Gent, D.C., and Engelward, B.P. 2007. DNA double-strand break repair: from mechanistic understanding to cancer treatment. *DNA Repair (Amst)* **6**(7): 923-935.

Heller, R.C. and Marians, K.J. 2005. The disposition of nascent strands at stalled replication forks dictates the pathway of replisome loading during restart. *Mol Cell* **17**(5): 733-743.

Heller, R.C. and Marians, K.J. 2006a. Replication fork reactivation downstream of a blocked nascent leading strand. *Nature* **439**(7076): 557-562.

Heller, R.C. and Marians, K.J. 2006b. Replisome assembly and the direct restart of stalled replication forks. *Nat Rev Mol Cell Biol* **7**(12): 932-943.

Hiasa, H. and Marians, K.J. 1994. Tus prevents overreplication of *oriC* plasmid DNA. *J Biol Chem* **269**(43): 26959-26968.

Hickson, I.D. 2003. RecQ helicases: caretakers of the genome. *Nat Rev Cancer* **3**(3): 169-178.

Higgins, N.P., Kato, K., and Strauss, B. 1976. A model for replication repair in mammalian cells. *J Mol Biol* **101**(3): 417-425.

Higuchi, K., Katayama, T., Iwai, S., Hidaka, M., Horiuchi, T., and Maki, H. 2003. Fate of DNA replication fork encountering a single DNA lesion during *oriC* plasmid DNA replication *in vitro. Genes Cells* **8**(5): 437-449.

Hill, T.M., Henson, J.M., and Kuempel, P.L. 1987. The terminus region of the *Escherichia coli* chromosome contains two separate loci that exhibit polar inhibition of replication. *Proc Natl Acad Sci U S A* **84**(7): 1754-1758.

Hill, T.M. and Marians, K.J. 1990. Escherichia coli Tus protein acts to arrest the progression of DNA replication forks *in vitro*. *Proc Natl Acad Sci U S A* **87**(7): 2481-2485.

Hill, T.M., Tecklenburg, M.L., Pelletier, A.J., and Kuempel, P.L. 1989. *tus,* the trans-acting gene required for termination of DNA replication in *Escherichia coli*, encodes a DNA-binding protein. *Proc Natl Acad Sci U S A* **86**(5): 1593-1597.

Hong, X., Cadell, G.W., and Kogoma, T. 1995. *Escherichia coli* RecG and RecA proteins in R-loop formation. *EMBO J* **14**: 2385-2392.

Ishioka, K., Iwasaki, H., and Shinagawa, H. 1997. Roles of the *recG* gene product of *Escherichia coli* in recombination repair: effects of the delta *recG* mutation on cell division and chromosome partition. *Genes Genet Syst* **72**(2): 91-99.

Iyer, V.N. and Rupp, W.D. 1971. Usefulness of benzoylated naphthoylated DEAE-cellulose to distinguish and fractionate double-stranded DNA bearing different extents of single-stranded regions. *Biochim Biophys Acta* **228**(1): 117-126.

Jaktaji, R.P. and Lloyd, R.G. 2003. PriA supports two distinct pathways for replication restart in UV-irradiated *Escherichia coli* cells. *Mol Microbiol* **47**(4): 1091-1100.

Janion, C. 2001. Some aspects of the SOS response system – a critical survey. *Acta Biochim Pol* **48**(3): 599-610.

Jonczyk, P. and Ciesla, Z. 1979. DNA synthesis in UV-irradiated *Escherichia coli* K-12 strains carrying *dnaA* mutations. *Mol Gen Genet* **171**(1): 53-58.

Kaguni, J. 2006. DnaA: Controlling the initiation of bacterial DNA replication and more. *Annu Rev Microbiol* **60**: 351-371.

Kanagaraj, R., Saydam, N., Garcia, P.L., Zheng, L., and Janscak, P. 2006. Human RECQ5beta helicase promotes strand exchange on synthetic DNA structures resembling a stalled replication fork. *Nucleic Acids Res* **34**(18): 5217-5231.

Kang, S., Lee, H., Han, J.S., and Hwang, D.S. 1999. Interaction of SeqA and Dam methylase on the hemimethylated origin of *Escherichia coli* chromosomal DNA replication. *J Biol Chem* **274**(17): 11463-11468.

Kasahara, M., Clikeman, J.A., Bates, D.B., and Kogoma, T. 2000. RecA protein-dependent R-loop formation *in vitro*. *Genes Dev* **14**(3): 360-365.

Katayama, T., Kubota, T., Kurokawa, K., Crooke, E., and Sekimizu, K. 1998. The initiator function of DnaA protein is negatively regulated by the sliding clamp of the *E. coli* chromosomal replicase. *Cell* **94**(1): 61-71.

Kelman, Z. and O'Donnell, M. 1995. DNA polymerase III holoenzyme: structure and function of a chromosomal replicating machine. *Annu Rev Biochem* **64**: 171-200.

Khatri, G.S., MacAllister, T., Sista, P.R., and Bastia, D. 1989. The replication terminator protein of *E. coli* is a DNA sequence-specific contra-helicase. *Cell* **59**(4): 667-674.

Khidhir, M.A., Casaregola, S., and Holland, I.B. 1985. Mechanism of transient inhibition of DNA synthesis in ultraviolet-irradiated *E. coli*: inhibition is independent of *recA* whilst recovery requires RecA protein itself and an additional, inducible SOS function. *Mol Gen Genet* **199**: 133-140.

Kitagawa, R., Mitsuki, H., Okazaki, T., and Ogawa, T. 1996. A novel DnaA protein-binding site at 94.7 min on the *Escherichia coli* chromosome. *Mol Microbiol* **19**(5): 1137-1147.

Kitagawa, R., Ozaki, T., Moriya, S., and Ogawa, T. 1998. Negative control of replication initiation by a novel chromosomal locus exhibiting exceptional affinity for *Escherichia coli* DnaA protein. *Genes Dev* **12**(19): 3032-3043.

Klein, H.L. 2007. Reversal of fortune: Rad5 to the rescue. *Mol Cell* **28**(2): 181-183.

Kogoma, T. 1997. Stable DNA replication: Interplay between DNA replication, homologous recombination, and transcription. *Microbiol Molec Biol Rev* **61**: 212-238.

Kogoma, T., Cadwell, G.W., Barnard, K.G., and Asai, T. 1996. The DNA replication priming protein, PriA, is required for homologous recombination and double-strand break repair. *J Bacteriol* **178**: 1258-1264.

Kogoma, T. and von Meyenburg, K. 1983. The origin of replication, *oriC*, and the *dnaA* protein are dispensable in stable DNA replication (*sdrA*) mutants of *Escherichia coli* K-12. *EMBO J* **2**(3): 463-468.

Krabbe, M., Zabielski, J., Bernander, R., and Nordstrom, K. 1997. Inactivation of the replication-termination system affects the replication mode and causes unstable maintenance of plasmid R1. *Mol Microbiol* **24**(4): 723-735.

Krejci, L., Van Komen, S., Li, Y., Villemain, J., Reddy, M.S., Klein, H., Ellenberger, T., and Sung, P. 2003. DNA helicase Srs2 disrupts the Rad51 presynaptic filament. *Nature* **423**(6937): 305-309.

Kreuzer, K.N. 2005. Interplay between DNA replication and recombination in prokaryotes. *Annu Rev Microbiol* **59**: 43-67.

Kuempel, P.L., Duerr, S.A., and Seeley, N.R. 1977. Terminus region of the chromosome in *Escherichia coli* inhibits replication forks. *Proc Natl Acad Sci U S A* **74**(9): 3927-3931.

Kurokawa, K., Nishida, S., Emoto, A., Sekimizu, K., and Katayama, T. 1999. Replication cycle-coordinated change of the adenine nucleotide-bound forms of DnaA protein in *Escherichia coli*. *EMBO J* **18**(23): 6642-6652.

Kuzminov, A. 1995. Collapse and repair of replication forks in *Escherichia coli*. *Mol Microbiol* **16**: 373-384.

Lambert, S., Watson, A., Sheedy, D.M., Martin, B., and Carr, A.M. 2005. Gross chromosomal rearrangements and elevated recombination at an inducible site-specific replication fork barrier. *Cell* **121**(5): 689-702.

Landoulsi, A., Hughes, P., Kern, R., and Kohiyama, M. 1989. *dam* methylation and the initiation of DNA replication on *oriC* plasmids. *Mol Gen Genet* **216**(2-3): 217-223.

Langston, L.D. and O'Donnell, M. 2006. DNA replication: keep moving and don't mind the gap. *Mol Cell* **23**(2): 155-160.

Lau, I.F., Filipe, S.R., Soballe, B., Okstad, O.A., Barre, F.X., and Sherratt, D.J. 2003. Spatial and temporal organization of replicating *Escherichia coli* chromosomes. *Mol Microbiol* **49**(3): 731-743.

Lecointe, F., Serena, C., Velten, M., Costes, A., McGovern, S., Meile, J.C., Errington, J., Ehrlich, S.D., Noirot, P., and Polard, P. 2007. Anticipating chromosomal replication fork arrest: SSB targets repair DNA helicases to active forks. *Embo J* **26**(19): 4239-4251.

Lee, E.H. and Kornberg, A. 1991. Replication deficiencies in *priA* mutants of *Escherichia coli* lacking the primosomal replication n' protein. *Proc Natl Acad Sci USA* **88**: 3029-3032.

Lee, E.H., Kornberg, A., Hidaka, M., Kobayashi, T., and Horiuchi, T. 1989. *Escherichia coli* replication termination protein impedes the action of helicases. *Proc Natl Acad Sci U S A* **86**(23): 9104-9108.

Lehmann, A.R. and Fuchs, R.P. 2006. Gaps and forks in DNA replication: Rediscovering old models. *DNA Repair (Amst)* **5**(12): 1495-1498.

Lindahl, T. and Wood, R.D. 1999. Quality control by DNA repair. *Science* **286**: 1897-1905.

Liu, J., Xu, L., Sandler, S.J., and Marians, K.J. 1999. Replication fork assembly at recombination intermediates is required for bacterial growth. *Proc Natl Acad Sci USA* **96**(7): 3552-3555.

Lloyd, R.G. 1991. Conjugational recombination in resolvase-deficient *ruvC* mutants of *Escherichia coli* K-12 depends on *recG. J Bacteriol* **173**: 5414-5418.

Lloyd, R.G. and Buckman, C. 1991. Genetic analysis of the *recG* locus of *Escherichia coli* K-12 and of its role in recombination and DNA repair. *J Bacteriol* **173**: 1004-1011.

Lloyd, R.G. and Sharples, G.J. 1991. Molecular organisation and nucleotide sequence of the *recG* locus of *Escherichia coli* K-12. *J Bacteriol* **173**: 6837-6843.

Lloyd, R.G. and Sharples, G.J. 1993. Dissociation of synthetic Holliday junctions by *E. coli* RecG protein. *EMBO J* **12**: 17-22.

Lobner-Olesen, A., Hansen, F.G., Rasmussen, K.V., Martin, B., and Kuempel, P.L. 1994. The initiation cascade for chromosome replication in wild-type and Dam methyltransferase deficient *Escherichia coli* cells. *EMBO J* **13**(8): 1856-1862.

Lobner-Olesen, A., Skarstad, K., Hansen, F.G., von Meyenburg, K., and Boye, E. 1989. The DnaA protein determines the initiation mass of *Escherichia coli* K-12. *Cell* **57**(5): 881-889.

Louarn, J., Patte, J., and Louarn, J.M. 1977. Evidence for a fixed termination site of chromosome replication in *Escherichia coli* K12. *J Mol Biol* **115**(3): 295-314.

Lu, M., Campbell, J.L., Boye, E., and Kleckner, N. 1994. SeqA: a negative modulator of replication initiation in *E. coli. Cell* **77**(3): 413-426.

Mahdi, A.A., Briggs, G.S., Sharples, G.J., Wen, Q., and Lloyd, R.G. 2003. A model for dsDNA translocation revealed by a structural motif common to RecG and Mfd proteins. *EMBO J* **22**(3): 724-734.

Mahdi, A.A., Buckman, C., Harris, L., and Lloyd, R.G. 2006. Rep and PriA helicase activities prevent RecA from provoking unnecessary recombination during replication fork repair. *Genes Dev* **20**(15): 2135-2147.

Mahdi, A.A., McGlynn, P., Levett, S.D., and Lloyd, R.G. 1997. DNA binding and helicase domains of the *Escherichia coli* recombination protein RecG. *Nucleic Acids Res* **25**(19): 3875-3880.

Mahdi, A.A., Sharples, G.J., Mandal, T.N., and Lloyd, R.G. 1996. Holliday junction resolvases encoded by homologous *rusA* genes in *Escherichia coli* K-12 and phage 82. *J Mol Biol* **257**: 561-573.

Maisnier-Patin, S., Nordstrom, K., and Dasgupta, S. 2001. Replication arrests during a single round of replication of the *Escherichia coli* chromosome in the absence of DnaC activity. *Mol Microbiol* **42**(5): 1371-1382.

Mandal, T.N., Mahdi, A.A., Sharples, G.J., and Lloyd, R.G. 1993. Resolution of Holliday intermediates in recombination and DNA repair: indirect suppression of *ruvA, ruvB* and *ruvC* mutations. *J Bacteriol* **175**: 4325-4334.

Marians, K.J. 2004. Mechanisms of replication fork restart in *Escherichia coli*. *Philos Trans R Soc Lond B Biol Sci* **359**(1441): 71-77.

Markovitz, A. 2005. A new *in vivo* termination function for DNA polymerase I of *Escherichia coli* K12. *Mol Microbiol* **55**(6): 1867-1882.

Masai, H., Asai, T., Kubota, Y., Arai, K., and Kogoma, T. 1994. *Escherichia coli* PriA protein is essential for inducible and constitutive stable DNA replication. *EMBO J* **13**: 5338-5345.

McGlynn, P., Al-Deib, A.A., Liu, J., Marians, K.J., and Lloyd, R.G. 1997. The DNA replication protein PriA and the recombination protein RecG bind D-loops. *J Mol Biol* **270**: 212-221.

McGlynn, P. and Lloyd, R.G. 1999. RecG helicase activity at three- and four-strand DNA structures. *Nucleic Acids Res* **27**(15): 3049-3056.

McGlynn, P. and Lloyd, R.G. 2000. Modulation of RNA polymerase by (p)ppGpp reveals a RecG-dependent mechanism for replication fork progression. *Cell* **101**: 35-45.

McGlynn, P. and Lloyd, R.G. 2001a. Action of RuvAB at replication fork structures. *J Biol Chem* **276**: 41938-41944.

McGlynn, P. and Lloyd, R.G. 2001b. Rescue of stalled replication forks by RecG: simultaneous translocation on the leading and lagging strand templates supports an active DNA unwinding model of fork reversal and Holliday junction formation. *Proc Nat Acad Sci USA* **98**: 8227-8234.

McGlynn, P. and Lloyd, R.G. 2002. Recombinational repair and restart of damaged replication forks. *Nature Reviews Mol Cell Biol* **3**: 859-870.

McGlynn, P., Mahdi, A.A., and Lloyd, R.G. 2000. Characterisation of the catalytically active form of RecG helicase. *Nucleic Acids Res* **28**: 2324-2332.

McInerney, P. and O'Donnell, M. 2004. Functional uncoupling of twin polymerases: mechanism of polymerase dissociation from a lagging-strand block. *J Biol Chem* **279**(20): 21543-21551.

McInerney, P. and O'Donnell, M. 2007. Replisome fate upon encountering a leading strand block and clearance from DNA by recombination proteins. *J Biol Chem* **282**(35): 25903-25916.

Meneghini, R. and Hanawalt, P. 1976. T4-endonuclease V-sensitive sites in DNA from ultraviolet-irradiated human cells. *Biochim Biophys Acta* **425**(4): 428-437.

Messer, W. 2002. The bacterial replication initiator DnaA. DnaA and *oriC*, the bacterial mode to initiate DNA replication. *FEMS microbiology reviews* **26**(4): 355-374.

Messer, W. and Weigel, C. 1997. DnaA initiator – also a transcription factor. *Mol Microbiol* **24**(1): 1-6.

Michel, B. 2005. After 30 years of study, the bacterial SOS response still surprises us. *PLoS Biol* **3**(7): e255.

Michel, B., Boubakri, H., Baharoglu, Z., LeMasson, M., and Lestini, R. 2007. Recombination proteins and rescue of arrested replication forks. *DNA Repair (Amst)* **6**(7): 967-980.

Michel, B., Ehrlich, S.D., and Uzest, M. 1997. DNA double-strand breaks caused by replication arrest. *EMBO J* **16**: 430-438.

Michel, B., Grompone, G., Flores, M.J., and Bidnenko, V. 2004. Multiple pathways process stalled replication forks. *Proc Natl Acad Sci U S A* **101**(35): 12783-12788.

Mirkin, E.V. and Mirkin, S.M. 2005. Mechanisms of transcription-replication collisions in bacteria. *Mol Cell Biol* **25**(3): 888-895.

Mirkin, E.V. and Mirkin, S.M. 2007. Replication fork stalling at natural impediments. *Microbiol Mol Biol Rev* **71**(1): 13-35.

Molina, F. and Skarstad, K. 2004. Replication fork and SeqA focus distributions in *Escherichia coli* suggest a replication hyperstructure dependent on nucleotide metabolism. *Mol Microbiol* **52**(6): 1597-1612.

Morimatsu, K. and Kowalczykowski, S.C. 2003. RecFOR proteins load RecA protein onto gapped DNA to accelerate DNA strand exchange: a universal step of recombinational repair. *Mol Cell* **11**(5): 1337-1347.

Mulcair, M., Schaeffer, P., Oakley, A., Cross, H., Neylon, C., Hill, T., and Dixon, N. 2006. A molecular mousetrap determines polarity of termination of DNA replication in *E. coli*. *Cell* **125**: 1309-1319.

Neylon, C., Kralicek, A.V., Hill, T.M., and Dixon, N.E. 2005. Replication termination in *Escherichia coli*: structure and antihelicase activity of the Tus-*Ter* complex. *Microbiol Mol Biol Rev* **69**(3): 501-526.

Nielsen, O. and Lobner-Olesen, A. 2008. Once in a lifetime: strategies for preventing re-replication in prokaryotic and eukaryotic cells. *EMBO Rep* **9**(2): 151-156.

Nievera, C., Torgue, J.J., Grimwade, J.E., and Leonard, A.C. 2006. SeqA blocking of DnaA-*oriC* interactions ensures staged assembly of the *E. coli* pre-RC. *Mol Cell* **24**(4): 581-592.

Ogawa, T. and Okazaki, T. 1984. Function of RNase H in DNA replication revealed by RNase H defective mutants of *Escherichia coli. Mol Gen Genet* **193**(2): 231-237.

Opperman, T., Murli, S., Smith, B.T., and Walker, G.C. 1999. A model for a *umuDC*-dependent prokaryotic DNA damage checkpoint. *Proc Natl Acad Sci USA* **96**(16): 9218-9223.

Pages, V. and Fuchs, R.P. 2003. Uncoupling of leading- and lagging-strand DNA replication during lesion bypass *in vivo. Science* **300**(5623): 1300-1303.

Pomerantz, R.T. and O'Donnell, M. 2007. Replisome mechanics: insights into a twin DNA polymerase machine. *Trends Microbiol* **15**(4): 156-164.

Possoz, C., Filipe, S.R., Grainge, I., and Sherratt, D.J. 2006. Tracking of controlled *Escherichia coli* replication fork stalling and restart at repressor-bound DNA *in vivo*. *EMBO J* **25**(11): 2596-2604.

Poteete, A.R. 2009. Expansion of a chromosomal repeat in *Escherichia coli:* roles of replication, repair, and recombination functions. *BMC Mol Biol* **10**: 14.

Reyes-Lamothe, R., Wang, X., and Sherratt, D. 2008. *Escherichia coli* and its chromosome. *Trends Microbiol* **16**(5): 238-245.

Robu, M.E., Inman, R.B., and Cox, M.M. 2001. RecA protein promotes the regression of stalled replication forks *in vitro. Proc Natl Acad Sci USA* **98**: 8211-8218.

Rudolph, C., Schürer, K.A., and Kramer, W. 2006. Facing Stalled Replication Forks: The Intricacies of Doing the Right Thing. In *Genome Integrity: Facets and Perspectives* (ed. D.-H. Lankenau), pp. 105-152. Springer, Berlin · Heidelberg.

Rudolph, C.J., Dhillon, P., Moore, T., and Lloyd, R.G. 2007a. Avoiding and resolving conflicts between DNA replication and transcription. *DNA Repair (Amst)* **6**(7): 981-993.

Rudolph, C.J., Upton, A.L., and Lloyd, R.G. 2007b. Replication fork stalling and cell cycle arrest in UV-irradiated *Escherichia coli*. *Genes Dev* **21**(6): 668-681.

Rudolph, C.J., Upton, A.L., and Lloyd, R.G. 2008. Maintaining replication fork integrity in UV-irradiated *Escherichia coli* cells. *DNA Repair (Amst)* **7**(9): 1589-1602.

Rupp, W.D. and Howard-Flanders, P. 1968. Discontinuities in the DNA synthesized in an excision-defective strain of *Escherichia coli* following ultraviolet irradiation. *J Mol Biol* **31**: 291-304.

Rupp, W.D., Wilde, C.E., Reno, D.L., and Howard-Flanders, P. 1971. Exchanges between DNA strands in ultraviolet-irradiated *Escherichia coli*. *J Mol Biol* **61**: 25-44.

Russell, D.W. and Zinder, N.D. 1987. Hemimethylation prevents DNA replication in *E. coli*. *Cell* **50**(7): 1071-1079.

Sancar, A. 1995. DNA repair in humans. *Annu Rev Genet* **29**: 69-105.

Sancar, A. 1996a. DNA excision repair. *Annu Rev Biochem* **65**: 43-81.

Sancar, A. 1996b. No "End of History " for photolyases. *Science* **272**(5258): 48-49.

Sancar, A., Lindsey-Boltz, L.A., Unsal-Kacmaz, K., and Linn, S. 2004. Molecular mechanisms of mammalian DNA repair and the DNA damage checkpoints. *Annu Rev Biochem* **73**: 39-85.

Sancar, G.B. 2000. Enzymatic photoreactivation: 50 years and counting. *Mutat Res* **451**(1-2): 25-37.

Sandler, S.J. 2000. Multiple genetic pathways for restarting DNA replication forks in *Escherichia coli* K-12. *Genetics* **155**(2): 487-497.

Sandler, S.J., Marians, K.J., Zavitz, K.H., Coutu, J., Parent, M.A., and Clark, A.J. 1999. *dnaC* mutations suppress defects in DNA replication- and recombination- associated functions in *priB* and *priC* double mutants in *Escherichia coli* K-12. *Mol Microbiol* **34**(1): 91-101.

Schlacher, K. and Goodman, M.F. 2007. Lessons from 50 years of SOS DNA-damage-induced mutagenesis. *Nat Rev Mol Cell Biol* **8**(7): 587-594.

Sclafani, R.A. and Holzen, T.M. 2007. Cell cycle regulation of DNA replication. *Annu Rev Genet* **41**: 237-280.

Sedgwick, S.G. 1975. Genetic and kinetic evidence for different types of postreplication repair in *Escherichia coli* B. *J Bacteriol* **123**(1): 154-161.

Seigneur, M., Bidnenko, V., Ehrlich, S.D., and Michel, B. 1998. RuvAB acts at arrested replication forks. *Cell* **95**: 419-430.

Seigneur, M., Ehrlich, S.D., and Michel, B. 2000. RuvABC-dependent double-strand breaks in *dnaBts* mutants require RecA. *Mol Microbiol* **38**(3): 565-574.

Sharma, B. and Hill, T.M. 1995. Insertion of inverted *Ter* sites into the terminus region of the *Escherichia coli* chromosome delays completion of DNA replication and disrupts the cell cycle. *Mol Microbiol* **18**(1): 45-61.

Sharples, G.J., Chan, S.C., Mahdi, A.A., Whitby, M.C., and Lloyd, R.G. 1994. Processing of intermediates in recombination and DNA repair: identification of a new endonuclease that specifically cleaves Holliday junctions. *EMBO J* **13**: 6133-6142.

Shereda, R.D., Kozlov, A.G., Lohman, T.M., Cox, M.M., and Keck, J.L. 2008. SSB as an organizer/mobilizer of genome maintenance complexes. *Crit Rev Biochem Mol Biol* **43**(5): 289-318.

Simmons, L.A., Breier, A.M., Cozzarelli, N.R., and Kaguni, J.M. 2004. Hyperinitiation of DNA replication in *Escherichia coli* leads to replication fork collapse and inviability. *Mol Microbiol* **51**(2): 349-358.

Singleton, M.R., Scaife, S., and Wigley, D.B. 2001. Structural analysis of DNA replication fork reversal by RecG. *Cell* **107**(1): 79-89.

Sista, P.R., Mukherjee, S., Patel, P., Khatri, G.S., and Bastia, D. 1989. A host-encoded DNA-binding protein promotes termination of plasmid replication at a sequence-specific replication terminus. *Proc Natl Acad Sci U S A* **86**(9): 3026-3030.

Slater, S., Wold, S., Lu, M., Boye, E., Skarstad, K., and Kleckner, N. 1995. *E. coli* SeqA protein binds *oriC* in two different methyl-modulated reactions appropriate to its roles in DNA replication initiation and origin sequestration. *Cell* **82**(6): 927-936.

Sogo, J.M., Lopes, M., and Foiani, M. 2002. Fork reversal and ssDNA accumulation at stalled replication forks owing to checkpoint defects. *Science* **297**(5581): 599-602.

Stein, H. and Hausen, P. 1969. Enzyme from calf thymus degrading the RNA moiety of DNA-RNA Hybrids: effect on DNA-dependent RNA polymerase. *Science* **166**(903): 393-395.

Sun, W., Nandi, S., Osman, F., Ahn, J.S., Jakovleska, J., Lorenz, A., and Whitby, M.C. 2008. The FANCM ortholog Fml1 promotes recombination at stalled replication forks and limits crossing over during DNA double-strand break repair. *Mol Cell* **32**(1): 118-128.

Suski, C. and Marians, K.J. 2008. Resolution of converging replication forks by RecQ and topoisomerase III. *Mol Cell* **30**(6): 779-789.

Sutton, M.D., Smith, B.T., Godoy, V.G., and Walker, G.C. 2000. The SOS response: recent insights into umuDC-dependent mutagenesis and DNA damage tolerance. *Annu Rev Genet* **34**: 479-497.

Tanaka, T., Taniyama, C., Arai, K., and Masai, H. 2003. ATPase/helicase motif mutants of *Escherichia coli* PriA protein essential for recombination-dependent DNA replication. *Genes Cells* **8**(3): 251-261.

Tippin, B., Pham, P., and Goodman, M.F. 2004. Error-prone replication for better or worse. *Trends Microbiol* **12**(6): 288-295.

Torrey, T.A. and Kogoma, T. 1982. Suppressor mutations *(rin)* that specifically suppress the *recA*$^+$ dependence of stable DNA replication in *Escherichia coli* K-12. *Mol Gen Genet* **187**(2): 225-230.

Tourriere, H. and Pasero, P. 2007. Maintenance of fork integrity at damaged DNA and natural pause sites. *DNA Repair (Amst)* **6**(7): 900-913.

Trautinger, B.W., Jaktaji, R.P., Rusakova, E., and Lloyd, R.G. 2005. RNA polymerase modulators and DNA repair activities resolve conflicts between DNA replication and transcription. *Mol Cell* **19**(2): 247-258.

Truglio, J.J., Croteau, D.L., Van Houten, B., and Kisker, C. 2006. Prokaryotic nucleotide excision repair: the UvrABC system. *Chem Rev* **106**(2): 233-252.

Truong, K., and Ikura, M. 2001. The use of FRET imaging microscopy to detect protein-protein interactions and protein conformational changes *in vivo*. *Curr Opin Struct Biol* 11(5): 573-578.

van Heemst, D., den Reijer, P.M., and Westendorp, R.G. 2007. Ageing or cancer: a review on the role of caretakers and gatekeepers. *Eur J Cancer* **43**(15): 2144-2152.

Veaute, X., Jeusset, J., Soustelle, C., Kowalczykowski, S.C., Le Cam, E., and Fabre, F. 2003. The Srs2 helicase prevents recombination by disrupting Rad51 nucleoprotein filaments. *Nature* **423**(6937): 309-312.

Vincent, S.D., Mahdi, A.A., and Lloyd, R.G. 1996. The RecG branch migration protein of *Escherichia coli* dissociates R-loops. *J Mol Biol* **264**: 713-721.

Viswanathan, M., Burdett, V., Baitinger, C., Modrich, P., and Lovett, S.T. 2001. Redundant exonuclease involvement in *Escherichia coli* methyl-directed mismatch repair. *J Biol Chem* **276**(33): 31053-31058.

von Freiesleben, U., Krekling, M.A., Hansen, F.G., and Lobner-Olesen, A. 2000. The eclipse period of *Escherichia coli. EMBO J* **19**(22): 6240-6248.

von Freiesleben, U., Rasmussen, K.V., and Schaechter, M. 1994. SeqA limits DnaA activity in replication from *oriC* in *Escherichia coli. Mol Microbiol* **14**(4): 763-772.

von Meyenburg, K., Boye, E., Skarstad, K., Koppes, L., and Kogoma, T. 1987. Mode of initiation of constitutive stable DNA replication in RNase H-defective mutants of *Escherichia coli* K-12. *J Bacteriol* **169**(6): 2650-2658.

Waldminghaus, T. and Skarstad, K. 2009. The *Escherichia coli* SeqA protein. *Plasmid*. doi:10.1016/j.plasmid.2009.02.004

Wang, T.C. 2005. Discontinuous or semi-discontinuous DNA replication in *Escherichia coli? Bioessays* **27**(6): 633-636.

Weinreich, M., Palacios DeBeer, M.A., and Fox, C.A. 2004. The activities of eukaryotic replication origins in chromatin. *Biochim Biophys Acta* **1677**(1-3): 142-157.

Wen, Q., Mahdi, A.A., Briggs, G.S., Sharples, G.J., and Lloyd, R.G. 2005. Conservation of RecG activity from pathogens to hyperthermophiles. *DNA repair* (Amst) **4**(1): 23-31.

Whitby, M.C. and Lloyd, R.G. 1995. Altered SOS induction by mutations in *recF*, *recO* and *recR*. *Mol Gen Genet* **246**: 174-179.

Zerbib, D., Mézard, C., George, H., and West, S.C. 1998. Coordinated actions of RuvABC in Holliday junction processing. *J Mol Biol* **281**: 621-630.

Appendix

```
         10        20        30        40        50
GTGTCACTTTCGCTTTGGCAGCAGTGTCTTGCCCGATTGCAGGATGAGTT
CACAGTGAAAGCGAAACCGTCGTCACAGAACGGGCTAACGTCCTACTCAA
 V  S  L  S  L  W  Q  Q  C  L  A  R  L  Q  D  E  L>

         60        70        80        90       100
ACCAGCCACAGAATTCAGTATGTGGATACGCCCATTGCAGGCGGAACTGA
TGGTCGGTGTCTTAAGTCATACACCTATGCGGGTAACGTCCGCCTTGACT
  P  A  T  E  F  S  M  W  I  R  P  L  Q  A  E  L>

        110       120       130       140       150
GCGATAACACGCTGGCCCTGTACGCGCCAAACCGTTTTGTCCTCGATTGG
CGCTATTGTGCGACCGGGACATGCGCGGTTTGGCAAAACAGGAGCTAACC
S  D  N  T  L  A  L  Y  A  P  N  R  F  V  L  D  W>

        160       170       180       190       200
GTACGGGACAAGTACCTTAATAATATCAATGGACTGCTAACCAGTTTCTG
CATGCCCTGTTCATGGAATTATTATAGTTACCTGACGATTGGTCAAAGAC
 V  R  D  K  Y  L  N  N  I  N  G  L  L  T  S  F  C>

        210       220       230       240       250
CGGAGCGGATGCCCCACAGCTGCGTTTTGAAGTCGGCACCAAACCGGTGA
GCCTCGCCTACGGGGTGTCGACGCAAAACTTCAGCCGTGGTTTGGCCACT
  G  A  D  A  P  Q  L  R  F  E  V  G  T  K  P  V>

        260       270       280       290       300
CGCAAACGCCACAAGCGGCAGTGACGAGCAACGTCGCGGCCCCTGCACAG
GCGTTTGCGGTGTTCGCCGTCACTGCTCGTTGCAGCGCCGGGGACGTGTC
T  Q  T  P  Q  A  A  V  T  S  N  V  A  A  P  A  Q>

        310       320       330       340       350
GTGGCGCAAACGCAGCCGCAACGTGCTGCGCCTTCTACGCGCTCAGGTTG
CACCGCGTTTGCGTCGGCGTTGCACGACGCGGAAGATGCGCGAGTCCAAC
 V  A  Q  T  Q  P  Q  R  A  A  P  S  T  R  S  G  W>

        360       370       380       390       400
GGATAACGTCCCGGCCCCGGCAGAACCGACCTATCGTTCTAACGTAAACG
CCTATTGCAGGGCCGGGGCCGTCTTGGCTGGATAGCAAGATTGCATTTGC
  D  N  V  P  A  P  A  E  P  T  Y  R  S  N  V  N>

        410       420       430       440       450
TCAAACACACGTTTGATAACTTCGTTGAAGGTAAATCTAACCAACTGGCG
AGTTTGTGTGCAAACTATTGAAGCAACTTCCATTTAGATTGGTTGACCGC
V  K  H  T  F  D  N  F  V  E  G  K  S  N  Q  L  A>

        460       470       480       490       500
CGCGCGGCGGCTCGCCAGGTGGCGGATAACCCTGGCGGTGCCTATAACCC
GCGCGCCGCCGAGCGGTCCACCGCCTATTGGGACCGCCACGGATATTGGG
 R  A  A  A  R  Q  V  A  D  N  P  G  G  A  Y  N  P>

        510       520       530       540       550
GTTGTTCCTTTATGGCGGCACGGGTCTGGGTAAAACTCACCTGCTGCATG
CAACAAGGAAATACCGCCGTGCCCAGACCCATTTTGAGTGGACGACGTAC
  L  F  L  Y  G  G  T  G  L  G  K  T  H  L  L  H>

        560       570       580       590       600
CGGTGGGTAACGGCATTATGGCGCGCAAGCCGAATGCCAAAGTGGTTTAT
GCCACCCATTGCCGTAATACCGCGCGTTCGGCTTACGGTTTCACCAAATA
A  V  G  N  G  I  M  A  R  K  P  N  A  K  V  V  Y>

        610       620       630       640       650
ATGCACTCCGAGCGCTTTGTTCAGGACATGGTTAAAGCCCTGCAAAACAA
TACGTGAGGCTCGCGAAACAAGTCCTGTACCAATTTCGGGACGTTTTGTT
 M  H  S  E  R  F  V  Q  D  M  V  K  A  L  Q  N  N>

        660       670       680       690       700
CGCGATCGAAGAGTTTAAACGCTACTACCGTTCCGTAGATGCACTGCTGA
GCGCTAGCTTCTCAAATTTGCGATGATGGCAAGGCATCTACGTGACGACT
  A  I  E  E  F  K  R  Y  Y  R  S  V  D  A  L  L>
```

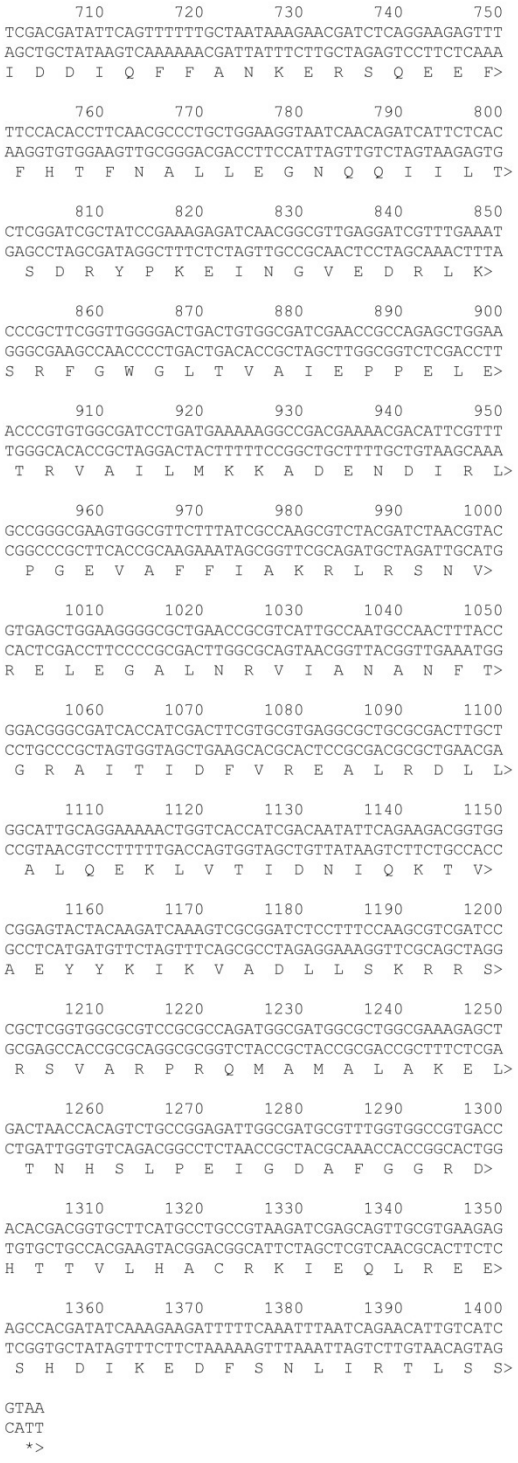

Figure 50. DnaA protein and DNA sequence.

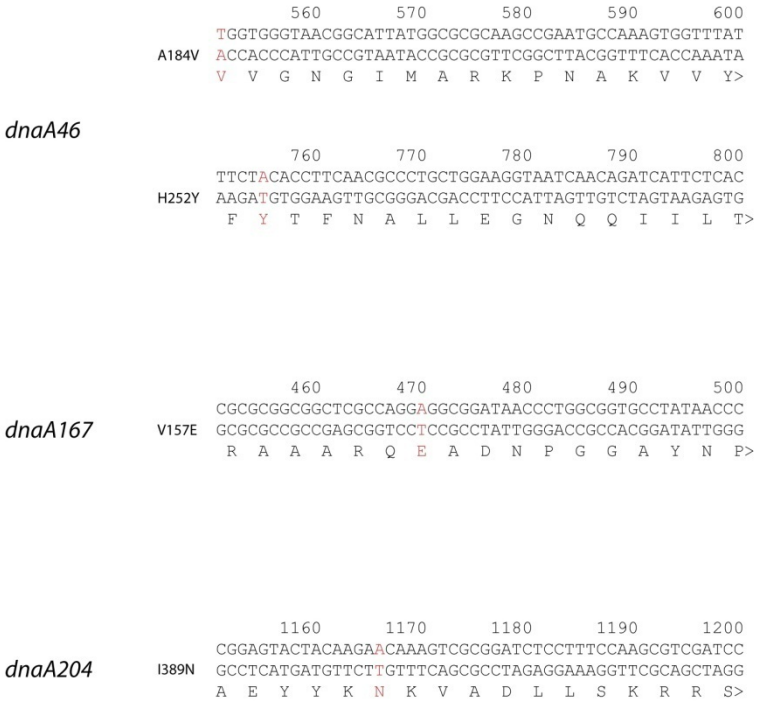

Figure 51. Temperature-sensitive *dnaA* alleles. The DNA and protein sequence changes are highlighted in red. DnaA has been divided into domain I (1–90), domain II (91–130), domain III (131–347) and domain IV (348–467). The mutations in *dnaA46* and *dnaA167* are located within the ATP binding cassette (domain III). The mutation in *dnaA204* is located in the DNA binding domain (domain IV) (Hansen *et al.* 1992; Erzberger *et al.* 2002).

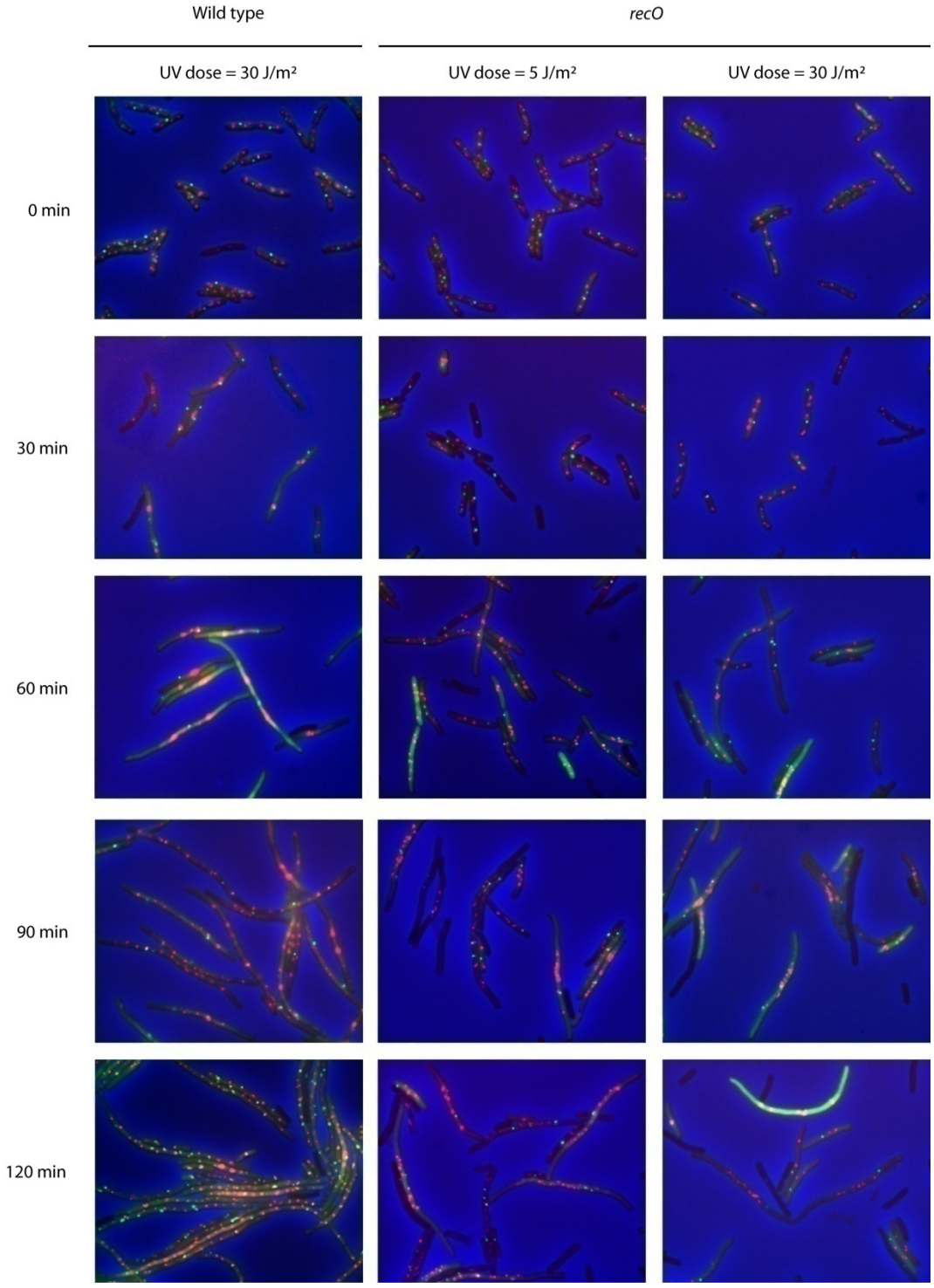
Wild type
recO
UV dose = 30 J/m²
UV dose = 5 J/m²
UV dose = 30 J/m²
0 min
30 min
60 min
90 min
120 min

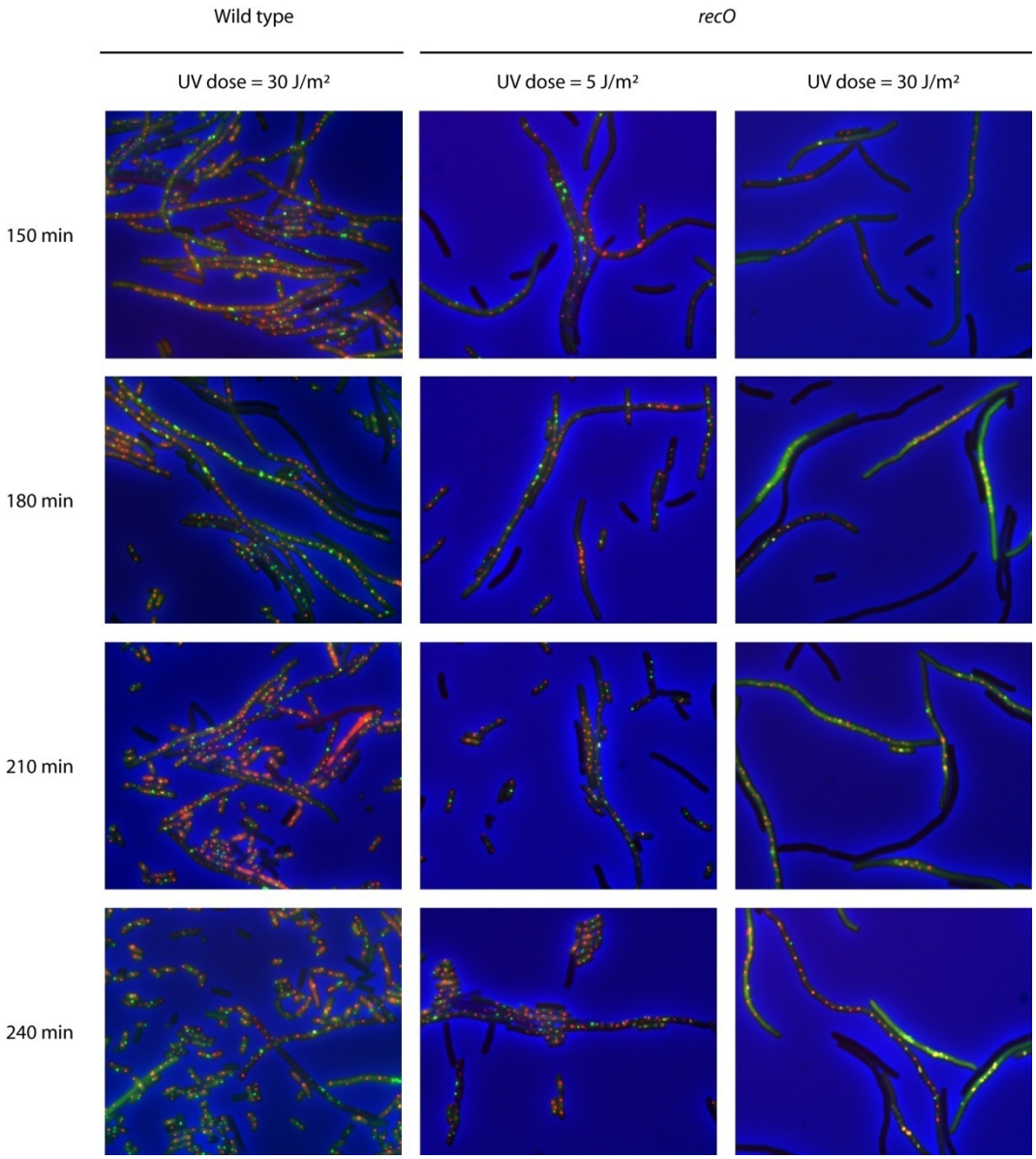

Figure 52. Effect of UV on cell cycle progression in *recO* cells. Fluorescence microscopy showing multiplication of the origin (red foci) and terminus (green foci) regions of the chromosome. Pictures are combined phase contrast and fluorescence images. The strain used was AU1101 (*recO*). The UV dose as well as incubation times after irradiation are indicated. Data for the wild type (APS345) were reproduced for comparison from Figure 12.

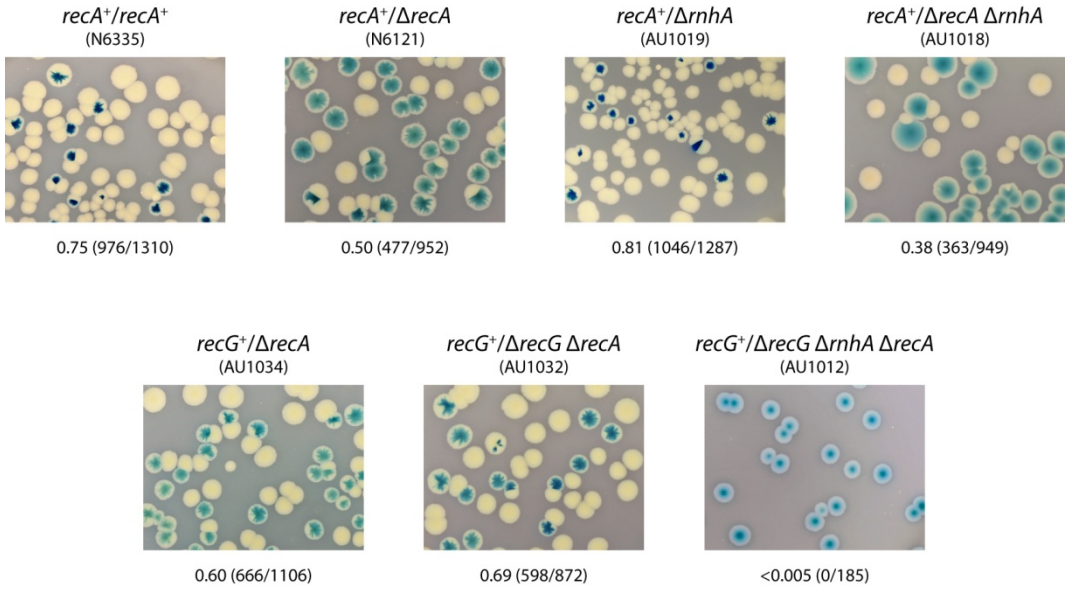

Figure 53. A *recA* mutation does not suppress the inviability of Δ*recG* Δ*rnhA* cells. The relevant genotype is shown above each image, along with the strain number. The fraction of white colonies is shown below each image, with the number of white colonies/total colonies analysed in parentheses.

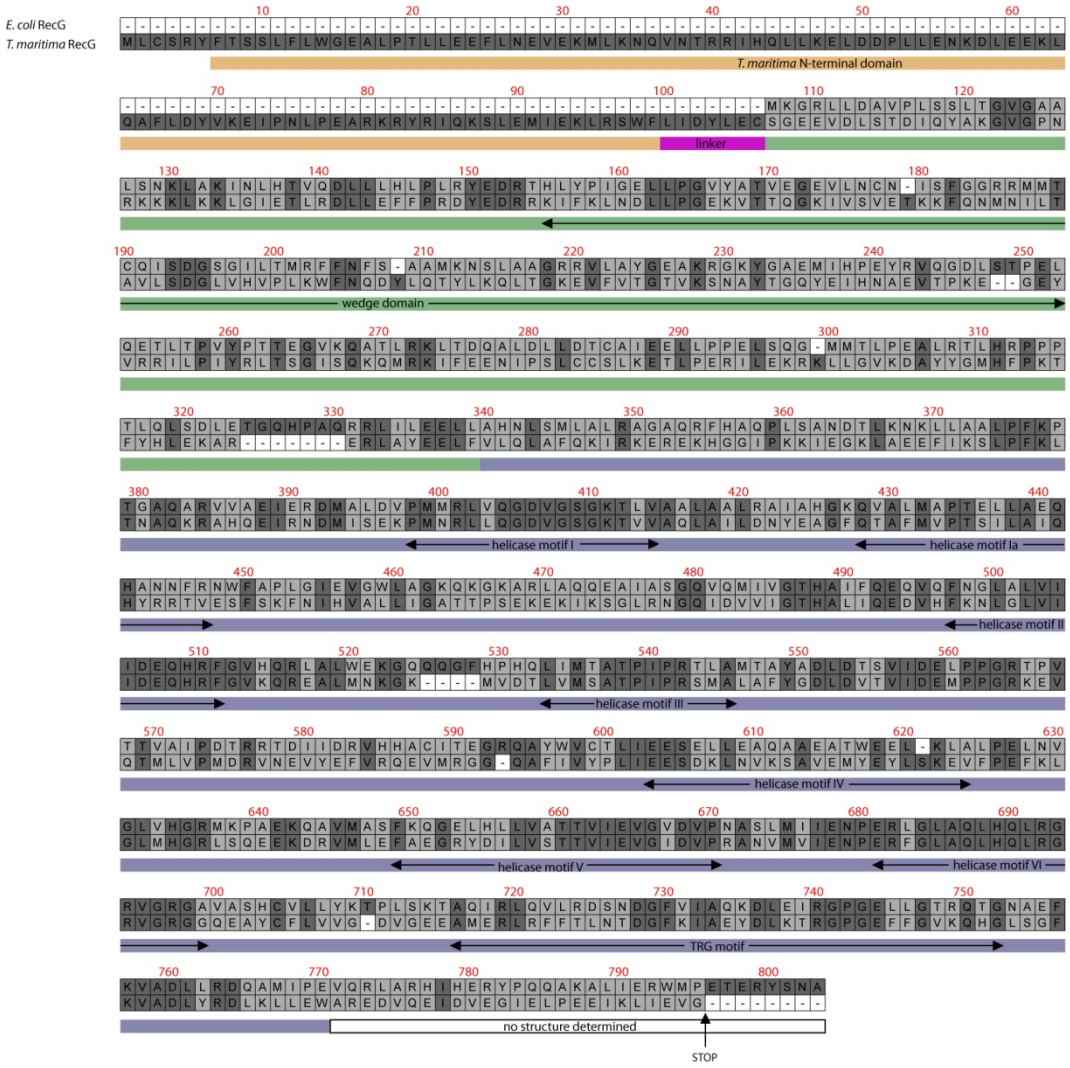

Figure 54. Amino acid sequence alignment of *Escherichia coli* and *Thermotoga maritima* RecG. The level of shading indicates percent identity (darker shaded residues have a higher percent identity). The colour coding corresponds to that used in Figure 37. Key functional domains have been labelled (Lloyd and Sharples 1991; Mahdi *et al.* 2003; Briggs *et al.* 2005). Alignment produced using clustalW.

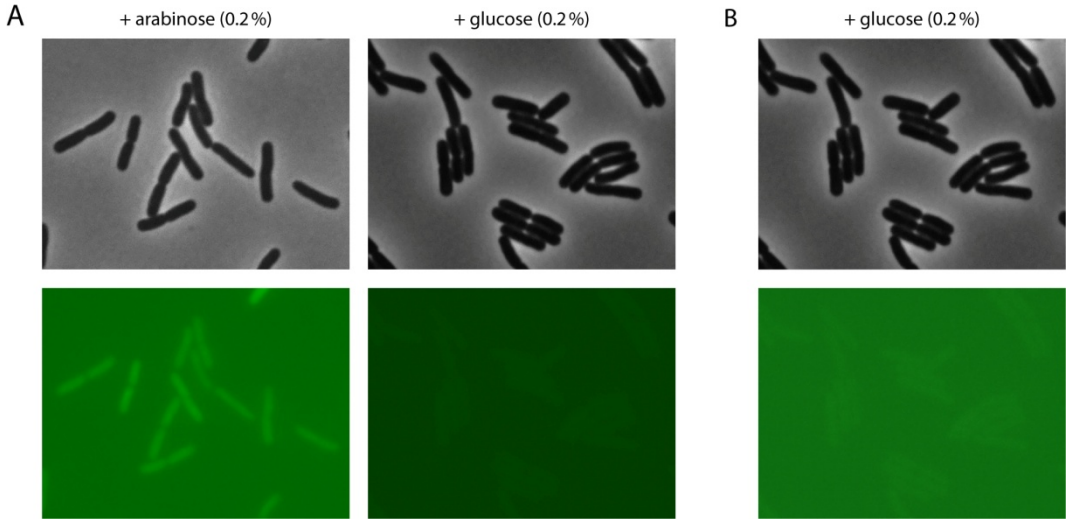

Figure 55. Cells expressing RecGΔC15 show an increased cellular fluorescence. (A) The signal in both fluorescent images has been enhanced in an identical way. (B) To compensate for the differing background intensities of the two fluorescent images shown in A, an additional enhancement step has been done for the image coming from the sample treated with glucose, generating an image with a comparable background. The strains used were N4256 pDIM071 and N4256 pAU112.

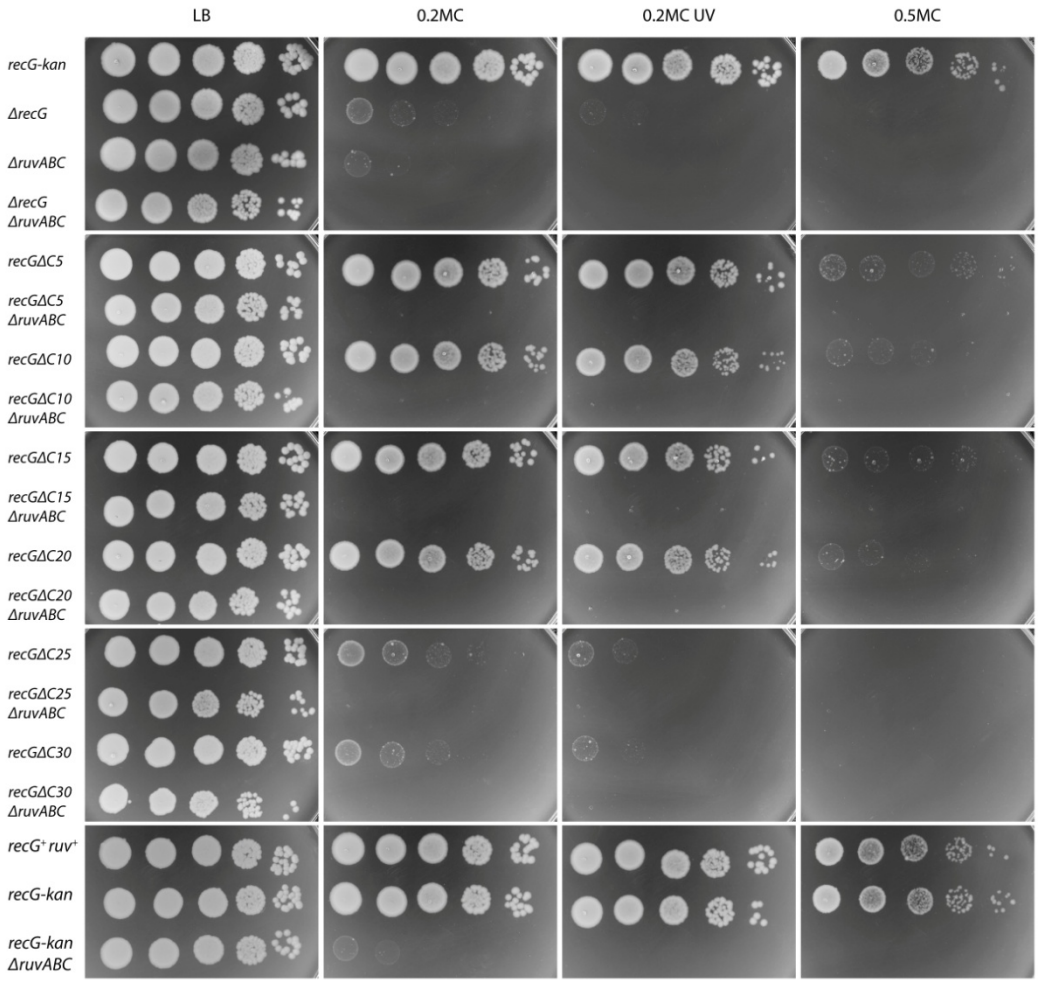
LB
0.2MC
0.2MC UV
0.5MC
recG-kan
ΔrecG
ΔruvABC
ΔrecG ΔruvABC
recGΔC5
recGΔC5 ΔruvABC
recGΔC10
recGΔC10 ΔruvABC
recGΔC15
recGΔC15 ΔruvABC
recGΔC20
recGΔC20 ΔruvABC
recGΔC25
recGΔC25 ΔruvABC
recGΔC30
recGΔC30 ΔruvABC
recG+ ruv+
recG-kan
recG-kan ΔruvABC

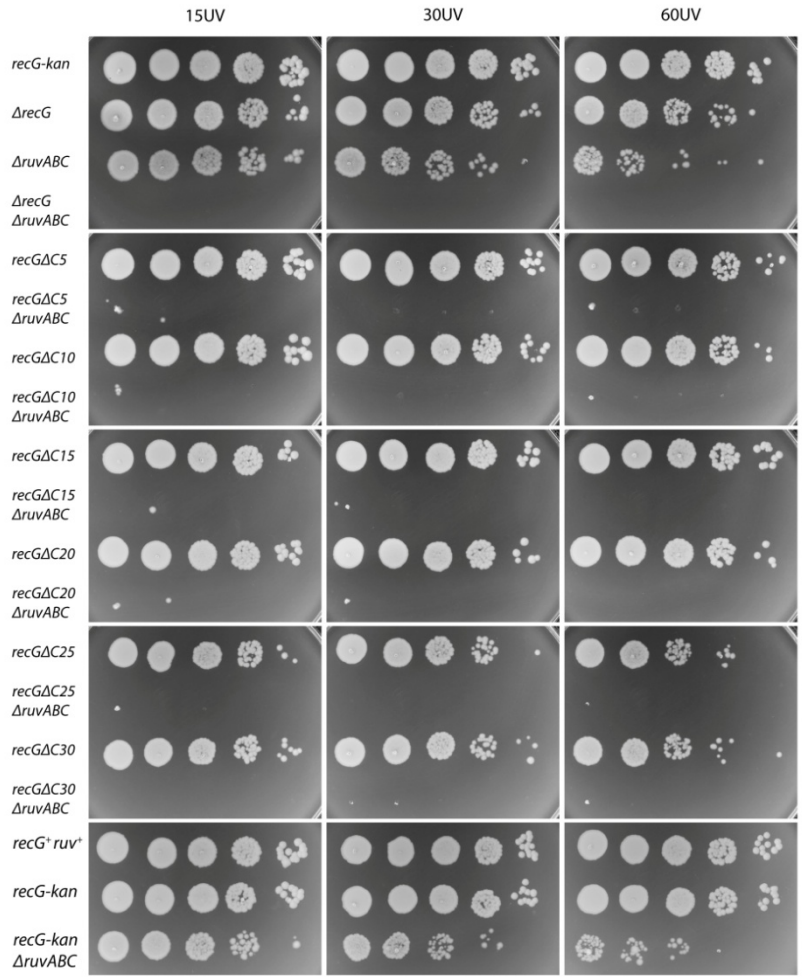

Figure 56. The *recG* C-terminus deletions are not like wild type. Mitomycin C survival assays illustrating the phenotypes of the recG C-terminus deletions. The strains used were MG1655 (*recG*$^{+}$ *ruv*$^{+}$), AU1218 (*recG-kan*), AU1232 (*recG-kan* Δ*ruvABC*), N4256 (Δ*recG*), N7105 (Δ*ruvABC*), N4971 (Δ*recG* Δ*ruvABC*), AU1200 (*recG*Δ*C5*), AU1219 (*recG*Δ*C5* Δ*ruvABC*), AU1201 (*recG*Δ*C10*), AU1220 (*recG*Δ*C10* Δ*ruvABC*), AU1202 (*recG*Δ*C15*), AU1221 (*recG*Δ*C15* Δ*ruvABC*), AU1203 (*recG*Δ*C20*), AU1222 (*recG*Δ*C20* Δ*ruvABC*), AU1204 (*recG*Δ*C25*), AU1223 (*recG*Δ*C25* Δ*ruvABC*), AU1205 (*recG*Δ*C30*) and AU1224 (*recG*Δ*C30* Δ*ruvABC*).

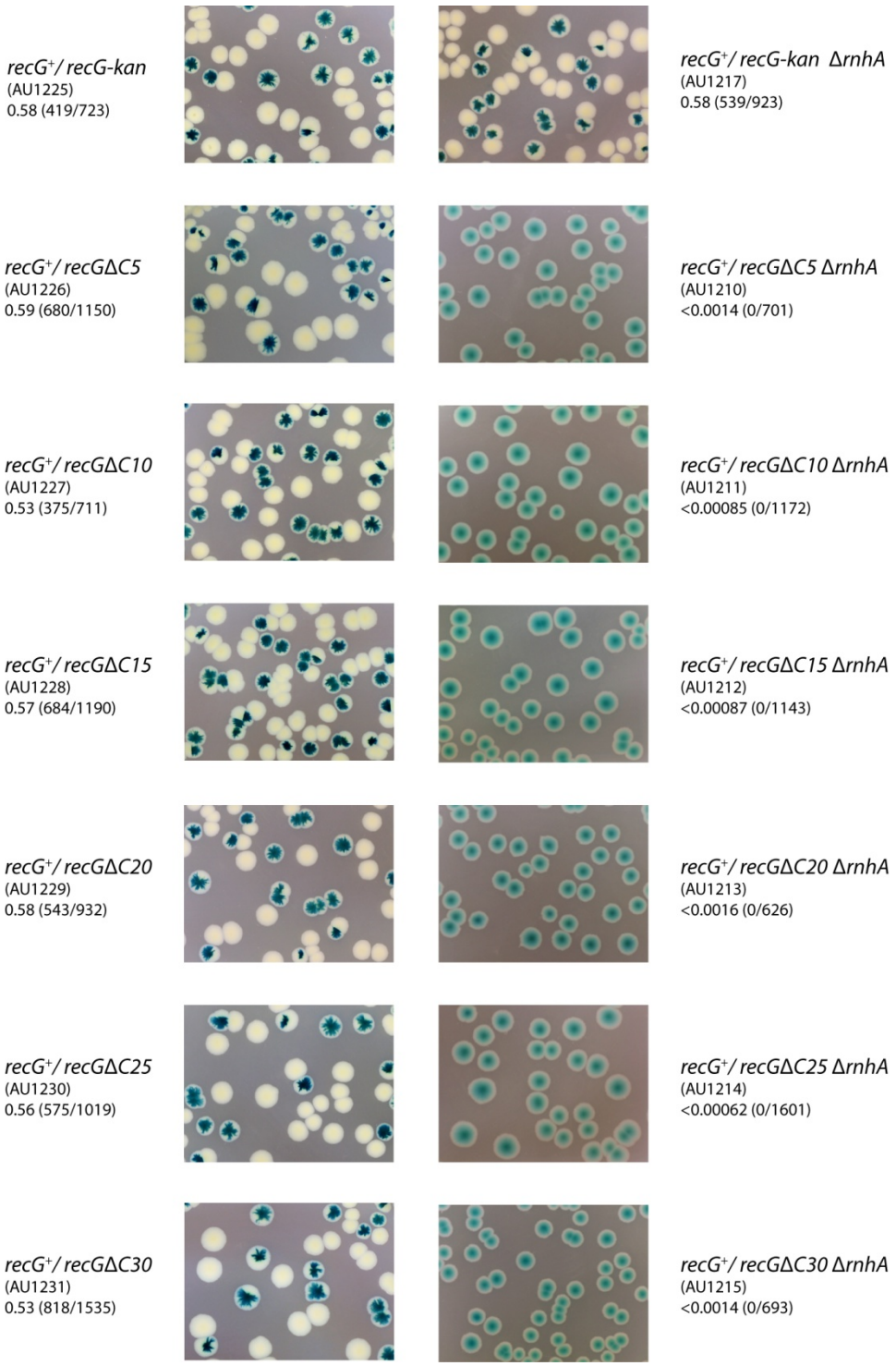

Figure 57. Deletions of the *recG* C-terminus are inviable when combined with Δ*rnhA*. Synthetic lethality assays demonstrating the inviability of *recGΔC5* Δ*rnhA*, *recGΔC10* Δ*rnhA*, *recGΔC15* Δ*rnhA*, *recGΔC20* Δ*rnhA*, *recGΔC25* Δ*rnhA* and *recGΔC30* Δ*rnhA*. The relevant genotype is shown above each image, along with the strain number. The fraction of white colonies is shown below each image, with the number of white colonies/total colonies analysed in parentheses.

Subject specific terms

A_{650}	absorption at 650 nm
ATP	adenosine 5′-triphosphate
bp	base pair
BrdU	5-Bromo-2′-deoxyuridine
BSA	bovine serum albumin
cSDR	constitutive stable DNA replication
Dam	methylates GATC sites in hemi-methylated DNA
D-loop	DNA loop
dNTP	deoxynucleoside triphosphate
DnaA	the replication initiator
DnaB	the replicative helicase
DnaC	involved in loading DnaB via protein-protein interactions
DnaG	produces RNA primers during replication
eCFP	enhanced cyan fluorescent protein
eYFP	enhanced yellow fluorescent protein
LexA	represses expression of genes as part of the SOS system
MBP	maltose binding protein
MC	mitomycin C
NER	nucleotide excision repair
oriC	the replication origin in *E. coli*
PriA	involved in loading the replicative helicase at sites away from *oriC*
PriC	involved in loading the replicative helicase at sites away from *oriC*
RecA	the recombinase – required to initiate strand exchange for recombination
RecBCD	double-stranded DNA exonuclease
replisome	the replication complex
R-loop	RNA-loop
RuvABC	the Holliday junction resolvase
iSDR	inducible stable DNA replication
SeqA	binds to hemi-methylated DNA behind a replication fork
SDR	stable DNA replication
SSB	single-strand DNA binding protein
Ter	sites at which Tus binds during termination of replication
Tus	acts as an anti-helicase during termination of replication
UvrA	required during nucleotide excision repair